Loughborough University

This item was submitted to Loughborough's Research Repository by the author.
Items in Figshare are protected by copyright, with all rights reserved, unless otherwise indicated.

Dynamic mechanical thermal properties of moulded poly(vinylchloride) swollen with organic liquids

PLEASE CITE THE PUBLISHED VERSION

PUBLISHER

© I. Hovell

PUBLISHER STATEMENT

This work is made available according to the conditions of the Creative Commons Attribution-NonCommercial-NoDerivatives 4.0 International (CC BY-NC-ND 4.0) licence. Full details of this licence are available at: https://creativecommons.org/licenses/by-nc-nd/4.0/

LICENCE

CC BY-NC-ND 4.0

REPOSITORY RECORD

Hovell, Ian. 2019. “Dynamic Mechanical Thermal Properties of Moulded Poly(vinylchloride) Swollen with Organic Liquids”. figshare. https://hdl.handle.net/2134/33149.

BLDSC No. - DX 80027

LOUGHBOROUGH
UNIVERSITY OF TECHNOLOGY
LIBRARY

AUTHOR/FILING TITLE

HOVELL, I

ACCESSION/COPY NO

014493/02

VOL. NO. | CLASS MARK

LOAN COPY

- 6 JUL 1990
- 6 JUL 1990
- 5 JUL 1991
- 5 JUL 1991
- 3 JUL 1992
~~2 JUL 1993~~
~~2 JUL 1993~~
26 JUN
- JUL
- 2 JUL 1993
- 2 JU 1993
- 1 JUL 1994
13 JAN 1995

001 4493 02

BLDSC No. - DX 80027

LOUGHBOROUGH
UNIVERSITY OF TECHNOLOGY
LIBRARY

AUTHOR/FILING TITLE

HOVELL, I

ACCESSION/COPY NO

014493/02

VOL. NO

CLASS MARK

25 JAN 1995

14 JAN 2000

26 JAN 1995

13 JAN 1995

001 4493 02

DYNAMIC MECHANICAL THERMAL PROPERTIES OF MOULDED POLY (VINYLCHLORIDE) SWOLLEN WITH ORGANIC LIQUIDS

by

IAN HOVELL

Supervisors: Professors J.V. Dawkins and R.E.Wetton

A Doctoral Thesis

Submitted in partial fulfilment of the requirements for the award of Doctor of Philosophy of the Loughborough University of Technology.

AUGUST 1987

Department of Chemistry

© by I. HOVELL 1987

Loughborough University
of Technology Library
Date NW 87
Class
Acc. No. 014493/02

To Mum and Dad for their guidance, help and encouragement over the years.

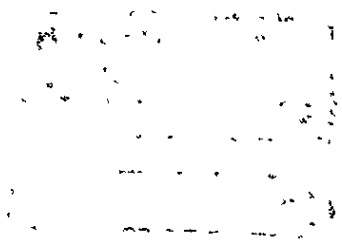

ACKNOWLEDGEMENTS

I would like to thank, Professor J. V. Dawkins, for his useful recommendations and interest shown throughout this research, Dr.'s P. V. Smallwood, A. Faraday and R. Stevenson all of I.C.I., Plastics and Petrochemicals Division, The Heath, Runcorn, Cheshire, U.K. for their many and helpful discussions and Professor R. E. Wetton for initiating the original programme. Thanks are also due to the S.E.R.C and I.C.I. for the provision of a Case Award research grant and to Professor F. Wilkinson for the use of the facilities in the Chemistry Department. Finally, I must pay tribute to Dr. A. M. C. Montenegro for her everlasting patience

ORIGINALITY

All the work presented in this thesis has been carried out by the author except where acknowledged and has not previously been presented for a degree at this University or any other institution.

ABSTRACT

Compression moulded unplasticised poly (vinylchloride) (uPVC) was swollen with various organic liquids at two temperatures, 60 and 30°C, both temperatures being below the glass transition temperature of uPVC. Liquids were chosen to give a range of solubility parameters, molecular sizes and ability to form hydrogen bonds. It was hoped to find a PVC-liquid system which behaved similarly to PVC swollen with vinyl chloride monomer (VCM).

The diffusion of the organic liquids into the PVC was followed by measuring the percentage gain in mass and the distance of penetration as a function of time. The experimental diffusion results were analysed by the use of the generalized diffusion equation which takes into account both Fickian and case II mechanisms. Some agreement was found between experimental and theoretically calculated liquid uptake. It is postulated that the swelling procedure produces an advancing front behind which there exists a swollen region of organic liquid and PVC in equilibrium with the concentration of liquid on the surface of the polymer.

The experimental probes used to investigate this swollen region have been the glass transition temperature and the rigidity modulus. These were determined using Dynamic Mechanical Thermal Analysis (DMTA). The ability of the swelling agent to "soften" the crystalline content of the polymer has been discussed. Differential Scanning Calorimetry (DSC) was also used to determine the glass transition temperature for the separate swollen region and for the glassy unswollen inner core.

The experimentally derived glass transitions for the swollen region were compared with values predicted with equations based on free volume. Reasonable agreement was found, the deviations being discussed in terms of swelling agent content in the swollen polymer and crystallinity. A theoretical model has been employed to calculate the modulus of the swollen PVC region while still in contact with the glassy unswollen inner core.

CONTENTS

ACKNOWLEDGEMENTS iii

ORIGINALITY iv

ABSTRACT v

CONTENTS vii

CHAPTER 1 - INTRODUCTION

1.1 DYNAMIC MECHANICAL THERMAL ANALYSIS OF POLYMERIC SYSTEMS 6

1.2 LIQUID UPTAKE BY PVC 8

1.3 VAPOUR UPTAKE BY PVC 10

1.4 SUMMARY OF THE WORK UNDERTAKEN IN THIS STUDY 13

CONTENTS PAGE

CHAPTER 2 - EXPERIMENTAL THEORY

2.1 DEFINITION OF MECHANICAL TERMS 14

2.1.1 Static terminology 14

2.1.1.1 Simple tension 14

2.1.1.2 Simple shear 14

2.1.1.3 Bulk compression 16

2.1.2 Dynamic terminology and interrelations ... 16

2.2 THE GLASS TRANSITION 22

2.2.1 Definition of the glass transition temperature 22

2.2.2 Kinetic theories 26

2.2.3 Thermodynamic theories 29

2.2.4 Factors affecting T_g values 33

2.2.4.1 Intramolecular effects 33

2.2.4.2 Intermolecular effects 36

2.3 POLYMER-SOLVENT INTERACTIONS 41

2.3.1 The solubility parameter 41

2.3.2 The thermodynamic interaction parameter ... 42

2.3.2.1 The interaction parameter value 43

2.4 ELASTICITY 45

2.4.1 Static moduli of rubbers from the rubber elasticity theory 45

2.4.2 Static moduli of swollen polymers 52

2.4.3 Swollen cross-linked networks 54

CONTENTS PAGE

2.5 SIMPLE RELAXATION BEHAVIOUR 58

2.5.1 Mechanical models describing viscoelasticity 58

2.5.1.1 The Maxwell model 61

2.5.1.2 Voigt-Kelvin model 61

2.5.1.3 The standard linear body 62

2.5.2 Molecular interpretations of viscoelastic behaviour 65

2.5.3 Moduli of partially crystalline polymers ... 66

2.5.3.1 Molecular models 66

2.5.3.2 The mechanical model of Takayanagi ... 67

2.6 DIFFUSION 71

2.6.1 Basic diffusion terminology 71

2.6.1.1 Fick's laws of diffusion 71

2.6.2 The free volume theory for diffusion into polymers 71

2.6.2.1 The concentration dependency of the diffusion coefficient 74

2.6.2.2 The temperature dependency of the diffusion coefficient 74

2.6.3 Diffusion in polymeric systems 77

2.6.3.1 Fickian diffusion (Case I) 79

2.6.3.1.1 Diffusion in a plane sheet 83

2.6.3.2 Case II diffusion 84

2.6.3.3 Non-Fickian or anomalous diffusion ... 87

2.6.4 A mathematical model for the superposition of Case I and Case II diffusion 89

CONTENTS PAGE

CHAPTER 3 - EXPERIMENTAL

3.1 MATERIALS 92

3.2 SAMPLE PREPARATION 97

3.2.1 Solid/liquid contact 97

3.2.2 Solid/vapour sorption 102

3.2.2.1 Operation of electro-microbalance ... 102

3.2.2.2 Vapour sorption using an electronic microbalance 104

3.3 ANALYSIS OF SWOLLEN SAMPLES 109

3.3.1 Dynamic mechanical thermal analysis of swollen samples 109

3.3.1.1 Analysis using shear mode 109

3.3.1.2 Analysis using dual-cantilever mode ... 113

3.3.1.3 Principle of PL-DMTA operation 114

3.3.1.4 Instrument calibration 118

3.3.2 Analysis by differential scanning calorimetry 118

3.3.3 Analysis of diffusion coefficients 121

CHAPTER 4 - RESULTS

4.1 DIFFUSION OF ORGANIC LIQUIDS INTO PVC PLAQUES 123

4.1.1 Classical treatment of diffusion into a plane sheet 123

4.1.2 The Case II contribution to diffusion into a system which swells 132

4.1.2.1 Equilibrium swelling in the swollen layer 132

4.1.2.2 Normalised mass uptake of swelling liquids in poly (vinylchloride) plaques 133

4.1.2.3 The measurement of the swelling agent-polymer interface 138

4.1.2.4 The movement of the liquid front in unplasticised poly (vinylchloride) plaques 144

4.2 DIFFUSION OF ORGANIC VAPOUR INTO POLY (VINYLCHLORIDE) PLAQUES 151

4.3 GLASS TRANSITIONS OF THE PURE LIQUIDS EMPLOYED 155

4.3.1 Dynamic mechanical thermal analysis of pure liquids 155

4.3.2 Calibration of the differential scanning calorimeter 165

4.3.3 Differential scanning calorimetric analysis of pure liquids 166

4.4 DYNAMIC MECHANICAL THERMAL ANALYSIS OF SWOLLEN POLY (VINYLCHLORIDE) PLAQUES 172

4.4.1 The capabilities of the Polymer Laboratories Dynamic Mechanical Thermal Analyser 172

4.4.1.1 Experimental variation 175

4.4.2 Analysis of highly swollen poly (vinylchloride) plaques using dual-cantilever dynamic mechanical thermal analysis methods 174

4.4.2.1 Systems thought to be fully swollen ... 175

4.4.2.2 Highly swollen diluent/Poly (vinylchloride) systems exhibiting an unplasticised poly (vinylchloride) glass transition 179

4.4.3 Examination of vapour swollen poly (vinylchloride) plaques using dual-cantilever, dynamic mechanical thermal analysis methods 191

4.4.4 Analysis of highly swollen PVC plaques using shear PL-DMTA methods 198

4.4.4.1 Loss of vapour during analysis 198

4.4.4.2 Shear log modulus thermograms of liquid swollen disc 199

4.4.4.3 Tan δ thermograms of swollen plaques 205

4.5 EXAMINATION OF SEPARATED CORE AND SWOLLEN LAYER 217

CHAPTER 5 - DISCUSSION

5.1 DIFFUSION OF LIQUIDS INTO uPVC 225

5.1.1 Validity of classical diffusion theories with changing sample thickness 226

5.1.2 The Case II contribution to diffusion into a system which swells 229

5.1.2.1 Validity of Case II theories with liquid diffusion into uPVC samples 229

5.1.2.2 Prediction of the thickness of the liquid swollen layer 235

5.1.3 The effect of diffusant size, hydrogen bonding number and solubility parameter on the diffusion coefficient 241

5.2 THE DYNAMIC THERMAL MECHANICAL ANALYSIS AND DSC ANALYSIS OF LIQUIDS AND PLASTICIZERS 245

5.3 THE DYNAMIC THERMAL MECHANICAL ANALYSIS OF SWOLLEN uPVC COMPRESSION MOULDED PLAQUES 247

5.3.1 The stability of the glass transition temperature of the swollen polymer 247

5.3.1.1 Movement of $T_g\alpha'$ peak on the rerunning of highly swollen samples using dual-cantilever PL-DMTA 247

5.3.1.2 Movement of $T_g\alpha'$ peak on the rerunning of vapour swollen samples using dual-cantilever PL-DMTA 251

5.3.1.3 Movement of $T_g\alpha'$ peak on the desorption of liquid swollen samples using shear PL-DMTA mode 253

5.3.2 Dynamic mechanical thermal analysis of shear mode results 259

5.3.2.1 Calculation of molecular weight between cross-links from PL-DMTA modulus results 260

5.3.2.2 Estimation of the variation between identical shear experiments 267

5.3.3 Glass transitions of swollen networks ... 270

5.3.3.1 Comparison of the glass transition temperature produced in highly swollen liquid sorbed uPVC plaques with the solubility parameter of swelling agent 275

5.3.3.2 The glass transition investigated using differential scanning calorimetry methods 277

5.3.4 Variation of $T_{g\alpha}$ peak height with volume fraction of unswollen core 277

5.4 General discussion 280

CHAPTER 6 - SUMMARY AND RECOMMENDATIONS

6.1 APPLICATIONS FOR THE TECHNIQUE 291

6.2 POSSIBLE IMPROVEMENTS IN INSTRUMENTATION 292

6.3 IMPROVEMENTS IN EXPERIMENTAL TECHNIQUE 293

REFERENCES 294

APPENDICES 304

CHAPTER 1 — INTRODUCTION

Poly (vinylchloride), (PVC) is one of the most important thermoplastics. The annual world production is approximately 30 million tons and about 80% of this is produced by the suspension process. The polymerization process is carried out in a pressurised stirred autoclave into which drops of vinylchloride monomer, (VCM), approximately 20 μm diameter are dispersed. The droplets, stabilized by a protective colloid, consolidate on polymerization giving a final granular product approximately 150 μm in diameter [1-3]. The suspension polymerization of VCM is confined to within the suspended VCM droplet. Each droplet can be considered as a small mass polymerization process. Consequently the mechanism for the formation of the particle microstructure is common to the two processes. Initiation of commercial suspension polymerization is by means of various azo or peroxide type materials that decompose to form monomer soluble free radicals when heated to the desired reaction temperature. PVC is almost completely insoluble in VCM and therefore when a growing PVC chain reaches a critical size, which is probably relatively few monomer units, it will precipitate. Mickley *et al.*[4] proposed that the precipitated polymer chain when coiled

upon itself forms the first and smallest PVC particle known as the basic particle or micro-domain approximately 20 nm in diameter. The particle morphology is described in figure 1.1. Behrens et al[5], although agreeing with the likely size of the basic particle, postulated that they are formed from a grouping of 5-10 macromolecules. These basic particles being highly unstable flocculate to form domains or primary nuclei of about 0.2 µm in diameter. It is thought[4] that the half-life of the basic particles is around 3 ms.

FIGURE 1.1

Model of uPVC grain morphology

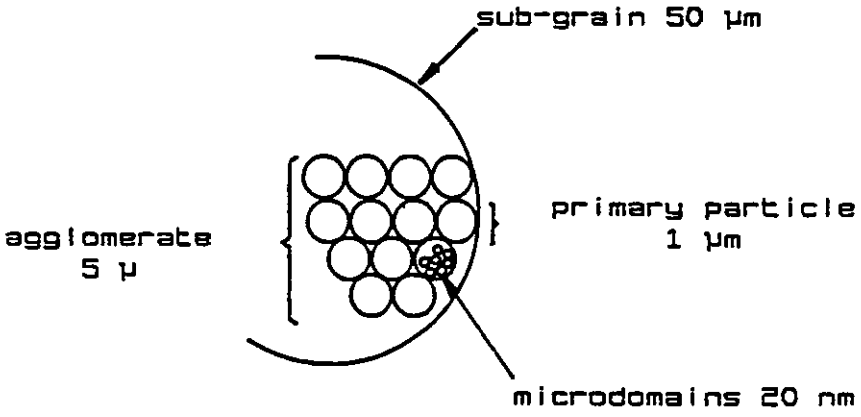

If the initiation rate is high it is possible for the growth rate of the basic particle to be fast enough to stabilize the basic particle without collisions occurring with other such particles. This produces a primary particle with no visible sub-structure. Once formed, at less than 5% conversion, the number of primary particles remains constant with little or no secondary nucleation occurring.

Polymerization, from 5% conversion onwards, occurs

almost exclusively in the monomer swollen polymer phase producing a uniform growth in the size of the primary particle first formed. These primary particles are in some manner stabilized from initial agglomeration. The mechanism of stabilization is unclear but is thought to be electrical in nature[6]. At around 5% conversion the primary particles flocculate into agglomerates of around 5µm in diameter. Suspension PVC particles usually possess a pericellular "skin" or "membrane" which extends almost continuously over the entire outer surface of the particle. This skin forms very early on, around less then 5% conversion. It is thought[7] the skin is formed by the primary particles being forced out by centrifugal forces onto the monomer/water interface and being destabilised, such that they fuse and form a continuous boundary that eventually grows to a thickness of about 1 µm.

Polymerization is normally continued to around 85-95% conversion and because of the 55% increase in density on polymerization a certain contraction of the droplet occurs causing some fusing of the agglomerates into a sub-grain particle. The sub-grain is a polymerised monomer droplet which aggregates to form the final morphologically recognised particle, the grain, which essentially is a porous network of primary particle aggregates, of around 150 µm in diameter.

The dried granular product is then processed in a variety of ways[8]. The processing characteristics of suspension PVC are largely determined by the granular morphology and molecular weight of the polymer. The smaller molecular weight favours ease of processing, but along with

reduced strength in the final product. The polymerization reaction temperature controls both the chain length and degree of syndiotacticity[9-12]. A porous granular product, which favours easy absorption of plasticizer additives, is used where flexibility is required in the final product, whilst, grains exhibiting a low porosity are favoured in rigid applications. Granular porosity is important in aiding the removal of remaining unreacted monomer at the end of the polymerization[1]. The grains are subsequently processed into the final product by a variety of means; from the melt, paste, latices or copolymer. The many possible variations and modifications to the processing of PVC grains has been summarised by Matthews[13]. Knowledge of the degree of fusion between the grains in the final, melt-processed, product is important for the, toughness and durability of PVC, accordingly many methods have been developed to assess the degree of fusion[14]. Of importance to this work are the techniques involving solvent testing and dynamic analysis. Fusion in compressed unplasticised-PVC, (uPVC), is often examined by immersing a portion of the polymer in propanone at room temperature following standard procedures, (BS3505:1968) and (ASTM D2152-67, reapproved 1972). The test has a number of limitations[14] and yields only a subjective analysis as to the degree of fusion present in the final product. More recently methods have been explored, using thermal analysis, by Gilbert and Vyvoda[15] to investigate the degree of fusion in the polymer. Dynamic mechanical thermal analysis techniques have been employed by Harrison et al.[16]. They investigated the extent of fusion in a compression moulded

uPVC plaque, as a function of moulding temperature, by using optically clear partially fused plaques annealed at a temperature above its glass transition temperature, (T_g), and modelled the volume recovery with loss of modulus.

CHAPTER 1 - INTRODUCTION

1.1 DYNAMIC MECHANICAL THERMAL ANALYSIS OF POLYMERIC SYSTEMS

The technique of dynamic mechanical thermal analysis of polymeric systems is of ever increasing importance since many applications of polymers involve the vibration of material, for example, as seen in the automobile industry. The dynamic thermal mechanical analysis, carried out at a single frequency, typically at a frequency between 0.1 and 90 Hz, over a temperature span of 320 degrees between -140 to 180°C yields valuable information as to the modulus behaviour of polymeric materials. Figure 1.2 shows idealised modulus-temperature curves for typical linear and cross-linked amorphous polymers. The curves show four regions of viscoelastic behaviour, glassy, transition, rubbery and linear. The line extending horizontally from the rubbery region would be that exhibited by a lightly cross-linked polymer. Of particular interest to the manufacturer is the temperature at which the transition region occurs, as this often describes the upper or lower working limit of a polymer.

FIGURE 1.2

Idealised modulus-temperature curves for typical linear and cross-linked amorphous polymers[17]

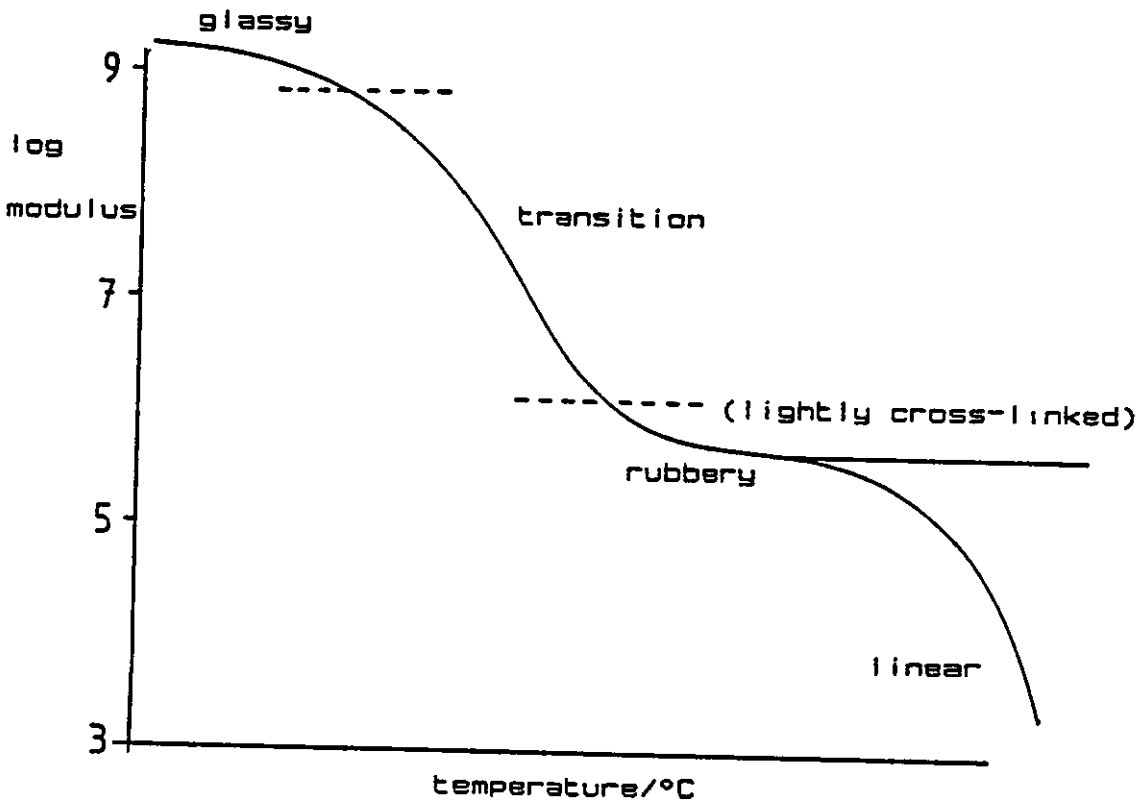

1.2 LIQUID UPTAKE BY PVC

Interest in the liquid uptake by PVC began as early as 1952[18]. The speed of penetration of the liquid into the polymer enabled Corbiere et al.[18] to distinguish three classes of liquids, (1) inert liquids producing no effect, (2) "disintegrating" liquids in which dissolution proceeded without previous visible swelling and (3) liquids which swelled the polymer followed in some cases by complete dissolution.

Some of the first investigations into PVC morphology by liquid uptake were carried out by Illers[19] and Lapcik and Valko[20]. Although no quantitative examination was reported, Illers concluded that the sorption of liquids by PVC is dependent upon thermal history. Lapcik and Valko studied the dissolution of commercial PVC in cyclohexanone at various temperatures between 20 and 70 °C and produced the apparent activation energy for the swelling and dissolution processes, by plotting the activation energy of swelling and dissolution of PVC in cyclohexanone as a function of molecular mass. The activation energy was found to reach a limiting value with increasing number average molecular weight, $\bar{M}_n$. This indicates that the chain ends make an important contribution to the swelling and dissolution. Lapcik et al.[21] later calculated the apparent Fickian diffusion coefficients for various organic solvents in PVC films produced from emulsion polymerized VCM. They found the activation energy for diffusion was dependent on the polarity of the solvent molecule. Working concurrently Kwei and co-workers in a series of papers[22-26]

demonstrated the similarity between the mathematically predicted mass uptake, and depth of penetration, of propanone into PVC sheeting and that obtained experimentally by using a generalized diffusion equation which includes the internal stress contribution.

1.3 VAPOUR UPTAKE BY PVC

It has become generally accepted [27] that there are two models for interpreting organic vapour transport in glassy polymers; Fickian (case 1) and non-Fickian (relaxation or case 2). For the system (PVC/VCM), Berens[28] has investigated the conditions where Fickian and case II diffusion can dominate. Berens has collected sorption and desorption data for VCM in a wide variety of PVC resins at temperatures from 25 to 110 °C and VCM pressures from zero to 700 mmHg. He has shown Fickian diffusion using an emulsion polymerized PVC resin, consisting of spherical particles of diameters from approximately 0.1 to 1 μm with very narrow size distributions; essentially a resin containing uniform spheres. When using suspension polymerized PVC resins, containing gross particles of roughly 100 μm in diameter, which are neither truly spherical nor uniform in size, Non-Fickian behaviour was observed. This behaviour was attributed to the presence of glassy particles - which arise in the polymerization process and appear as nonporous structures. They are believed to arise from excessive fusing together of primary particles during polymerization to form solid PVC regions which may be as large as the gross agglomerated particles of the resin, i.e. up to 100 μm. The presence of a few such particles in an otherwise porous resin could well account for slow sorption or desorption of the last fraction of the total VCM.

Berens[27] discusses the theory proposed by Michaels *et al.*[29] who suggested that the sorption of gases and

organic vapours in polymers below their T_g follows a dual-mode sorption model, the total sorption being ascribed to contributions of normal dissolution and Langmuirian "hole-filling". A sorption isotherm for VCM in PVC under these conditions shows a pronounced downward curvature, see figure 1.3[28]. This situation exists when the polymer is in its glassy state, in its rubbery region normal dissolution behaviour occurs. Berens[28] further suggested that the extent of hole-filling can be used as a measure of the microvoid content in the PVC resin.

Summers[30] re-examined the action of propanone on PVC suspension resin. He suggested the presence of a cross-linked network where the propanone only enters into the amorphous region leaving the crystallites intact which act as cross-links, limiting the amount by which the PVC swells. This work has been carried further by Guerrero[31] who prepared 10%(w/w) solutions of PVC in various solvents and prepared PVC gels and studied the network structure, as a function of polymer crystallinity and polymer-solvent interaction. A correlation between gel-forming ability and solubility parameter was found.

FIGURE 1.3

The sorption of VCM into PVC grains at 30°C[28]

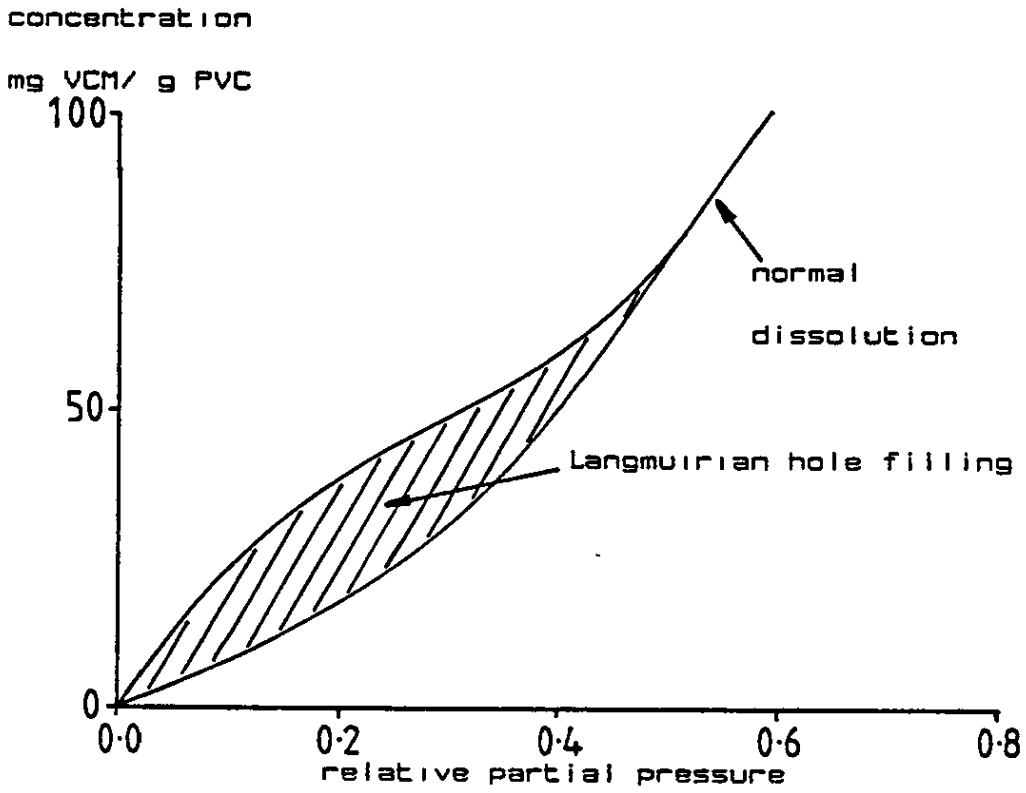

1.4 SUMMARY OF THE WORK UNDERTAKEN IN THIS STUDY

The previous two sections describes how organic vapours and liquids have been used as tools for investigating the morphology of uPVC. All the work described has dealt with emulsion or suspension polymerized PVC resins that have received little or no heat treatment. The experiments described in this report deal with suspension polymerized resin of average molar mass, 200,000 g mol^{-1} and of gross particle size upto 100 μm diameter pressed into a sheet at 169 °C for 6 minutes at a pressure of 9800 KNm^{-2}. A certain amount of modification will have occurred in particle structure and void content. At this temperature and pressure the primary particles will have begun to break down.

The uptake of various liquids into PVC plaques has been followed using two parameters, total mass uptake per unit surface area and depth of penetration. The mathematical model[22-26] used to follow these parameters required the use of a constant equilibrium concentration of liquid in the swollen polymer. The mechanical properties of the partial swollen (in some cases fully swollen) polymer were investigated using a Polymer Laboratories Dynamic Mechanical Thermal Analysis (PL-DMTA) instrument supplied by Polymer Laboratories, The Technology Centre, Epinal Way, Loughborough, Leicestershire, LE11 0QE UK. The information extracted from PL-DMTA consisted of T_g and modulus data and was modelled to the concentration of liquid in the swollen polymer.

CHAPTER 2 — THEORY

2.1 DEFINITION OF MECHANICAL TERMS

2.1.2 Static terminology

Amorphous and to some extent partially crystalline polymeric materials may be considered to be isotropic in nature. These materials can undergo three elementary forms of elastic deformation when subjected to (1) simple tension, (2) simple shear and (3) uniform or bulk compression, as shown diagramatically in figure 2.1[32].

2.1.2.1 Simple tension

If Hooke's law is assumed, the tensile stress σ is proportional to the tensile strain γ. The proportionality constant is known as the modulus which is defined by the Young's modulus E for elastic solids by

$$\sigma = E\gamma \qquad (2.1)$$

2.1.2.2 Simple shear

The base of the sample is held rigid and a

FIGURE 2.1

Different forms of elastic deformation (1) simple tension (2) simple shear (3) bulk compression

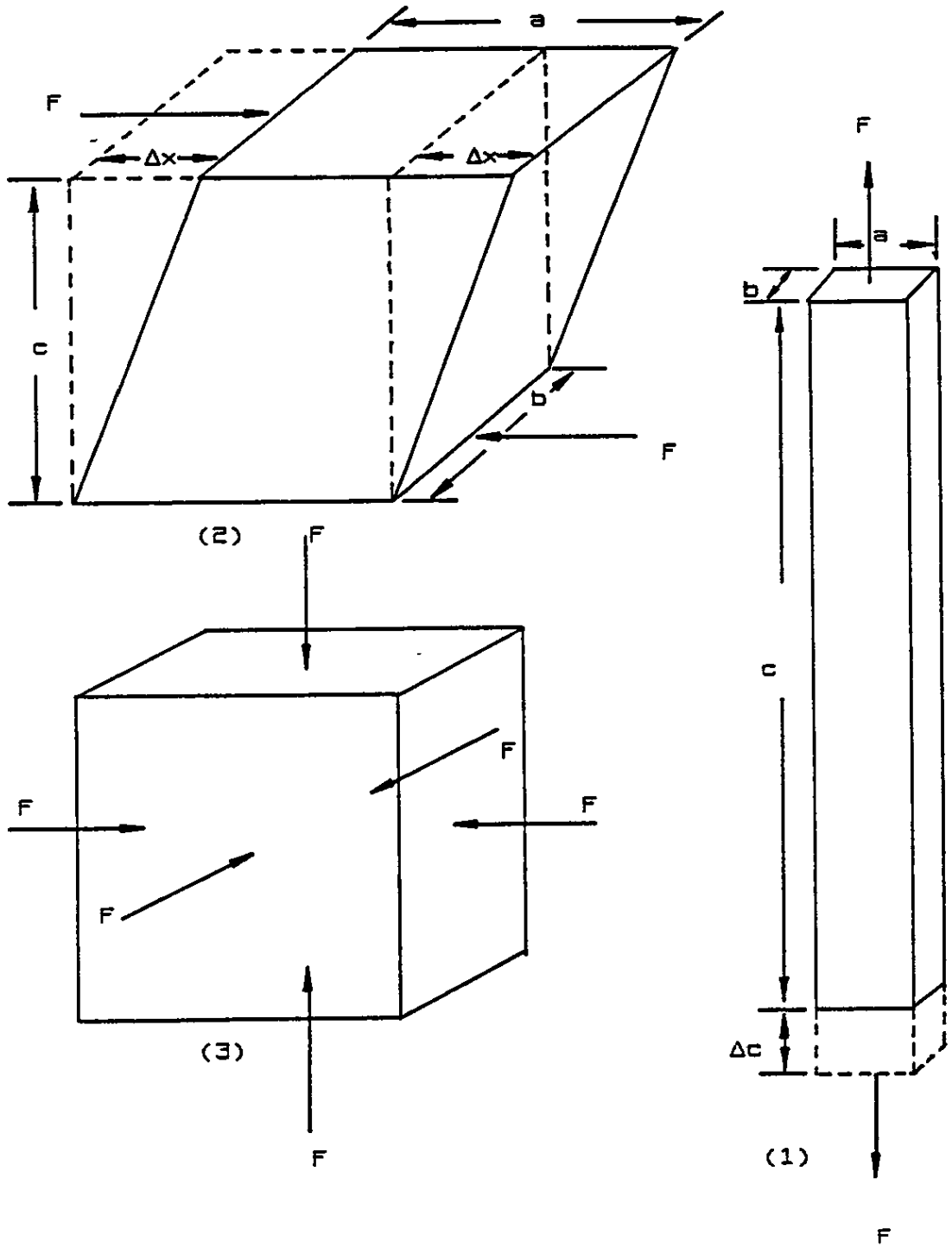

transverse force is applied. The shear modulus G is given by the quotient of the shearing force per unit area and the shear per unit distance between shearing surfaces.

$$G = \sigma_s/\gamma_s \qquad (2.2)$$

2.1.1.3 Bulk compression

When a hydrostatic pressure $-p$ is applied to a body having a volume V_o a change in volume is produced, ΔV. The bulk modulus B can be defined as

$$B = -p/(\Delta V/V_o) \qquad (2.3)$$

In simple shear and tension there is a change in shape without change in volume. Bulk compression brings about a change in volume with no change in shape. The three moduli G, B and E are interrelated by

$$E = 3B(1 - 2\mu) = 2(1 + \mu)G \qquad (2.4)$$

where μ is Poisson's ratio and is a characteristic of the material under test. Poisson's ratio varies from 0.5, when no volume change occurs, to about 0.2. This shows for a incompressible elastic solid, such as rubber, the Young's modulus is three times that for shear modulus.

2.1.2 Dynamic terminology and interrelations

Upon the application of stress a viscoelastic body

develops a strain which builds up slowly. If the stress is applied in a sinusoidal manner, the strain also alternates sinusoidally but lags in phase behind the applied stress. The situation is illustrated in figure 2.2.

A sinusoidal stress of frequency (ω) is applied to the sample. The stress and strain may be expressed in the following equations[33]

$$\sigma = \sigma_p \sin \omega t \tag{2.5}$$

$$\gamma = \gamma_p \sin(\omega t - \delta) \tag{2.6}$$

where σ_p and γ_p is the stress and strain amplitudes, respectively. The stress may be resolved vectorally into two components, one in phase with the strain and the other out of phase, by 90° with the strain. If each of these components is divided by the strain the modulus may be expressed, using complex notation, as in-phase (or real) and out-of-phase (imaginary) components. This is shown in figure 2.3(a). The complex dynamic modulus is given by.

$$E^* = E' + iE'' \tag{2.7}$$

The seperate components are defined as

$$E^* = \frac{\text{stress amplitude}}{\text{strain amplitude}} \tag{2.8}$$

FIGURE 2.2

Continuous sinusoidal deformation

of a viscoelastic body

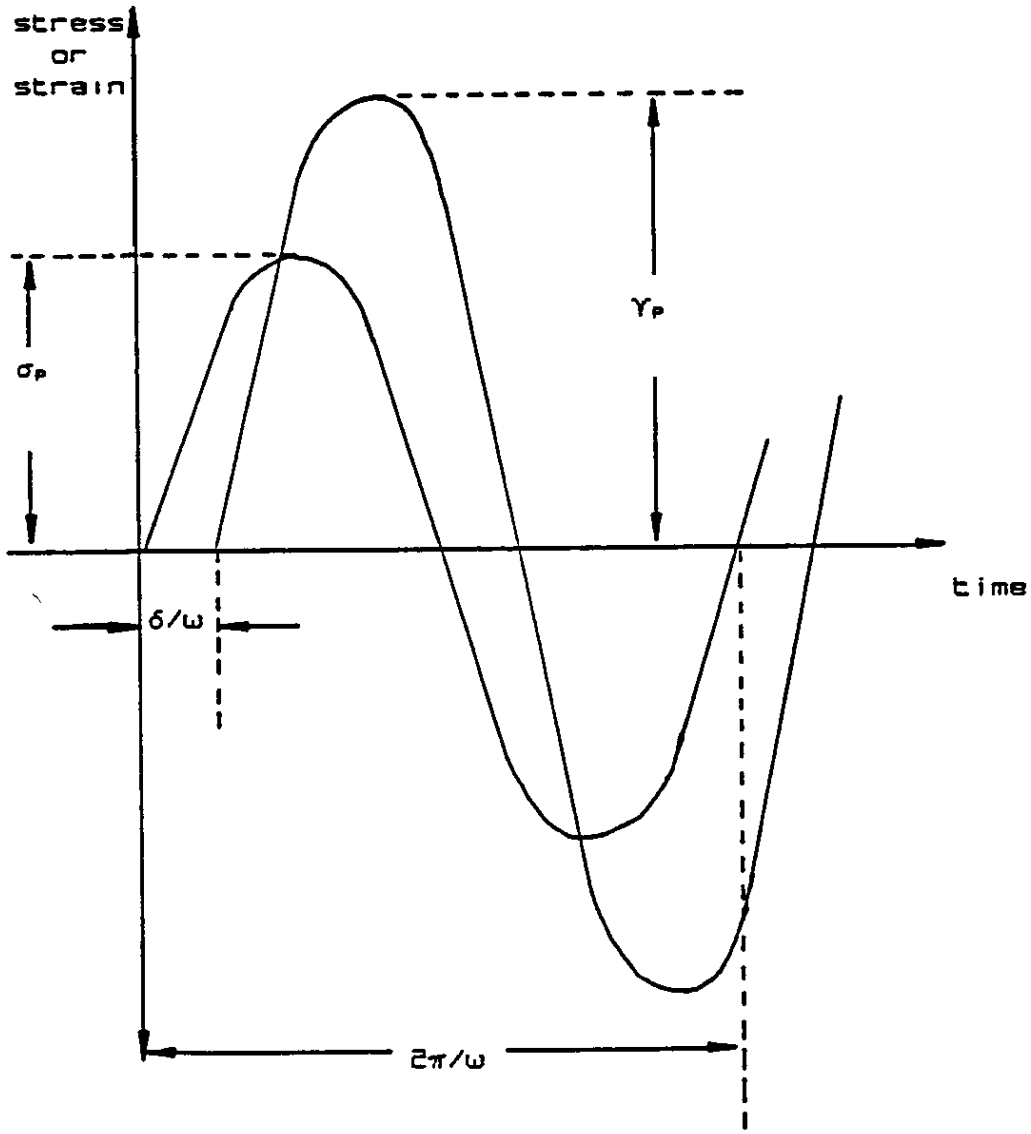

FIGURE 2.3

The vectorial analysis of dynamic modulus and compliance

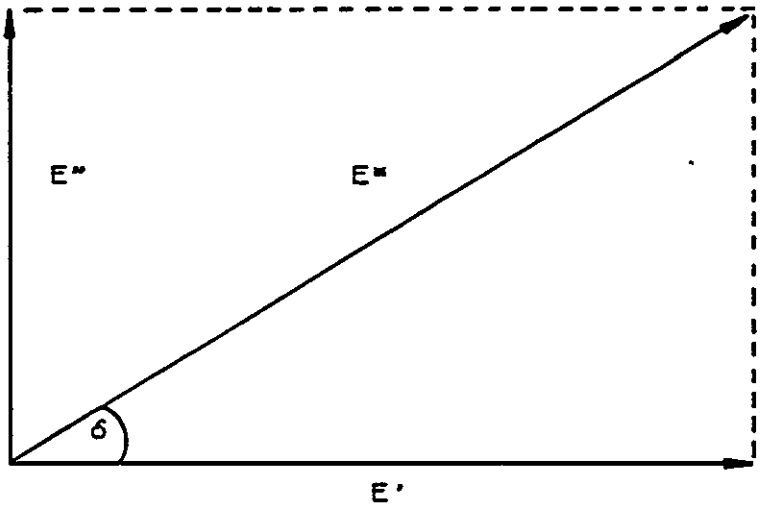

(a)

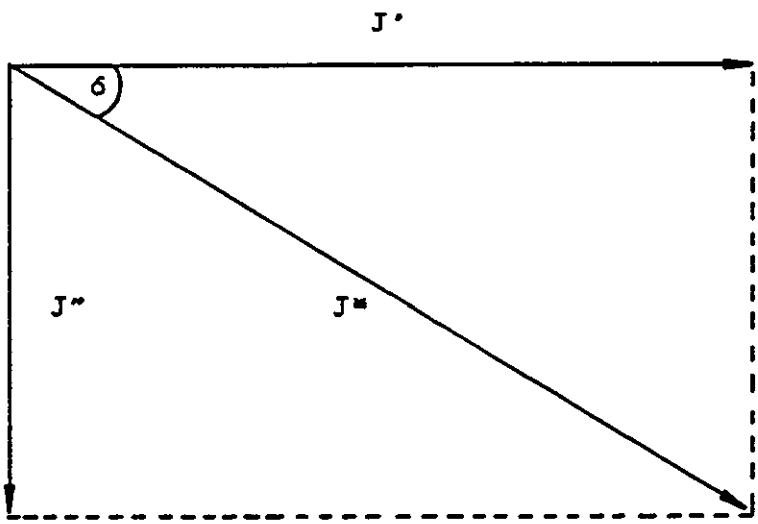

(b)

and

$$E' = \frac{\text{stress amplitude in phase with strain}}{\text{strain amplitude}} \qquad (2.9)$$

$$E'' = \frac{\text{stress amplitude 90° out of phase}}{\text{strain amplitude}} \qquad (2.10)$$

The in-phase or storage modulus E' is associated with the recoverable stored energy and the out-of-phase or loss modulus E" is associated with the amount of energy dissipated by the material.

The damping in the system or the energy loss per cycle can be measured from the "loss tangent" tan δ. This is a measure of the internal friction and is related to the complex moduli by

$$\tan \delta = E''/E' \qquad (2.11)$$

From figures 2.2 and 2.3 it can be seen that instead of producing complex modulus data by dividing stress by strain it is possible to produce strain by stress data. This is shown in figure 2.3(b). This is termed the complex compliance J*.

$$J^* = 1/G^* = J' - iJ'' \qquad (2.12)$$

The storage compliance J' is the ratio of the strain in

phase with the stress and J", the loss compliance is the ratio of the strain 90° out of phase with the stress. From figure 2.3 it can be seen that

$$G^* = 1/J^* \qquad (2.13)$$

Their individual components do not however follow the same relationships. They are connected by the following equations[33].

$$J' = \frac{G'}{(G'^2 + G''^2)} = \frac{1/G'}{1 + \tan^2\delta} \qquad (2.14)$$

$$J'' = \frac{G''}{(G'^2 + G''^2)} = \frac{1/G''}{1 + (\tan^2\delta)^{-1}} \qquad (2.15)$$

These equations may be used to calculate G' and G" simply by substituting J' and J" into the right hand sides of equations 2.14 and 2.15 for G' and G" respectively.

2.2 THE GLASS TRANSITION

2.2.1 Definition of the glass transition temperature

When the temperature of an amorphous high molecular weight polymer is lowered, a region may be reached where the properties of the polymer change from those of a soft, flexible rubber to those of a hard, brittle glass. This point is known as the glass transition temperature (T_g). At this point rotational molecular motion ceases to occur. The thermodynamic and physical properties of a polymer undergo a marked change at this temperature.

The temperature dependence, at constant pressure, of quantities such as the volume and enthalpy, have been well described in the literature[34,35]. An example of this is shown in figure 2.4. In both cases an inflection in the property-temperature curve is observed. The volume temperature relationship is shown for an amorphous polymer (curve A-D). A hypothetically pure crystalline polymer (curve A-B-H). In the region C-D the amorphous polymer is a glass. The inflection observed at C is the T_g temperature beyond which the polymer softens and becomes rubber-like. A continuing increase in temperature along C-B-A leads to a change of the rubbery polymer to a viscous liquid.

In a perfectly crystalline polymer, all the chains would be incorporated in regions of three-dimensional order, called crystallites and no glass transition would be observed, because of the absence of disordered chains in the polymer. The crystalline polymer, on heating would melt ($T_m°$) and become a viscous liquid. In practice perfectly

FIGURE 2.4

Change of specific volume (v) of a polymer with temperature

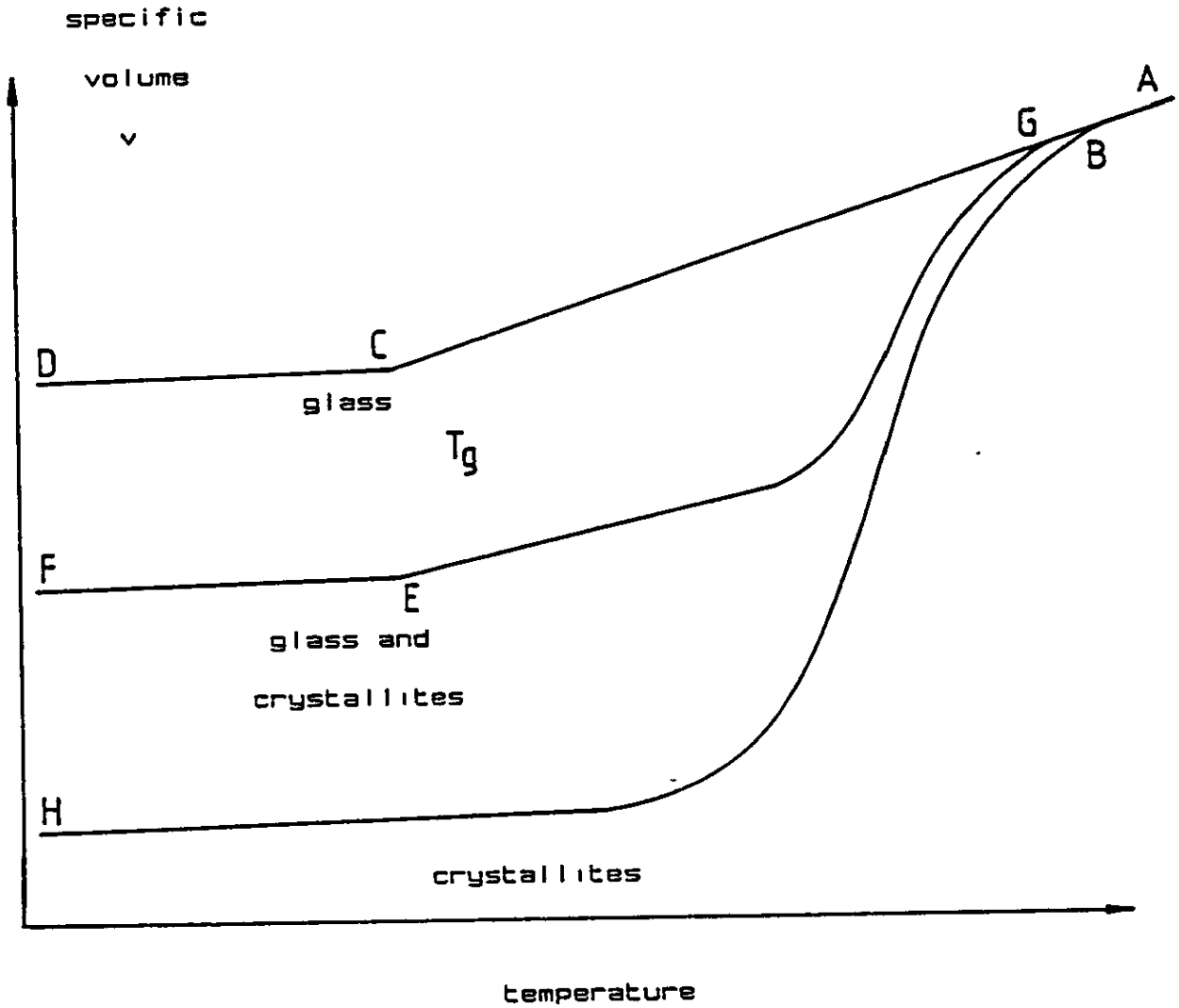

crystalline polymers are not encountered and instead polymers may contain varying proportions of amorphous and crystalline regions. These exhibit both T_g and T_m corresponding to the disordered and ordered portions and would follow a curve similar to F-E-G-B-A. The T_m for a semi-crystalline would be lower than T_m° due to crystal defects and a range of chain lengths. The rate of cooling an amorphous polymer is important. This is shown in figure 2.5, where more than one glass type may be formed from the same melt if different cooling rates are used. It is immediately apparent that T_g is in part dependent upon thermal history.

FIGURE 2.5

volume-temperature relationship for a typical amorphous polymer

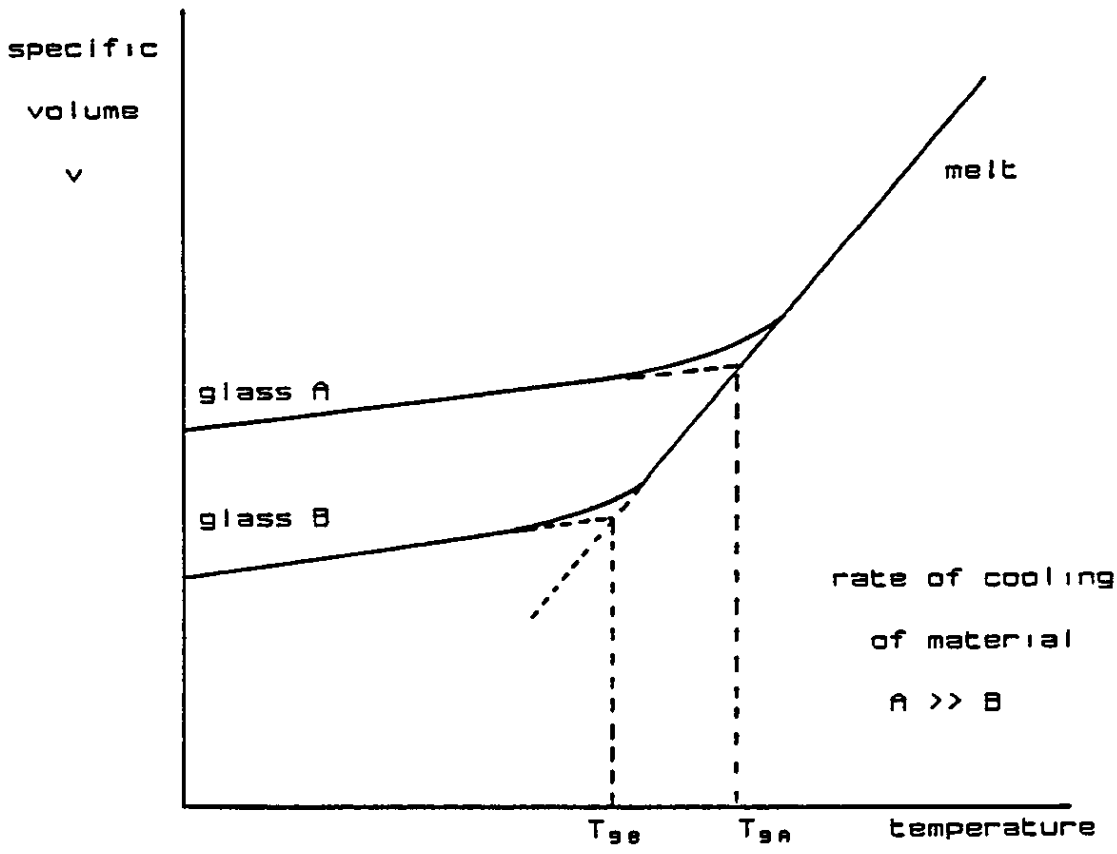

CHAPTER 2 - THEORY

The transition from a glass to a rubber-like state is accompanied by marked changes in the specific volume, the modulus, the heat capacity, the refractive index and other physical properties of the polymer. Since no discontinuity is observed when the entropy or volume of the polymer is measured as a function of temperature the glass transition is not a first-order transition, in a thermodynamic sense. If the first derivative of the property-temperature curve is measured, a change in the vicinity of T_g is found; for this reason it is sometimes called a second-order transition. Rehage and Borchard[36], however, have shown that the rate of the experiment can affect the T_g, thus, showing the T_g not to be a true second order transition and is not a divide between equilibrium thermodynamic states.

On a molecular level the T_g is widely interpreted as the temperature above which the polymer has acquired sufficient thermal energy for conformational changes to occur. These are explained as rotation of the bonds in the backbone of the molecule. Small-scale motion along the backbone does occur within the glassy state, as shown by sub-T_g transitions[37-39]. These transitions are subject to severe restrictions and occurs on a much more limited scale than above T_g.

The phenomenon of the T_g cannot be explained by a single theoretical treatment which enjoys widespread agreement. The two most popular treatments give either a kinetic or a thermodynamic explanation. Neither explanation has proved wholly successful and it seems likely that the interpretation lies somewhere in between.

2.2.2 Kinetic theories

One quantifying method is the kinetic free volume theory. Unfortunately the concept of free volume is difficult to define in a precise manner. In an approximate way it is possible to represent the segments of a polymer chain by rigid bodies and the free volume as the holes present between these segments as a result of the inefficient packing of the rigid bodies. This idea was demonstrated by Simha and Boyer[40] and is shown in figure 2.6. Below T_g the free volume reaches a constant value which is too small to allow the large-scale conformational rearrangements of the chain backbones associated with T_g to occur. Above T_g, however, the free volume increases and becomes sufficiently large to allow such motions to occur. These ideas are borne out in the following equations

$$f = f_g + \alpha_f (T - T_g) \qquad T > T_g$$

$$f = f_g \qquad T < T_g \qquad (2.16)$$

where the fractional free volume (f) reaches a constant value, f_g, at T_g and increases linearly above T_g with the coefficient of expansion α_f in the region of the T_g. If the thermal expansion coefficients immediately above and below T_g are given by

$$\alpha_r = 1/V_g(dV/dT)_r \quad \text{and} \quad \alpha_g = 1/V_g(dV/dT)_g \qquad (2.17)$$

FIGURE 2.6

Variation of specific volume with temperature

from Simha and Boyer[40]

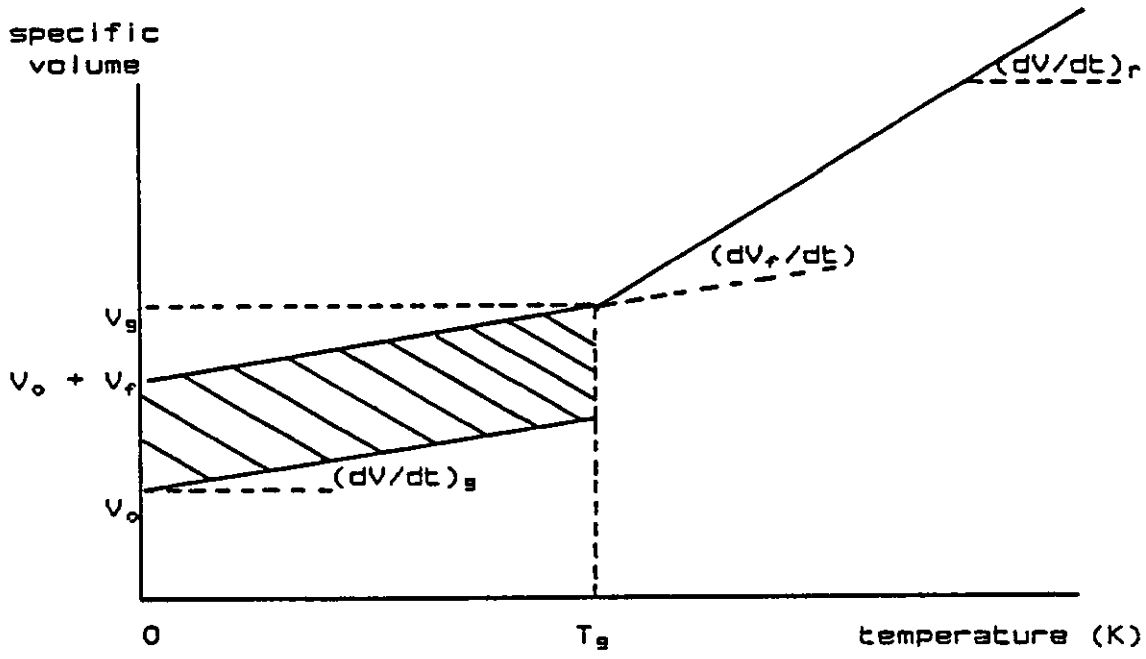

then the volume expansion of free volume in the region of T_g is given by $\alpha_r - \alpha_g = \alpha_f$.

Doolittle[41,42] used the concept of free-volume in his empirical relationship between viscosity and volume which proved successful in treating small molecular liquids. In this equation A and B are constants and η is the viscosity of the liquid.

$$\ln\eta = \ln A + B\frac{(V - V_f)}{V_f} \qquad (2.18)$$

Where V is the specific volume of the polymer and is the sum of the unoccupied and occupied volumes, V_o and V_f. When the fractional free volume f is defined as V_f/V, equation 2.18 can be rewritten as:

$$\ln \eta = \ln A + B(1/f - 1) \qquad (2.19)$$

If T_g is used as the reference point, the viscosity of a liquid at a temperature T ($T > T_g$) is given by

$$\ln (\eta / \eta_g) = B(1/f - 1/f_g) \qquad (2.20)$$

where η_g and f_g represent the viscosity and fractional free volume at T_g. Substitution of equation 2.16 into equation 2.20 yields.

$$\ln (\eta / \eta_g) = B/f_g\left[\frac{T - T_g}{f_g/\alpha_f + (T - T_g)}\right] \qquad (2.21)$$

Equation 2.21 is of the same form as the empirical relationship developed by Williams Landel and Ferry[43] (WLF) found to be suitable for describing mechanical and electrical behaviour in the region from T_g to $(T_g + 100)$. For many polymers particularly amorphous polymers, the following expression has proved valid.

$$\ln (\eta / \eta_g) = \frac{-17.44\ (T - T_g)}{51.5 + (T - T_g)} \qquad (2.22)$$

Rewriting equation 2.21 in terms of logs and assuming that the value of B is unity as found for simple liquids, one obtains.

$$\log (\eta/\eta_g) = \frac{-(T - T_g)}{2.303 f_g\ (f_g/\alpha_g + (T - T_g))} \qquad (2.23)$$

By comparing equations 2.22 and 2.23 values for f_g (0.025) and α_f (4.8×10^{-4} K^{-1}), which were thought at one time to be universal constants, may be found. It has since been shown experimentally that α_f does vary between polymers, yielding a range of values for the fractional free volume in the glassy state in the range 0.015 to 0.036 It is clear that the WLF equation predicts that T_g represents an iso-free volume state. While this concept is not strictly true it is nevertheless of wide utility.

2.2.3 Thermodynamic theories

The glassy state of a polymer has already been described on a molecular level as a liquid which is frozen into a locked immobile state. The amount of disorder present is dependent on the rate at which the glassy state is approached. It is proposed that if the melt is cooled at a infinitely slow rate then a transition can be achieved which may be interpreted in terms of theoretical thermodynamics.

By examining thermodynamic data for materials that produced a glassy state upon cooling Kauzmann[44] demonstrated that the extrapolated entropy of a supercooled liquid at absolute zero was less than the entropy shown in the crystalline state. This was held to be impossible. If the extrapolated entropy curve was drawn so that equilibrium was achieved the curve would have to curve round sharply to remain above the values for the crystal. This idea has been formalized diagrammatically by Rehage[36], as shown in figure 2.7. He described the intersection of the entropy

versus temperature plots for the equilibrium transition temperature.

FIGURE 2.7

The variation of configurational entropy with temperature for a glass forming liquid

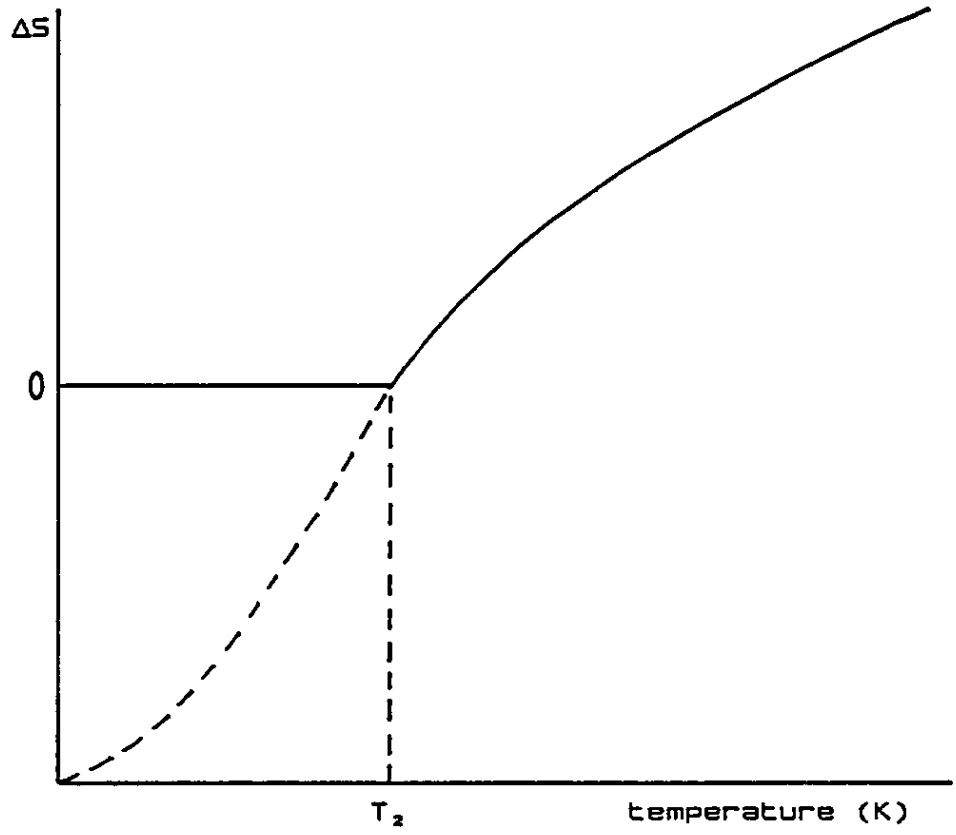

Gibbs and DiMarzio[45-48] have considered the T_g to be a true equilibrium. They did acknowledge though that kinetic effects are inevitably encountered when measuring T_g. Their theory is based on a lattice treatment similar to one used by Flory[49] and Huggins[50-52] for polymer solutions. The observed T_g of a polymer can be shown to decrease[53] if the polymer is held, after rapid cooling, at sub T_g temperatures for a sufficiently long time. Gibbs and

DiMarzio considered this by defining a new transition temperature T_2 at which the configurational entropy of the system is zero. This temperature can be considered to be the limiting value of T_g which would be obtained if infinitely long time experiments were employed. The experimentally detectable T_g is a time dependent relaxation process the observed T_g value being a function of the time scale of the measurement. The temperature T_2 is considered to be a true second order transition temperature. The main term used by Gibbs-DiMarzio in calculating the configurational entropy of a system is the energy barrier between one conformation of the main chain and another. The energy associated with this hindered rotation is very high at temperatures just above T_2 and hence a slow response would be expected to the application of any external force. Evidence for the existence of T_2 is shown by the fact that dielectric and viscoelastic relaxation times fall towards T_2. The temperature T_2 is not an experimentally measurable quantity but is calculated to lie approximately 50 K below the experimental T_g. The main weaknesses of this theory are (a) a chain of zero stiffness would have a T_g of 0 K and (b) that the T_g would be independent of any intermolecular interactions. The Adam-Gibbs[54] theory is an attempt to unite both the kinetic approach used in the WLF equation and the equilibrium treatment of Gibbs-DiMarzio. The Adams-Gibbs theory is based on a molecular kinetic theory. They relate the temperature dependence of the size of a region which is shown as a volume large enough to allow rearrangement to take place without affecting a neighbouring region. The volume of this region by definition will

decrease with temperature and will equal the volume of the smallest unit that can undergo a transition to a new configuration. This region is termed the "co-operatively rearranging region" (CRR). The temperature dependency of such a region leads to an expression for the co-operative transition probability w(T). The final expression of the Adam-Gibbs theory is of a similar form to the WLF equation.

$$-\log [W(T_o)/W(T)] = c_1(T - T_o) / [c_2 + (T - T_o)] \quad (2.24)$$

Where $c_1 = 2.3035 S_c \Delta\mu / k \Delta C_p T_o \ln(T_o/T_2)$

and $c_2 = T_o \ln(T_o/T_2)/[1 + \ln(T_o/T_2)]$

The temperature T_o is the WLF reference temperature, T_2 is as defined in the Gibbs-DiMarzio theory, S_c is the macroscopic configurational entropy for the smallest region, ΔC_p is the change in specific heat capacity between the melt and the glass at T_g and $\Delta\mu$ is the height of the potential energy barrier per monomer unit for a co-operative rearrangement.

If T_o, the reference temperature, is chosen such that it represents the glass transition the values of c_1 and c_2 closely approximate to the WLF constants. Also the difference between T_g and T_2 is 55 K. These two facts seem to point towards the molecular kinetic theory of Adams and Gibbs resolving the differences between the kinetic and thermodynamic T_g theories.

2.2.4 Factors affecting T_g values

Free volume, thermodynamic and kinetic theories can be used to explain the differences in the T_g temperature for a wide variety of polymeric systems. The main factors influencing changes in T_g may be separated into two parts intramolecular and intermolecular effects.

2.2.4.1 Intramolecular effects

The most important factor affecting the T_g is the chain stiffness or flexibility of the polymer[55]. Long chain aliphatic groups, ether linkages and siloxane groups build flexibility into the main chain of the polymer and lower T_g. If one considers a vinyl type polymer $(CH_2CHX)_n$ the size of the side group X has a profound influence on T_g. For instance increasing X from hydrogen to a methyl group increases T_g by over a hundred degree. If X is a phenyl group T_g is raised over two hundred degrees above that of the original poly(ethylene). Adding such rigid groups has the effect of decreasing chain flexibility thus raising T_g. Alternatively, the flexibility of the group, not its size, can determine T_g. Thus it is possible to lower the T_g by considering X to be an alkyl group changing from methyl to ethyl when it is possible to lower T_g by some fifteen degrees. The expected rise in T_g due to the size increase of the pendant group is outweighed by the increase in flexibility brought about by the pendant group. The Gibbs-DiMarzio[56] theory can be used to explain the substituent size in terms of the "flex energy". The flex

energy (ε) is the energy difference between the potential energy minimum of the located bond and the potential minima of the remaining possible orientations which the polymer chain may orientate itself. As the size of the side group increases so does the steric hindrance and hence the flex energy.

A second factor important in determining the value of T_g is backbone symmetry. Generally as symmetry increases the T_g decreases. This effect is illustrated by the following two pairs of polymers: poly(propylene) (T_g = -10°C) and poly(isobutylene) (T_g = -70°C), and poly(vinyl chloride) (T_g = 88°C), and poly(vinylidene chloride) (T_g = -19°C). Despite the extra side group the ..symmetrical polymers, poly(isobutylene) and poly(vinylidene chloride), have lower T_g values.

A third factor influencing the value of T_g is the chain microstructure. When two chemically different monomers are polymerized together to form a random, amorphous copolymer the T_g of the copolymer lies somewhere between the respective T_g's of the homopolymers. The Gibbs-DiMarzio[56] theory can be utilised to demonstrate the calculation of T_g of a random copolymer. The Gibbs-DiMarzio model is characterized by two parameters; the hole-formation energy, u_o and the flex energy. The parameter u_o describes the intermolecular energy contributions and ε describes the intramolecular energy contributions. According to the theory, it is found that u_o is directly proportional to T_2 and that ε/kT_2 is a constant for all polymers. Rewriting this ratio in terms of T_g it has been shown that ε/kT_g possesses a "universal" value of 2.26 for all amorphous

polymers[56]. The flex energy of a random copolymer composed of A and B monomer units is given by

$$\varepsilon = X_A\varepsilon_A + X_B\varepsilon_B \qquad (2.25)$$

where X_A and X_B are the mole fractions of monomer units A and B. Substituting the "universal" value of

$$\varepsilon = 2.26kT_g \qquad (2.26)$$

in equation 2.25 leads to

$$T_g = X_AT_{gA} + X_BT_{gB} \qquad (2.27)$$

which is of the same form as the empirical equation found by Wood[57]

$$k_AW_A(T_g - T_{gA}) + k_BW_B(T_g - T_{gB}) = 0 \qquad (2.28)$$

where W_i are the weight fractions of the comonomers A and B and k_A and k_B are constants characteristic of A and B respectively. When equation 2.28 is rearranged in terms of T_g, the Gordon and Taylor[58] equation is derived.

$$T_g = \frac{T_{gA} + (kT_{gA} - T_{gA})W_B}{1 - (1 - k)W_B} \qquad (2.29)$$

In deriving this equation they assumed that in an ideal

copolymer the partial specific volumes of the components are constant and equivalent to the specific volumes of the two homopolymers. They also assumed that the thermal expansion coefficients of the rubbery and glassy states are the same in the copolymer as in the respective homopolymers. Hence k in equation 2.29 is

$$k = k_B/k_A = \frac{(\alpha_B / \rho_B)_r - (\alpha_B / \rho_B)_g}{(\alpha_A / \rho_A)_r - (\alpha_A / \rho_A)_g} \qquad (2.30)$$

The term α_i/ρ_i is the specific thermal expansivity of component i and W_B is the weight fraction of repeat unit B in the copolymer.

In addition to copolymer composition, geometrical and steric isomerism determine the chain stiffness and thus the value of T_g. For instance the cis and trans isomers of polybutadiene exhibit T_g's of -108°C and -18°C respectively. Poly(vinyl chloride) and poly(vinylidene chloride) may both exist in three different forms, isotactic syndiotactic and atactic. It has been found that steric isomerism has no effect on the T_g of poly(vinyl chloride) but greatly affects the T_g of poly(vinylidene chloride). The isotactic form of poly(vinylidene chloride) is generally considered as having the lower T_g. This clearly, also, can be rationalized on the basis of the Gibbs-DiMarzio theory.

2.2.4.2 Intermolecular effects

Intermolecular effects can mainly, but not wholly, be explained using the free volume theory. The value of T_g

may be affected by the polarity or cohesive energy density of the polymer. This is easily explained using the following series as an example: poly(propylene) (T_g = -10°C), poly (vinyl chloride) (T_g = 88°C) and poly(acrylonitrile) (T_g = 101°C). The size of the pendant group in each polymer is roughly the same size. Then according to free volume theories the T_g's should be about the same. Infact the difference in T_g in the extremes of the series is over 100 degrees. This difference can be explained in terms of polarity. As the polymer polarity increases so does the T_g. Bueche[55] has interpreted this observation in terms of the reduced expansion of a polymer with strong intermolecular attractions. Upon heating, the required fractional free volume for T_g to occur is achieved at higher temperatures.

The effect of cross-linking on the T_g of polymers has been reviewed by Nielson[59-61]. In considering cross-linking two effects must be considered (a) cross-linking itself and (b) the complicating factor of the cross-link producing a copolymer effect[56]. The chemical composition of the polymer changes as the extent of cross-linking increases. Hence the copolymer effect can either raise or lower T_g. Thermodynamic treatments explain the effect of cross-linking on T_g in terms of the decreased configurational entropy available to the chain. In cross-linking a polymer the free volume is reduced so the required fractional free volume necessary for the glass transition to occur is attained at higher temperatures.

It has been shown, for many polymers, that the T_g varies in an inverse fashion with respect to a change in

molecular weight. This relationship is explained directly from free volume theory[61]. If the argument that the chain ends contribute more free volume than the main chain bonds is used, an increase in the molecular weight leads to a decrease in the number of chain ends per unit volume. This gives a decrease in the fractional free volume giving a corresponding rise in T_g. It has been shown[55,62-64] that equation 2.31 can describe the change in T_g with molecular weight.

$$T_g = T_{g\infty} - c/M_n \qquad (2.31)$$

where M_n is the number average molecular weight, $T_{g\infty}$ is the asymptotic value of T_g at infinite molecular weight. The constant c has a characteristic value for the polymer.

The free volume theory finds ready application in predicting the effect on T_g of diluents or plasticizers. From equation 2.16 the free volume of a polymer system reduces to a near constant value below the T_g of the polymer and increases linearly above T_g according to the product of the thermal expansion coefficient and the temperature difference above T_g. With the presence of diluent the free volume is increased according to equation 2.32.

$$f = f_{gP} + \alpha_p(T - T_g)V_p + \alpha_d(T - T_g)V_d \qquad (2.32)$$

where subscripts p and d refer to polymer and diluent respectively, and V is the volume fraction. At the T_g of the mixture the free volume

$$f = f_{gp} \tag{2.33}$$

and replacing V_d with $1 - V_p$ equation 2.33 becomes

$$T_g = \frac{\alpha_p V_p T_{gp} + \alpha_d (1 - V_p) T_{gd}}{\alpha_p V_p + \alpha_d (1 - V_p)} \tag{2.34}$$

This is essentially another form of the Gordon and Taylor equation derived in equation 2.29.

It is seen that plasticizers or diluents lower T_g by introducing free volume into the system, the final T_g being between that of the plasticizer or diluent and that of the polymer.

A theoretical treatment of the plasticizer effect has been developed by Bueche[55]. He rewrote the Gordon and Talyor equation calculating k using volume coefficients of expansion for the respective polymer and plasticizer components, as follows

$$k = \text{constant} = \frac{\alpha_{ld} - \alpha_{gs}}{\alpha_{lp} - \alpha_{gp}} \tag{2.35}$$

The constant k was found to have values between 1 and 3. The subscripts l and g denote liquid and glass respectively. They refer to the volume coefficient of expansion above and below T_g respectively. Using Bueche's form of the Gordon Taylor equation

$$T_g = \frac{T_{gp} + (kT_{gs} - T_{gp}) V_s}{1 + (k - 1) V_s} \tag{2.36}$$

and rearranging

$$\frac{T_{gp} - T_g}{T_{gp} - T_{gs}} = \frac{1 - V_p}{1 - V_p(1 - 1/k)} \qquad (2.37)$$

where V_p is the volume fraction of polymer. Van Krevelen[65] has surveyed the available data and shown that an average for k would be 2.5. Hence the T_g of any mixture may be calculated so long as the T_g of the plasticizer or diluent together with the composition is known.

2.3 POLYMER-SOLVENT INTERACTIONS

2.3.1 The solubility parameter

The degree of swelling will depend on the interactions between the polymer-polymer intermolecular forces, due to cross-linking, crystallinity or strong hydrogen bonding, and the strength of polymer-swelling agent interactions. Maximum swelling in lightly cross-linked polymers will occur when the free energy of mixing

$$\Delta G = \Delta H - T\Delta S \qquad (2.38)$$

is negative.

ΔS, the entropy of mixing, is generally considered to be positive, therefore, maximum swelling occurs with a limiting positive value of ΔH, the enthalpy of mixing. Hildebrand[66] in correlating cohesive energy to solubility, cohesive energy being defined as the increase in internal energy per mole of substance eliminating all intermolecular forces, proposed the term solubility parameter, δ and defined it as being the square root of the cohesive energy divided by molar volume i.e the cohesive energy density (CED). The cohesive energy of a species is defined as the increase in internal energy per mole if all the intermolecular forces are discounted. According to Hildebrand[66], the enthalpy of mixing can be calculated by

$$\Delta H = v_1 v_2 (\delta_1 - \delta_2)^2 \qquad (2.39)$$

where v is the volume fraction and the subscripts 1 and 2 refer to swelling agent and polymer respectively. Equation 2.39 predicts, $\Delta H = 0$, and hence maximum swelling when $\delta_1 = \delta_2$.

2.3.2 The thermodynamic interaction parameter

The most obvious feature of a polymer-solvent system (as compared with a mixture of small molecules) is the disparity in size between the two components. The first attempts to theoretically treat the compatibility of a polymer with a liquid were made by Flory and Huggins[67,68]. Both chose a simple lattice representation for the polymer solution and calculated the entropy change on a statistical basis by estimating the total number of ways the polymer and solvent molecules could be arranged on the lattice. The final expression being

$$\Delta G = RT[\ln(1 - v_2) + v_2 + \chi v_2^2] \qquad (2.40)$$

Here the dimensionless parameter χ is known as the Flory-Huggins interaction parameter and

$$\chi = z\Delta e/RT \qquad (2.41)$$

where z is a lattice coordination number and Δe is the energy of formation of a liquid-polymer contact.

Attempts to correlate δ with χ from the Flory-Huggins equation have met with limited success because of the following assumptions used in its derivation.

Firstly, a uniform lattice density was assumed, secondly that the segment locating process was purely statistical, only true if Δe was zero, and finally the flexibility of a chain is unaltered on passing into solution from the solid state. It is thought[69-71] that χ is actually a free energy parameter composed of entropic ,χ_s, and enthalpic ,χ_h, contributions given by

$$\chi = \chi_h + \chi_s \qquad (2.42)$$

Limited correlation between δ and χ is given by

$$\chi = 1/z + V_1/RT(\delta_1 - \delta_2)^2 \qquad (2.43)$$

where $1/z = \chi_s$ and is thought to compensate for the lack of a non-combinatorial entropy contribution in the Flory-Huggins treatment. It has been found that χ_s approximates to 0.34.[72]

2.3.2.1 The interaction parameter value

χ has been evaluated for a number of liquid-PVC systems[73]. In section 2.3.1 it was stated that maximum swelling in a lightly cross-linked polymer will occur when the respective CED's of liquid and polymer are approximately equal in this region, equation 2.43 simplifies giving an approximate value of χ as being 3.4. The work of Doty and Zable[73] produced values of χ from negative values through zero to positive values for fifty different liquid-PVC systems at two elevated temperatures. In their study they

employed solvents, plasticizers and non-solvents and correlated their solvent ability to the value of χ. It has been shown theoretically[74,75] and experimentally[73] that a χ value of 0.55 is the dividing line between poor solvents and non-solvents, values greater correspond to non-solvents, the degree of interaction varying continuously with increasing χ. Doty and Zable[73] showed that the swelling of PVC (cross-linked or linear) will vary with different non-solvents, the swelling being less the larger the χ value, except for the effect of molar volume. Also shown was the independency of χ towards temperature for values around 0.2 to 0.4 as predicted[76].

2.4 ELASTICITY

2.4.1 Static moduli of rubbers from the rubber elasticity theory

By examining a rubber network undergoing small deformations Kuhn[77] and later Treloar[78,79] produced a theory to explain the elasticity of a molecular network. They restricted their theory to the following assumptions.

1. The chains forming the rubber network give a chain density of N chains per unit volume, a chain being defined as the segment of the macromolecule between successive points of cross-linkage.
2. There is a Gaussian distribution of distances between the chain ends.
3. There is no change in volume on deformation.
4. A change in the dimensions of the sample causes a corresponding change in the distance between ends of each chain in the network.
5. The sum of the entropies of the individual chains is the entropy of the network.

The reference made to the chain refers to that portion of the macromolecule between junction points or entanglements. Assumption (2) is based on the material being amorphous prior to any cross-linking taking place, and the Gaussian distribution of distances between chain ends remaining unaltered upon cross-linking. Assumption (3) is based on observation and (4), the affine deformation assumption is the main corner post for the whole theory. It relates the

deformation of an individual chain to the macroscopic strain of the material. It s validity was proven by James and Guth[80].

The development of this theory proceeds through the following stages. Consider a single chain in the network having an end-to-end distance, given by r_o and having components in space of x_o, y_o and z_o in the unstrained state. In the strained state after deformation the end-to-end distance is given by the vector r with spatial coordinates of x_1, y_1, z_1, see figure 2.8. Affine deformation is

FIGURE 2.8

Affine deformation of a chain

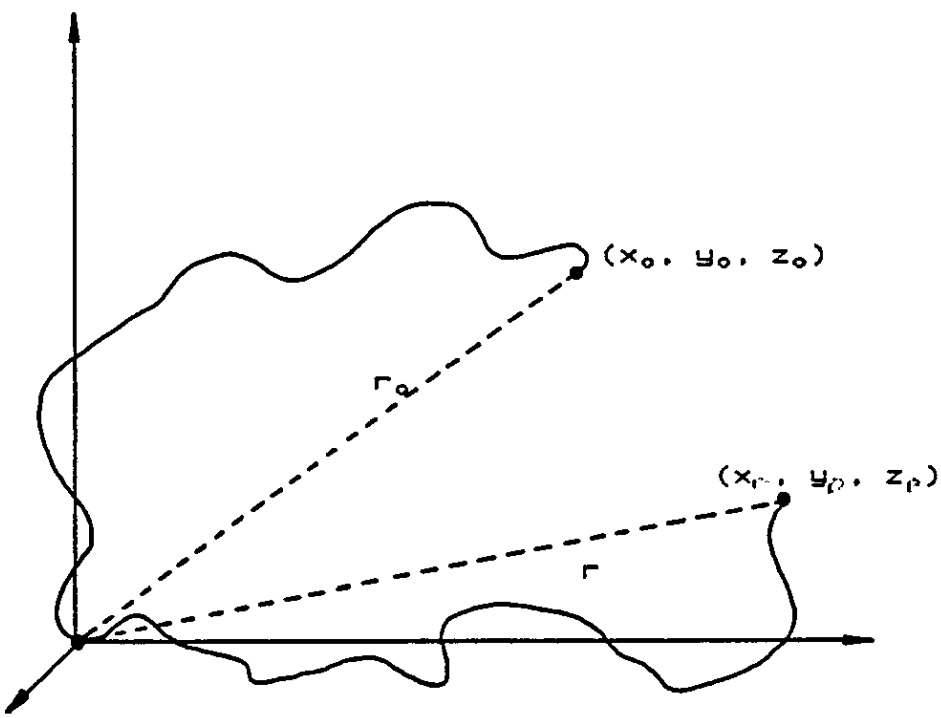

$$x = \lambda_1 x_o, \qquad y = \lambda_2 y_o, \qquad z = \lambda_3 z_o \tag{2.44}$$

where λ_1, λ_2 and λ_3 are the principal axes of strain and coincide with the axes of coordinates. The entropy of a single chain in the unstrained state is given by

$$S_o = C - kb^2 r_o^2 = C - kb^2(x_o^2 + y_o^2 + z_o^2) \qquad (2.45)$$

where b^2 is a constant and gives the probability that the components of the vector r lie within a value between r_o and r. The same chain in the strained state will have an entropy given by

$$s = C - kb^2(\lambda_1^2 x_o^2 + \lambda_2^2 y_o^2 + \lambda_3^2 z_o^2) \qquad (2.46)$$

where C is a numerical constant and k is Boltzmann's constant. The contribution this chain makes towards the total entropy of deformation is therefore

$$\Delta s = s - s_o$$

$$= kb^2[(\lambda_1^2 - 1)x_o^2 + (\lambda_2^2 - 1)y_o^2 + (\lambda_3^2 - 1)z_o^2] \qquad (2.47)$$

The total entropy for N chains contained in the unit volume will be the summation of equation 2.47. Hence

$$\Delta S = \Sigma s \qquad (2.48)$$

$$\Delta S = - kb^2\{[\lambda_1^2 - 1]\Sigma x_o^2 + [\lambda_2^2 - 1]\Sigma y_o^2 + [\lambda_3^2 - 1]\Sigma z_o^2\} \qquad (2.49)$$

In a unit volume of N chains the expression Σx_o^2 is the sum of the squares of the x_o components, in the unstrained network. The chain vectors r_o in the unstrained state are

entirely random, hence

$$\Sigma x_o^2 + \Sigma y_o^2 + \Sigma z_o^2 = \Sigma r_o^2 \qquad (2.50)$$

and

$$\Sigma x_o^2 = \Sigma y_o^2 = \Sigma z_o^2 = 1/3\Sigma r_o^2 \qquad (2.51)$$

but, the unit volume contains N chains, then

$$\Sigma r_o^2 = N\bar{r}_o^2 \qquad (2.52)$$

where $\bar{r}_o^2$ is the mean-square length of the chains in the unstrained state. Substituting 2.52 into 2.49 the total entropy of deformation becomes

$$\Delta S = Nkb^2\bar{r}_o^2(\lambda_1^2 + \lambda_2^2 + \lambda_3^2 - 3) \qquad (2.53)$$

The mean-square chain vector length for a free chain is given by[81]

$$\bar{r}_o^2 = 3/2b^2 \qquad (2.54)$$

Substituting equation 2.56 into 2.53, hence removing the parameter b, then the dependence of the entropy on the extension ratios is given by

$$\Delta S = 1/2Nk(\lambda_1^2 + \lambda_2^2 + \lambda_3^2 - 3) \qquad (2.55)$$

From basic principles the Helmholtz free energy of work of deformation is found using $W = -T\Delta S$, and

$$W = 1/2NkT(\lambda_1^2 + \lambda_2^2 + \lambda_3^2 - 3) \qquad (2.56)$$

The force (f) required to produce a change in extension ratio is given by

$$f = dW/d\lambda \qquad (2.57)$$

Differentiation of equation 2.56 provides a relationship between f and λ

$$f = G(\lambda - \lambda^{-2}) \qquad (2.58)$$

$$G = NkT = \rho RT/M_c \qquad (2.59)$$

where R is the gas constant, ρ, the polymer density. The modulus factor is G = NkT and shows that G depends on the number of cross-links in the sample. The physical properties of rubbers are thus shown to be independent of the chemical nature of the molecule and are dependent on the extent of cross-linking. The quantity N is related to the molecular weight (M_c) between cross-links. The product ρ/M_c is then a measure of the cross-link density of the sample. The statistically derived equation 2.58 was first tested by Treloar[82].

The major fundamental objection to the above theory is that the junction points of the network are thought to be fixed points in space. The freedom of movement of the system is thus limited to the lengths of chain between these fixed points. By considering micro-Brownian motion of these fixed points James and Guth[80] were able to predict a model

which more closely resemebles that of the physical structure of a rubber than the Kuhn[77] model. In the James-Guth treatment the only junction points which are fixed are those located on the boundary surfaces of the rubber. The modulus G from this treatment is given by

$$G = kT\Sigma n_T \lambda_T^2 \qquad (2.60)$$

where n_T is the number of links in the t th chain and λ_T is its mean fractional extension in the unstrained state of the network. Equation 2.60, assuming that the distribution of the mean end-to-end lengths of the network and the free chain is the same, reduces to equation 2.59. The Gaussian treatment described above assumes that the mean end-to-end lengths of the network and the free chain is unity. This has since been found to be incorrect[83]. Infact, a slight temperature dependency has been found[84]. For systems which are only slightly cross-linked[83], however, the mean end-to-end lengths of the network and the free chain can be approximated to unity.

The theory assumes that there are no defects in the network. i.e. no interlooping entanglements or ineffective links. Flory[85] refined the theory to account for these defects. The simplest defect to evaluate is the ineffective link i.e. the chain which is linked at one end only. Flory stated that starting with N primary uncross-linked molecules, (N - 1) intermolecular linkages will be sufficient to produce a simple branched structure without closed loops. Any more cross-links would produce closed loops or network circuits. For each of these cross-linkages

there would be one loop or two network chains; it follows that

$$1/2V = 1/2V_o - N \qquad (2.61)$$

where $1/2V$ is the actual number of cross-links and $1/2V_o$ is the number of effective cross-links and N is written for (N - 1). The effective number of chains would be twice this quantity.

$$V = V_o(1 - 2N/V_o) = V_o(1 - 2M_c/M) \qquad (2.62)$$

M is the molecular weight of the molecules prior to cross-linking and M_c is the mean molecular weight between cross-links. The effect of other network defects is represented by Flory by introducing an empirical entanglement factor g. The expression for G now becomes.

$$G = gpRT/M_c(1 - 2M_c/M) \qquad (2.63)$$

Flory[86] gave this empirical quantity, a value of 3.3. The factor g will only affect the active chains in the network, and not the inactive chains given by the factor $(-2M_c/M)$. Furthermore, the value of g is directly affected by the value of M_c. As the cross-link density increases, and M_c correspondingly decreases, the opportunity of chain entanglements decreases, hence the factor g decreases. The value of 3.3 given by Flory is for a rubber gum vulcanized to give a rubber network with a M_c = 35000.

2.4.2 Static moduli of swollen polymers

It is possible to derive an equation in similar form to the stored-energy function, equation 2.56, for the swollen polymer. To simplify the argument proposed by Treloar[81] the nature of the swelling liquid will not be dealt with, nor the question of equilibrium between the swelling liquid and swollen polymer. Also, the free-energy changes associated with the process of the mixing of liquid and polymer molecules will not be dealt with, only the change in the configurational entropy of the polymer network.

Consider a unit cube of unswollen polymer containing N chains per unit volume. The degree of swelling is defined by the volume fraction v_2 of polymer in the mixture of polymer and liquid. The volume swelling ratio is given by $1/v_2$ and the length of one edge of the cube, in the unstressed state by $\lambda_o = 1/v_2^{1/3}$. Then a unit cube swollen to the ratio $1/v_2$ and deformed to dimensions l_1, l_2, l_3 gives the total change in network entropy, $\Delta S_o'$ in passing from the unstrained unswollen state to the strained swollen state as being,

$$\Delta S_o' = -1/2Nk(l_1^2 + l_2^2 + l_3^2 - 3) \qquad (2.64)$$

The change in entropy, $'S_o$ due to the isotropic swelling in the ratio $\lambda_o = 1/v_2^{1/3}$ without any applied stress is

$$\Delta S_o = -1/2Nk(3\lambda_o^2 - 3) = -1/2Nk(3v_2^{-2/3} - 3) \qquad (2.65)$$

The difference between equations 2.64 and 2.65 yields $\Delta S'$ the entropy of deformation of the swollen network

$$\Delta S' = \Delta S_o' - \Delta S_o$$
$$= -1/2Nk(I_1^2 + I_2^2 + I_3^2 - 3v_2^{-2/3}) \qquad (2.66)$$

Rewriting in terms of extension ratios, λ, where $I_1 = \lambda_1/v_2^{1/3}$ etc.,

$$\Delta S' = 1/2Nkv_2^{-2/3}(\lambda_1^2 + \lambda_2^2 + \lambda_3^2 - 3) \qquad (2.67)$$

To derive the stored energy function per unit volume, equation 2.67 needs to be expressed in terms of entropy of deformation per unit volume, ΔS, measured in the swollen state.

$$\Delta S = v_2\Delta S' = 1/2Nkv_2^{1/3}(\lambda_1^2 + \lambda_2^2 + \lambda_3^2 - 3) \qquad (2.68)$$

and the stored energy function becomes

$$W = -T\Delta S = 1/2Nkv_2^{1/3}(\lambda_1^2 + \lambda_2^2 + \lambda_3^2 - 3) \qquad (2.69)$$

Comparing equations 2.57 and 2.69 it is seen that the stored-energy function differ only by the factor $v_2^{1/3}$. Thus, if G and G_r are the respective moduli in the unswollen and swollen states then

$$G_r = Gv_2^{1/3} = (\rho RT/M_c)(1 - 2M_c/M)v_2^{1/3} \qquad (2.70)$$

where ρ is the density in the unswollen state. This result

shows that the effect of swelling a rubber is to reduce the modulus in proportion to the factor, $v_2^{1/3}$. An alternative method in calculating the entropy of deformation has been made by Flory[87] and Wall and Flory[88]. They based their treatment on the consideration of forming a rubber network using a set of independent chains. The entropy change differs from equation 2.64 with the inclusion of $-\ln(l_1 l_2 l_3)$.

$$\Delta S_o' = -1/2Nk(l_1^2 + l_2^2 + l_3^2 - 3 - \ln(l_1 l_2 l_3)) \qquad (2.71)$$

This extra term disappears with an unswollen rubber and the equation reduces to that of equation 2.64. The method of derivation of this formula remains inconclusive and it is thought [80] that the extra term $-\ln(l_1 l_2 l_3)$ in most cases is rather small.

2.4.3 Swollen cross-linked networks

A three-dimensional network polymer such as vulcanized rubber and to some extent PVC, assuming crystallites are left intact, although incapable of disolving completely may imbibe large quantities of liquids. There is the opportunity for the entropy to increase due to the added volume. The tendency to mix, expressed as the entropy of dilution may be increased or decreased by the solvent. The chains between the network cross-links, or insoluble crystallites, are stretched and assume elongated configurations. A force somewhat akin to the retractive force in rubber is produced which is preventing further

swelling. Eventually this retractive force reaches equilibrium with the swelling forces. There is a close analogy between swelling equilibrium and osmotic equilibrium.

For a material which is cross-linked the Flory-Huggins equation, for free energy of dilution, is insufficient[86]. It is necessary to take account ot the configurational entropy of the network[87]. Then the total free energy of dilution ΔG_1 is

$$\Delta G_1 = \Delta G_{1m} + \Delta G_{1\ell} \qquad (2.72)$$

where ΔG_{1m} is the free energy of dilution for the pre-cross-linked polymer and $\Delta G_{1\ell}$ is the free energy due to the expansion of the network on imbibing one mole of liquid. $\Delta G_{1\ell}$ is obtained from equation 2.56. In a simple swelling situation a unit cube of material will swell in all dimensions by the same ratio, λ. Equation 2.56 may be rewritten as

$$W = \rho RT/2M_c(3\lambda^2 - 3) = 3\rho RT/2M_c(\lambda^2 - 1) \qquad (2.73)$$

The volume of the swollen cube is

$$\lambda^3 = 1/v_2 = 1 + n_1V_1 \qquad (2.74)$$

and equation 2.73 becomes

$$W = 3\rho RT/2M_c(v_2^{-2/3} - 1) \qquad (2.75)$$

where n_1 is the number of moles of liquid and V_1 is the molar volume of the liquid. The free energy of dilution may be calculated

$$\Delta G_{1\ell} = \rho RT/M_c V_1 v_2^{1/3} \qquad (2.76)$$

Expressing ΔG_{1m} using the Flory-Huggins equation as[81]

$$\Delta G_{1m} = RT[\ln(1 - v_2) + v_2 + \chi v_2^2]$$

substituting equations 2.76 and 2.77 into 2.72 the total free energy of dilution becomes

$$\Delta G_1 = RT[\ln(1 - v_2) + v_2 + \chi v_2^2 + (\rho V_1/M_c)v_2^{1/3}] \qquad (2.78)$$

and the equation for equilibrium swelling is

$$\ln(1 - v_2) + v_2 + \chi v_2^2 = -V_1\rho/M_c v_2^{1/3} \qquad (2.79)$$

Using the alternative Flory equation, equation 2.71 for the entropy of a swollen rubber network equation 2.73 is replaced with

$$W = \rho RT/2M_c(3v_2^{-2/3} - \ln v_2^{-1} - 3) \qquad (2.80)$$

and the final equation for equilibrium swelling would become

$$\ln(1 - v_2) + v_2 + \chi v_2^2 = -V_1\rho/M_c(v_2^{1/3} - v_2/2) \qquad (2.81)$$

by expanding the logarithm on the left hand and ignoring powers of v_2 greater than two Flory[65,89] and Gee[90] were able to deduce the following approximation.

$$(V_1\rho/M_c) = (1/2 - \chi)V_2^{5/3} \qquad (2.82)$$

The term $\rho V_1/M_c$ is proportional to the shear modulus developed by Gaussian network theory in section 2.4.1. The modulus thus gives a relationship with the equilibrium degree of swelling for a particular liquid for differing degrees of cross-linking.

2.5 SIMPLE RELAXATION BEHAVIOUR

2.5.1 Mechanical models describing viscoelasticity

The classical theory of elasticity governs the mechanical properties of perfectly elastic solids. If Hooke's law is obeyed the stress is always directly proportional to strain for small deformations but is independent of the rate of strain.

The classical theory of hydrodynamics deals with the properties of viscous liquids. In obeying Newtons law, the stress applied to a viscous liquid is always directly proportional to the rate of strain but independent of the strain itself.

$$\sigma = \eta \frac{d\gamma}{dt} \qquad (2.83)$$

where σ and γ are stress and strain respectively. η is the Newtonian viscosity and t the time.

It is true to say that the behaviour of many solids and liquids approach ideal behaviour when undergoing infinitesimal strains and rates of strain respectively. Under other conditions deviations from the classical behaviour is observed. It is found that elastic behaviour is not instantaneous but dependent on time and the stress-strain history of the body.

Both of these laws adequately describe the behaviour of most liquids and solids. However, in some cases a

material may exhibit the characteristics of both a liquid and a solid which neither of these laws are able to describe. The system is then said to be in a viscoelastic state.

One of the first attempts to explain the mechanical behaviour of viscoelastic materials was made by Maxwell[91]. He modelled the exponential decay of stress at constant strain. He discussed the behaviour in terms of a mechanical model comprising an ideal elastic element, represented by a Hookian spring, in series with an ideal viscous element, the dashpot.

More complicated models were proposed by Voigt[92] and Kelvin[93] who independently examined the change of strain at constant stress, i.e. creep, using similar methods to Maxwell. Their models consisted of a spring and dashpot in parallel (see figure 2.9).

The use of Maxwell and Voigt-Kelvin models forms the basis for the phenomenological treatment of viscoelasticity. The use of such models relies on the Boltzmann superposition principle[94]. This principle states that the total effect of applying stresses is the sum of the effects of applying each one separately. The removal of such stresses also follows a linear function.

The motion of such springs and dashpots, representing Hookian solids and Newtonian liquids, can be mathematically defined. These elements, or their combinations, may be used to describe the linear mechanical response of polymeric materials[33]. The simplest combinations of springs and dashpots represents single relaxation time models. Two models have already been

FIGURE 2.9

Maxwell (A) and Voight-Kelvin (B) models

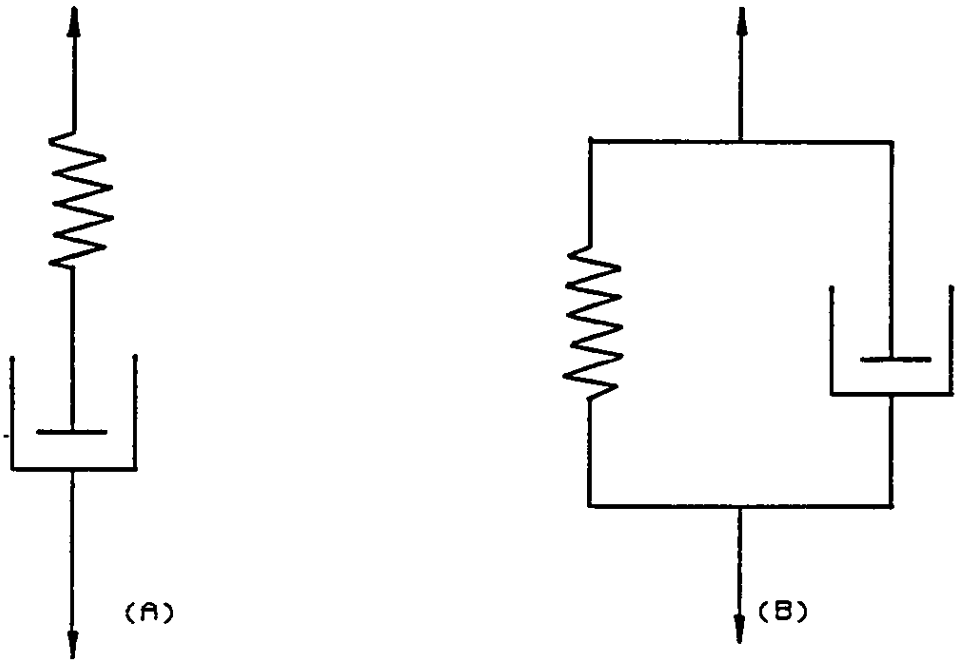

FIGURE 2.10

Standard linear model[95]

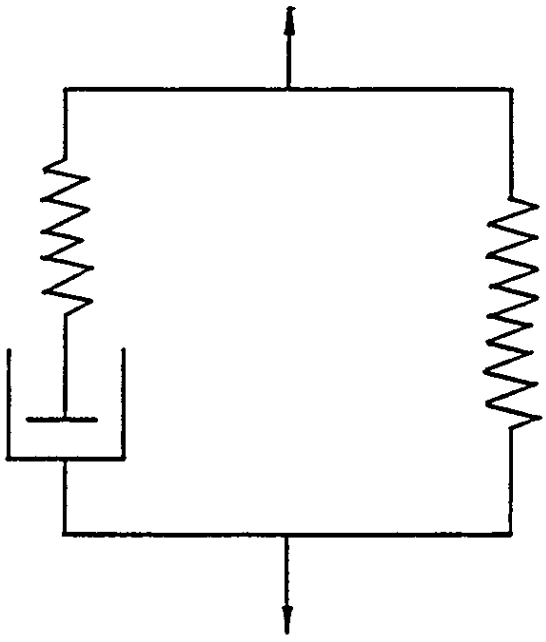

mentioned in figure 2.9. A third is shown in figure 2.10. Their behaviour is now discussed.

2.5.1.1 The Maxwell model

The Maxwell model consists of a spring having a modulus E_m and a dashpot of viscosity η_m in series. The movement of the strained element can be described by the following equation

$$\frac{d\gamma}{dt} = \frac{1}{E}\frac{d\sigma}{dt} + \frac{\sigma}{\eta} = 0 \qquad (2.84)$$

Since $\gamma = \sigma/E$, equation 2.1, and $\sigma/\eta = d\gamma/dt$, equation 2.83, the solution of equation 2.84 is

$$\sigma/\sigma_o = e^{-(Et/\eta)} = e^{-t/\tau} \qquad (2.85)$$

where $\tau = \eta/E$ and is the relaxation time and σ_o = stress at zero time.

2.5.1.2 Voigt-Kelvin model

In considering the Voigt-Kelvin model the spring of modulus E_v and dashpot of viscosity η_v are connected in parallel. Any applied stress is now equally shared between the elements of the model. The corresponding equation for the strain is.

$$\gamma = E_v\sigma + d\sigma/dt\eta \qquad (2.86)$$

If a stress is applied and after a period of time removed the deformation- time curve is given by

$$\sigma = \gamma/E_v(1 - e^{-(E/\eta)t}) = \gamma/E_v (1 - e^{-t/\tau}) \qquad (2.87)$$

where τ is a retardation time. The dashpot acts as a damping resistance to the establishment of the equilibrium of the spring.

The simple models of Maxwell and Voigt-Kelvin with their single relaxation and retardation times are insufficient to describe viscoelastic behaviour of polymer materials as a whole. In certain cases they can prove helpful, however, in the elucidation in viscoelastic processes.

2.5.1.3 The standard linear body

The third model depicted in figure 2.10 represents a simplified model for an ideal cross-linked polymer. The model possesses single relaxation and retardation times and a relaxed and unrelaxed modulus. If a sinusoidal stress is applied and its behaviour is followed as a function of frequency, the response is shown in figure 2.11. The dynamic moduli are shown in the following equations[33,95].

FIGURE 2.11

Real E' and imaginary E" components of the complex modulus for the standard linear model

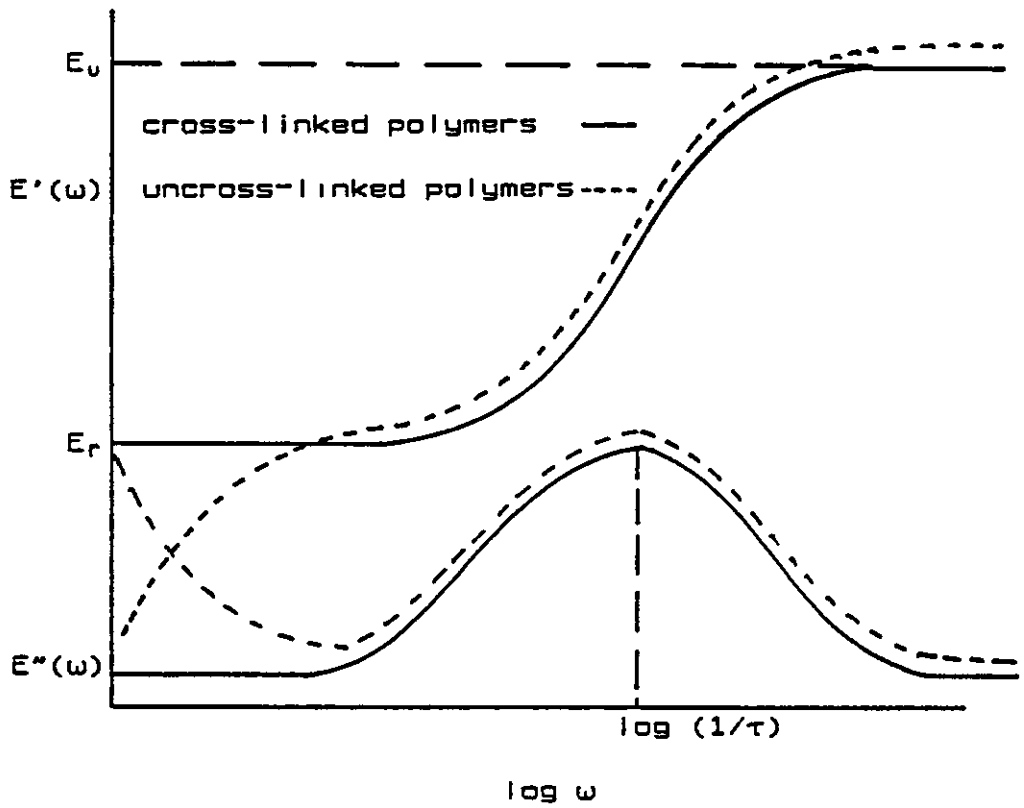

$$E'(\omega) = E_r + \frac{(E_u - E_r)\omega^2\tau^2}{1 + \omega^2\tau^2} \qquad (2.88)$$

$$E''(\omega) = \frac{(E_u - E_r)\omega\tau}{1 + \omega^2\tau^2} \qquad (2.89)$$

and

$$\tan\delta = \frac{(E_u - E_r)\omega\tau}{(E_uE_r)^{1/2}(1 + \omega^2\tau^2)} \qquad (2.90)$$

The compliances of the system may also be defined using

these equations substituting τ with τ_r. However, again this model is a simplification. This model displays a sharp transition. Real polymeric materials exhibit many different transitions. Each transition being brought about by its own single relaxation (or retardation) time.

This range of relaxations $H(\tau)$ and retardations $L(\tau_r)$ times were introduced to describe real polymer behaviour first by Weichart[96]. A continuous spectra of relaxation (or retardation) is found in practice and is defined as $H(d\ln\tau)$, the contribution to the modulus being given by the relaxation times in the range $\ln\tau$ and $\ln\tau + d\ln\tau$. The expressions for the dynamic moduli analogous to equations 2.88 and 2.89 in terms of relaxation spectra , H are

$$E'(\omega) = E_r + \int_{-\infty}^{+\infty} \frac{H(\tau)\omega^2\tau^2 d\ln\tau}{1 + \omega^2\tau^2} \qquad (2.91)$$

$$E''(\omega) = \int_{-\infty}^{+\infty} \frac{H(\tau)\omega\tau d\ln\tau}{1 + \omega^2\tau^2} \qquad (2.92)$$

The acquisition of $H(\tau)$ and $L(\tau_r)$ allows viscoelastic behaviour to be modelled[33,97]

2.5.2 Molecular interpretations of viscoelastic behaviour behaviour

The use of Maxwell and Voigt-Kelvin models enables the elucidation of macroscopic behaviour and does not necessarily provide an explanation into the molecular basis of viscoelastic behaviour. In an attempt to explain viscoelastic behaviour on a molecular level Rouse[98] and Bueche[99] have used arguments based on a chain model consisting of a series of sub-units. Each sub-unit is connected via a spring. Sufficient sub-units are considered to provide a Gaussian distributions of segment lengths.

The application of stress on a single isolated unstressed chain will cause distortion, by altering the equilibrium conformation to a less probable one, resulting in a decrease in entropy and a corresponding increase in the free energy of the system. If the stress is maintained, strain relief is found by converting the excess free energy into heat and providing thermal motion of the segments back into their original positions. This is known as stress relaxation. The chain molecule is composed of a large number of segments. The movement of the chain molecule depends on the cooperative movement of all the segments. The stress relaxation depends on the number of ways the molecule can return to its most probable conformation. Each movement will have a characteristic relaxation time. If the chain is long enough, say 50 carbon atoms long, it will possess a wide distribution of relaxation times. Applying this idea to a viscoelastic material[33], instead of dilute solutions of monodisperse coils, it is possible to calculate

continuous relaxation and retardation spectra.

Rouse's theory together with a similar theory developed by Bueche[99] both accurately describe the sample moduli below the values of 10^8 Nm^{-2}. The theory explains the viscoelastic function through the regions of rubber to the melt.

A theory introduced by Ferry et al.[100] allowed the Rouse-Bueche theories to account for the second order transition by postulating a second friction factor. Williams[101] pointed out that these theories were only applicable to the rubber-like motion found at low frequencies and hence the unrelaxed modulus calculated is some two orders of magnitude lower than experimentally determined values.

2.5.3 Moduli of partially crystalline polymers

2.5.3.1 Molecular models

Jackson et al.[102] extended the statistical theory of rubber elasticity developed in the previous section to calculate the modulus of partially crystalline polymers. They suggested that since the crystallites would be rigid compared with the amorphous regions most of the strain accompanying deformation of a bulk sample would occur in the amorphous regions. Secondly, the chains would be incorporated into the crystalline regions causing them to behave as cross-links similar to those found in vulcanized rubber and thus the rubber elasticity theory could be applied to partially crystalline polymer networks. The

major drawback of Jackson's extension was that the number of effective network chains in the partially crystalline polymer could not be calculated. To overcome this they produced copolymers with non-crystallizable comonomer units randomly along the chains in order to subdivide the molecule into crystallizable units. The number of elastic elements in the amorphous phase can be equated to the number of crystalline sequences providing the necessary information on the sequence distribution between "crystallite cross-links". A crystallite cross-link has a much larger volume than a chemical cross-link. It is not unreasonable therefore to postulate that the crystallites will give a filler action on the Gaussian network.[103]

Both of the above theories calculated the moduli to be lower than the experimentally determined values. The above theories assumed the amorphous regions were in an unperturbed conformation when the crystalline regions were introduced. Indeed this would be correct for infinitely small crystallites. The introduction of the filler effect[104] improved correlation with experimental data. If it is assumed the amorphous chains are near to their fully extended lengths, the distribution of conformations cannot be described by Gaussian statistics. Using such considerations it is possible to calculate the moduli of partially crystalline polymers which give better agreement with experimental data.

2.5.3.2 The mechanical model of Takayanagi

By considering a phenomenological model

Takayanagi[105-107] developed a theory to account for the value of the Young's modulus shown by partially crystalline polymers. The model, see figure 2.12, represents the structure of the partially crystalline polymer, being divided into completely rubbery and crystalline regions. The shaded area represents the rubbery region. A completely rubbery region would exhibit a modulus of 10^8 Nm^{-2}. A fully rubbery polymer is a limiting case in the Takayanagi model and the unit square would be fully shaded. The converse would be true for a fully crystalline polymer exhibiting a modulus around 10^{11} Nm^{-2}. The viscoelastic behaviour of the model is defined by the mechanical coupling of the overall complex modulus E^*, the complex moduli of the crystalline and rubbery phases E_c^* and E_R^* respectively and the volume fraction V_R of the rubbery region. The rubbery and crystalline coupling is in turn defined by the parallel λ - parameter and the series ϕ - parameter, so that $\phi\lambda = V_R$. Figure 2.12(b) represents how the model A may be represented by an equivalent model B. According to figure 2.12(b) the overall modulus is expressed as[107]

$$E^* = \left[\frac{\phi}{[\lambda E_R^* + (1 - \lambda)E_c^*]} + \frac{1 - \phi}{E_c^*} \right]^{-1} \qquad (2.93)$$

If the value of ϕ, the degree of series connection, tends to unity, the model C in figure 2.12 is produced. Since ϕ is 1 then $\lambda = V_R$, substituting these into equation 2.93, which reduces to

$$E^* = V_A E_A^* + (1 - V_A) E_C^* \qquad (2.94)$$

and describes the modulus for parallel connection between rubbery and crystalline regions.

FIGURE 2.12

mechanical model of Takayanagi

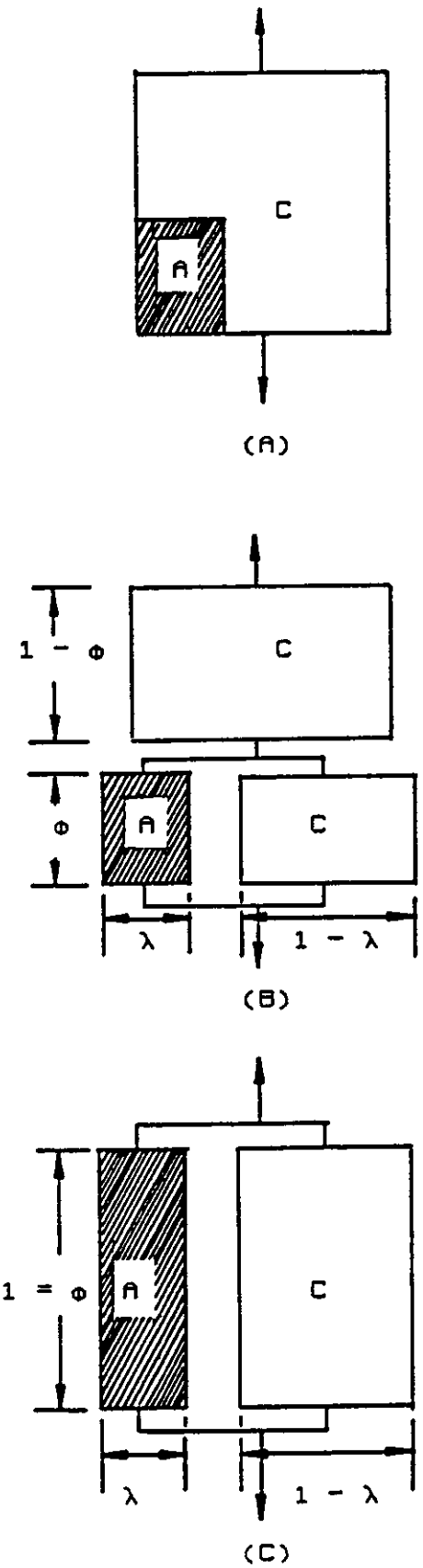

2.6 DIFFUSION

2.6.1 Basic diffusion terminology

2.6.1.1 Fick's laws of diffusion

Ficks first law of diffusion[108] is based on the hypothesis that the rate of transfer of diffusing substance through unit area of a section is proportional to the concentration gradient measured normal to the section, i.e.

$$F = -D * c/x \qquad (2.97)$$

where F is the rate of transfer per unit area of section, c is the concentration of diffusing substance and x is the space coordinate measured normal to the section. If F and c are expressed in the same unit of quantity, e.g. grams or moles, then D is independent of this unit and has dimensions $(length)^2\ (time)^{-1}$.

The differential form of equation 2.97 can be derived as[109]

$$\frac{dc}{dt} = D\ \frac{d^2c}{dx^2} \qquad (2.98)$$

2.6.2 The free volume theory for diffusion into polymers.

If no porosity is present, as in homogeneous amorphous polymeric materials, the diffusion mechanism is an activated process i.e. a process in which the gas or vapour

dissolves into the polymer at the surface and diffuses through the polymer under a concentration gradient. Activated diffusion is characterised by a large positive temperature dependence together with the solubility and diffusivity of the sorbent.

The diffusion of a molecule through the polymer can be regarded as the movement of the molecule through the free volumes formed between adjacent polymer molecules by thermal motion. Polymers with low glass transition temperatures (i.e. less than room temperature) require, by definition, low energy for segmental motion to occur. Diffusion is thus a fast process in such polymers. On the other hand polymers with high T_g values, such as, PVC (88°C), require much higher energy for the formation of free volumes large enough to accommodate the diffusing molecule, and diffusion is a relatively much slower process. This is because on approaching the T_g the movements of the polymer segments become more and more restricted, and more energy is required to displace the polymer chains. It is generally true that raising the T_g of a polymer will lead to slower diffusion of a penetrant.

The diffusion coefficients of liquids sorbing into amorphous polymers above T_g have been found to be very dependant in many cases on concentration[110-115]. Many suggestions have been put forward in attempts to explain such phenomena. Some of the earliest theories put forward were in terms of non-ideality in polymer-diluent mixtures[116], and of immobilization of penetrant molecules in the polymer network[117]. These have since been shown to be inconsistent with experimental data. Zone theories

developed by Brandt[118] and Barrer[119] both suffer, in explaining the diffusion coefficient dependency on concentration, in the range above T_g because of the rapid variation of activation energy with temperature and consequently the large number of degrees of freedom involved in the calculation.

The free volume approach[110,111,120], however, offers a quantitative treatment which explains both the temperature and concentration dependence of D. The origin of the free volume concept was the equation derived by Doolittle[41,42] to explain the dependence of viscosity of simple liquids on temperature. Doolittle pictured a liquid as being a mixture of free volume and occupied volume. The larger the free volume, the easier it is for molecular motion to occur. The viscosity of a liquid can be expressed as

$$\eta = A \exp(B/f) \qquad (2.99)$$

the symbols taking the same meaning as given in equations 2.16 and 2.17. It has already been shown that from the Doolittle treatment the WLF expression[43] may be derived, equation 2.21, which describes the dependency of viscosity of a bulk polymer on temperature.

If the fractional free volume is assumed to be proportional to the concentration of added diluent to a concentrated solution, the viscosity is shown to be dependent on the diluent concentration[121].

2.6.2.1 The concentration dependency of the diffusion coefficient

Using free volume ideas Cohen and Turnbull[122] developed the notion of a liquid consisting of "hard spheres" where molecules reside within cages bound by their neighbours. Thermal fluctuations allow considerable displacement of the molecule allowing the formation of voids in the liquid. Diffusion occurs as a result of the redistribution of the free volume within the liquid. The total probability $P(v^*)$ of finding a hole of a size exceeding a volume of v^* is given by

$$P(v^*) = \exp(-bv^*/v_A) \qquad (2.100)$$

where b is a numerical factor near unity and is a correction for overlap of free volume. v_A is the average free volume of one molecule.

In order to apply equation 2.100 to polymer systems the parameters have to be redefined. Fujita[120] regarded v^* as the fractional free volume, (f), of the system. The product bv^* is rewritten as B and defined as the measure of the hole size. Thus for polymeric systems.

$$P(B) = \exp(-B/f) \qquad (2.101)$$

The mobility of a diluent in the polymer medium should depend on the probability of its finding a hole in its neighbourhood large enough to allow its displacement. If the minimum hole size for a particular diluent displacement

is B_d, then

$$m_d = A_d \exp(-B_d/f) \qquad (2.102)$$

where m_d is the mobility of the diluent molecule and A_d is a constant depending upon the size and shape of the diluent. By their definitions A_d and B_d are independent of temperature and diluent concentration, so that the mobility of a diluent is determined by the average fractional free volume of the system. The thermodynamic diffusion coefficient, D_T[123], of the diluent is related to the molar mobility m_d by the expression[124]

$$D_T = RTm_d \qquad (2.103)$$

where R is the gas constant and T is the absolute temperature of the system. Combining equation 2.102 and 2.103 yields

$$D_T = A_d RT \exp(-B_d/f) \qquad (2.104)$$

f, the fractional free volume, is dependent on the temperature and diluent concentration, and is hence written as $f(v_1,T)$, where v_1 is the volume fraction of the diluent. If proportionality between free volume and the volume of the added diluent is assumed[124], then $f(v_1,T)$ is a linear function of v_1

$$f(v_1,T) = f(0,T) + \beta(T)v_1 \qquad (2.105)$$

where

$$\beta(T) = \gamma(T) - f(0,T) \qquad (2.106)$$

and $\gamma(T)$ is the proportionality factor between the free volume increase and the volume of added diluent. $f(0,T)$ is the value of f at zero diluent concentration.

Substituting equation 2.105 into 2.106 and assuming a fixed temperature, then it is possible to derive the following simplified equation.

$$D_T = D \exp(K v_1) \qquad (2.107)$$

where

$$K = B_d \beta(T)/[f(0,T)]^2 = \text{a constant} \qquad (2.108)$$

Equation 2.107 represents the concentration dependence of a diffusion coefficient often observed experimentally.

2.6.2.2 The temperature dependency of the diffusion coefficient

For amorphous polymers above the T_g the fractional free volume increases linearly with the coefficient of expansion, as shown in equation 2.16 Substituting 2.16 into 2.104 at $T > T_g$ and writing D for D_T equation 2.104 becomes

$$D = A_d RT \exp[-B_d/f_g + \alpha_f (T - T_g)] \qquad (2.109)$$

At temperatures below T_g

$$Do = A_d RTo \exp[-B_d/f_g] \qquad (2.110)$$

Assuming A_dRT and A_dRTo to be almost equal and combining equations 2.109 and 2.110, we have

$$(T - T_g)/\ln(D/Do) = f_g^2/B_d\alpha_f + f_g(T - T_g)/B_d \qquad (2.111)$$

so that $(T - T_g)/\ln(D/Do)$ is linearly related to $(T - T_g)$. It can also be seen that f_g, B_d, and α_f are independent of temperature. Equation 2.111 can therefore be rewritten as

$$(T - T_g)/\ln(D/Do) = K_1 + K_2(T - T_g) \qquad (2.112)$$

and rearranged to

$$\ln(D/Do) = (T - T_g)/K_1 + K_2(T - T_g) \qquad (2.113)$$

where K_1 and K_2 are constants. Equation 2.113 resembles equation 2.20 the WLF equation derived from viscosity considerations.

It is seen, therefore, that the free volume theory can be applied successfully to explain the concentration and temperature dependence of diffusion of organic diluents in polymers, and possibly to predict the diffusion coefficient from a knowledge of T_g, or vice versa.

2.6.3 Diffusion in polymeric systems

The observed behavioural features shown by the diffusion of hydrocarbons in glassy polystyrene systems have been described by Hopfenberg and Frisch[125], as shown in figure 2.13. Hopfenberg and Frisch suggested the behavioural

FIGURE 2.13

The behavioural features exhibited on the diffusion of hydrocarbons in glassy polystyrene systems

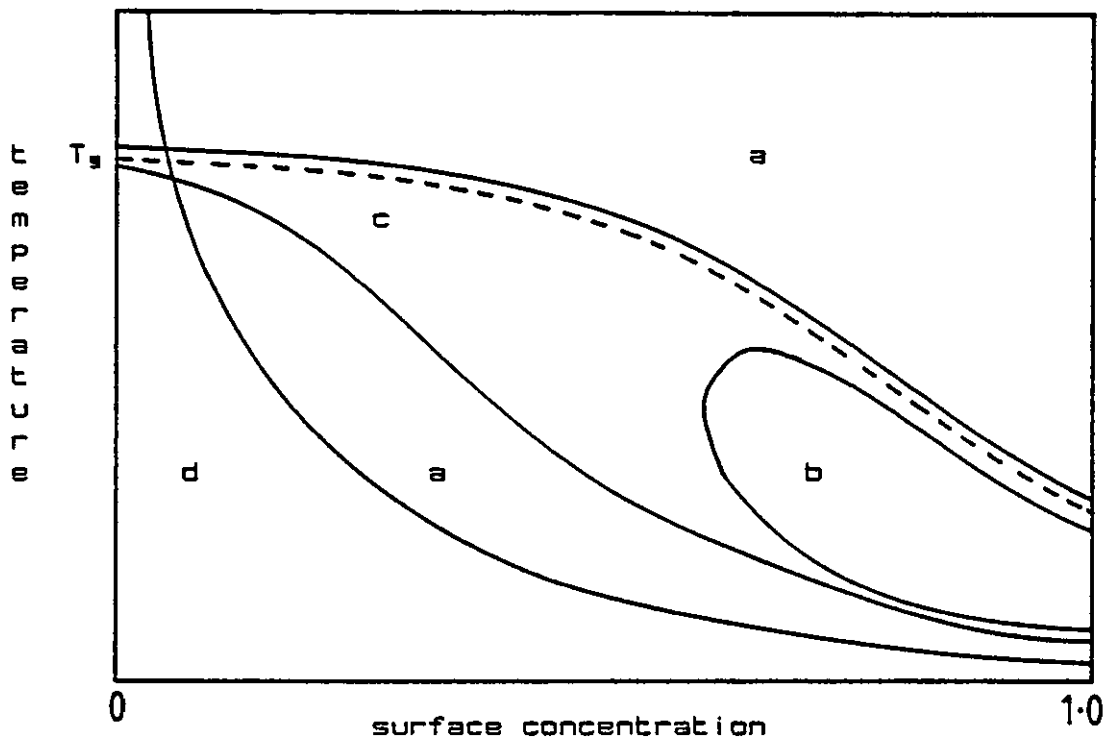

features exhibited in polystyrene would probably occur in most amorphous systems of a sufficient temperature and penetrant concentration range is employed. Region a describes concentration dependent diffusion or Fickian diffusion. Region d or concentration-independent diffusion will occur at low surface concentrations, e.g. for vapour sorption. Between these regions is situated Case II[126] transport regions b and c where time-dependent or anomalous diffusion occurs. Regions b and c are confined to high penetrant surface concentration and temperatures in the vicinity of and below the prevailing T_g of the system. The T_g of the system is shown by the dashed line in figure 2.13.

A useful classification which describes regions a, b and c as shown in figure 2.13, in terms of their relative rates of diffusion and polymer relaxation, has been proposed by

Alfrey et al.[126]. They described the three thus:

a. Case I or Fickian diffusion in which the rate of diffusion is much smaller than relaxation in the polymer.

b. Case II diffusion, an extreme case where diffusion is very rapid when compared with the relaxation processes and is controlled by the relaxation of the polymer.

c. This region describes non-Fickian or anomalous diffusion which occurs when the diffusion and relaxation rates are comparable.

Case I and Case II are both simple cases in that their behaviour can be described in terms of a single parameter. Case I diffusion is controlled by the diffusion coefficient (D). The parameter describing Case II is the constant velocity of an advancing front which indicates the extent of penetration of the swelling agent. The advancing front is the boundary between swollen outer layer and glassy unswollen centre. By examining curves for the mass sorbed versus time, it can be shown that Case II is a limiting or extreme case. If the amount of penetrant sorbed at time t is Kt^n where K and n are constants then case I systems show N=1/2, as shown in figure 2.14. Case II systems exhibit an n equal to 1. Non-Fickian behaviour systems give n values between 1/2 and 1.

2.6.3.1 Fickian diffusion (Case I)

For many organic vapours in polymers, D depends very markedly on concentration. If M_T is mass sorbed at time, t and M_∞ is mass sorbed at equilibrium, a plot of M_T/M_∞ versus

FIGURE 2.14

Fickian and case II sorption, mass sorbed versus square root time behaviour

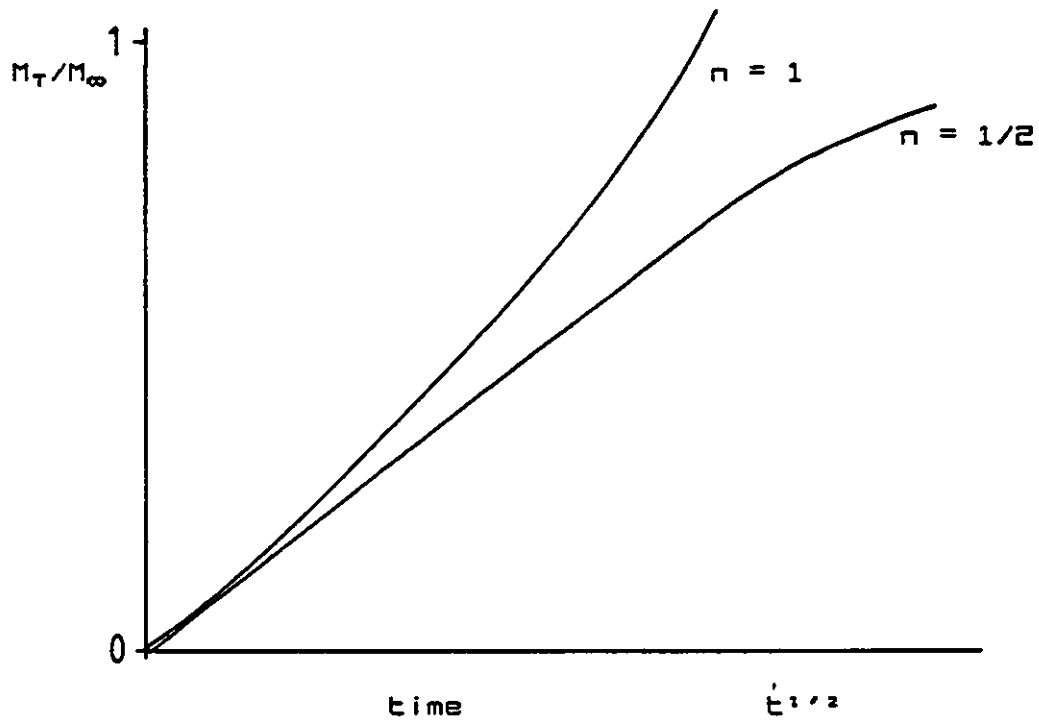

(time)$^{1/2}$ produces the general plot in figure 2.15. The derivation of such plots is described in the following section using equation 2.119.

In the early stages, when diffusion take place essentially in a semi-infinite medium, the amount sorbed or desorbed is directly proportional to the square root of time. When the sorption and desorption curves cease to be linear when plotted against (time)$^{1/2}$, as shown in figure 2.15, each tend towards a limiting value. When D increases with concentration increasing, the linear behaviour may extend well beyond 50% of the final equilibrium uptake in the case of sorption. This is similar to the corresponding curve for a constant D, since the sorption curves are

FIGURE 2.15

Fickian sorption and desorption

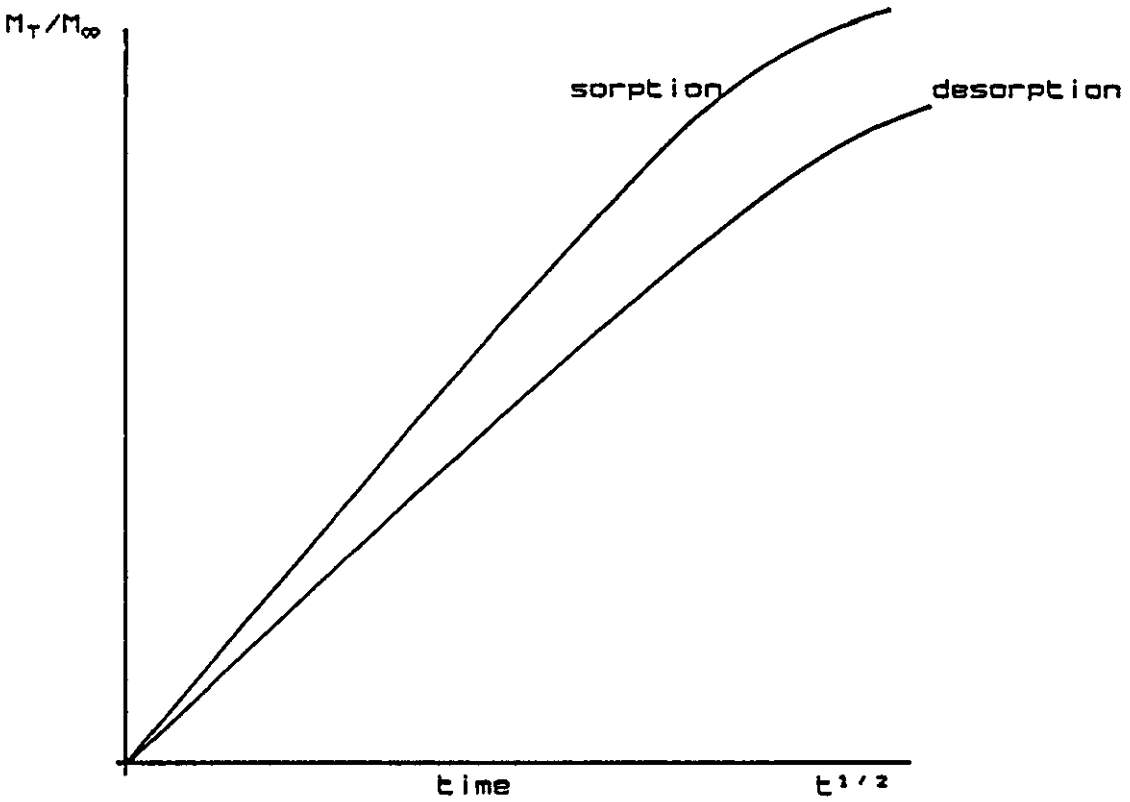

parabolic, i.e. linear when plotted against (time)$^{1/2}$ over most of their long time interval. Finally, with Case I models the desorption is always slower than sorption.[108]

The mathematical model describing Fickian or Case I sorption into amorphous polymers is simplified by two observations[127]

1. The movement of liquid into the polymer occurred by molecular diffusion is satisfied by Fick's laws.

2. Since an equilibrium is rapidly produced the boundary conditions at the film surfaces $x = 0$ and the film thickness, ℓ, are constant with the concentration c, of penetrant.

The diffusion equation for a homogeneous film of a large area is[128]

$$\partial c/\partial t = \frac{\partial}{\partial x}[D(c)\partial c/\partial x] \qquad 0 < x < \ell \qquad (2.114)$$

D(c) is defined as the binary diffusion coefficient and is the product of a thermodynamic factor (the chemical potential of the penetrant) and a mobility factor, sometimes known as the thermodynamic diffusion coefficient. The normal boundary conditions used in describing Fickian diffusion are

$$c(0, t) = co \quad c(\ell, t') = c_1 \qquad (2.115)$$

where co and c_1 are constants. The boundary condition for the initial situation is

$$c(x, 0) = C_i \qquad (2.116)$$

and c_i is chosen experimentally to be constant. When $co = c_1 > c_i$ the boundary conditions describe sorption. By choosing suitable boundary conditions it is also possible to describe desorption and permeation mathematically.

To completely describe Fickian diffusion, D(c), Fick's equations must be differentiable with respect to x and must satisfy

$$0 < D(c) \leq Do < \infty \qquad (2.117)$$

The simple mathematics of Fickian diffusion allows Fick's equations and equation 2.114, to be dimensionally scaled from which follows the early time behaviour of figure 2.14.

2.6.3.1.1 Diffusion in a plane sheet

If a sheet of polymer is exposed to a vapour or liquid capable of sorbing into the polymer and the surfaces of the polymer are assumed to immediately attain a concentration value equal to the equilibrium concentration value, the mass uptake of the sorbent by the polymer can be expressed as[109]

$$M_T/M_\infty = 1 - \frac{8}{\pi^2} \sum_{m=0}^{\infty} \frac{1}{(2m+1)^2} \exp[-D(2m+1)^2\pi^2 t/\ell^2] \quad (2.118)$$

where M_T is the total amount of the vapour sorbed by the sheet at time t, and M_∞ is the equilibrium sorption attained theoretically after infinite time. The thickness of the polymer sheet is given by ℓ and the experiment carried out at a constant temperature. The value of D obtained in equation 2.118 is only approximate since the polymer sheet, in particularly PVC, swells on sorption of some liquids and vapours and is dependent on the surface concentration of sorbent. At the early stages of sorption equation 2.118 approximates to

$$M_T/M_\infty = 4/\pi^2 (Dt/\ell^2)^{1/2} \quad (2.119)$$

Thus, it is possible to deduce an average diffusion coefficient from the initial gradient of the sorption curve when plotted against the square root of time.

2.6.3.2 Case II diffusion

Case II diffusion is often described as a simple limiting case[126] although transport has been observed which obeys M_T/M_∞ versus Kt^n curves where $n > 1$[129]. The main features of Case II diffusion first reported by Alfrey et al.[126] involving a glassy polymer are now described:

1. As the sorbent penetrates into the polymer a sharp advancing boundary separates the glassy centre from the outer plasticised surface layer. Such visible advancing sharp boundaries are commonly observed during the sorption of liquids in cross-linked glassy polymers and constitute a necessary condition for Case II swelling.

2. Behind the advancing front, there is a surface layer constrained due to entanglements with molecules in the internal core layers and will not have reached equilibrium concentration.

3. The boundary between the surface layer and glassy core advances at a constant velocity.

4. The initial gain in mass, represented by M, is consequently directly proportional to time, represented by t, rather than to the square root time($t^{1/2}$). On a classical plot of gain in mass versus square root of time, this appears as a parabola, since

$$M = D(t^{1/2})^2 \qquad (2.120)$$

5. The kinetics of ideal Fickian penetration into specimens of simple geometries (plaques, long cylinders and spheres) can be reduced to one parameter - the diffusion

constant. The kinetics of Case II diffusion can also be reduced to one parameter - the velocity of the advancing front.

6. As the temperature decreases in a sorption experiment a distinct critical point is reached when the velocity of the advancing front falls to zero.

7. The velocity of the advancing front in Case II sorption is very sensitive to the thermal history of the glassy polymer.

8. For specimens of simple geometry the stresses involved in Case II diffusion can be calculated from the shear modulus of the surface layer and the equilibrium swelling factor.

9. With mixed solvents it is possible to observe a superposition of Case II and Fickian sorption. Frisch et al.[22] studied the diffusion of methylene chloride in glassy epoxy polymer measuring the gain in mass and the distance of penetration as a function of time. They analysed experimental results by taking into account both Fickian and Case II mechanisms and obtained good agreement between experimental and theoretical results.

In equation 2.114 the diffusion coefficient in a homogeneous film of a large area, D(c) is defined as being the product of a thermodynamic factor and a mobility factor and may be expressed as

$$\partial c/\partial t = -\frac{\partial}{\partial x}(uc) \qquad (2.121)$$

where u is the mass velocity of the penetrant in one plane.

In Case II swelling this is considered to be constant. Hence substituting v for u in equation 2.121 results in

$$\partial c/\partial t = -v\partial c/\partial x \qquad (2.122)$$

If the initial concentration profile is $c(x,0) = co(x)$ the solution to 2.122 is,

$$(x,t) = co(x-vt) \qquad (2.123)$$

and if the initial distribution is a step function then this profile is kept with time and is described in figure 2.16. The moving boundary location x and the weight gain M_T are given by

FIGURE 2.16

The concentration profile for case II diffusion

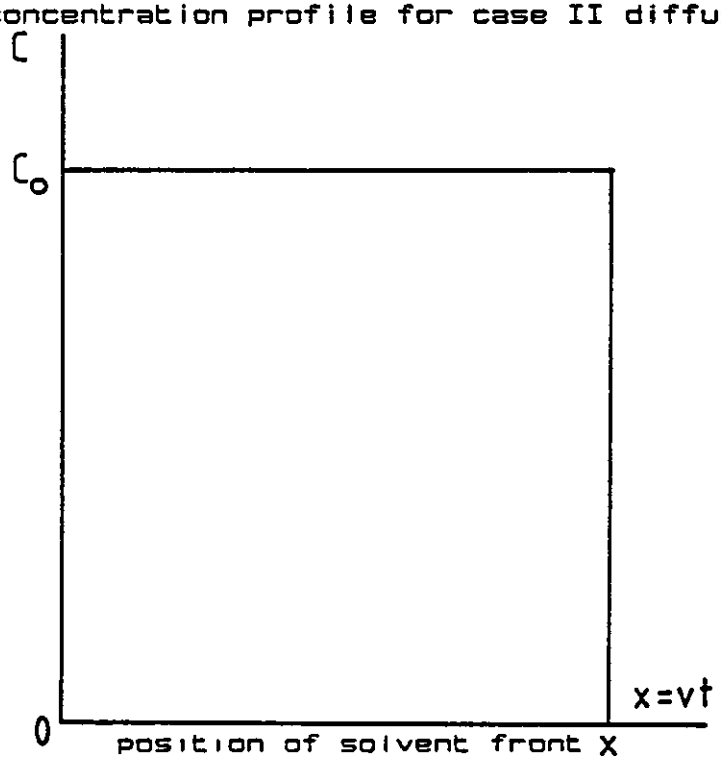

$$x = vt \qquad (2.124)$$

and

$$M_T = covtA \qquad (2.125)$$

where A is the cross-sectional area transverse to the flow. Equations 2.124 and 2.125 describe points 3 and 4 in the above description of Case II diffusion.

2.6.3.3 Non-Fickian or anomalous diffusion

Rogers[130] summarized the various types of diffusion behaviour exhibited by polymers using mass sorption-desorption curves and compared these curves with Fickian type diffusion, see figure 2.17. Rogers used the term "pseudo-Fickian" to describe curves of the same general shape to Fickian curves but exhibiting an initial linearity for a much shorter period of time as shown by figure 2.17(d). If a single inflexion, at around 50% equilibrium sorption, is observed, sigmoid sorption[127] as shown by figure 2.17(b) is said to occur. When a vapour is brought into contact with a polymer sheet, a surface sorption equilibrium is attained which involves the swelling and extension of the surface. This surface layer is constrained by the entanglement with molecules in the internal core. At sub-T_g temperatures the modulus is large and the surface layer is effectively restrained preventing the establishment of a equilibrium surface concentration until some vapour has penetrated into and has plasticized the internal core. The

rate of sorption then speeds up towards its final equilibrium resulting in sigmoid behaviour. Figure 2.17(c) describes two-stage sorption[131]. It is thought that the second stage is brought about with an increase in surface concentration which occurs slowly compared with the diffusion process. The surface concentration is the overall rate determining step for sorption.

FIGURE 2.17

The various types of diffusion behaviour exhibited by polymers

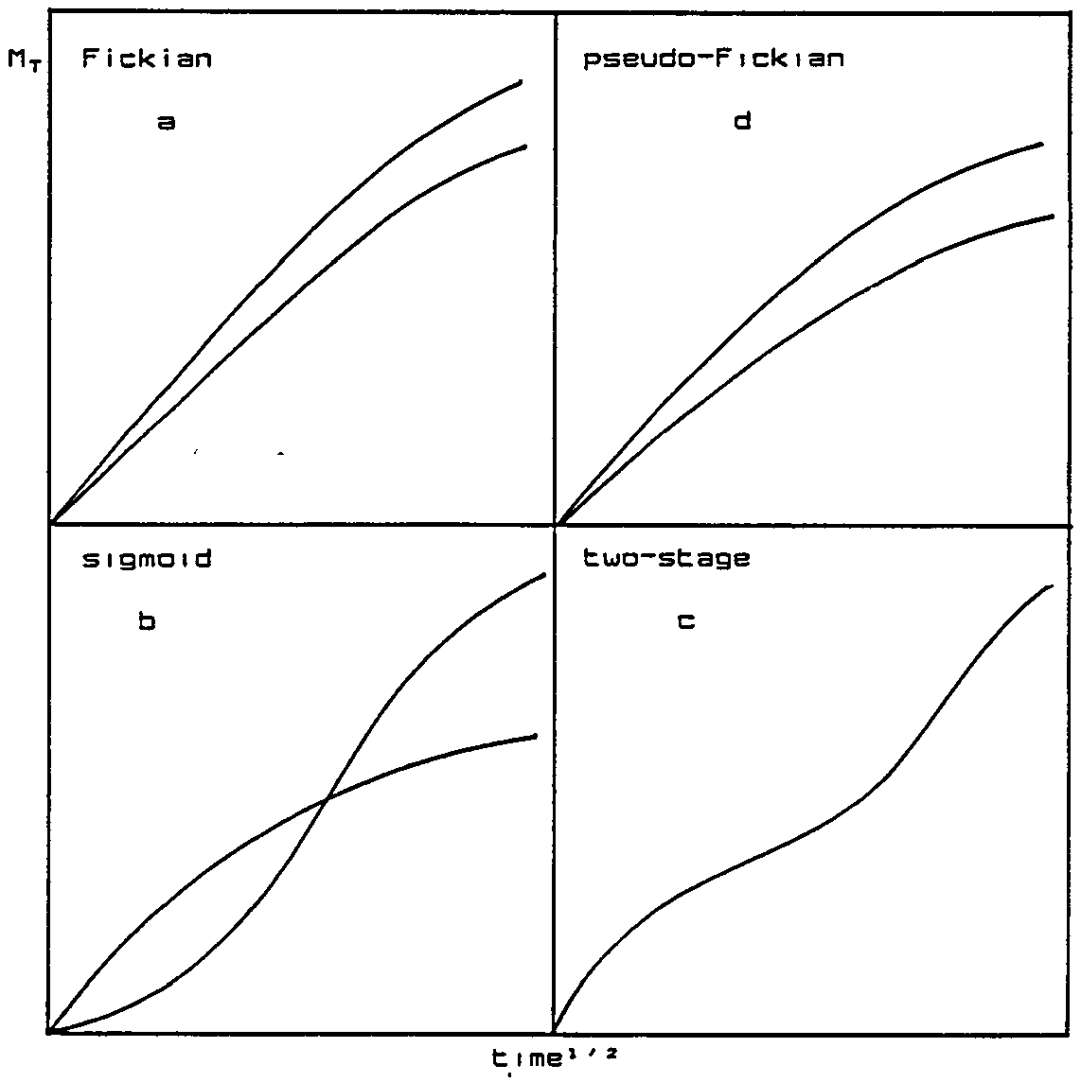

2.6.4 A mathematical model for the superposition of Case I and Case II diffusion

Points 2 and 8, in section 2.6.3.2, in the description of Case II diffusion give evidence that internal stresses arise between the constrained outer swollen layer and the internal core. Attempts have been made to relate anomalous diffusion behaviour to these stresses[24,25,132]. Of particular interest is the procedure developed by Kwei et al.[22]. They described sorption experiments for the system PVC-propanone well below the T_g for PVC. They argued that D would decrease as the temperature decreases and the internal stress effects would increase until a situation is reached where the system is not in equilibrium. They rewrote equation 2.97 to include not only the gradient of chemical potential but a second term derived from the stress produced by the penetrant. For a system, not in equilibrium, the thermodynamics of irreversible processes leads to the following modification of equation 2.97.

$$F = -BC\left(\frac{\partial \mu}{\partial x} - \frac{1}{C}\frac{\partial S}{\partial x}\right) \qquad (2.126)$$

where B is a mobility coefficient, μ the chemical potential and S the partial stress tensor for one direction. On assuming proportionality between S and the total uptake of penetrant, then Kwei et al. derived

$$S(c) = s\int_0^x C dx' \qquad (2.127)$$

where s is a proportionality constant. Hence it is possible to rewrite equation 2.114, the generalized Fickian diffusion equation.

$$\partial c/\partial t = \frac{\partial}{\partial x}[D\partial c/\partial x - \beta s C] \qquad (2.128)$$

This is further simplified by showing $v = \beta s$[24], where the quantity v represents the velocity of solvent penetration. The solution for equation 2.128 has been shown[124] for diffusion into a penetrant free semi-infinite medium with a constant concentration, Co to be

$$C(x, t) = \frac{Co}{2}[\exp(xv/D)\operatorname{erfc}(\frac{x + vt}{2\sqrt{(Dt)}}) + \operatorname{erfc}(\frac{x - vt}{2\sqrt{(Dt)}})] \qquad (2.129)$$

where erfc is a standard mathematical function, called the error-function complement[133], extensive tables of which may be found in the CRC handbook[134]. The total amount M_T of penetrant per unit area sorbing to the polymer is

$$M_T = -\int_0^t [D(\partial c/\partial x - vc]dt \qquad (2.130)$$

from time, 0 to t. The solution of equation 2.130 is,

$$M_T = Co(\frac{D}{v}\operatorname{erfc}[\frac{v}{2}\sqrt{\frac{t}{D}}] + \frac{vt}{2}\operatorname{erfc}[-\frac{v}{2}\sqrt{\frac{t}{D}}] + \sqrt{\frac{Dt}{\pi}}\exp(-v^2t/4D)) \qquad (2.131)$$

which tends at large times to

$$M_T = [(D/v) + vt] \qquad (2.132)$$

When x tends to small values when compared with vt in equation 2.129, the second term in the square bracket, an inspection of the error-function complement becomes much larger than the first, so that except for small values of t the movement of the penetrant front X with a given concentration will have the form.

$$X = 2h\sqrt{(Dt)} + vt \qquad (2.133)$$

where h is a constant. Using the above model Kwei et al.[22] were able to model successfully the rates of sorption and penetration of propanone into PVC. Their model also describes the two extreme cases of Fickian and Case II where Fickian is described by $D << v$ and Case II is shown to hold when $D >> v$.

CHAPTER 3 — EXPERIMENTAL

3.1 MATERIALS

Suspension polymerized PVC grade S71/102, particle size ranging between 50 μm to 100 μm obtained from I.C.I., Petrochemicals and Plastics Division, Runcorn, Cheshire U.K., was compression moulded into plaques using equipment provided by I.C.I. The weight average molecular mass of the polymer was approximately 200,000.

Four plaques were prepared simultaneously, each plaque requiring approximately 40g of PVC. The press after reaching the operating temperature was charged with the mould containing PVC. The mould was preheated for two minutes in order to allow the PVC to equilibrate with the pressing temperature of 169°C. The mould was compressed at 9600 $KN m^{-2}$ pressure for 6 minutes, cooled in situ to room temperature before removing the mould from the press. The dimensions of the plaques were approximately 11.5x11.5x0.2 cm. No antioxidants or lubricants were added since they would interfere with subsequent analysis of the PVC. Because of the absence of stabilizers a small amount of dehydrochlorination takes place and the plaques are red-brown in colour. The samples were stored at room temperature in the dark to prevent further

dehydrochlorination taking place.

The degree of fusion that takes place during pressing of the plaques varies as a consequence of temperature and time. Faulkner[135] described a technique for determining the temperature-torque profile of a PVC compound in a Brabender Plasticorder mixing chamber from room temperature to the polymer degradation temperature. In this temperature range PVC shows three characteristic peaks in the torque temperature trace. These peaks are thought to be associated with the breakdown of the powder particles. At 124°C a torque peak occurs which Gonze[136] stated is due to the densification of the 100 μm grains. As the temperature rises the grains begin to break open, producing a minimum on the torque trace which rises to a maximum at 160°C. This is due to the densification of primary particles. This temperature is also referred[137] to as the "threshold temperature" for fusion. The threshold temperature for sample S71/102 is 165°C. Above this temperature primary particles break down. The processing temperature of 169°C was chosen so that the primary particles have just begun to break down, producing a homogenous plaque of fused primary particles with the minimum amount of dehydrochlorination.

Initially, liquids, subsequently referred to as swelling agents, were chosen purely on their ability to swell moulded PVC samples. The main factor taken into account when choosing which liquids to use, was the solubility parameter. The solubility parameter for PVC, is 19.6 $J^{1/2}/cm^{3/2}$[138]. It is known[31] that liquids are good swelling agents when the solubility parameter difference

between liquid and polymer is less than between 3.5 to 4.1 $J^{1/2}/cm^{3/2}$. A larger solubility parameter difference indicates the liquid is likely to be a non-solvent for the polymer and demonstrated to be the case for PVC[139].

The first liquids examined were ketones. These have solubility parameter values between 20.3 to 16.0 $J^{1/2}/cm^{3/2}$.

Consideration of the solubility parameter alone is insufficient in predicting whether the liquid is a swelling agent for PVC. By considering the hydrogen bonding ability of various liquids together with their solubility parameter, Vincent and Raha[140] were able to produce a plot depicting a region where the liquid would be a solvent or swelling agent for PVC. Vincent and Raha's data are reproduced in figure 3.1 for the interaction of various liquids with PVC. Although the hydrogen bonding data are incomplete for the liquids employed in this work, figure 3.1 does show that swelling agents and solvents fall within the shaded area. The hydrogen bonding parameter is based on the work of Gordy and Stanford[141-143], who measured the displacement of the OD infrared absorption band in the 4 μm range when different liquids were added to a solution of deuterated methanol (CH_3OD) in benzene. The size of the displacement measured in wave numbers divided by ten is defined as the hydrogen bonding parameter. Using the solubility parameter and hydrogen bonding parameters it is possible to predict the likelihood of a liquid being a swelling agent for PVC.

Other classes of compounds examined were acrylates, nitroalkanes, halogenated aromatics and halogenated alkanes. A small number of well known PVC plasticizers were employed and supplied by ICI. Lists of swelling agents and

FIGURE 3.1

Solvent and swelling agents for PVC,

after Vincent and Raha[140], legend on following page

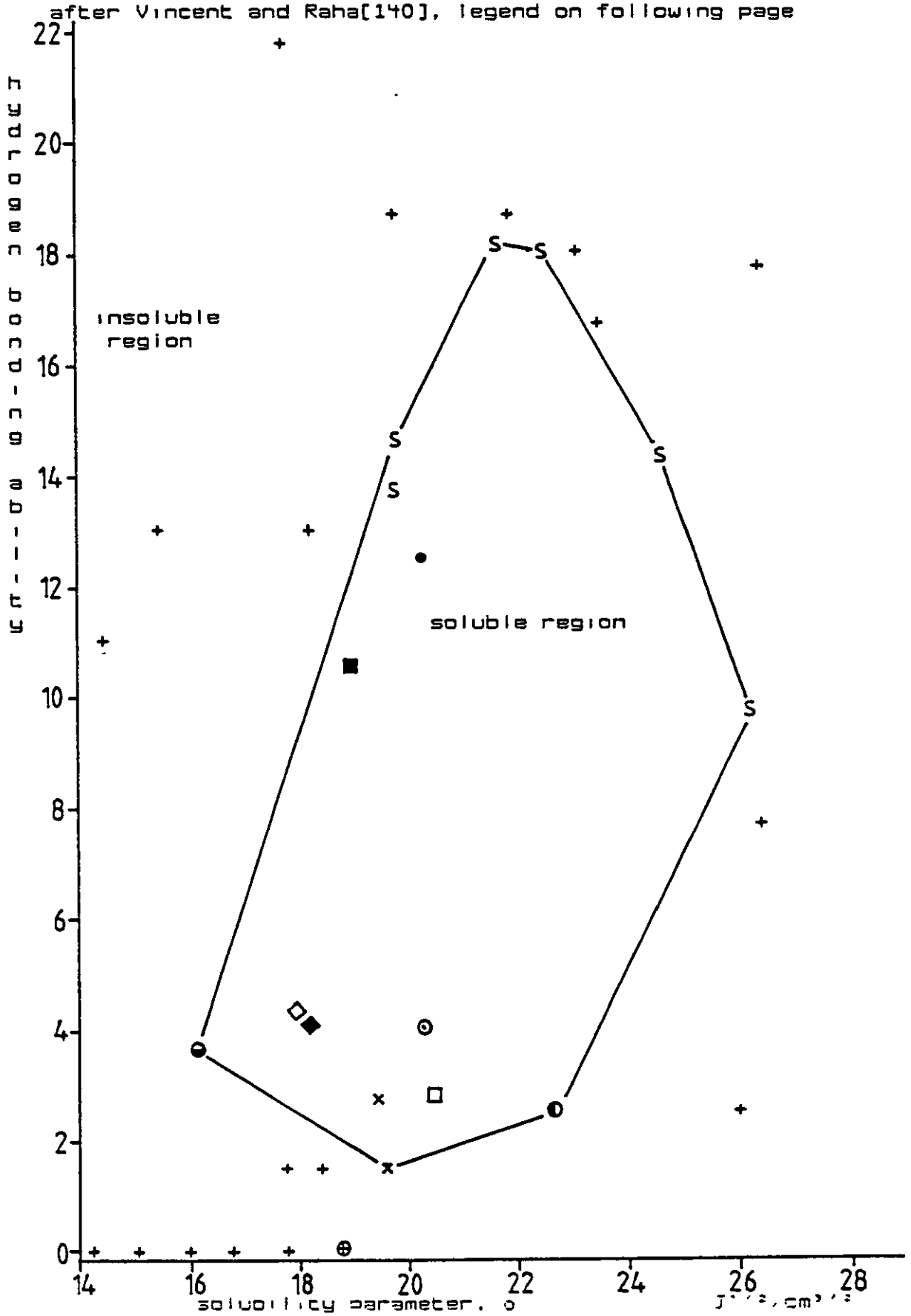

FIGURE 3.1 (cont.)

legend

⊕ benzene	◐ nitroethane
• propanone	✱ trichloroethane
■ methylethyl ketone	◆ methylbenzene
⊙ 2-nitropropanone	◇ ethylbenzene
□ 1-nitrobutane	◒ dioctyl phthalate
× chlorobenzene	

Vincent and Raha data

S solvents

\+ non-solvents

plasticizers are shown in tables 3.1 and 3.2. All liquids were standard laboratory reagents and were used as received except 1-nitrobutane which was produced following the procedure given by Kornblum[144]

3.2 SAMPLE PREPARATION

Two principal methods were used to produce swollen PVC samples for analysis using PL-DMTA methods. The samples were either brought into contact with the vapour or the liquid form of the swelling agent.

3.2.1 Solid/liquid contact

A sample of suitable dimensions for analysis by PL-DMTA instrument was cut from a plaque. The sample was placed in a suitable air tight container and the swelling agent was introduced so that the sample was covered. The samples were weighed before any swelling agent was introduced in order to calculate the percentage mole content of imbibed liquid.

The weighing procedure was standardized in order to eliminate errors due to loss of swelling agent by evaporation. The samples were held in a water bath at 60°C for varying amounts of time. Once swollen to the required degree the samples were removed from the swelling agent. The excess liquid was removed using tissue paper. The samples were then quenched and stored in liquid nitrogen until required to prevent loss of imbibed liquid. The thickness of the swollen samples was recorded by allowing the sample to warm to room temperature and taking an average of three micrometer readings of the thickness. The extreme edges of the sample were avoided when taking these measurements since a raised edge is produced due to the sorption occurring at the sample edge, as shown in figure 3.2.

TABLE 3.1

Ketones used in PVC sorption experiments

liquid	molar mass	molar volume	δ parameter	ν	hydrogen bonding ability	source$^{\phi}$
	g/mol	cm^3/mol	$J^{1/2}/cm^{3/2}$	cm^{-1}		
propanone	58.1	73.3	20.3	9.7/12.5	M	a
2-butanone	72.1	89.6	19.0	7.7/10.5	M	b
2-pentanone	86.1	106.1	18.3	8.0	M	c
3-pentanone	86.1	105.6	18.0	7.7	M	c
MBK	100.2	123.4	17.5	8.4	M	c
DIBK	142.2	176.4	16.3	8.4/9.8	M	c

ϕ - legend in table 3.3

MBK - methylbutylketone

DIBK - diisobutylketone

TABLE 3.2

Liquids used in PVC sorption experiments

liquid	molar mass	molar volume	solubility parameter	ν	hydrogen bonding ability	sourceϕ
	g/mol	cm^3/mol	$J^{1/2}/cm^{3/2}$	cm^{-1}		
Nitroethane	75.1	71.4	22.7	2.5	P	c
benzene	78.1	89.0	18.8	0.0	P	b
DCM	84.9	63.6	22.9	1.5		b
2-nitropropane	89.1	89.0*	20.3	4.0	P	c
methylbenzene	92.1	106.0	18.2	4.2	P	a
fluorobenzene	96.1	89.0	16.0		P	d
DCE	99.0	78.7	20.1	1.5		b
ethylacrylate	100.1	109.0*	17.6		M	c
MMA	100.1	106.0*	18.0		M	e
nitrobutane	103.1		20.3			
ethlybenzene	106.2	122.0	18.0	4.2	P	e
DMB	106.2	123.2	17.9	4.5	P	e
chlorobenzene	112.6	101.7	19.5	2.7	P	b
TCM	119.0	80.0	19.0	1.3	P	b
nitrobenzene	123.1	102.3	20.5	2.8	P	b
TCE	133.4	100.7	17.5	1.5	P	b
BMA	142.2	160.0*	16.9		M	f
DCB	147.0	493.3*	20.5		P	e
DEO	153.1	136.2*	17.6		M	b
CF	154.8	96.5	17.7	0.0		b

ϕ -legend in table 3.3

DCM - dichloromethane
DCE - 1,2-dichloroethane
MMA - methylmethacrylate
DMB - dimethylbenzene
TCM - trichloromethane
TCE - trichloroethane
BMA - butylmethacrylate
DCB - o-dichlorobenzene
DEO - diethyloxalate
CF - tetrachloromethane

TABLE 3.3

Plasticizers used in PVC sorption experiments

liquid	molar mass g/mol	molar volume cm^3/mol	solubility parameter $J^{1/2}/cm^{3/2}$	hydrogen bonding ability	source
BBP	298.0	360.0	22.3		g
DOP	390.6	377.0	18.2*	M	g
DMP	194.2	163.2	21.9*	M	d
Cereclor S52	440.0	352.0			g

BBP - butylbenzylphthalate
DOP - dioctylphthalate
DMP - dimethylphthalate

Legend for tables 3.1 and 3.2

* source of data, reference [145]

a Careless Solvents Ltd.,St. James House, Romford, Essex.

b Fisons Ltd., Laboratory Supplies, Bishop Meadow, Loughborough, Leics.

c Aldrich Ltd., The Old Brick Yard, New Road, Gillingham, Dorset.

d Fluka Ltd., Peakdale Road, Glossop, Derbyshire.

e BDH, Fourways Road, Carlyon Industrial Estate, Atherstone, Warks.

f Kock Light Ltd., Rookwood Way, Haverhill, Suffolk.

g I.C.I., Petrochemicals and Plastics Division, Runcorn, Cheshire.

FIGURE 3.2

Micrograph of a section through a uPVC plaque swollen with dimethylbenzene swollen at 60°C showing the raised edge of the sample

This figure shows a micrograph of a slice cut through the edge of the sample. The symbol (A) is pointing to the inner core region, (B) and (C) refer to the core-swollen polymer interface and swollen outer edge. The raised edge resembles a "window frame". Two discs were punched from each sample with an 8 mm diameter die again avoiding the edges of the sample. A thin slice was cut from the remaining sample with a scalpel, at right angles from one edge of the sample, and examined under a Leitz polarizing microscope (50x magnification). The thickness of the core was recorded from this slice using a graticule fitted in the microscope (see figure 3.3) each division of the graticule being 0.02 mm. Region (A) in figure 3.3 is the inner core. The slice was cut from right to left in the figure. It can be seen that the left hand side of the core-swollen polymer interface, (B), is jagged possibly due to the glassy polymer shattering on cutting. The thickness of the swollen layer on the left hand side is also smaller, shown by the swollen edge (C), due to deformation occurring on cutting. Wherever possible the measurements were carried out on the core and total thickness, using micrometer readings, to avoid regions which were deformed on cutting. The two discs were now ready for PL-DMTA.

3.2.2 Solid/vapour sorption

3.2.2.1 Operation of electro-microbalance

The Mark II vacuum head with a Robal Digital control unit supplied by C.I. Electronics Salisbury Wiltshire U.K.,

FIGURE 3.3

Micrograph of a section through a uPVC plaque swollen with dimethylbenzene swollen at 60°C

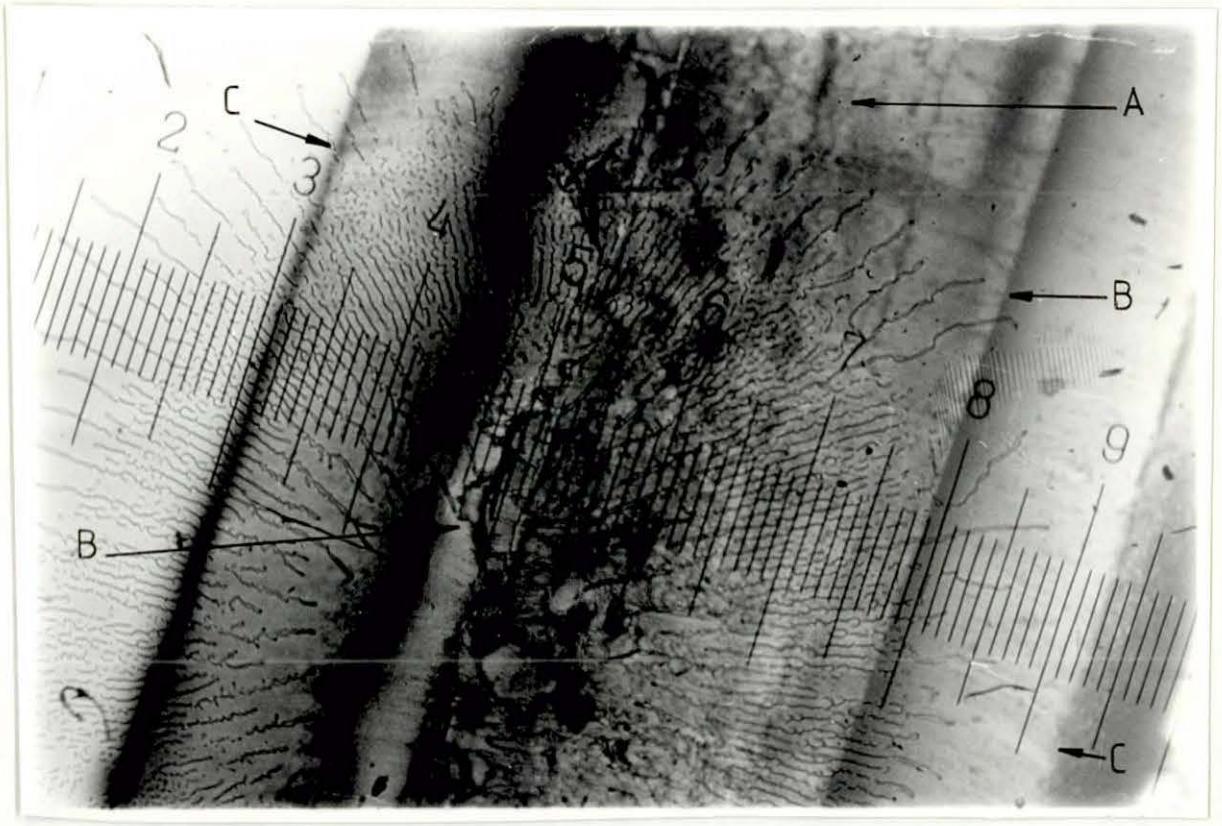

was an electronic bridge circuit maintained in continuous balance by a servo system. The head unit, shown in figure 3.4, electro-magnetically balanced the torque produced by the sample mass. A current flowed through the head in exact proportion to the applied mass and this current operated the indicating meter and provided an electrical output for a pen recorder.

Figure 3.4 shows the construction of the balance head unit. The balance arm carried a shutter interposed between a lamp and a pair of silicon photocells. A small displacement of this arm caused an imbalance in the light falling on the photocells, and hence the current flowing through the photocells. This current was amplified and passed through the movement coil restoring it to its original position. This rapid response to mass change helped to make the balance insensitive to external vibration.

The simple bridge circuit of figure 3.5 illustrates the principle. With the arm central the photocells have equal resistance and no bridge current flowed. A slight arm movement changed the relative illumination on the photocells, unbalancing their resistances and causing bridge current. This current passing through the movement coil rapidly produced a new equilibrium in which the residual bridge current just counteracts the external torque applied to the balance arm.

3.2.2.2 Vapour sorption using an electronic microbalance

Using a C.I. Electronics Microbalance it was

FIGURE 3.4

A schematic diagram of the

C.I. Electronics microbalance head.

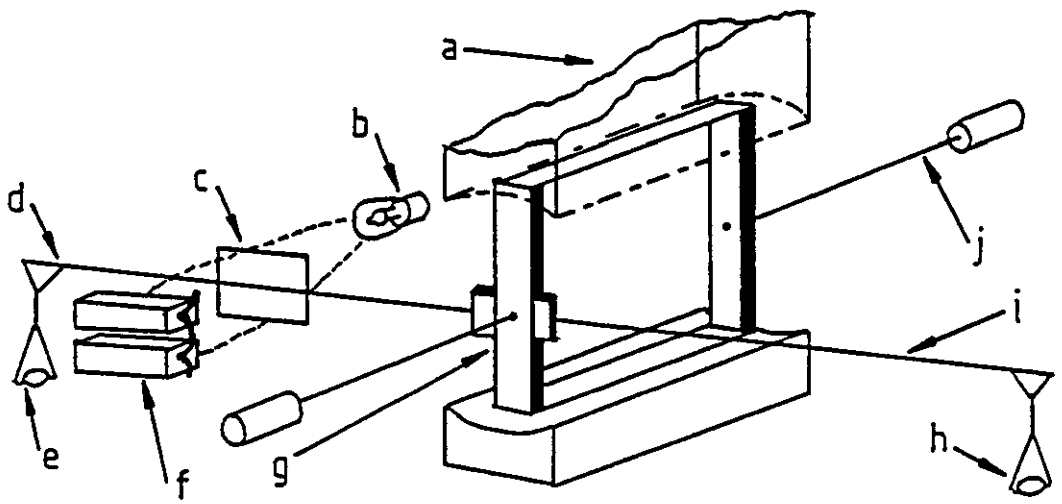

legend

a	magnets	f	photocells
b	lamp	g	electromagnet
c	shutter	h	tare pan
d	sample arm	i	balance arm
e	sample pan	j	fulcrum wire

FIGURE 3.5

The microbalance bridge circuitry

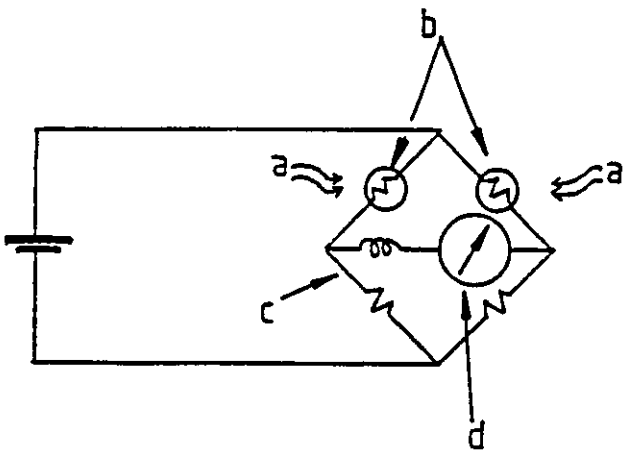

legend

a light focused on photocells

b photocells

c coil

d meter

possible to continuously follow the uptake of swelling in a PVC sample. A schematic view of the microbalance apparatus is shown in figure 3.6. The Robal control unit contained a IEEE computer interface allowing continuous acquisition of data on a Commodore 4032 computer. An example program allowing data collection via the IEEE interface is shown in Appendix 5.

The balance head was operated in a controlled environment and was kept at a temperature at least 5°C higher than the sample and the reservoir was kept at least 3°C or more below that of the sample. This prevented distillation of the swelling agent onto the balance and sample.

The swelling agent, around 30 cm^3, was introduced into the reservoir. A bar shaped sample of PVC of dimensions 3.5x0.2x1.0 cm. was suspended from the left hand side of the balance using fine copper wire. The mass of this bar was approximately 0.3 g

Copper wire was placed on the right hand side to counterbalance the balance arm so that a near balance point was reached. The balance was electrically zeroed using the Robal control unit. A maximum of 200 mg can be tared electronically. The apparatus was closed and allowed to equilibrate thermally.

The apparatus was evacuated by opening taps A and C. Tap C was then closed. The swelling agent was degassed by closing tap A, when opening tap B allowed any dissolved gas to come out. Tap B was then closed and tap A opened. This procedure was repeated until all the dissolved gas had been

FIGURE 3.6

A schematic view the of microbalance apparatus, the dashed line shows the environmental chamber

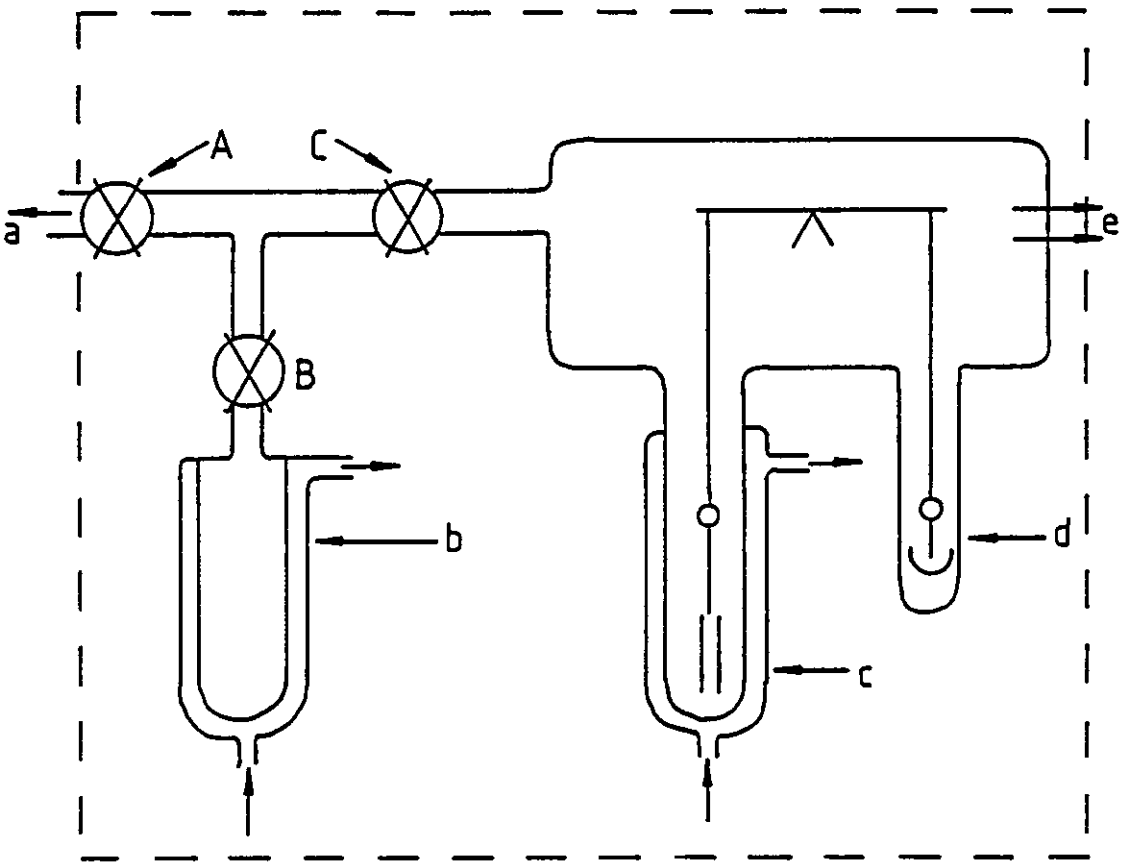

legend

a feed line to cold trap and vacuum pump

b reservoir

c sample water jacket

d tare

e signal to control unit and computer

removed. This ensured that the vapour over the sample was purely that of the swelling agent.

After the system had been degassed and evacuated the taps A and C are closed. The zero setting on the balance was checked, tap C was opened, and tap B was opened admitting the swelling vapour onto the sample. Simultaneously the computer was set running. The sample was left until the required sorption had occurred and removed for analysis using a PL-DMTA instrument.

3.3 ANALYSIS OF SWOLLEN SAMPLES

3.3.1 Dynamic mechanical thermal analysis of swollen samples

Mechanical properties were obtained using a PL-DMTA instrument. The information obtained from the PL-DMTA instrument was a plot of the logarithum of the Young's modulus (E') giving an indication of the stiffness of the sample and a plot of tan δ, the loss factor, an indication of the absorption of mechanical energy within the sample as the temperature increased at constant frequency and fixed strain. The PL-DMTA head and a block diagram of the electronics are shown in figures 3.7 and 3.8. The instrument was ran in either dual-cantilever or shear mode.

3.3.1.1 Analysis using shear mode

With the shear clamp frame detached from the PL-DMTA head, see figure 3.9, two sample discs were placed into the shear clamp with an intervening aluminium disc. The samples were held finger tight using the screws situated in a horizontal plane with the samples. The clamp frame together with the sample discs were frozen in liquid nitrogen and the discs finally tightened in position while still frozen. The frame was then placed in the PL-DMTA head using the four fixing screws, the drive shaft released, and the environmental chamber positioned, locked into place using the three knurled nuts on the PL-DMTA bulkhead, and cooled to between -130 to -160°C depending on the sample, using

FIGURE 3.7

Polymer Laboratories Dynamic Thermal Mechanical Analyser

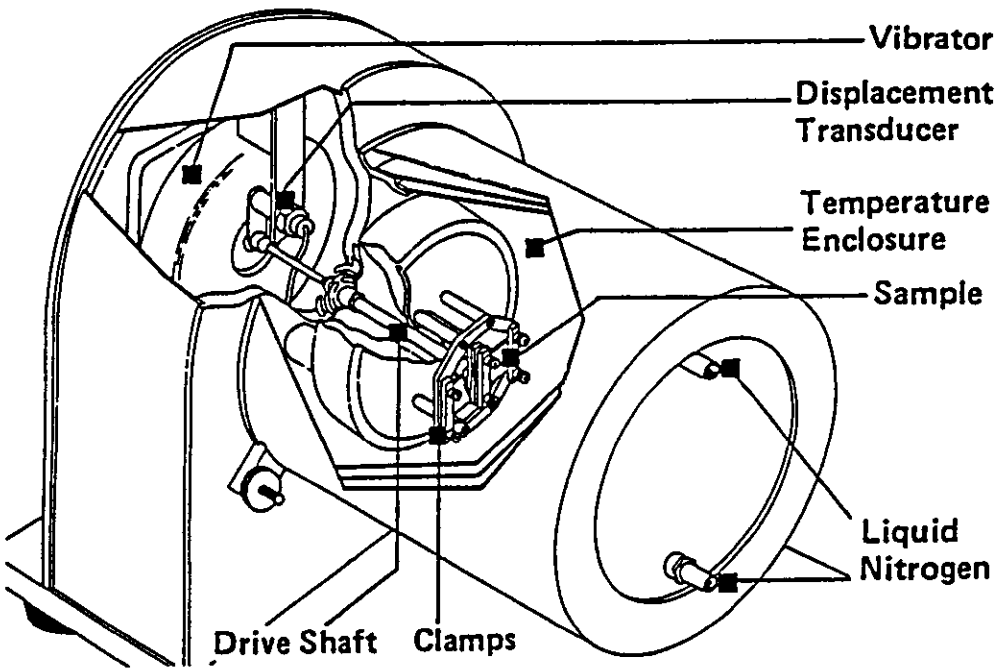

FIGURE 3.8

Block diagram of microprocessor unit

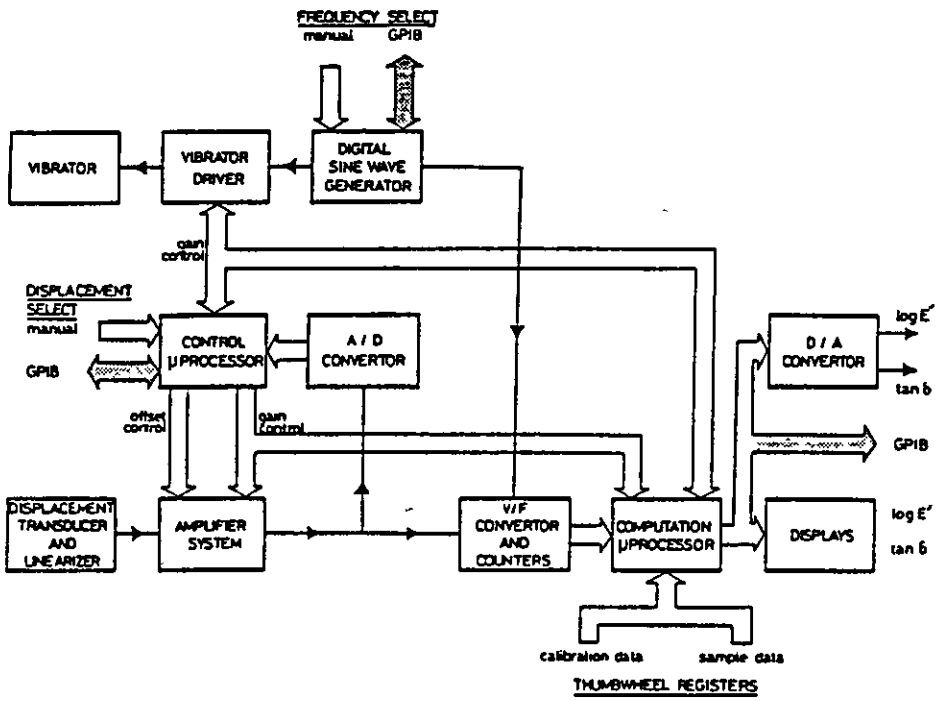

FIGURE 3.9

Shear clamp frame

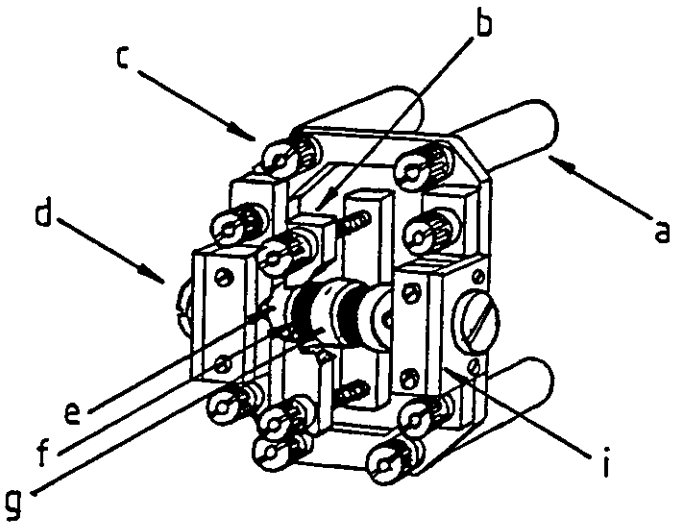

legend

a ceramic clamp supports

b central driven clamp

c clamp nuts

d sample screw

e mushroom

f sample

g central aluminium spacer

i mushroom carrier

liquid nitrogen being introduced into the cooling chamber via a glass funnel. The main criterion for the starting temperature was that the tanδ, the loss factor, reading should be as low as possible, i.e. around 0.0008. This indicated that side chain and chain backbone motions were frozen. The PL-DMTA proximetry head detects drive shaft displacement from a transducer situated at the rear of the drive shaft, as shown in figure 3.7. This transducer operates on a 2 mm air gap and requires, initially, to be manually adjusted to this gap. This is shown by the central L.E.D. in the vertical row of L.E.D.'s in the STATUS display on the PL-DMTA instrument shown in figure 3.10. The gap was altered by the knurled nut on the back of the spectrometer

FIGURE 3.10

Front panel of the microprocessor controlled analyser

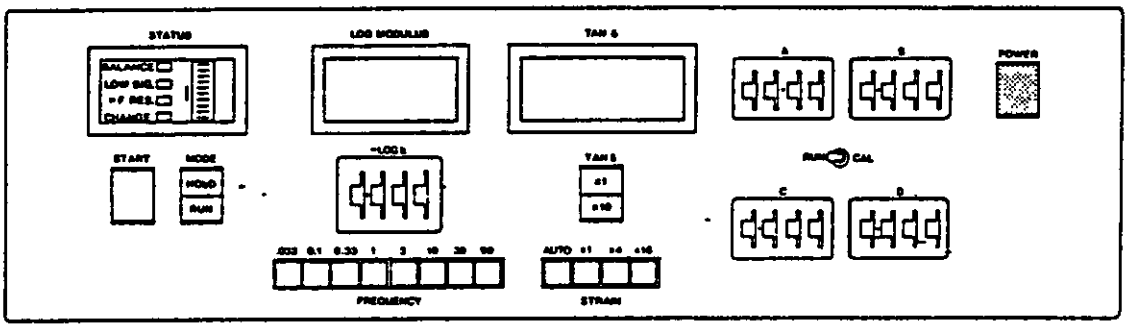

head. As soon as the required starting temperature was reached, as shown on the UTP L.E.D. display, the head was set into the running mode by depressing the MODE button on the PL-DMTA and vibrated at 1Hz. The temperature was raised, at a constant rate of 2°C/min. to 140°C, or to the point where the sample fractures, by setting the three thumbwheels temperatures. The heating rate for all the shear work was set at 2°C/min. The central thumbwheel on the UTP showing the minimum temperature was adjusted to be 4°C above that shown by the sample. The sample was allowed to warm up naturally to the minimum set temperature and when the two temperatures were identical the heating process was started by depressing the HEAT button followed by the RESET button. After a few seconds the lit "min" light on the LIMIT display extinguished indicating that the sample was heating at the required rate. The sample was heated at the set rate with the LOAD running light flashing intermittently as energy was inputted to the head until the maximum set temperature was reached, as shown in the UTP thumbwheel temperature setting. The PL-DMTA head was continually flushed with nitrogen gas to prevent the formation of ice on

the sample. The flow of gas over the sample was kept to a minimum to minimise heating effects on the sample by the gas. The UTP unit was reset by depressing the HEAT and RESET buttons, the spectrometer motor stopped, and the sample removed.

3.3.1.2 Analysis using dual-cantilever mode

The prepared samples were placed into the clamping frame situated on the proximetry head, as shown in figure 3.7. Care was taken to ensure the sample was installed squarely in the frame. The sample was secured in the frame using the four clamp nuts, compressing the sample evenly. The driven clamp was secured using the two nuts on the drive shaft. The transducer air gap was adjusted and the sample cooled as described in the previous section. The heating rate was set at 4°C/min and the sensitivity of the J.J. Lloyd chart recorder, model number PL 2500, was set to enable the acquisition of tan δ values lower than 0.1. The clamping arrangement is shown in figure 3.11.

It was possible to vary the length of the sample between the rigid and driven clamp by changing the size of the clamp frame and driven clamp. By using different combinations of frames and driven clamps it was possible to utilise a sample length between 2 and 16 mm (see section 3.3.1.1) to optimise the sample geometry although all the results discussed will have a sample length, L, of 10 mm unless otherwise stated.

FIGURE 3.11

Dual-cantilever clamp frame

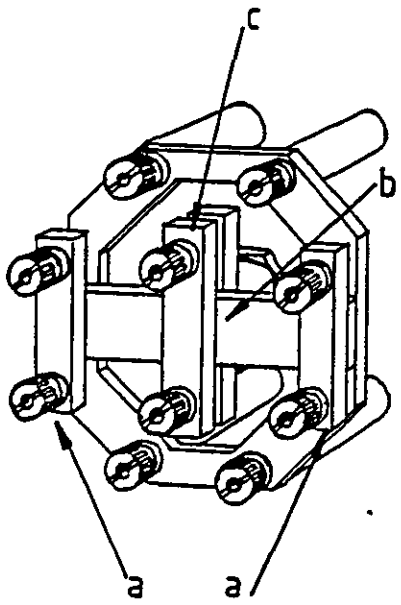

legend

a clamp bars

b sample

c central driven clamp

3.3.1.3 Principle of PL-DMTA operation

The use of dynamic mechanical thermal analysis allows information to be obtained when a polymer is subjected to non-intrusive stresses. For a polymer subjected to a sinusoidally varying stress of angular frequency (ω) the information obtained reflects the delayed response of the polymer to such a stress. If the polymer is believed to behave as a classical linear viscoelastic solid, damping characteristics can be obtained. Elastic materials when deformed by a stress will store the energy as potential energy which is recoverable in reforming its initial shape.

If no energy is lost, through heat, the material is acting as an ideal spring. Liquids on the other hand, flow if subjected to a stress. They dissipate the energy almost entirely as heat and hence they possess high damping characteristics.

Viscoelastic polymers, for example PVC, exhibit both elastic and damping properties. If a sinusoidal stress is applied to PVC, the resulting strain will also be sinusoidal and will be out of phase when there is energy dissipation or damping in the polymer. The resulting phase difference is known as the phase angle (δ) between the stress and the strain. The resulting strain can be described by complex notation in terms of the angular frequency (ω) and the maximum amplitude ε_o.

$$\varepsilon^* = \varepsilon_o \exp(i\omega t) \qquad (3.1)$$

where $\omega = 2\pi\nu$, the frequency is ν and $i=-1^{1/2}$.

The relation between the alternating stress and strain is written as

$$\sigma^* = \gamma^* E^*(\omega) \qquad (3.2)$$

where $E^*(\omega)$ is the frequency dependent complex dynamic modulus defined by

$$E^*(\omega) = E'(\omega) + iE''(\omega) \qquad (3.3)$$

Here, $E'(\omega)$ is the real part in phase with the strain called the storage modulus and $E''(\omega)$ is the loss

modulus.

The damping in the system or energy loss per cycle can be measured from the " loss tangent"; tan δ. This is a measure of the internal friction and is related to the complex moduli by

$$\tan \delta = (E''(\omega))/E'(\omega)) \qquad (3.4)$$

For this particular non-resonance forced vibration method the complex elastic modulus for a rectangular beam sample undergoing dual-cantilever deformation is given by

$$Fo \sin \omega t = M\ddot{x} + (\eta + S_n/\omega + kE''/\omega)\dot{x} + (S + kE')x \qquad (3.5)$$

where M is the mass of the vibrating system, (Kg), x is the linear displacement of the driven clamp, in metres; Fo is the maximum driving force, in newtons; $(S + iS_n)$, a machine constant, is a term to account for the complex rigidity of the suspension, $(E' + iE'')$ is the complex Youngs modulus of the specimen, t is time, ω is the angular frequency of the driving current, k is the sample geometry factor in metres; η is a viscous damping term (air damping) of the mechanical spectrometer.

The monitored drive current is proportional to the force applied to the sample and the transducer output voltage is proportional to the displacement. Accurate measurement of the relative amplitudes and of the output signals allows the instrument to compute the storage and loss moduli via

$$kE' = kA + M_l\omega^2 - S \qquad (3.6)$$

$$kE'' = kB + \omega S_n \qquad (3.7)$$

and hence tan δ by equation 3.4. Calibration terms relating to the instrument constants M, S and s_n measuring A and B without a sample at two different frequencies and with a sample of known modulus. The k constant, sometimes known as the geometry factor, is found for dual cantilever geometry

$$k = 2b(h/L)^3 \qquad (3.8)$$

where L is the length of each half between the faces of rigid and driven clamp, b is the breadth and h is the thickness. All measurements are taken in metres giving the geometry constant in metres. This figure is typically very small i.e. 3.159×10^{-3} and hence converted to -log k which converts the constant to a more manageable number in this example 3.500

For shear sandwich geometry E^* is replaced by G^* (complex shear modulus) in equation 3.3 and the geometrical factor becomes

$$k = 2Q/L \qquad (3.9)$$

where Q is the cross-sectional area of each disc and L is the sample length as previously defined.

3.3.1.4 Instrument calibration

Calibration of the PL-DMTA instrument was accomplished by running the instrument without a sample present at 1 Hz with the instrument set in calibration mode using the central calibration switch on the front panel as shown in figure 3.10. In accordance with the PL-DMTA operation manual[146] the readings obtained in the log modulus and tan δ windows were entered in to the thumbwheel switches A and B respectivly. The instrument was set to run at 90 Hz and the new reading in the log modulus window was entered into the thumbwheel switch C. With a PVC calibration bar[147], supplied by Polymer Laboratories fitted in dual cantilever mode and running at 1 Hz, the thumbwheel D was adjusted to give the correct modulus reading at room temperature. This calibration was carried out on a fortnightly basis. A complete scan using a PVC calibration sample was carried out every six months.

3.3.2 Analysis by differential scanning calorimetry

Differential scanning calorimetry (DSC) was used to measure the T_g of the swollen and dry regions in selected PVC/swelling agent systems. The T_g of the swelling agents were also determined. The systems chosen were those that exhibited clear liquid fronts.

The Perkin Elmer differential scanning calorimeter, (model: DSC-4), fitted with the liquid nitrogen subambient accessory (part no. 0419-0295), was used in conjunction with a Perkin Elmer System 4 Microcomputer Controller. This

controller was used to program the DSC-4 from the initial temperature to the final temperature. The subambient accessory allowed the use of the temperature range -170°C to 200°C.

Two platinum alloy "cups" functioned as the sample holders in the DSC-4. The reference sample pan was placed in the right hand cup, the sample pan in the left hand cup. Owing to the volatility of the swelling agents the sample pans were stainless steel with reusable copper sealing rings. The cups were mounted on platinum-iridium posts and the heater and sensor leads to each sample holder were made of thin platinum ribbons. Each sample holder was held in a cavity, within the sample enclosure, insulated from draughts, any exhaust fumes from the samples under investigation being removed by a helium purge gas. Cooling was provided by an aluminium "cold-finger", attached to the bottom of the sample enclosure sitting in a liquid nitrogen bath.

The amount of power required to maintain the sample holder temperature to the temperature of the reference holder during a heating or cooling experiment was recorded together with the actual sample temperature on a J.J. Lloyd XYY chart recorder, model number PL 2500.

Normal conventions for presenting data will be adhered to in this work. Typical DSC traces, for a glass transition, are shown in figure 3.12. Scanning starts below the polymer's T_g and proceeds from left to right. The starting transient is a machine characteristic due to the pans coming under temperature control. The shift in baseline occurred as a result of an increase in the heat

FIGURE 3.12

A typical DSC thermogram produced on heating uPVC swollen with dimethylphthalate at a rate of 40 °C/min showing principle of T_g measurement

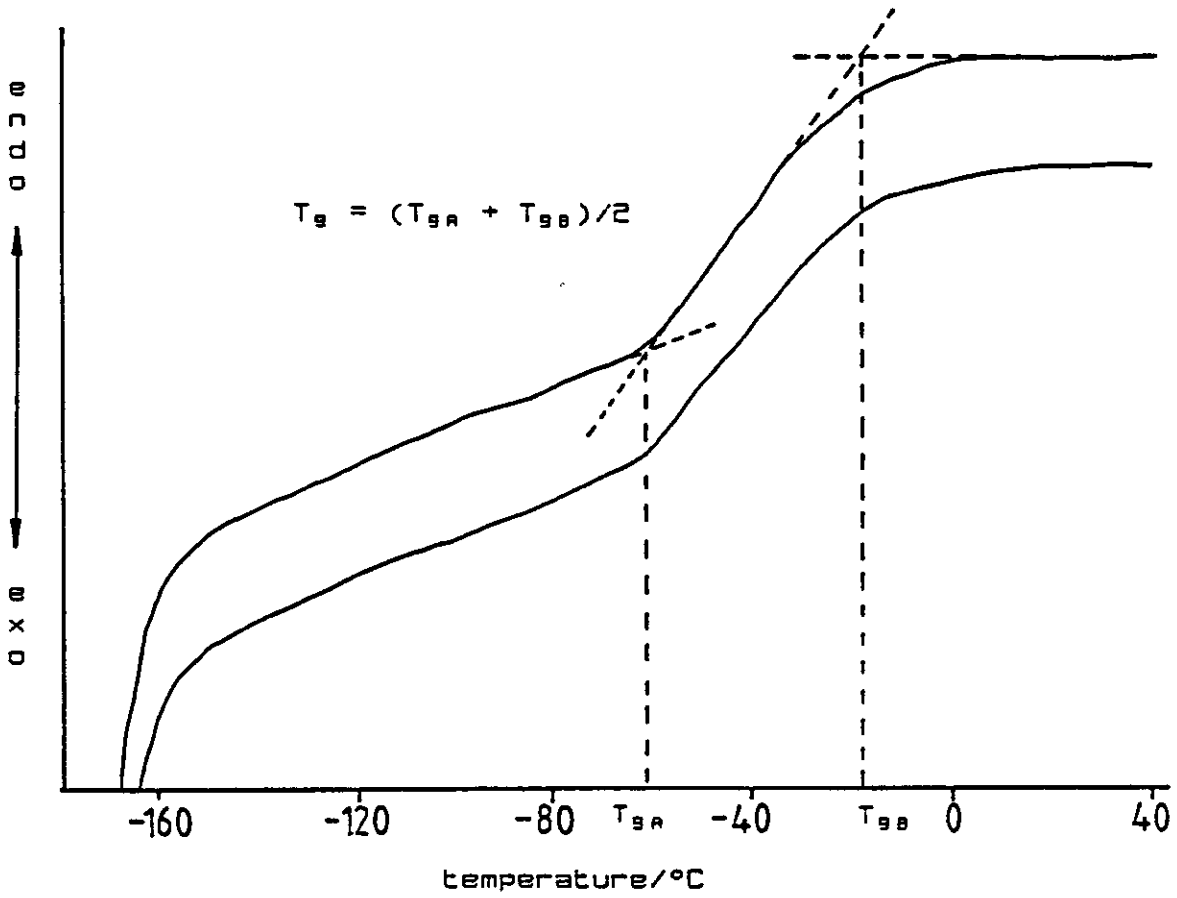

capacity of the polymer, which was characteristic of a polymer changing from a glass to a rubber. The T_g was defined, in this work, as the midpoint of the straight line drawn between the onset and conclusion of this baseline shift and is the average of at least two consecutive runs on the same sample excluding the first run. The overall downward curvature of the baseline above the T_g was due, partly to the physical contact between polymer and platinum holder, and to differences in the platinum sample holders

which was minimised prior to calibration; programming, with empty sample holders, over the temperature range of interest.

3.3.3 Analysis of diffusion coefficients

Data acquisition for the analysis of diffusion coefficients of swelling agents into PVC plaques has been restricted to situations where a clear measurable liquid front has been observed. The data used have therefore been obtained using liquid sorption. Liquid sorption was carried out at two temperatures 30°C and 60°C unless otherwise stated. The swelling agents and plasticizers used are shown in table 3.4. The methodology concerning data acquisition has already been dealt with in section 3.2.1 for the experiments conducted at 60°C. The measurement of the core thickness with these systems allowed full analysis of both the diffusion coefficient and liquid front movement using the methods described by Kwei et al.[25]. The lower temperature experiments were restricted to the measurement of mass uptake only.

TABLE 3.4

Liquids employed for sorption analysis.

sorption at 30°C	sorption at 60°C
propanone	propanone
dimethylbenzene	dimethylbenzene
ethylbenzene	ethylbenzene
	nitroethane
	fluorobenzene
2-nitropropane	
methylbenzene	
benzene	
1-nitrobutane	
chlorobenzene	
1,2-dichlorobenzene	
	butylbenzylphthalate
	dioctylphthalate
	dimethylphthalate
	Cereclor S52

CHAPTER 4 - RESULTS

4.1 DIFFUSION OF ORGANIC LIQUIDS INTO PVC PLAQUES

4.1.1 Classical treatment of diffusion into a plane sheet

The diffusion of organic liquids into uPVC plaques was carried out at two different temperatures, 30 and 60°C. In order to compare experiments the mass uptake of liquid was normalised to the amount of liquid sorbed per gram of uPVC. The experiments at 30°C were run until the uptake of liquid was thought to have reached equilibrium. The mass uptake at time t, M_T, per gram of uPVC at 30°C for the various liquids employed is shown in figure 4.1. The numbers in figure 4.1 refer to the liquids in table 4.1. It is clearly seen that in some liquid-PVC systems equilibrium uptake may not have been reached, in particular for the 1,2-dichloroethane and 1-nitrobutane systems, curve numbers 1 and 4 respectively.

Sorption isotherms showing the dependence of M_T/M_∞ on the square root of time, for some of the liquids shown in tables 3.1 to 3.3, are given in figures 4.2 and 4.3 for 30 and 60°C respectively, where the mass uptake of liquid per gram of uPVC at time t is given as M_T and M_∞ is the total uptake of liquid per gram at equilibrium sorption of the

FIGURE 4.1

Mass uptake per unit area of uPVC with respect to time; the numbers refer to the liquids in table 4.1

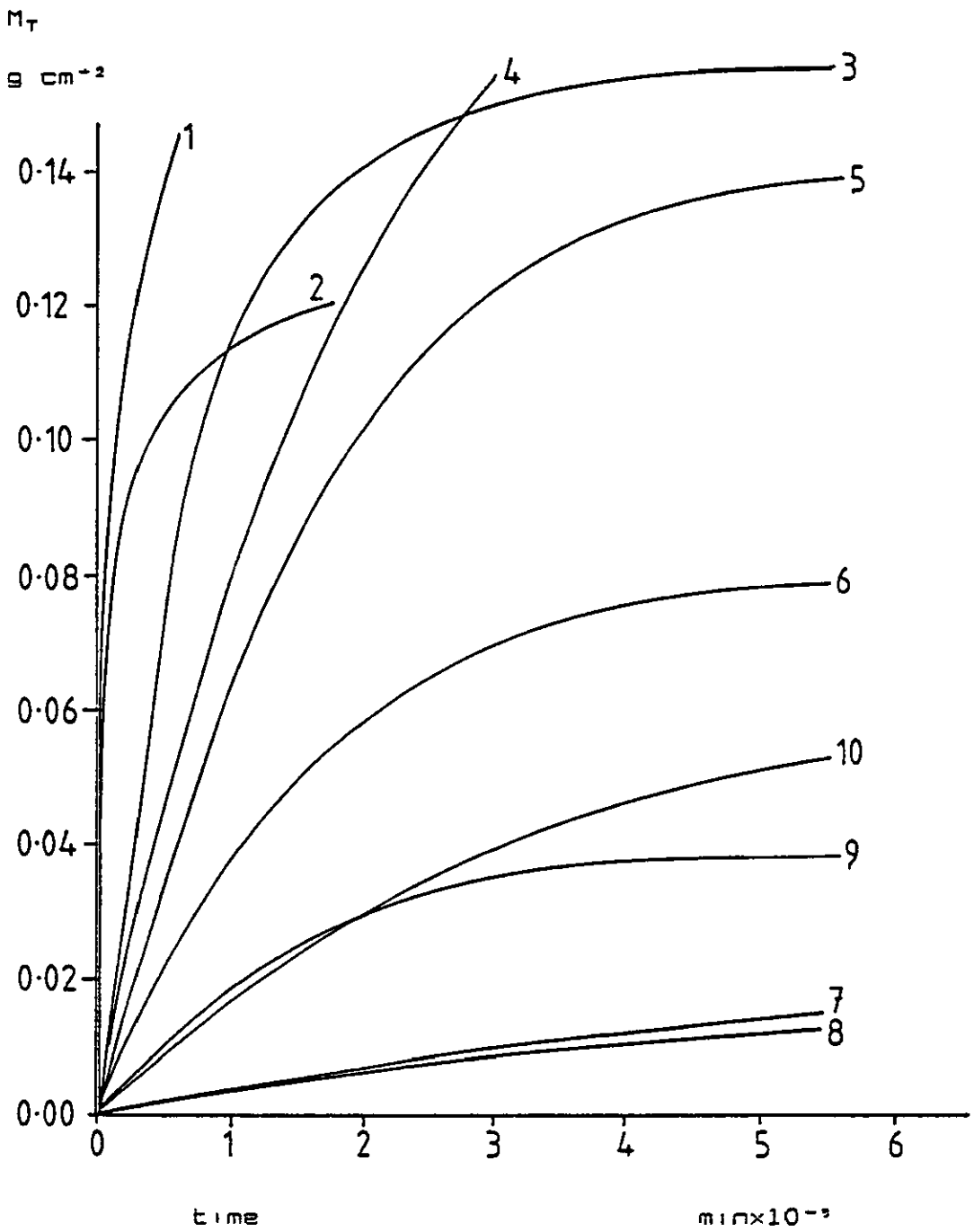

TABLE 4.1

Initial diffusion coefficients for various liquids sorbing into PVC at 30°C

Number*	liquid	D $\times 10^{10}$ $cm^2 s^{-1}$
1	1,2-dichloroethane	35.80
2	propanone	8.27
3	chlorobenzene	1.99
4	nitrobutane	1.03
5	2-nitropropane	0.81
6	fluorobenzene	0.62
7	dimethylbenzene	0.62
8	ethylbenzene	0.62
9	benzene	0.46
10	methylbenzene	0.26

*liquid numbers refer to the curves in figures 4.1 and 4.2

FIGURE 4.2

Sorption isotherms for various liquid in uPVC plaques at 30°C; the numbers refer to liquids in table 4.1

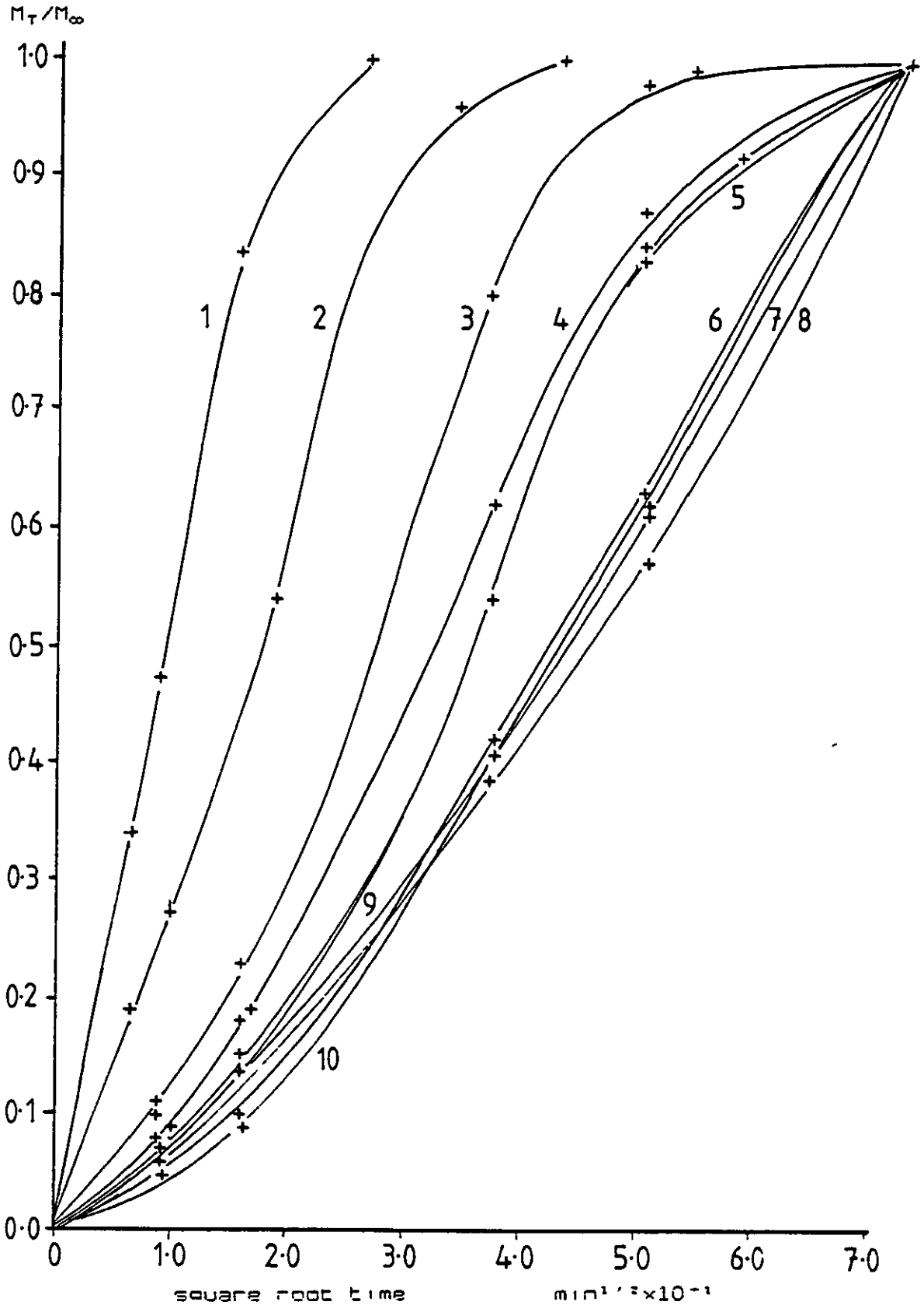

FIGURE 4.3

Polynomial regression[149] fit on curves showing sorption isotherms of various liquids into PVC plaques at 60°C

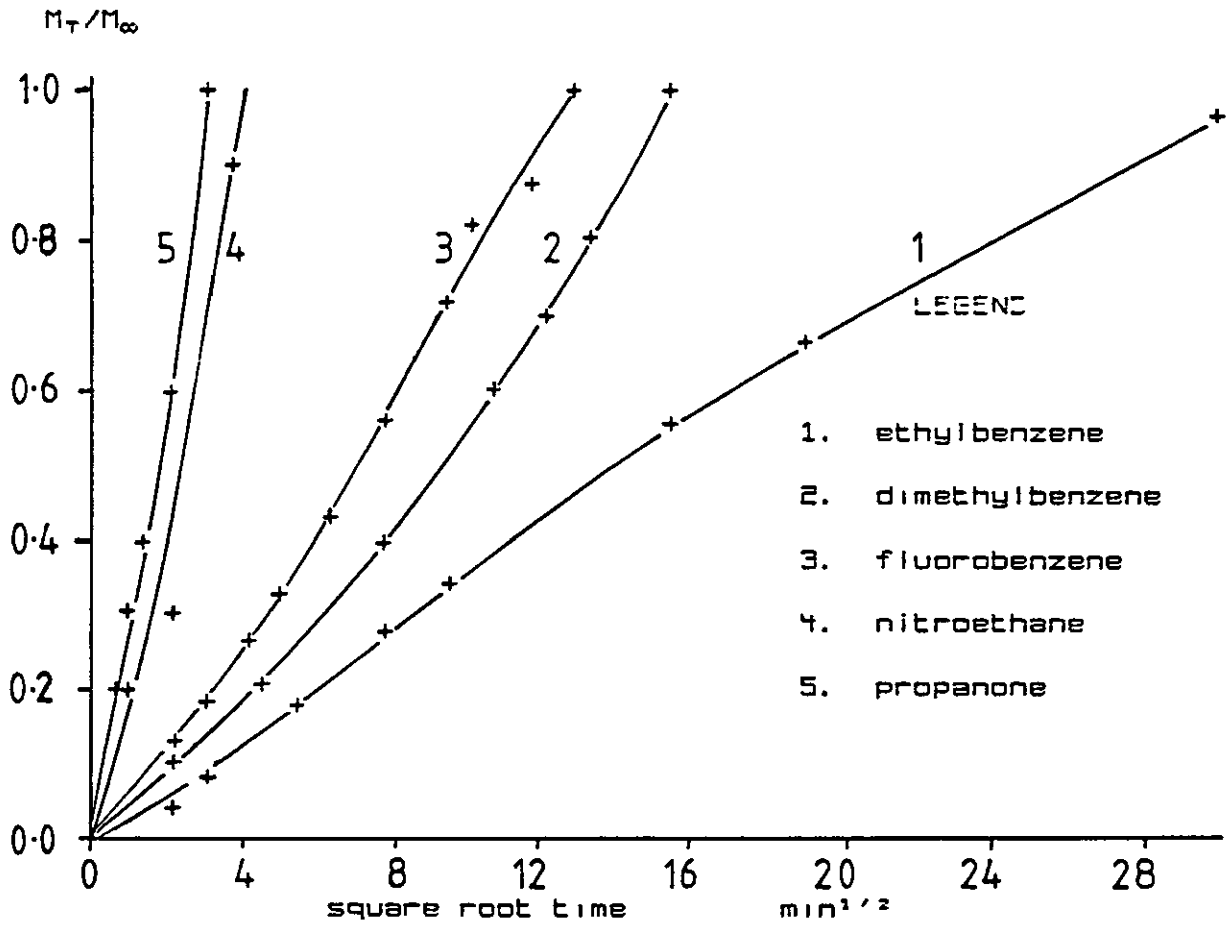

whole plaque. The numbers on the curves in figure 4.2 refer to the liquids in table 4.1. The initial diffusion coefficients for the sorption of the liquids at 30°C are given in table 4.1. The diffusion coefficients were calculated from the initial slopes of the plots for mass uptake for the first 100 mins in figure 4.2 using equation 2.119. Fickian sorption behaviour was assumed to be occurring during the first 100 mins of sorption due to the absence of a liquid front moving through the polymer. The original thickness of the plaques employed was around 2.35 mm. The penetration of liquid after 100 minutes would not have been very great. Indeed, as it will be shown later the extent of penetration, for example, for fluorobenzene sorption at 60°C, was as little as 0.007 mm after 100 mins but for propanone, under the same conditions, penetration was calculated to be 3.3 mm. The sample thickness employed in equation 2.119 was assumed therefore not to be the total plaque thickness (2.35 mm) but an average approximate value (1.50 mm). No swollen layer thickness measurements were made for 30°C sorption systems. Although the absolute values of D in table 4.1 are therefore in doubt, the data serve to indicate the relative diffusivity of the liquids.

There are no reported values of D for liquids in the literature which use a straight Fickian analysis for liquid diffusion into a moulded uPVC plaque. However, D has been calculated for the liquid sorption at 30°C for a small number of liquids by examining the distance of penetration as a function of time[21]. The values obtained from the literature, using liquid sorption, are compared with values obtained with this work where liquids are common to both in

TABLE 4.2

Initial diffusion coefficient values for liquid sorption, at 30°C, compared with literature reported values

liquid	D $cm^2 s^{-1}$	
	this work	literature values Lapcik[21]
	$\times 10^{10}$	$\times 10^{7}$
1,2-dichloroethane	35.80	11.50
propanone	8.27	-----
chlorobenzene	1.99	4.93
fluorobenzene	0.81	1.45

table 4.2. The difficulty in comparing D values is the difference in material type, structure, thermal history, and mode of experiments. The samples used by Lapcik et al.[21] were produced by solvent casting a fractionated emulsion PVC resin into a 0.1 mm thick film, whereas the samples in this work were produced by compression moulding of suspension polymerised grains. The main observation possible is that the ranking order with respect to D is the same as the literature values. It was assumed that the sample thickness did not change during the first 100 mins. Diffusion coefficients for the isotherms at 60°C were not computed, except for fluorobenzene, see section 5.1.1, due to the observation of a solvent front and a rapid increase in the overall sample thickness.

From figure 4.1 the concentration of liquid, at equilibrium (or long time interval) for sorption at 30°C, was calculated. The density of unswollen uPVC is known, (ρ = 1.369 g cm^{-3}) and this allows the computation of liquid content per unit volume of uPVC at equilibrium (or long time interval). Data for the equilibrium (or long time interval) concentration expressed as C_∞ in units g cm^{-3}, for systems at 30°C are shown in table 4.3. It is evident from figure 4.1 that equilibrium sorption has not been obtained for some systems, for 1,2-dichloroethane and 1-nitrobutane the equilibrium concentration values were calculated from the last recorded data point for these two systems. 1,2-dichloroethane and 1-nitroethane sorption lead to disintegration of the plaque.

TABLE 4.3

Liquid concentration at equilibrium (or long time) swelling in complete plaque (30°C) and equilibrium swelling within the swollen layer (60°C)

Liquid	system at 30°C g cm^{-3}	system at 60°C g cm^{-3}
nitrobutane	1.21	----
1,2-dichlorobenzene	1.12	----
chlorobenzene	1.12	----
2-nitropropane	1.01	----
propanone	0.88	0.28
fluorobenzene	0.48	0.32
methylbenzene	0.39	----
benzene	0.27	----
dimethylbenzene	0.11	0.22
ethylbenzene	0.08	0.25
nitroethane	----	0.48
BBP	----	0.48
DOP	----	0.30
Cereclor 552	----	0.05
DMP	----	0.36

4.1.2 The Case II contribution to diffusion into a system which swells

4.1.2.1 Equilibrium swelling in the swollen layer

In order to make use of equation 2.123 and to model the mass uptake with respect to time, taking the effect of case II sorption into account, the surface equilibrium concentration was required. The equilibrium concentration, C_o g cm^{-3}, of liquid in the polymer was taken as being equal to the concentration of liquid in the surface layer for samples displaying a picture frame (see figures 3.2 and 3.3).

Since the liquid sorption experiments at 60°C were not taken to a position where the whole plaque was at equilibrium, as in the case of most of the 30°C systems, calculation of C_o was not so straightforward as for the systems at 30°C already discussed. It was possible however to plot the mol fraction content of liquid in the swollen layer with respect to time and evaluate an equilibrium mol fraction content of liquid in the swollen layer. The mol fraction content was calculated from:-

$$\text{Mol fraction content} = \frac{\text{diluent mass/diluent MM}}{\text{diluent mass/diluent MM} + 0.0155} \qquad (4.1)$$

where 0.0155 is the number of moles of 1 g of uPVC. The liquid sorbed is only present in the outer swollen layer and by evaluating the respective volume fractions of swollen and unswollen portions in the sample, using core thickness

measurements, the molar content of liquid in the swollen region was calculated. Plots describing the mol fraction of liquid in the swollen layer, at 60°C, are show in figures 4.4 to 4.10, the dotted curves being a plot through the averaged mol fraction contents in the swollen layer. The maximum values attained by these dotted curves, are shown by the symbol, M_f, in figures 4.4 to 4.10, and were the mol fraction values employed in calculating C_o values. This M_f value was transformed into a concentration term, C_o using the method outlined in Appendix 1. The C_o values obtained, using the methods described above, for liquid sorption experiments at 30 and 60°C are shown in table 4.3.

4.1.2.2 Normalised mass uptake of swelling liquids in poly (vinylchloride) plaques

All the liquid sorption experiments, plotted as a function of mass uptake per initial surface area of material with respect to time, are shown in figures 4.11 to 4.18. The plots describe the uptake of liquids into uPVC plaques at 60°C. Each point in each figure signifies a different experiment, hence the normalisation of the data to mass uptake per surface area. The surface area of 1 gram of unswollen PVC is 4.886 cm^2, division of the mass uptake of liquid per gram of uPVC by 4.886 cm^2 yields the mass uptake per unit surface area. M_T in figures 4.11 to 4.18 denotes the mass uptake, per unit surface area of uPVC, of liquid in the sample expressed in units, g cm^{-2}. Examination of the least-squares linear regression fit on the data, shown by the dotted line, gave an unrealistic Y-intercept value,

FIGURE 4.4

Equilibrium swelling of ethylbenzene in PVC at 60°C

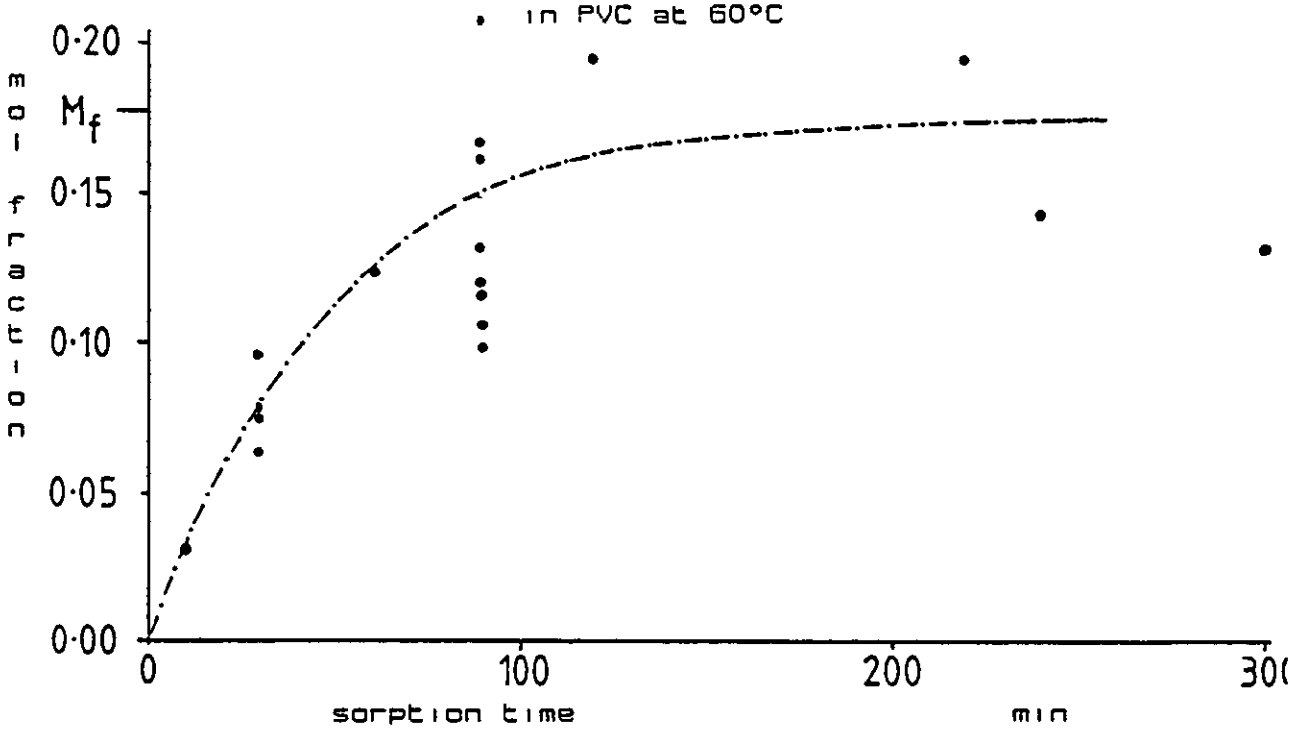

FIGURE 4.5

Equilibrium swelling of fluorobenzene in PVC at 60°C

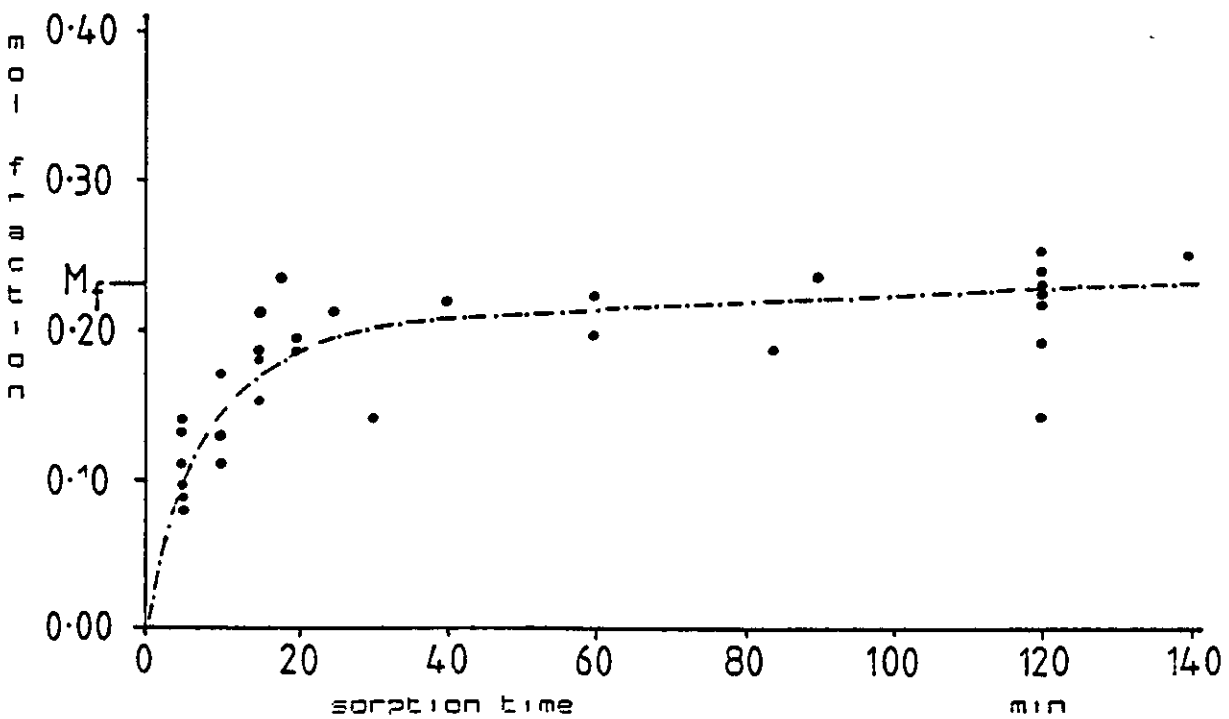

FIGURE 4.6

Equilibrium swelling of propanone in PVC at 60°C

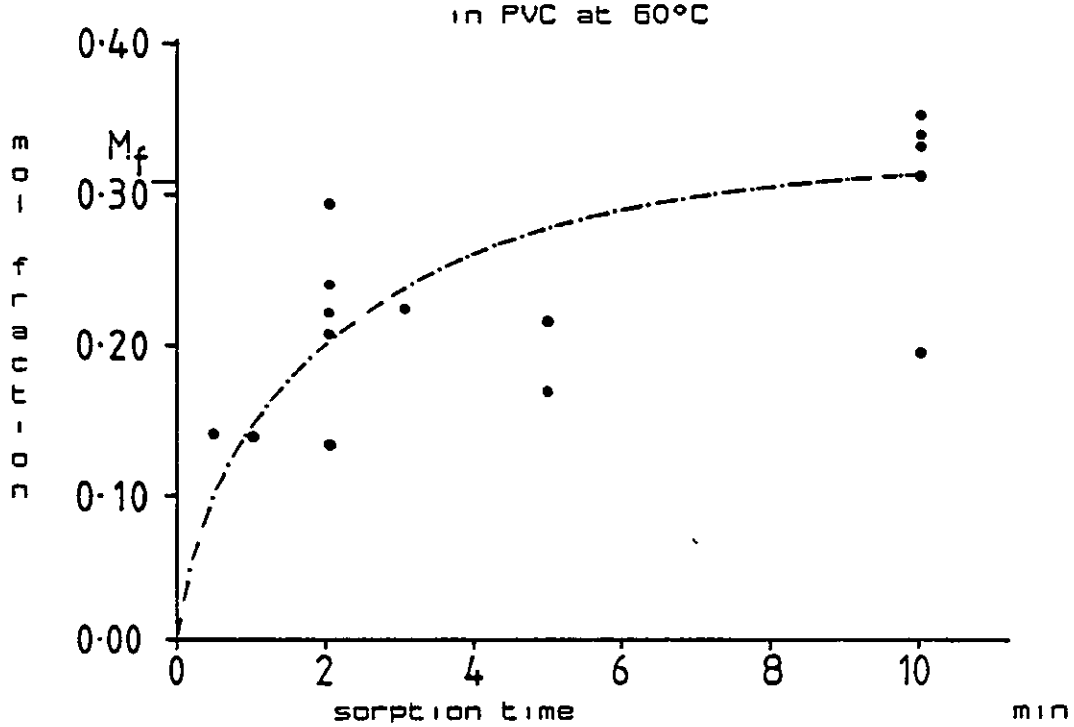

FIGURE 4.7

Equilibrium swelling of nitroethane in PVC at 60°C

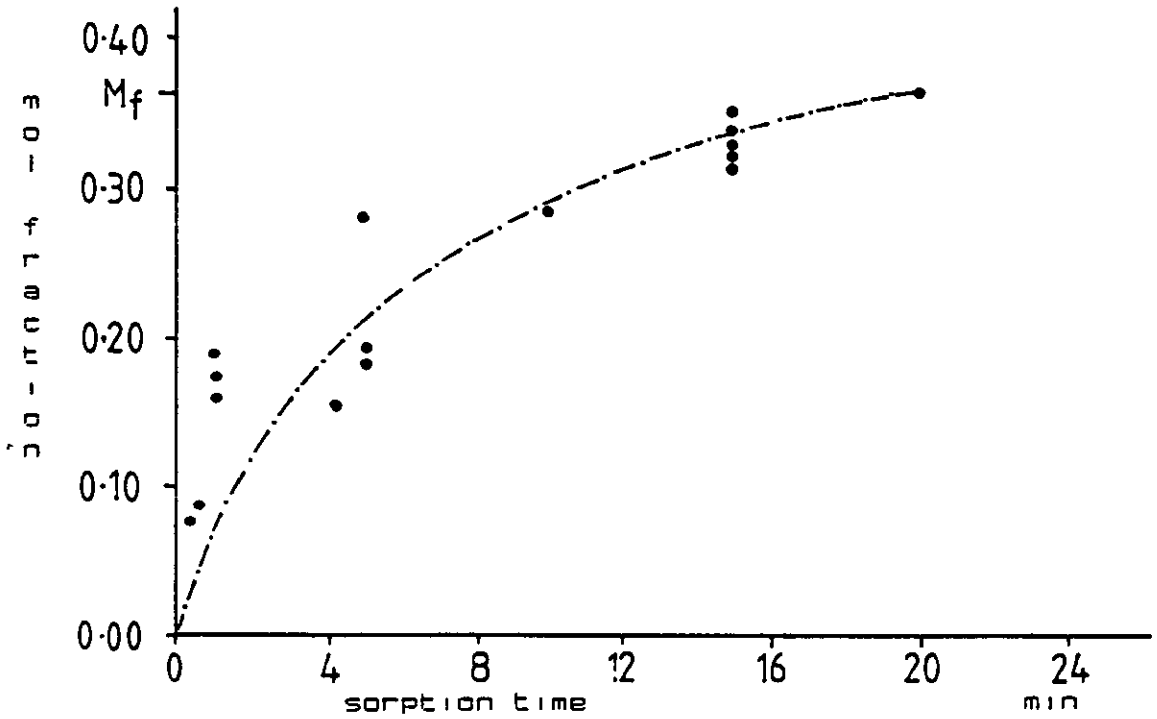

FIGURE 4.8

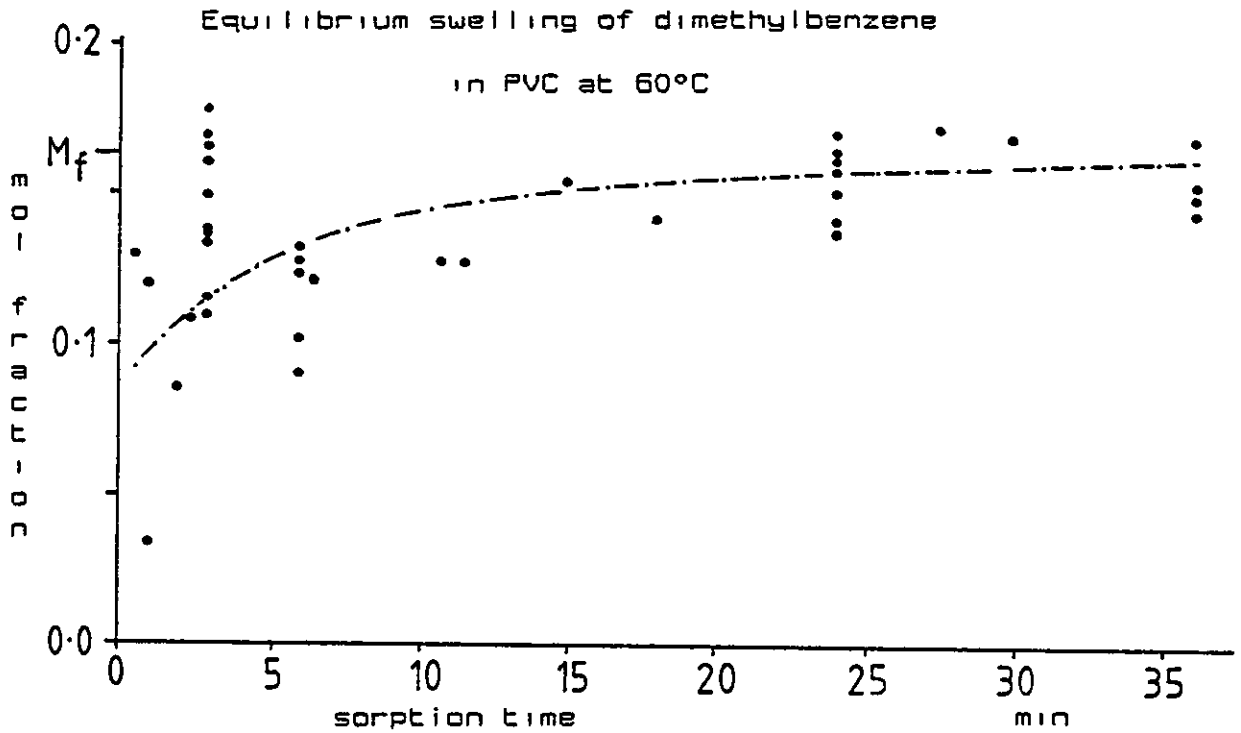

FIGURE 4.9

Equilibrium swelling of DOP (⊙) and Cereclor S52 (●)
plasticizer in PVC at 60°C

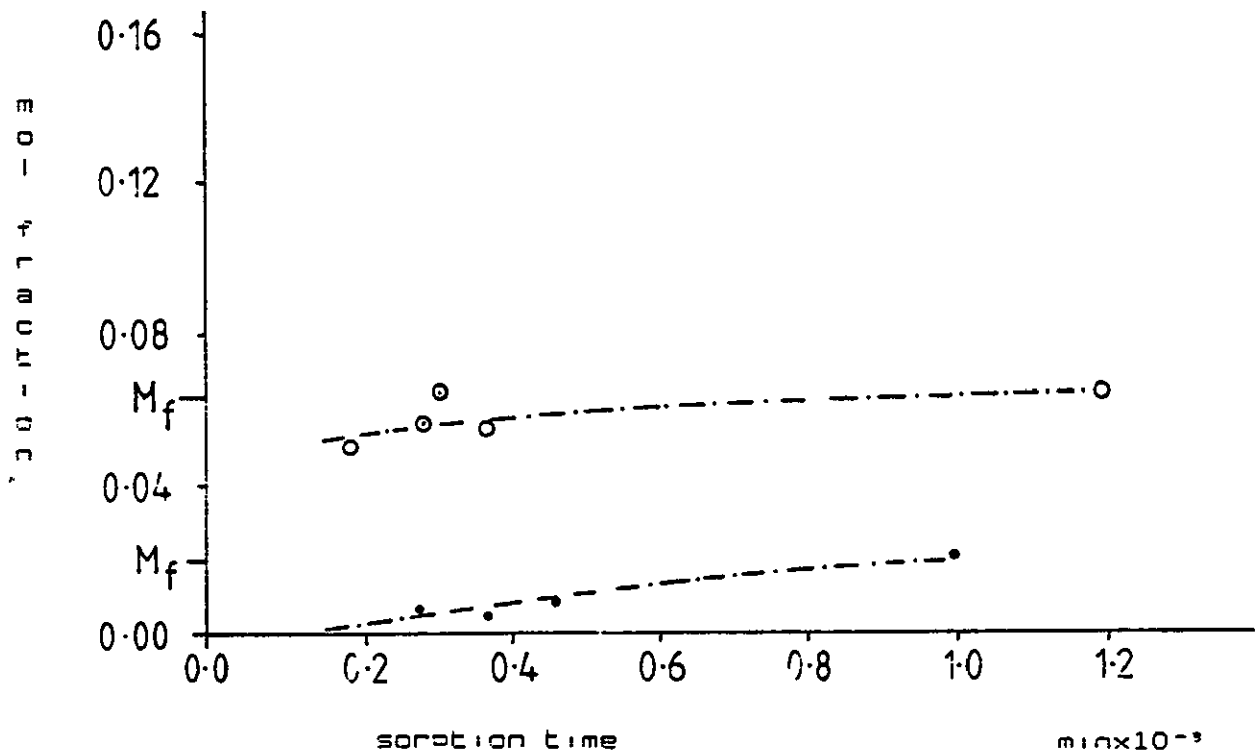

FIGURE 4.10

Equilibrium swelling of

BBP plasticizer in PVC at 60°C

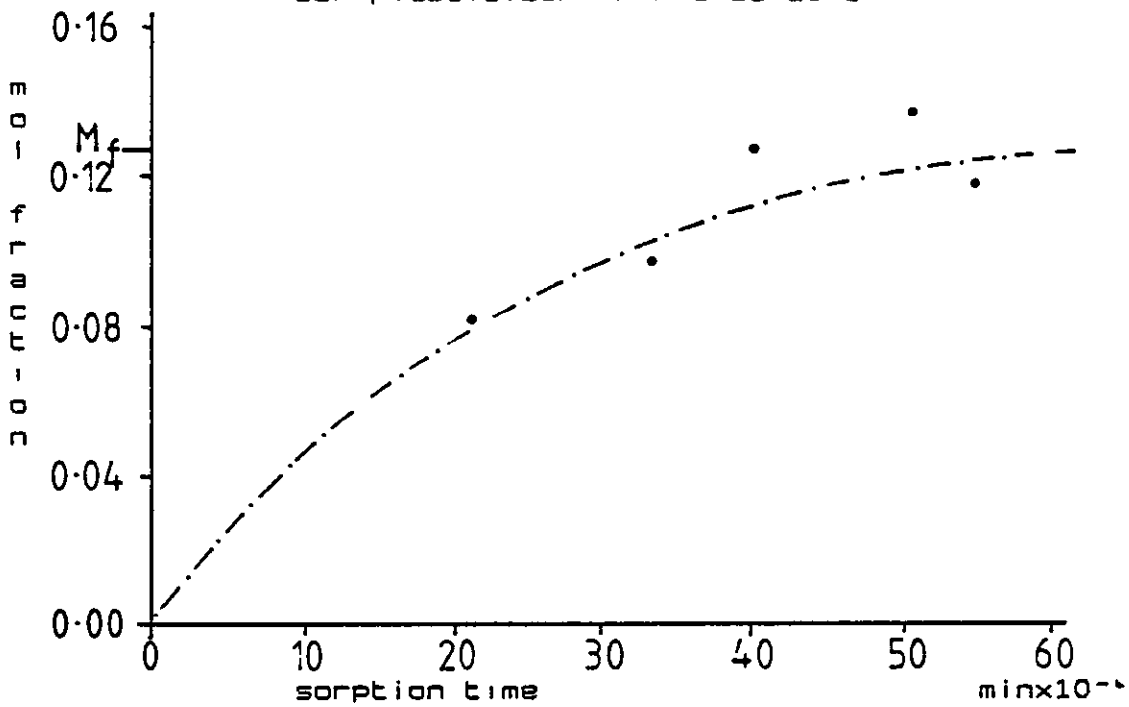

suggesting the presence of diluent at time zero. The least-squares fit was recalculated with zero mass uptake at time zero. Table 4.4 shows the Y-intercept and slope of the least-squares linear regression fit on the data and compares the resulting difference in the values when the zero mass uptake at time zero data point was included. The effect of including the "zero data" point on the values of slope and Y-intercept are small and subsequent calculations using data from table 4.4. will use the slope and Y-intercept values calculated without the zero data point.

4.1.2.3 The measurement of the swelling agent-polymer interface

The measurement of the unswollen PVC core thickness was accomplished by microscopy using a thin cross-sectional slice of polymer cut from the swollen plaque. For each plaque three core measurements were made. The standard deviation in original thickness of a plaque from three micrometer measurements is 0.03 mm. This would imply that the standard deviation of the core thickness would be the same. In practice, a standard deviation of 0.04 mm was found by taking three measurements from each of three slices, in systems where the swelling agent-uPVC boundary was clearly defined. The increase in the standard deviation was attributed to the experimental measurement using the graticule. This results in a 2% error in the measurement of the volume fraction of the swollen outer layer or dry inner core, and hence an error of the same magnitude in the swollen layer liquid content. However, in the situations

FIGURE 4.11

Diffusion of propanone into uPVC at 56°C

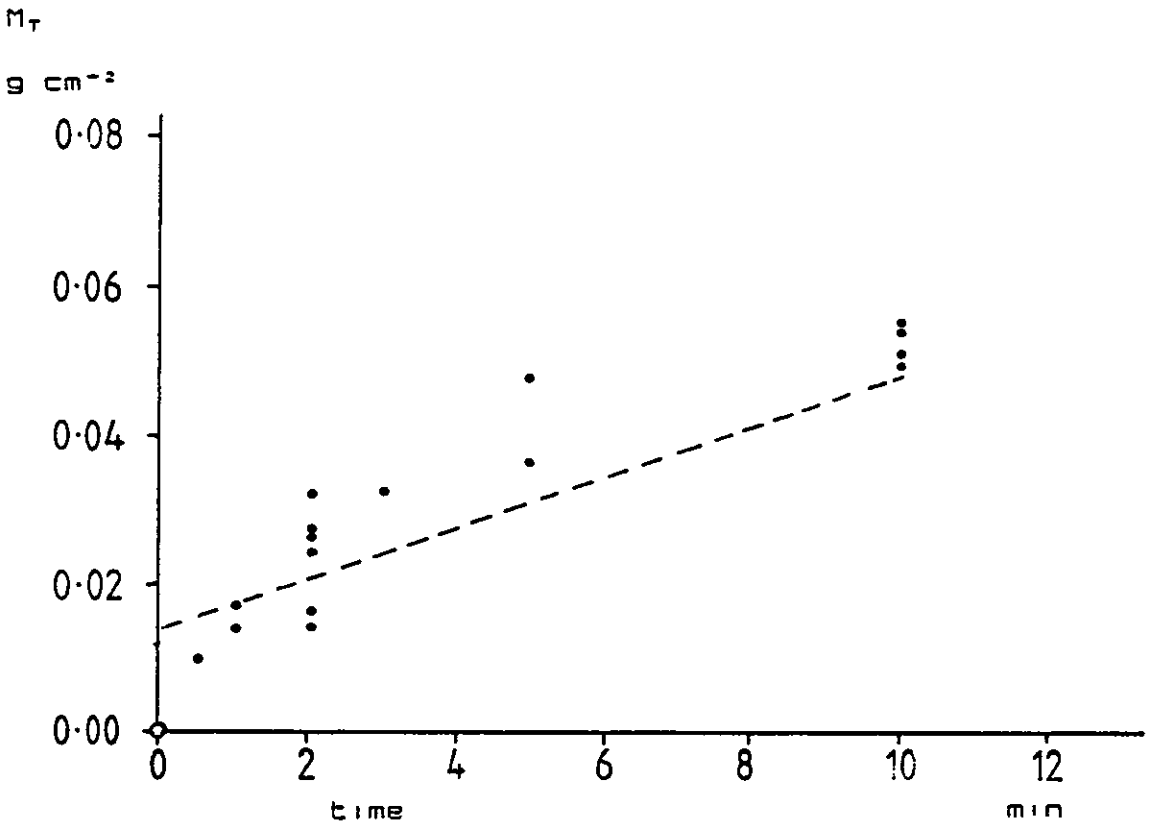

FIGURE 4.12

Diffusion of ethylbenzene into uPVC at 60°C

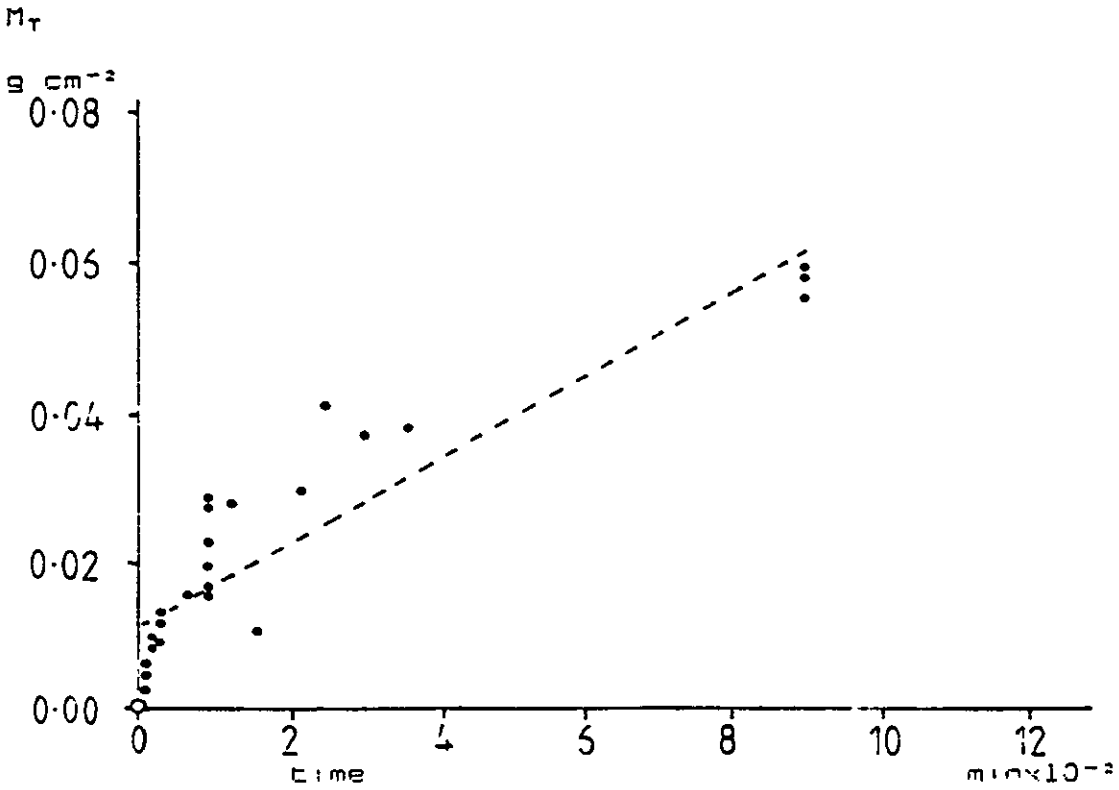

FIGURE 4.13

Diffusion of dimethylbenzene into uPVC at 60°C

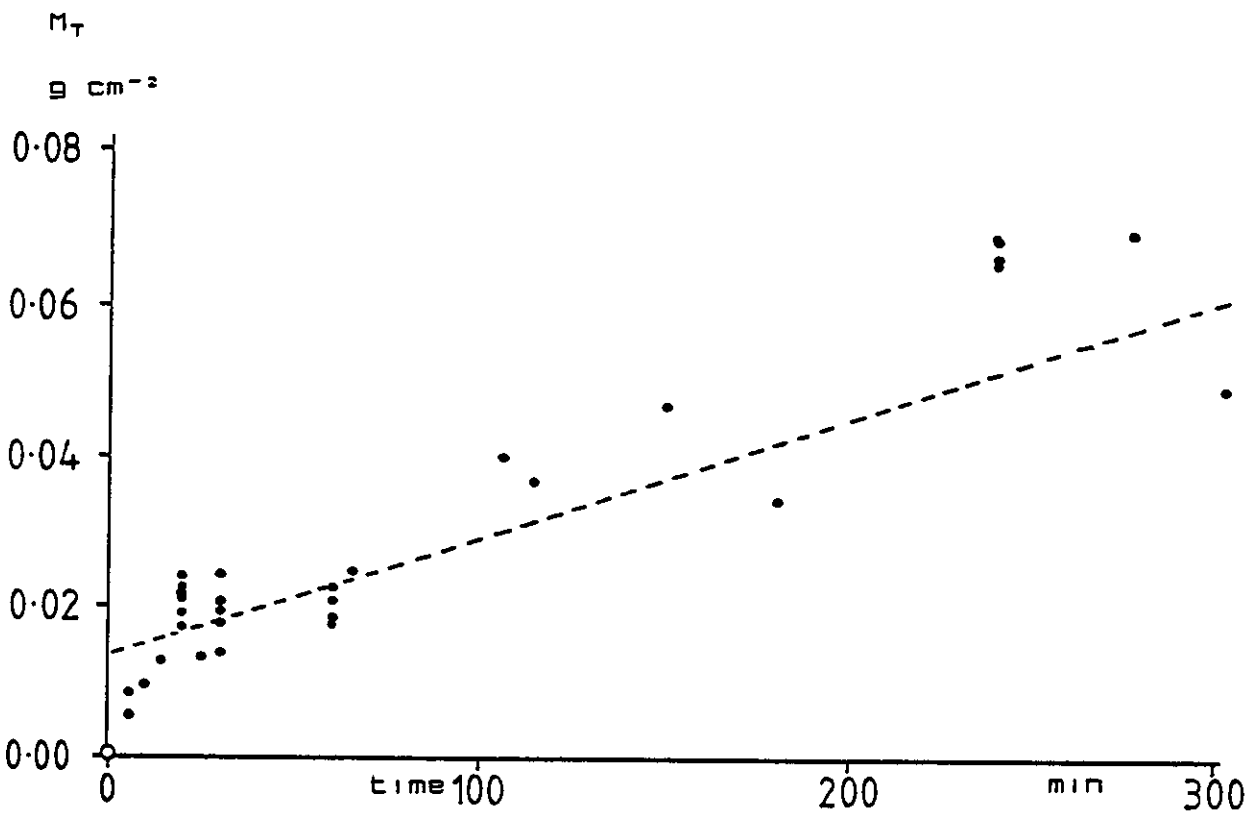

FIGURE 4.14

Diffusion of nitroethane into uPVC at 60°C

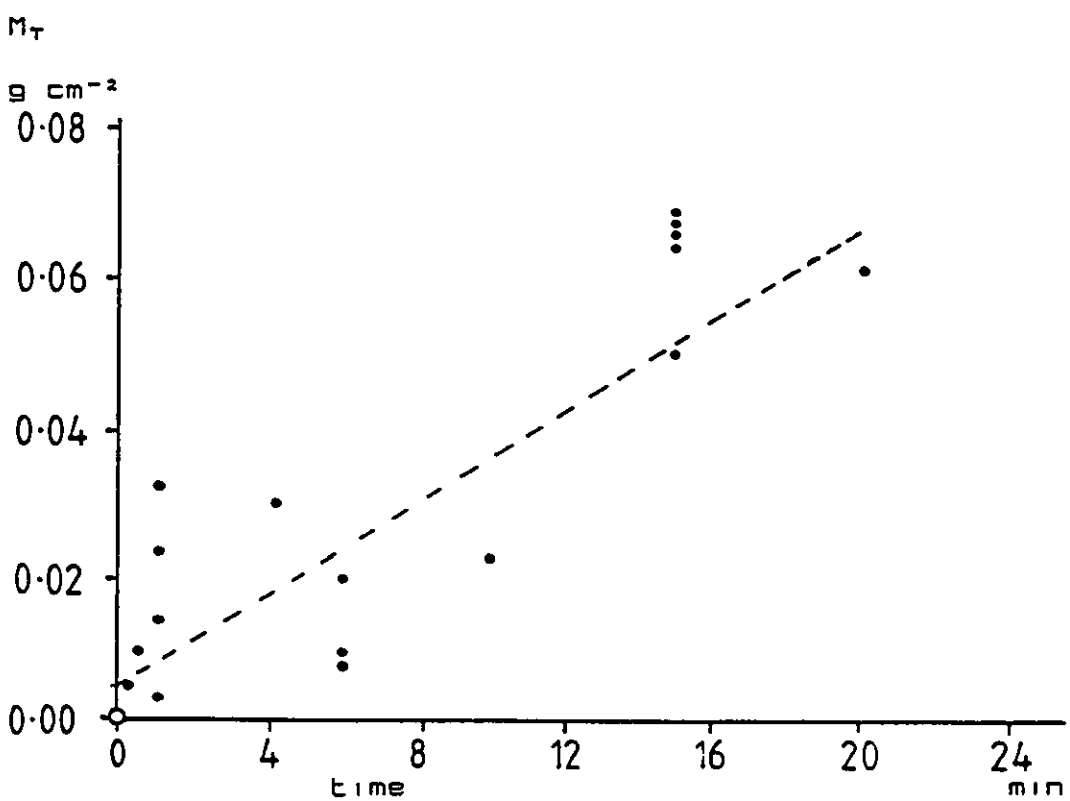

FIGURE 4.15

Diffusion of fluorobenzene into uPVC at 60°C

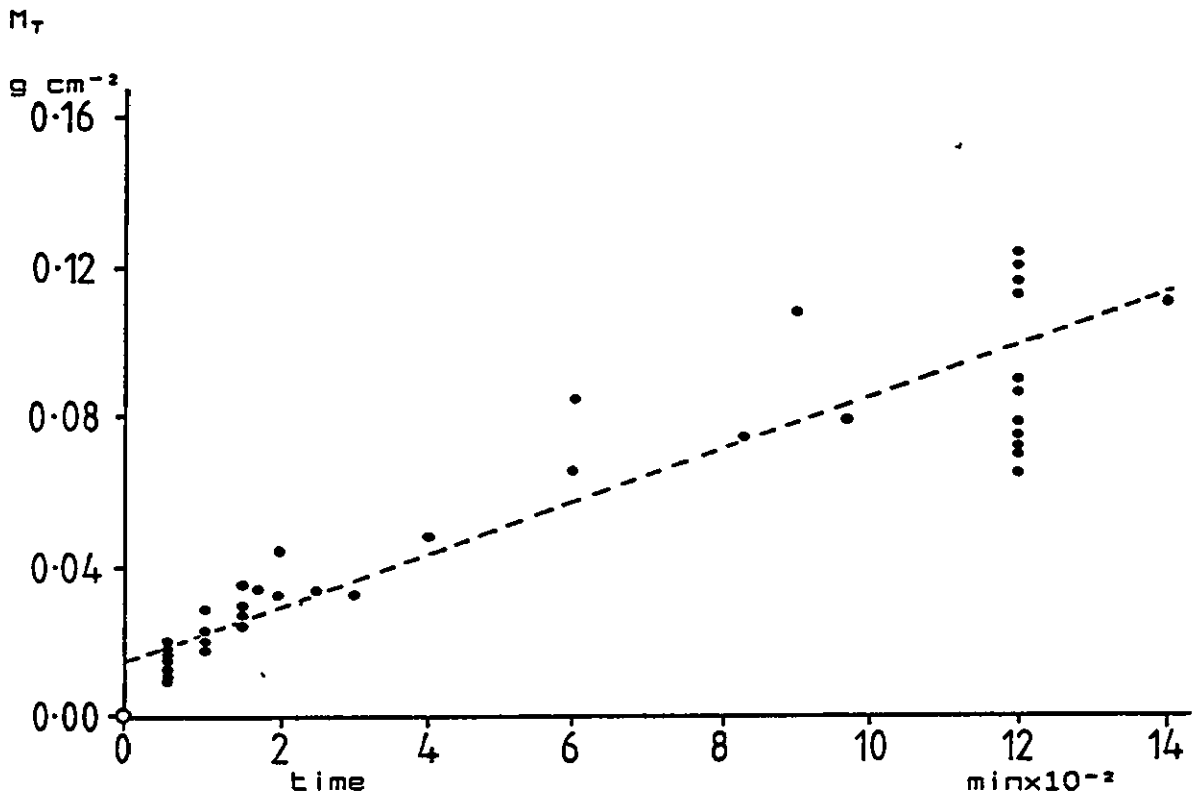

FIGURE 4.16

Diffusion of BBP (•) and DMP (o) plasticizers into uPVC at 60°C

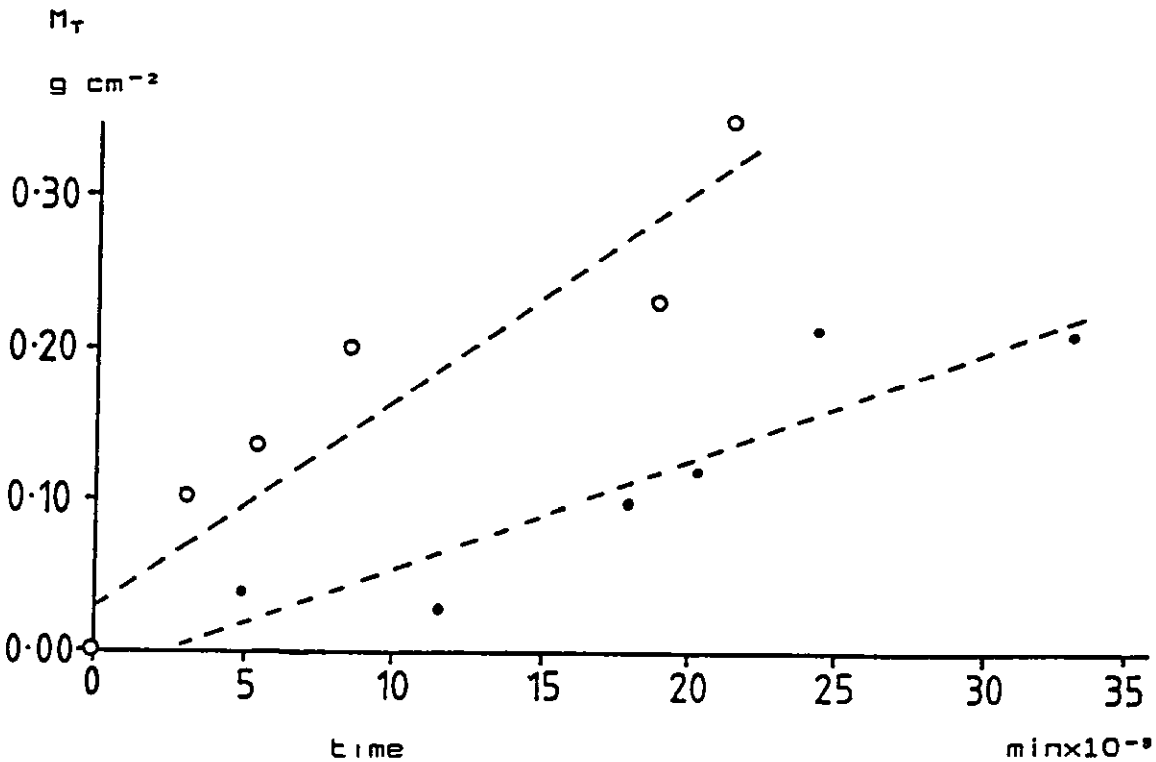

FIGURE 4.17

Diffusion of DOP plasticizer into uPVC at 60°C

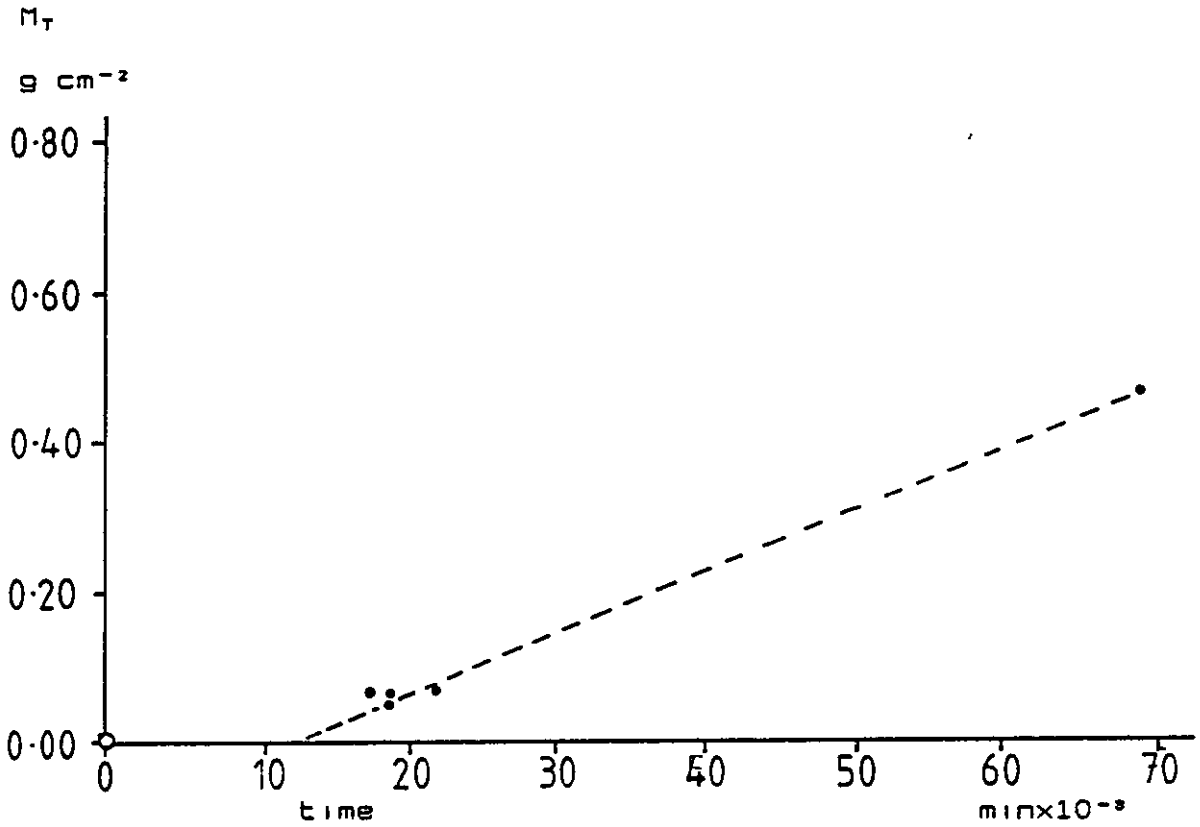

FIGURE 4.18

Diffusion of Cereclor 552 plasticizer into uPVC at 60°C

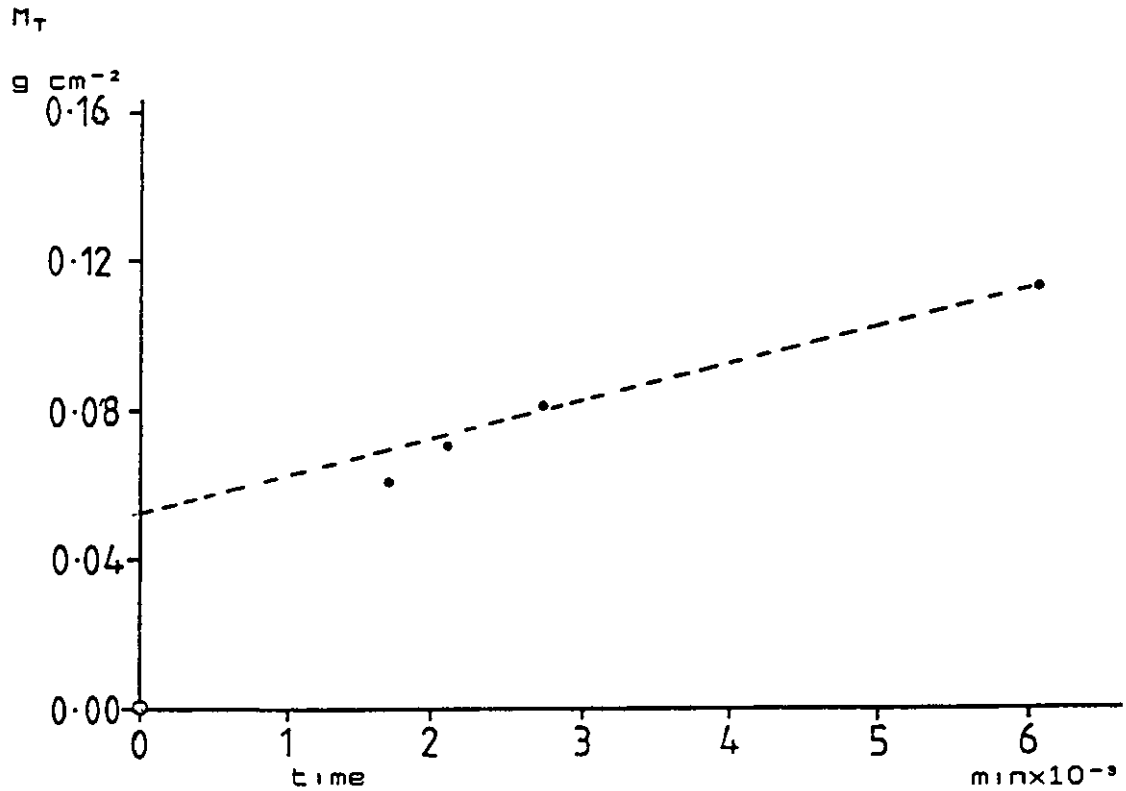

TABLE 4.4

Slope and Y-intercept values for

figures 4.11 to 4.18

liquid	original data		including zero data point, M_T=0 at t=0	
	slope	Y-intercept	slope	Y-intercept
	gcm^2s^{-1}	gcm^2	gcm^2s^{-1}	gcm^2
	$\times10^6$	$\times10^2$	$\times10^6$	$\times10^2$
nitroethane	51.68	0.36	52.25	0.32
propanone	63.74	1.50	68.33	1.30
fluorobenzene	11.79	1.68	11.95	1.59
dimethylbenzene	2.42	1.48	2.47	1.40
ethylbenzene	0.80	1.25	0.81	1.19
DMP	0.23	2.83	0.23	1.91
DOP	0.14	-10.5	0.12	-6.48
BBP	0.13	-3.60	0.12	-1.43
Cereclor 552	0.002	0.47	0.003	0.22

where the swollen layer thickness was small (around 0.05 volume fraction) great difficulty was experienced in measuring the swelling agent-uPVC interface since the thickness of the swollen layer became smaller than the margin of error expressed in the measurement. Samples were thus swollen to an extent where the volume fraction in the prepared sample was greater than 0.05.

4.1.2.4 The movement of the liquid front in unplasticised poly (vinylchloride) plaques

Using Danckwert's[148] treatment describing the measurement of a liquid front, it was possible to follow the ingress of liquid in a uPVC sample with respect to time. From each sample, measurements were made of the total thickness, L_T, via micrometer readings and either the swollen thickness, L, or the core thickness, L_c, via microscopy, depending on which was less than 1 mm - this being the size of the graticule. The quantities measured are shown in figure 4.19. The dimension L for the various liquids employed, is plotted against sorption time and is shown in figures 4.20 to 4.27. The least squares-linear regression line is shown as a dotted line, calculated in the same manner as described in section 4.1.2.2 and includes a zero time data point which by definition of the method of measurement would be zero. Table 4.5 shows the calculated slopes and Y-intercept values for figures 4.20 to 4.27.

FIGURE 4.19

Schematic diagram of the swollen layer

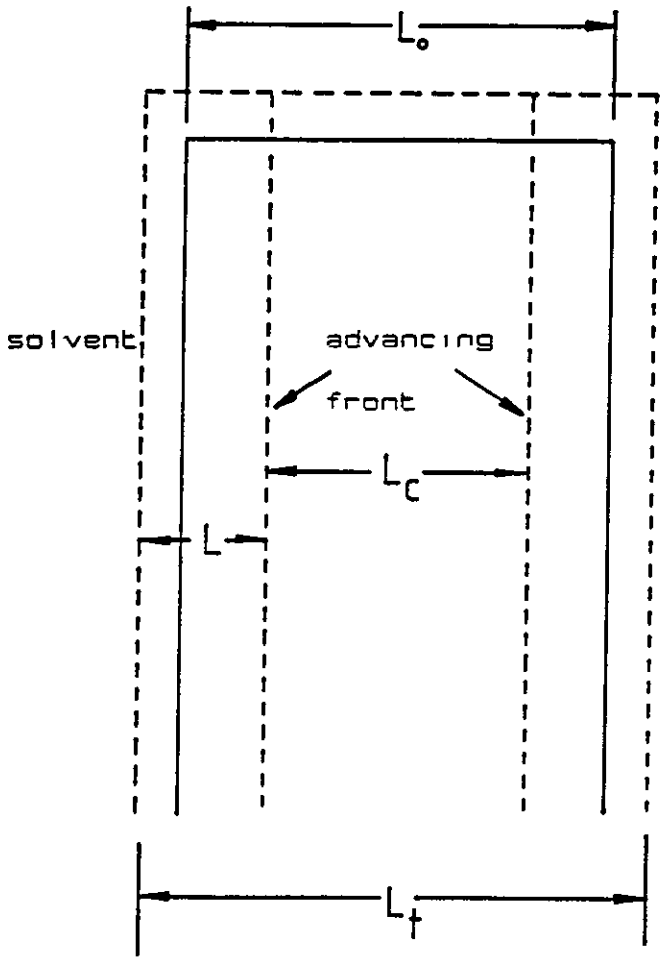

FIGURE 4.20

Diffusion of propanone into uPVC at 56°C,

movement of liquid front into plaque

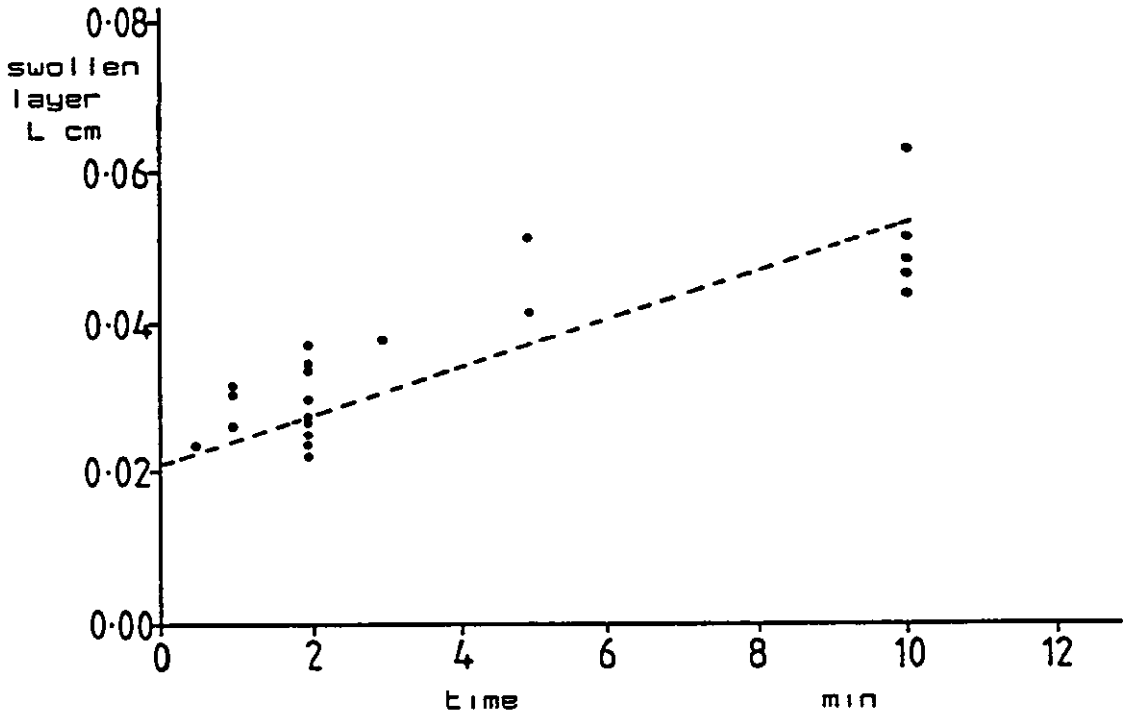

FIGURE 4.21

Diffusion of ethylbenzene into uPVC at 60°C,

movement of liquid front into plaque

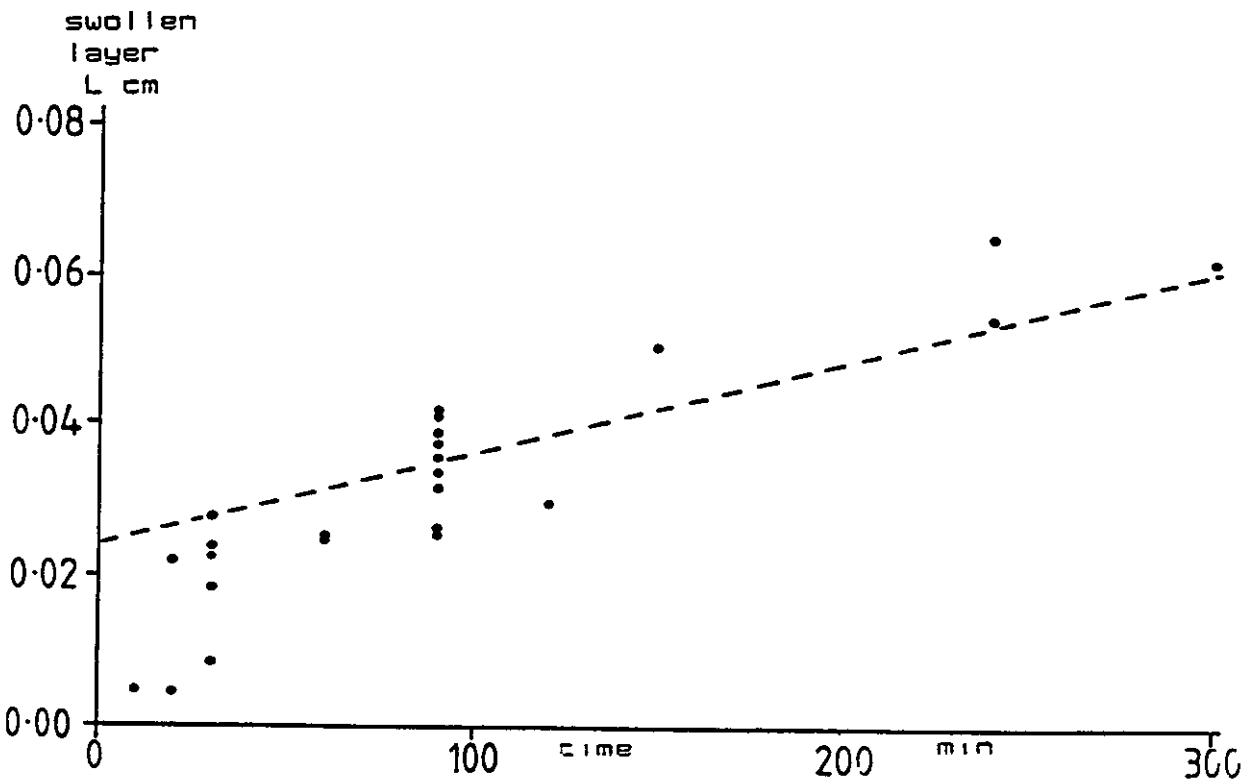

FIGURE 4.22

Diffusion of dimethylbenzene into uPVC at 60°C,

movement of liquid front into plaque

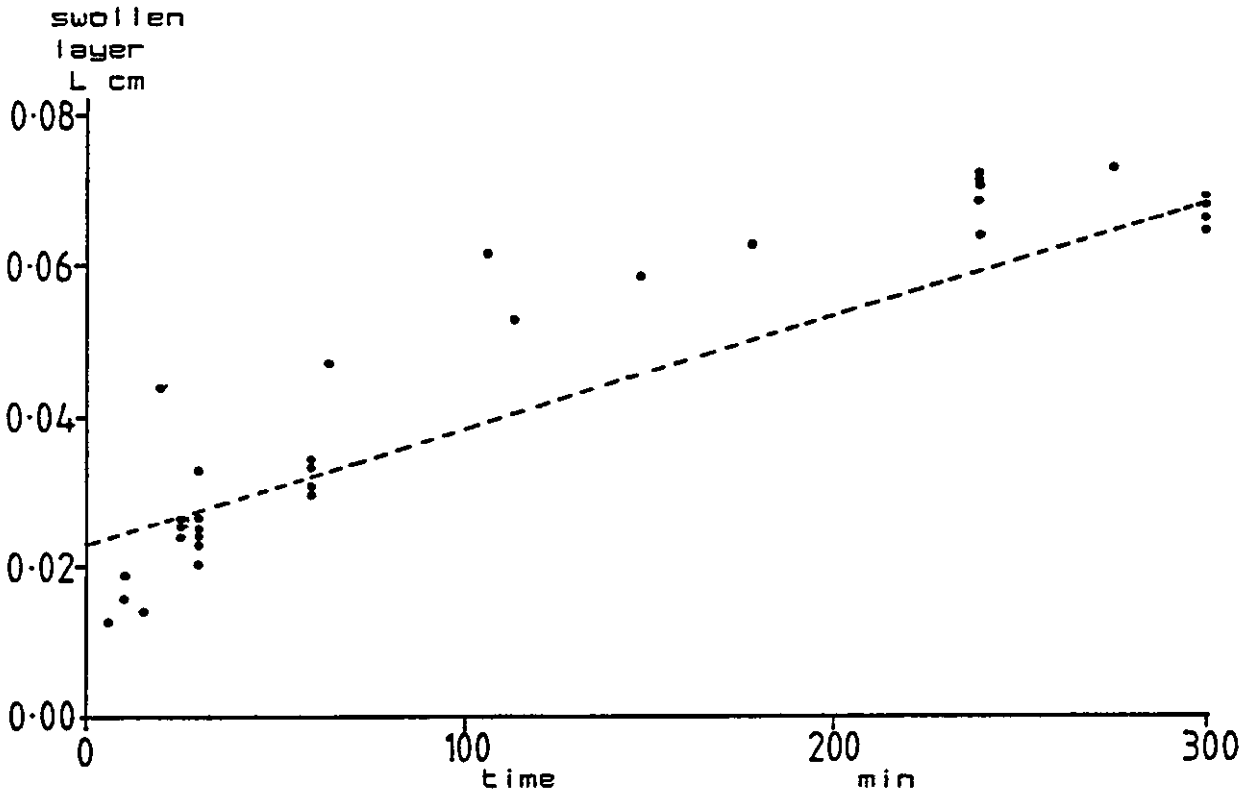

FIGURE 4.23

Diffusion of fluorobenzene into uPVC at 60°C,

movement of liquid front into plaque

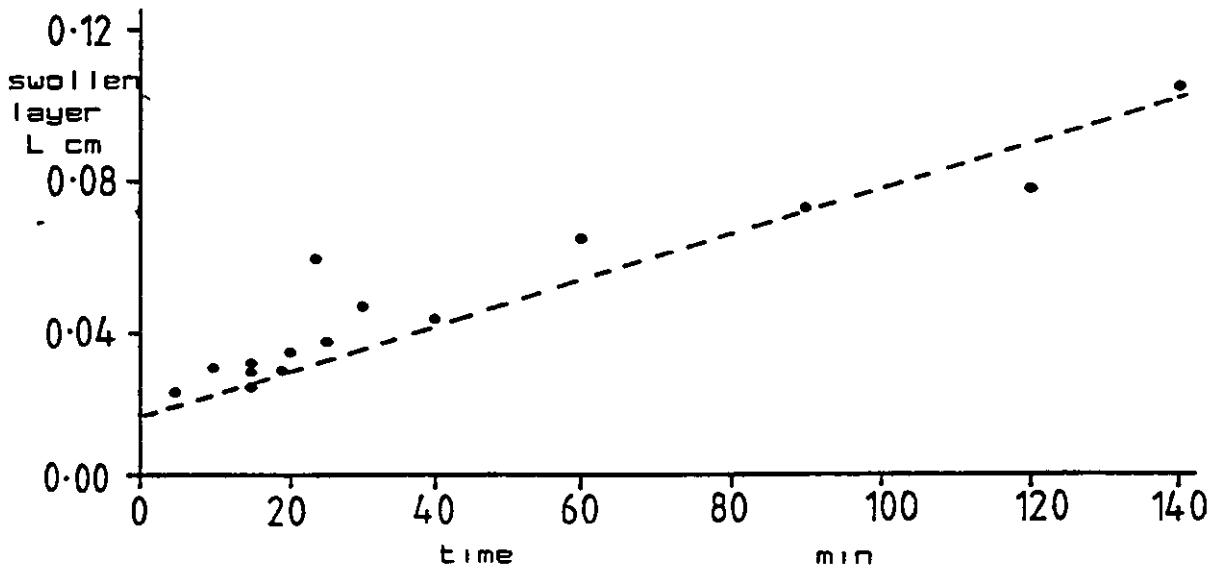

FIGURE 4.24

Diffusion of nitroethane into uPVC at 60°C, movement of liquid front into plaque

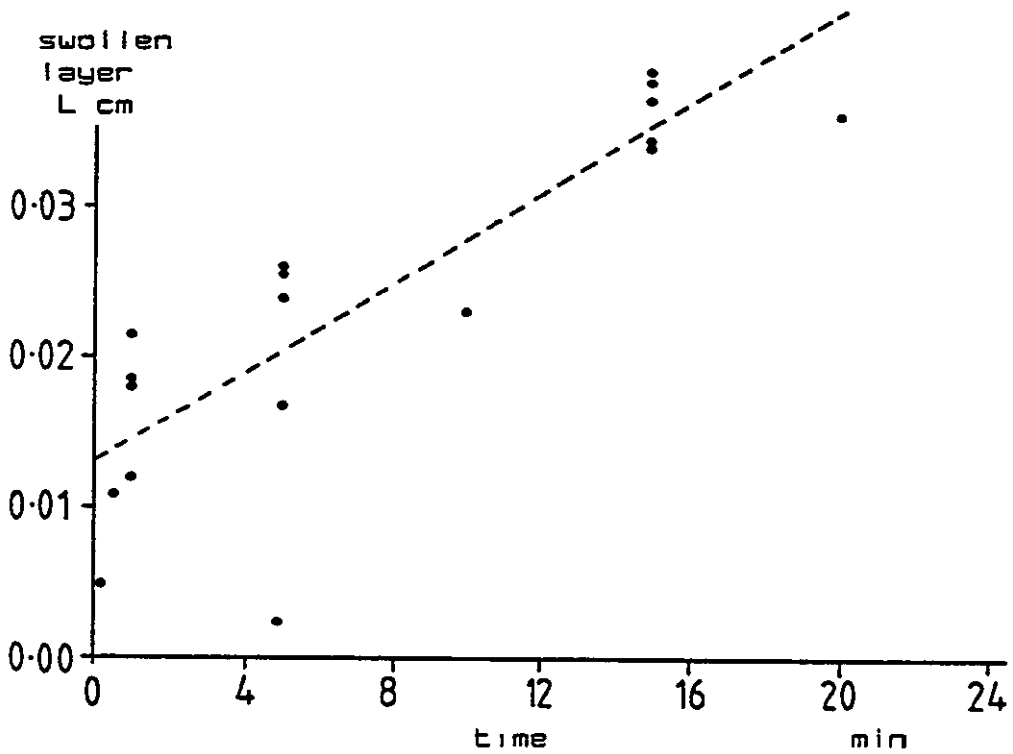

FIGURE 4.25

Diffusion of BBP (•) and DMP (⊙) plasticizers into uPVC at 60°C, movement of liquid front into plaque

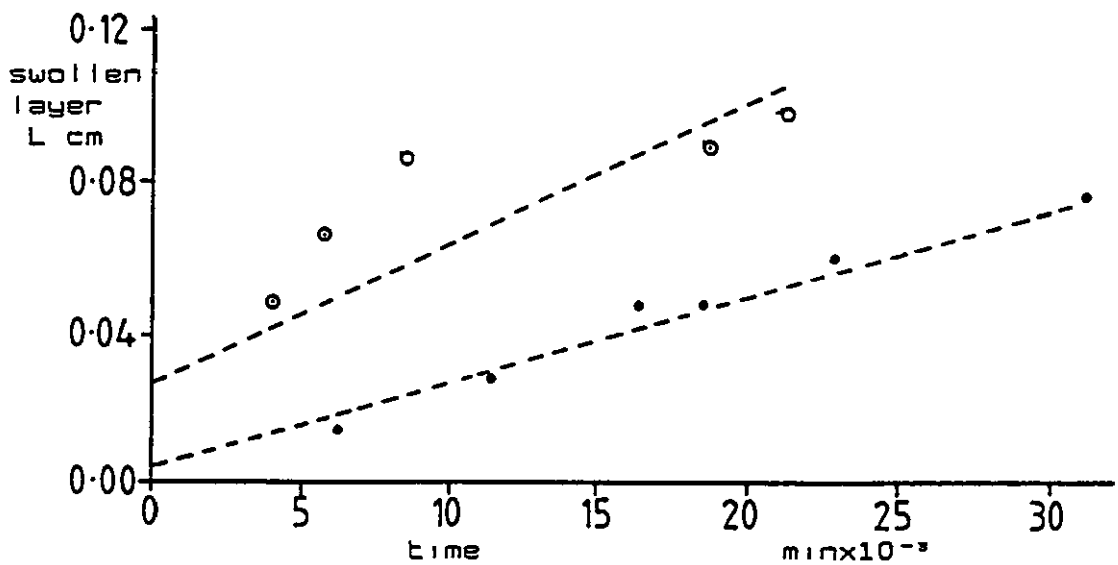

FIGURE 4.26

Diffusion of Cereclor S52 plasticizer into uPVC at 60°C,

movement of liquid front into plaque

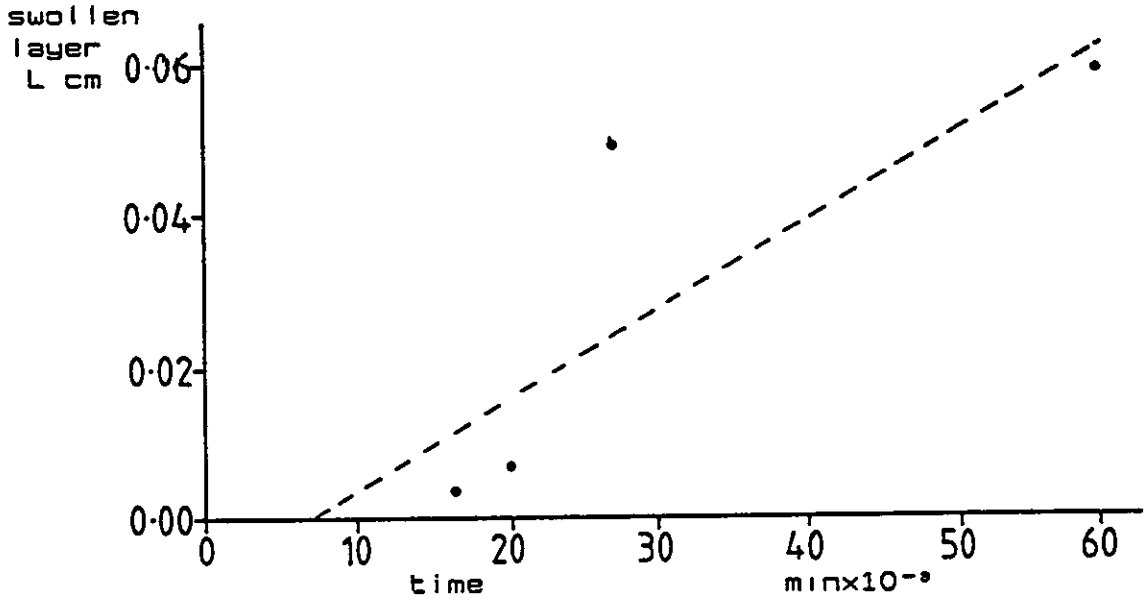

FIGURE 4.27

Diffusion of DOP plasticizer into uPVC at 60°C,

movement of liquid front into plaque

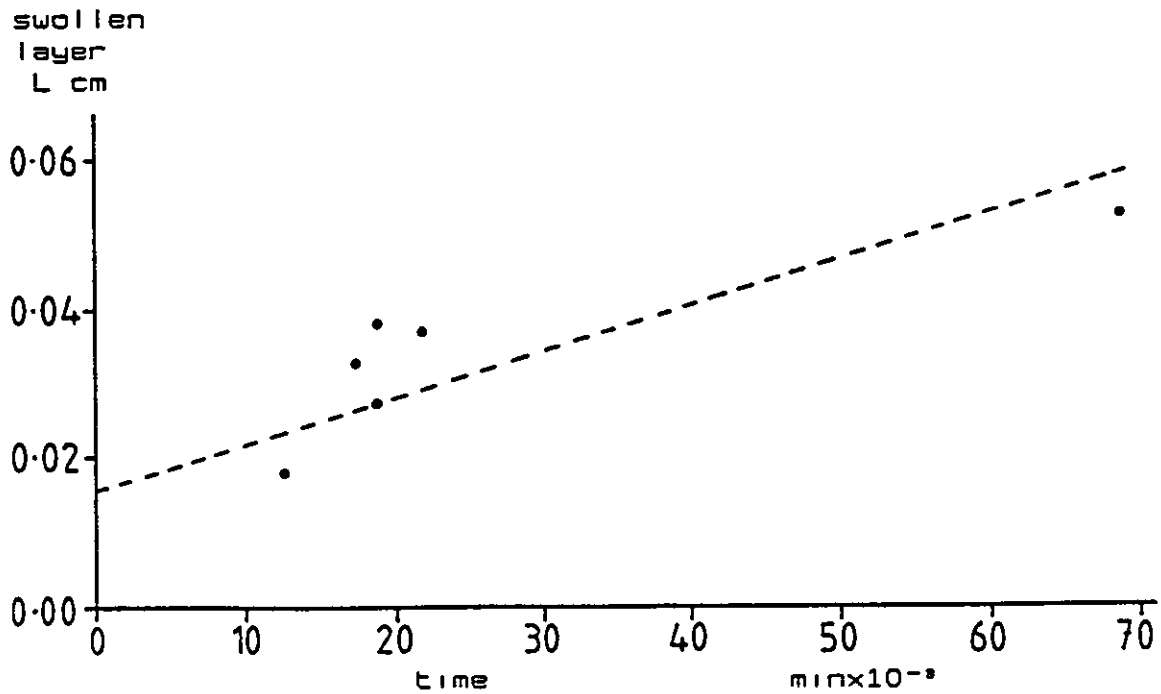

TABLE 4.5

Slope and Y-intercept values for figures 4.20 to 4.27

Liquid	slope $g\ cm^2\ s^{-1} \times 10^6$	Y-intercept $g\ cm^2 \times 10^2$
propanone	52.40	2.10
nitroethane	24.70	1.29
fluorobenzene	9.96	1.73
dimethylbenzene	2.49	2.33
ethylbenzene	2.08	2.41
DMP	0.06	2.88
BBP	0.04	0.52
Cereclor 552	0.02	-0.35
DOP	0.01	1.64

the vapour sorption experiments employed in this work.

Since this value was obtained using a different vapour pressure around the sample due to the 5°C temperature difference between reservoir and sample, it is not possible to compare this experiment with the other experiments run with a temperature difference of 10°C. At lower vapour pressures PVC/propanone systems at 50°C did not reach equilibrium. The sorption mechanism was shown to be Fickian, see figure 4.28, when mass uptake was examined with respect to the square root of the sorption time interval. The induction period seen in figure 4.28 is thought to be due to the development of the vapour around the sample.

4.2 DIFFUSION OF ORGANIC VAPOUR INTO POLY (VINYLCHLORIDE) PLAQUES

The range of vapours employed was restricted to those with low boiling points, as it was then possible to readily produce a vapour surrounding the sample without using elevated temperatures above 100°C. This temperature was the upper working limit of the microbalance vacuum head. Table 4.6 shows the liquids employed with vapour sorption techniques together with the respective initial rate of vapour uptake measured at 50°C and a temperature difference between liquid reservoir and sample of 10°C. It was not possible to measure diffusion coefficients via Equation 3.99,with the exception of propanone, since it was not possible to produce an equilibrium within the system at such low surface concentrations indicated by the partial pressure in the unit in the time interval employed. When propanone sorbed into a PVC plaque at a temperature of 50°C with a temperature difference between the reservoir and sample of 5°C, it was possible to produce a system which reached equilibrium. This enabled the diffusion coefficient to be computed, 1.46×10^{-16} cm^2 s^{-1}. Berens[28] has calculated D for the sorption of VCM, propanone and methanol vapour into uPVC microspheres at 30°C, he found D for propanone to be 50×10^{-12} cm^2 s^{-1}, This value is greater by a factor of 10^5 for D calculated for propanone in this work. The difference may be attributed to the surface area of the uPVC. The specific surface area of the emulsion polymerised powder used by Berens[28] was 9.8 m^2 g^{-1}, a factor of approximately 2×10^4 greater than the surface area of the plaques used in

TABLE 4.6

Initial rate of vapour sorption of various vapours into PVC plaques

Vapour	rate g/minx10^7
1,2-dichloroethane	155.0
2-nitropropane	8.2
fluorobenzene	4.5
dimethylbenzene	3.8
propanone	3.5
benzene	3.2

FIGURE 4.28

The vapour sorption of 1,2-dichloroethane into uPVC at 30°C

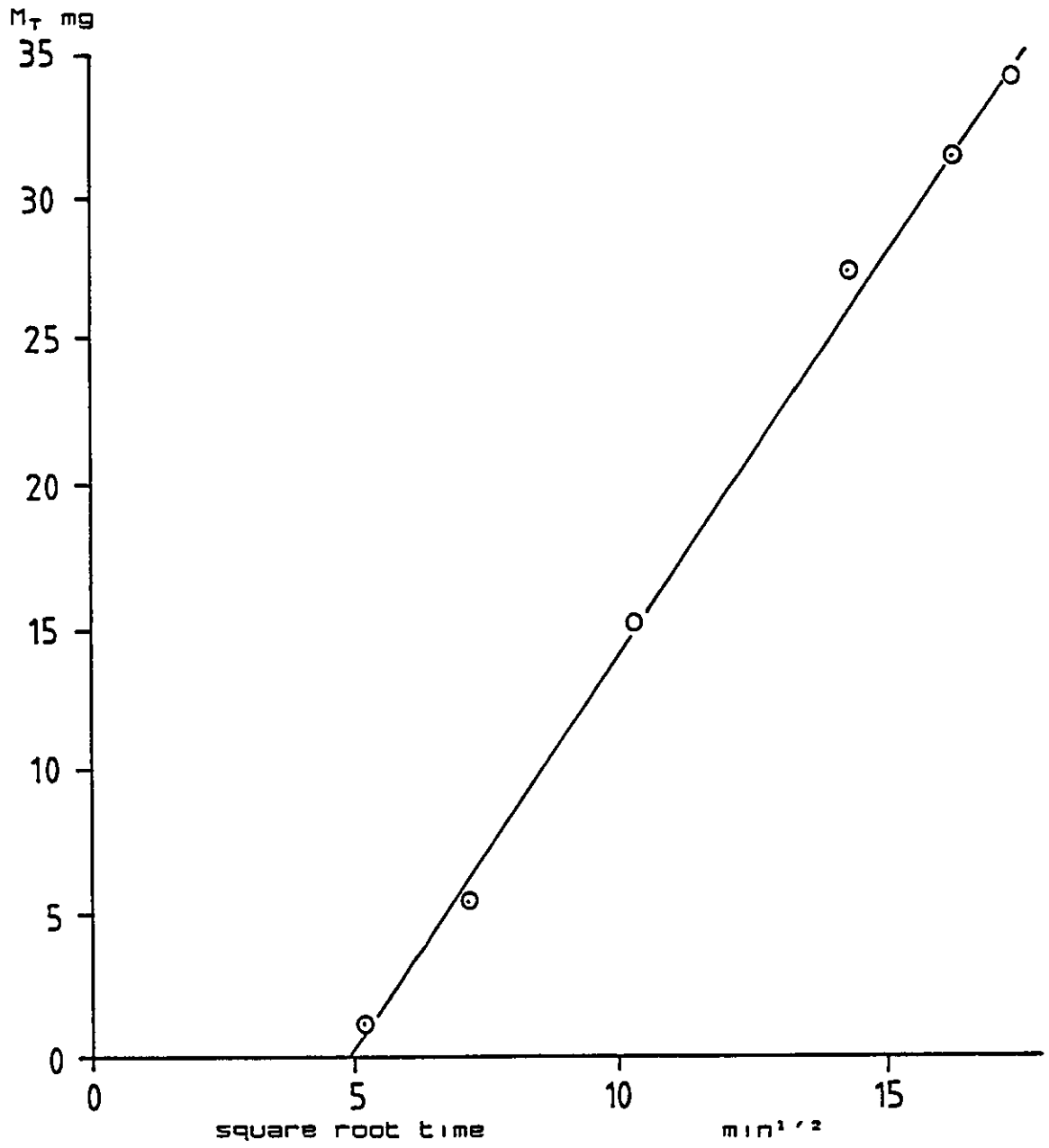

4.3 GLASS TRANSITIONS OF THE PURE LIQUIDS EMPLOYED

The T_g's of the swelling agents which exhibited clear solvent fronts in the swollen uPVC systems were determined experimentally by PL-DMTA and/or DSC methods. The results are shown in table 4.7.

4.3.1 Dynamic mechanical thermal analysis of pure liquids

The PL-DMTA results were obtained using a support of micro-glassfibre filter paper[150], (Whatman GF/A), soaked with the respective liquid and then quenched in liquid nitrogen. It was not possible to produce PL-DMTA thermograms for all the liquids. It was often found that the glassfibre filter paper soaked with liquid became extremely brittle on cooling with liquid nitrogen making sample clamping impossible. Examples of PL-DMTA thermograms on heating are shown in figures 4.29 to 4.35. The T_g's for nitroethane and ethylbenzene are not fully resolved and some speculation as to their values must be assumed. The traces for the DMP and DOP plasticizers became noisy after passing through their T_g's making the evaluation of their melting points difficult. The BBP thermogram seen in figure 4.34 shows two tan δ peaks. The lower temperature and smaller peak possibly being due to a β relaxation transition.

TABLE 4.7

T_g values of various liquids using PL-DMTA and DSC methods and literature quoted melting points. (PL-DMTA dual cantilever mode at 4°C/min using soaked filter paper), and DSC on pure liquid at 40°C/min corrected to a heating rate of 4°C/min according to figure 4.36

swelling liquid	PL-DMTA		DSC		literature
	T_g °C	T_m °C	T_g °C	T_m °C	T_m °C
ethylbenzene	-112	-86	-159(-162)[1]	-102	-93[1]
fluorobenzene	-108	-34	-155	-46	-45[2]
nitroethane	-120	-80	-140	-98	-50/-80[1]
propanone	---	---	---	-100	-95[1]
dimethylbenzene	---	15	---	14	13[1]
methylbenzene	---	-86	-167[1]	-100	-95[1]
1,2-dichloroethane	---	---	-98	-36	-35
2-nitropropane	---	---	---	-92	-93
chlorobenzene	---	---	---	-42	-46
1,2-dichlorobenzene	---	---	(-63,-44)	-21	-17
trichloromethane	---	---	---	-61	-63
DOP	-62(-63)[3] *	---	-80	---	-50
DMP	-52	---	-75(-79)[5]	---	2
Cereclor S52	-28	---	-45	---	---
BBP	(-75)*-48	---	-64	---	---

1 - experimental values obtained by van Krevelen[65]

2 - Morrison and Boyd[151]

3 - Faucher and Koleske[152]

4 - Scandola and Ceccorulli[153]

5 - Scandola *et al.*[154]

* - a possible β relaxation

FIGURE 4.29

Dual-cantilever PL-DMTA of nitroethane on a glassfibre filter paper support

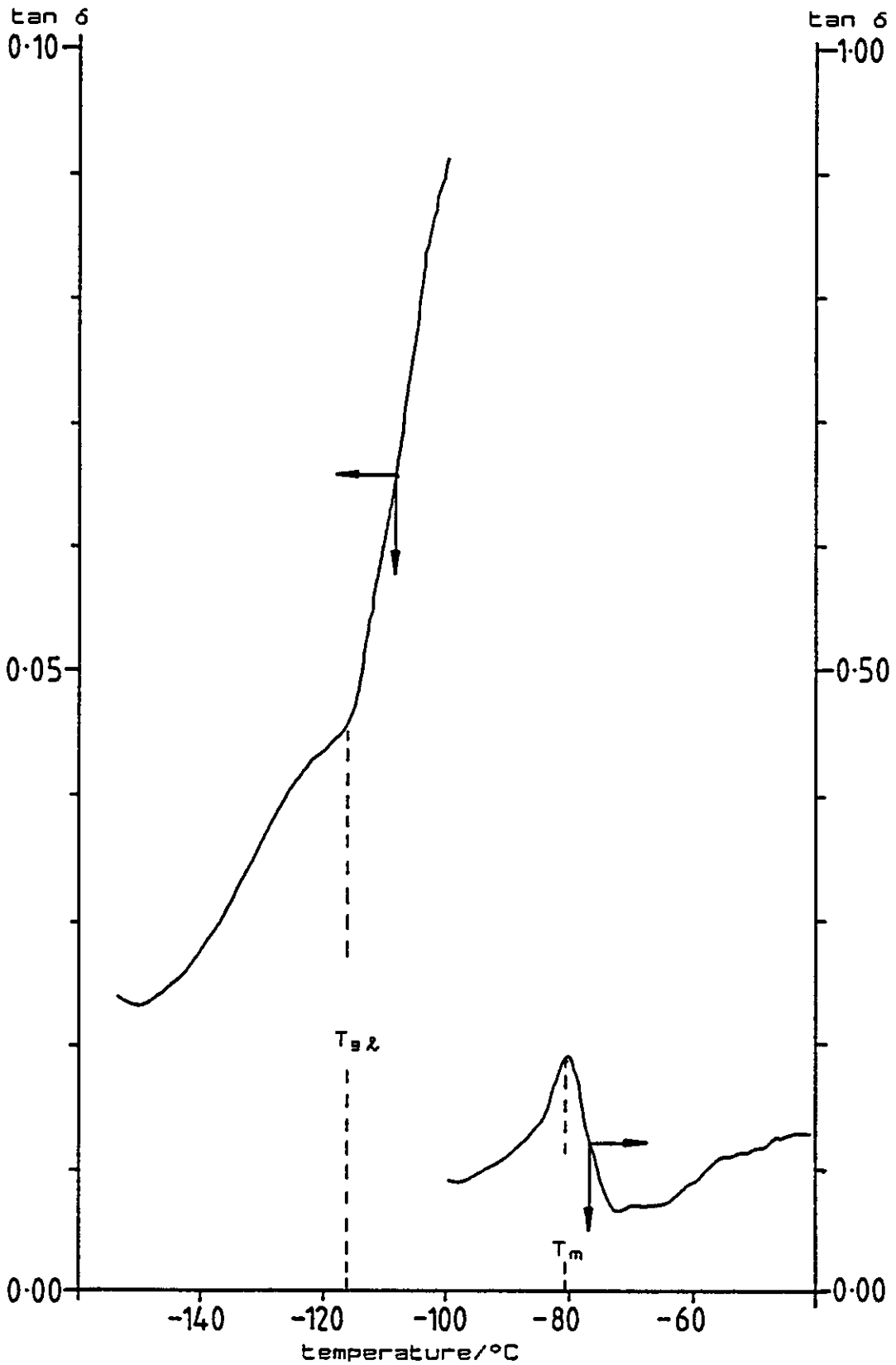

FIGURE 4.30

Dual-cantilever PL-DMTA of ethylbenzene on a glassfibre filter paper support

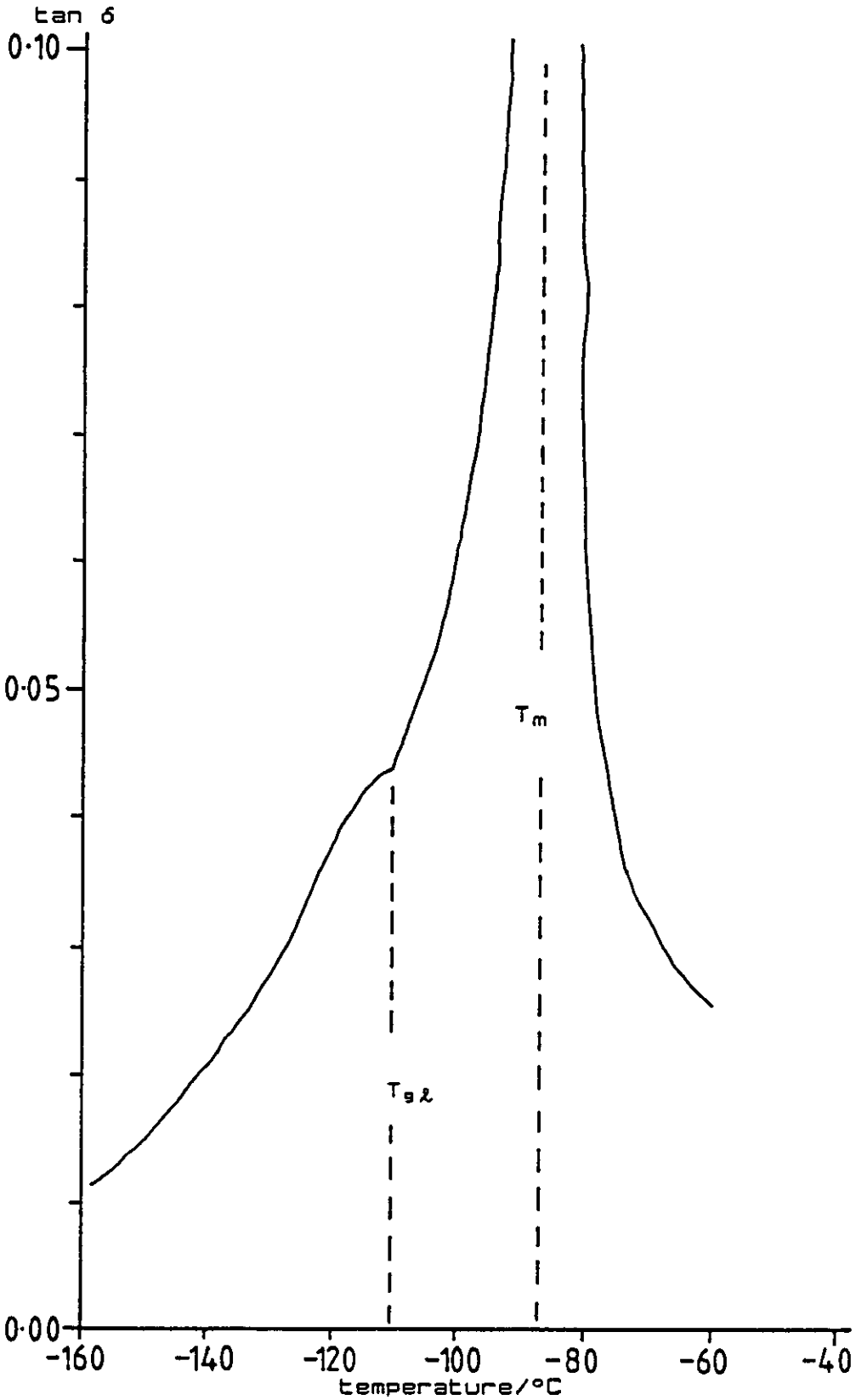

FIGURE 4.31

Dual-cantilever PL-DMTA of fluorobenzene on a glassfibre filter paper support

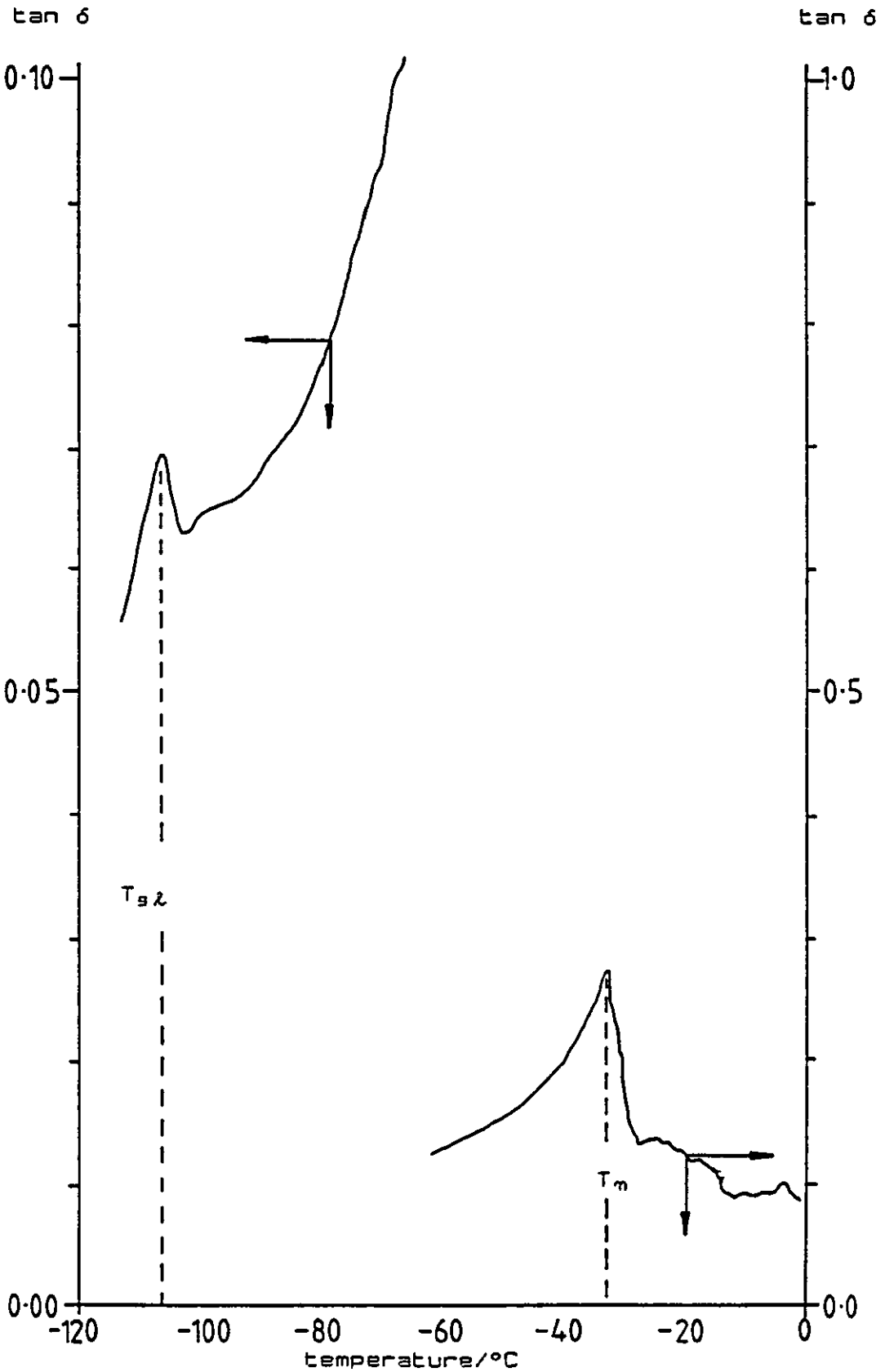

FIGURE 4.32

Dual-cantilever PL-DMTA of Cereclor 552 plasticizer on a glassfibre filter paper support

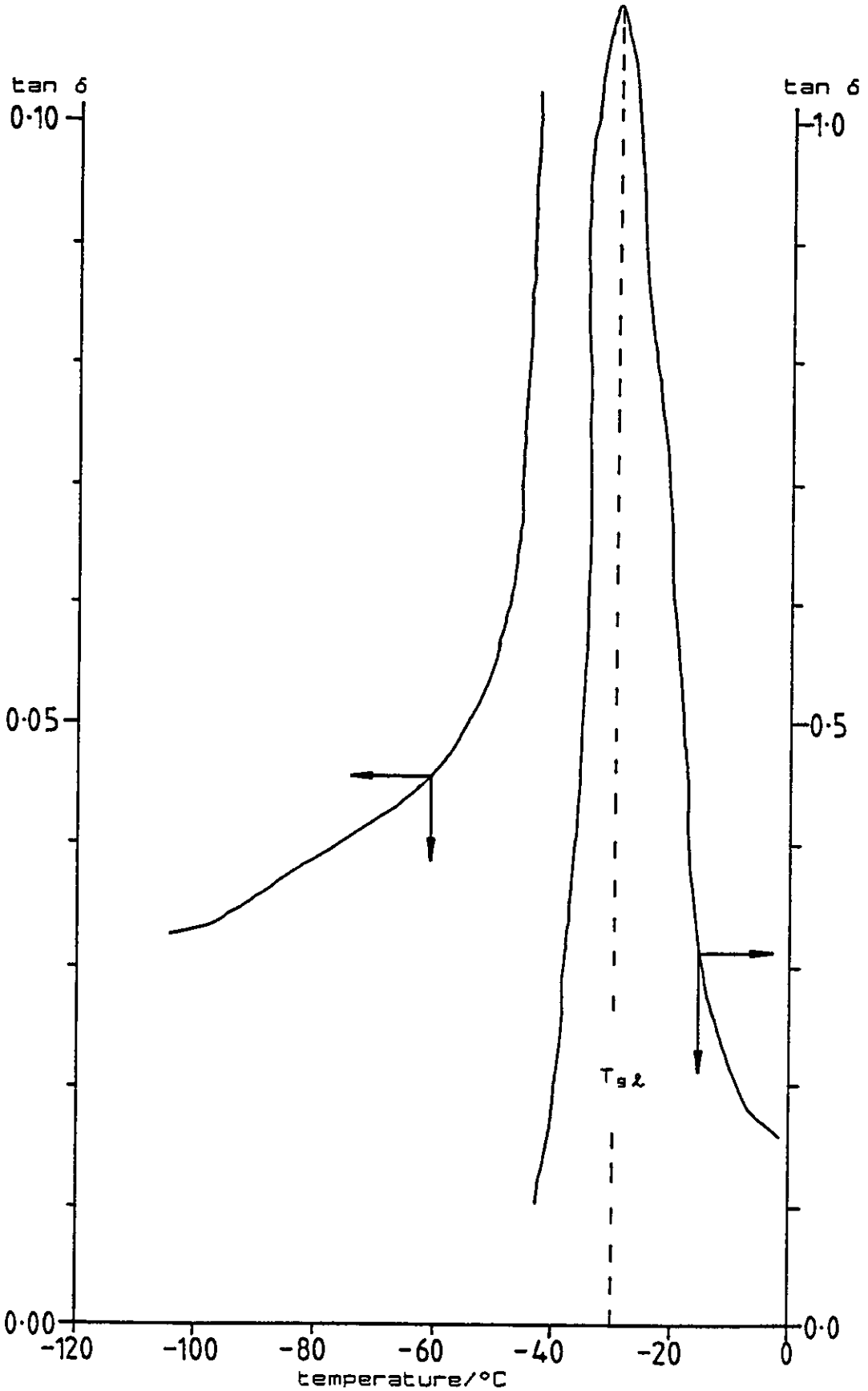

FIGURE 4.33

Dual-cantilever PL-DMTA of DMP plasticizer on a glassfibre filter paper support

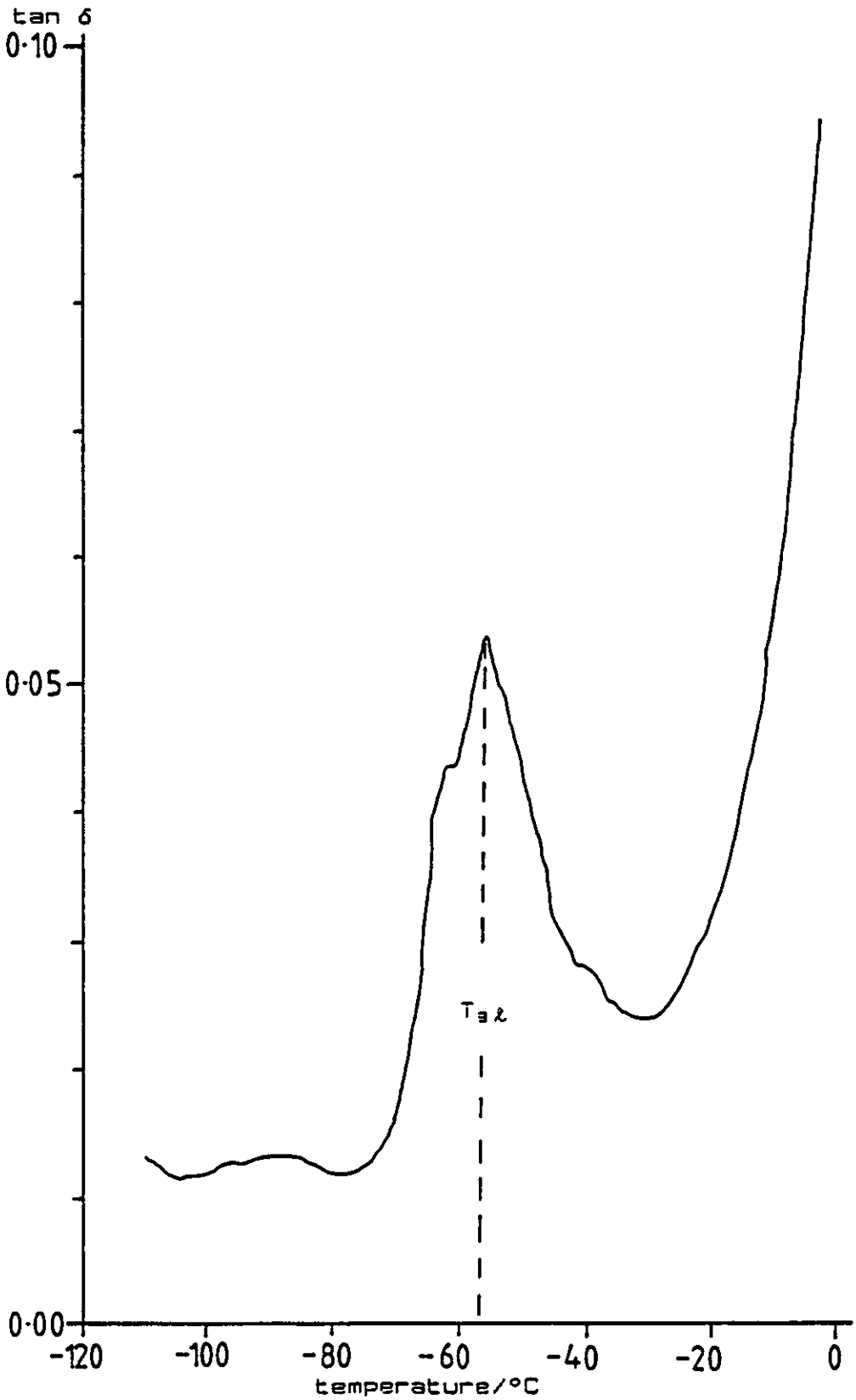

FIGURE 4.34

Dual-cantilever PL-DMTA of BBP plasticizer on a glassfibre filter paper support

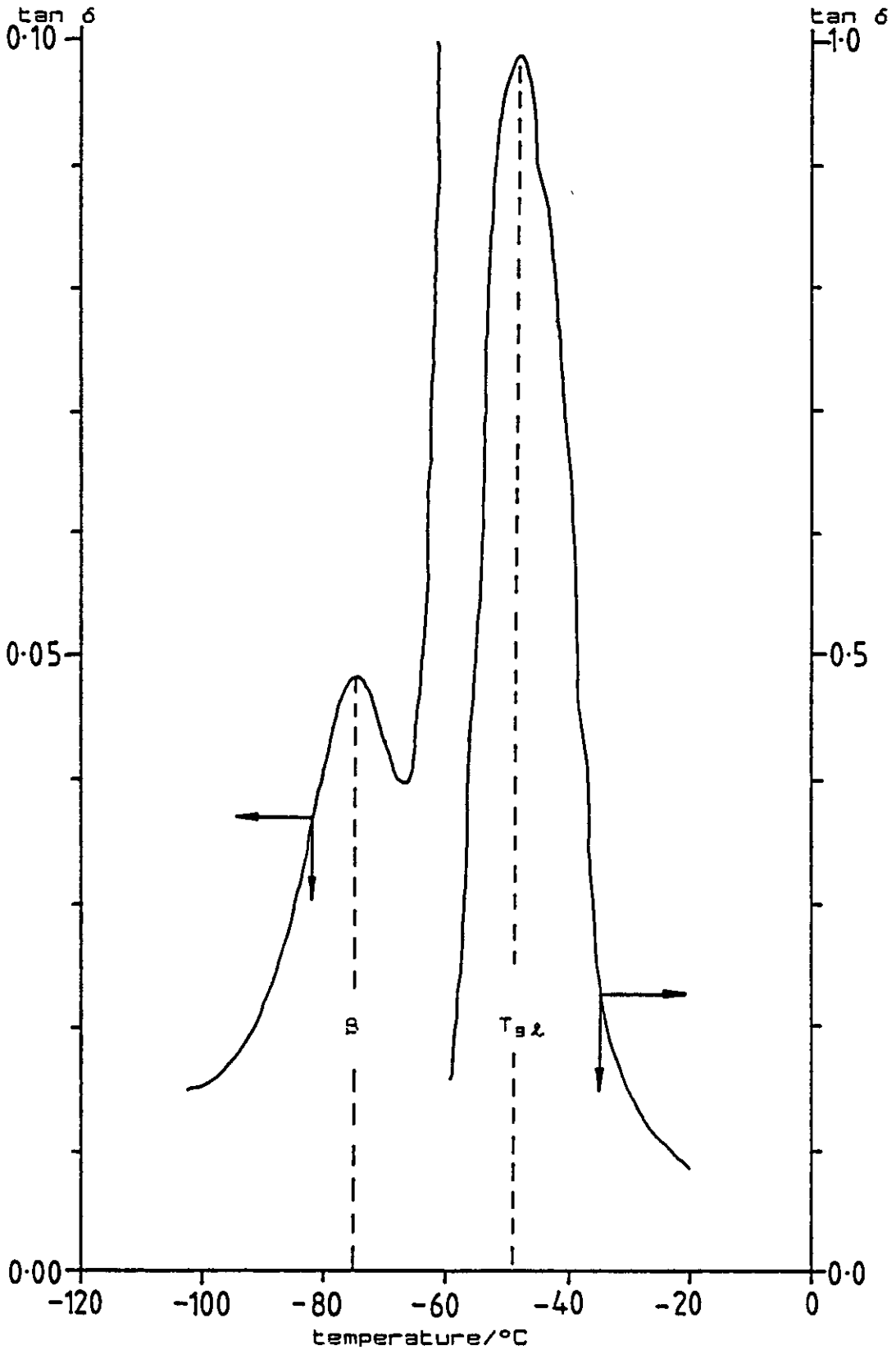

FIGURE 4.35

Dual-cantilever PL-DMTA of DOP plasticizer on a glassfibre filter paper support

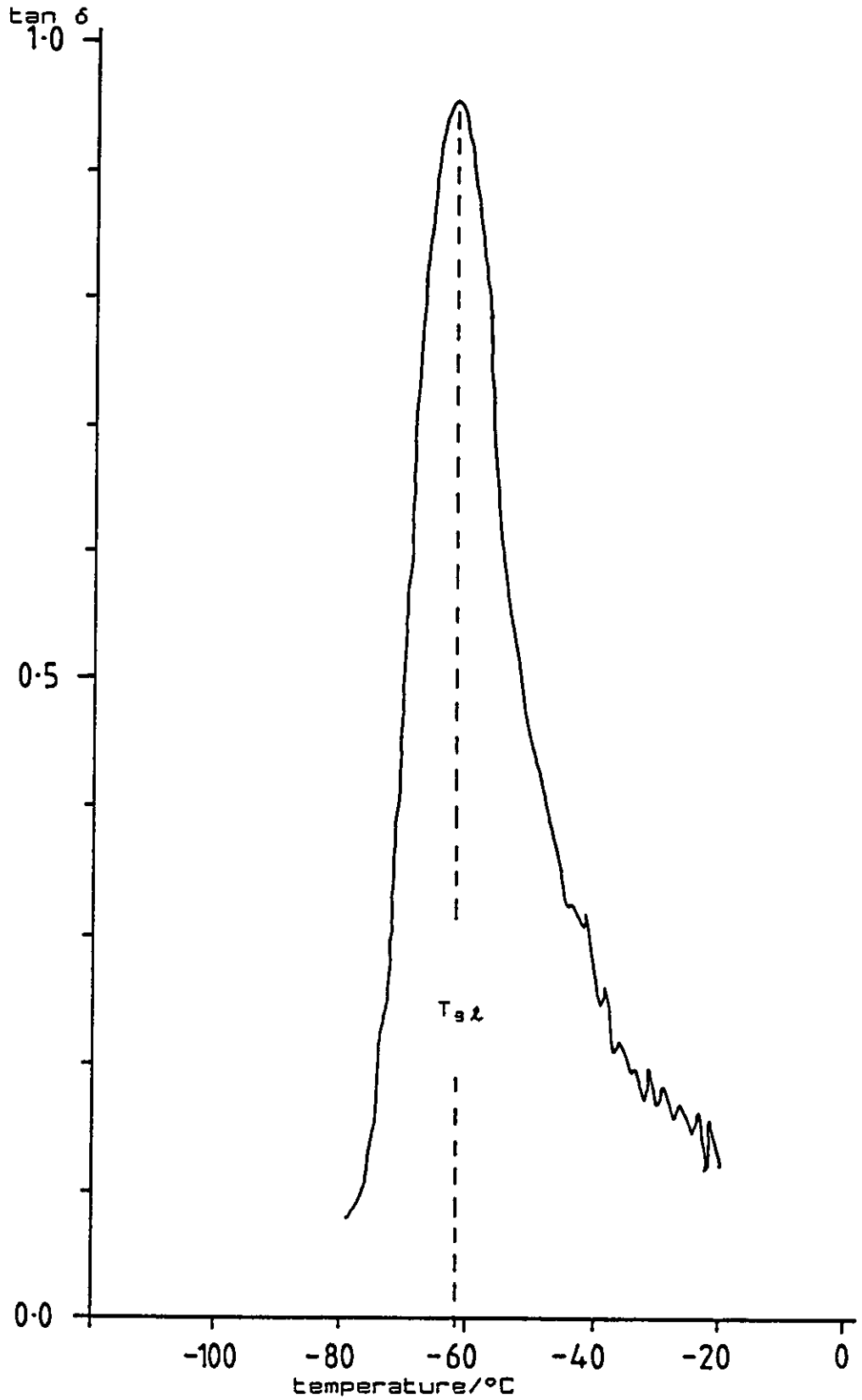

FIGURE 4.36

Differential scanning calorimeter calibration plot using cyclohexane

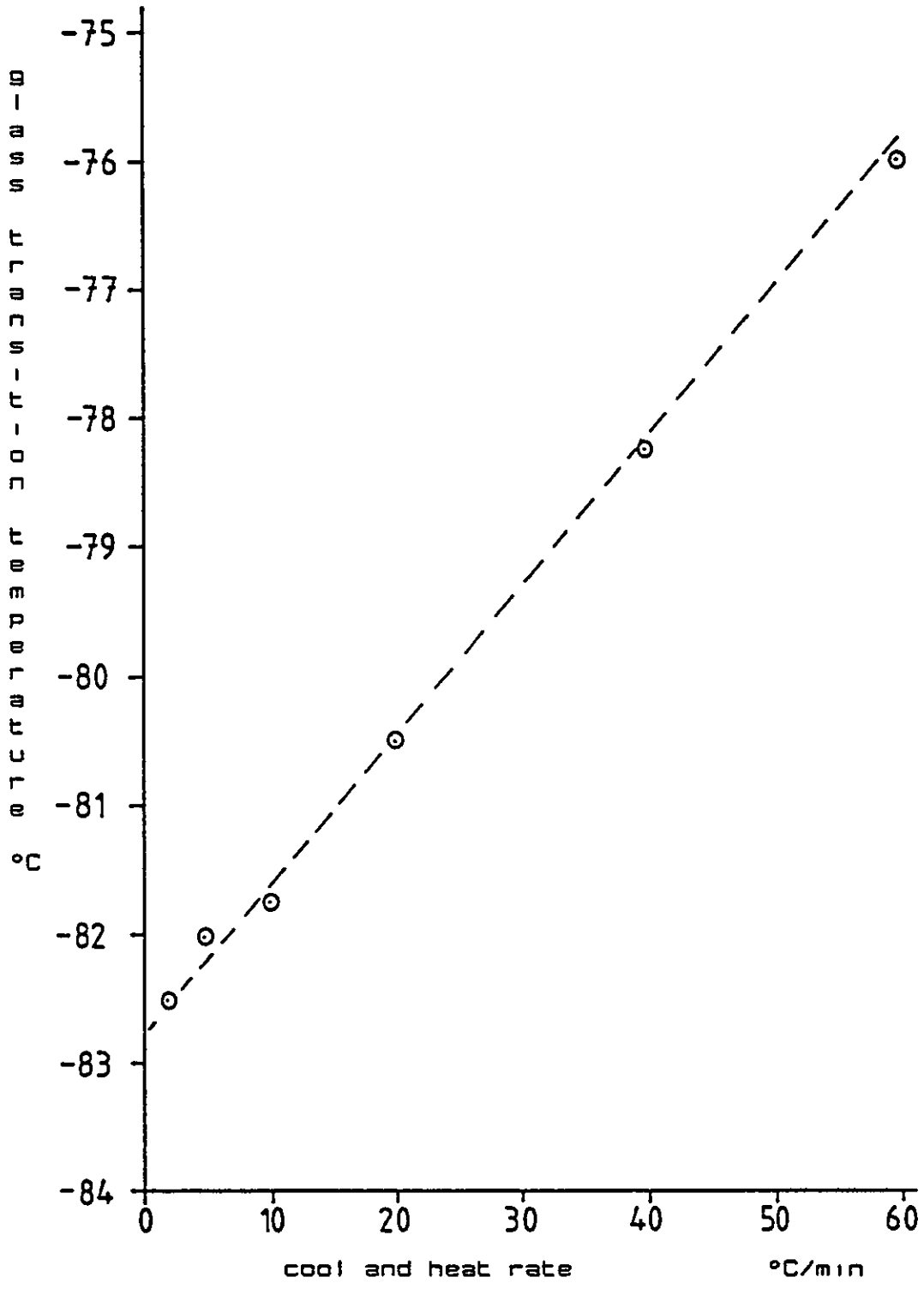

4.3.2 Calibration of the differential scanning calorimeter

The Perkin-Elmer DSC4 was calibrated using a glass transition (-87.06°C)[155] associated with A.R. grade cyclohexane, (supplied by, BDH, Fourways Road, Carlyon Industrial Estate, Atherstone, Warks.), and the indium melting point of 156.6°C. A series of experiments was conducted at increasing cool and heat rates using cyclohexane and the actual glass transition temperature was plotted against the cool/heat temperature. The resulting calibration graph is seen in figure 4.36. The maximum heating rate employed using the PL-DMTA in the dual-cantilever mode for the analysis of pure liquid transitions was 4°C/min. According to figure 4.36 the recorded cyclohexane T_g at this rate would be 4.3°C higher than the actual cyclohexane T_g, at a cool/heat rate of 40°C/min the recorded transition will be 8°C higher than the actual cyclohexane T_g. The difference between a T_g measured at a cool/heat rate of 4°C/min and 40°C/min is 3.7°C. Consequently, DSC quoted values will be adjusted to give a value at a heating rate of 4°C/min to facilitate comparison between PL-DMTA results as shown in table 4.7. To make an absolute comparison between the two methods (PL-DMTA and DSC) the effect of frequency in the dynamic method must be investigated in a similar manner to that shown in figure 4.36, as the tan δ peak position found using PL-DMTA extrapolated to zero frequency is predicted to be several degrees lower[156].

In order to prevent crystallization, since fast cooling rates were employed in the DSC analysis of the

liquids, the effect of changing the cooling rate on the observation of the T_g on subsequent heating was investigated. The results are shown in figures 4.37 and 4.38 where T_c is the crystallization exotherm and T_m is the melting point. The thermograms were produced on heating the liquids the heating rate, in all cases, being kept at 40°C/min, and the prior cooling rate was varied between 2 to 200°C/min. It is clearly seen that the cooling rate is ineffective in changing the T_g position.

4.3.3 Differential scanning calorimetric analysis of pure liquids

Typical DSC thermograms on heating showing T_g values for the swelling agents can be seen in figures 4.39 to 4.42. A crystallization exotherm and melting point endotherm is clearly observed in the trace for ethylbenzene following the T_g of the liquid. By quenching (200°C/min) nitroethane, shown in figure 4.40, it was possible to minimize the crystallization of the liquid in the second and third traces. The second trace was terminated before the crystalline region could melt. The sharp downward turn of the DMP trace in figure 4.41 is due to crystallization occurring in the sample.

FIGURE 4.37

DSC thermograms on heating fluorobenzene, effect of different cooling rates prior to heating at 40°C/min

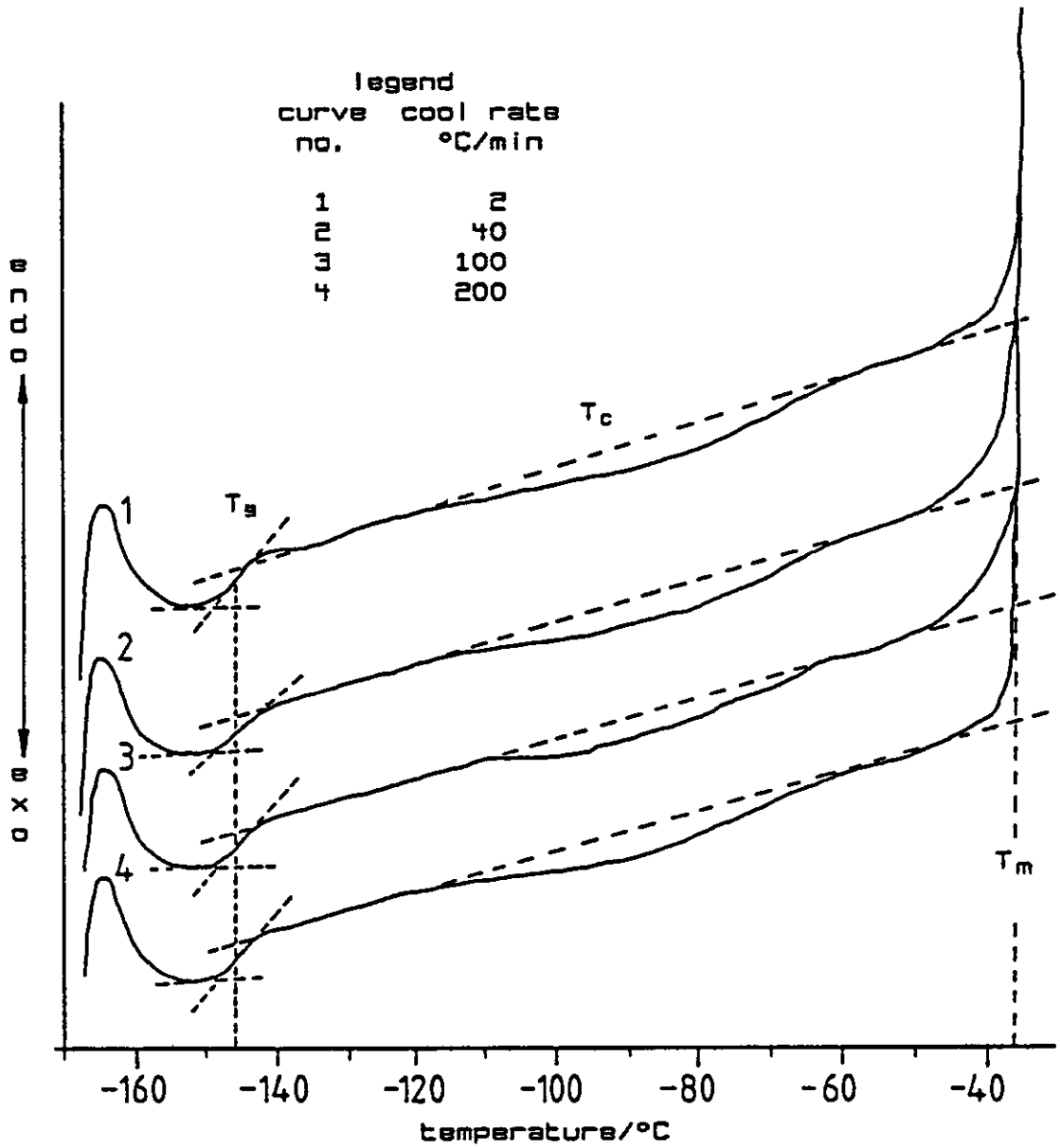

FIGURE 4.38

DSC thermograms on heating ethylbenzene, effect of different cooling rates prior to heating at 40°C/min

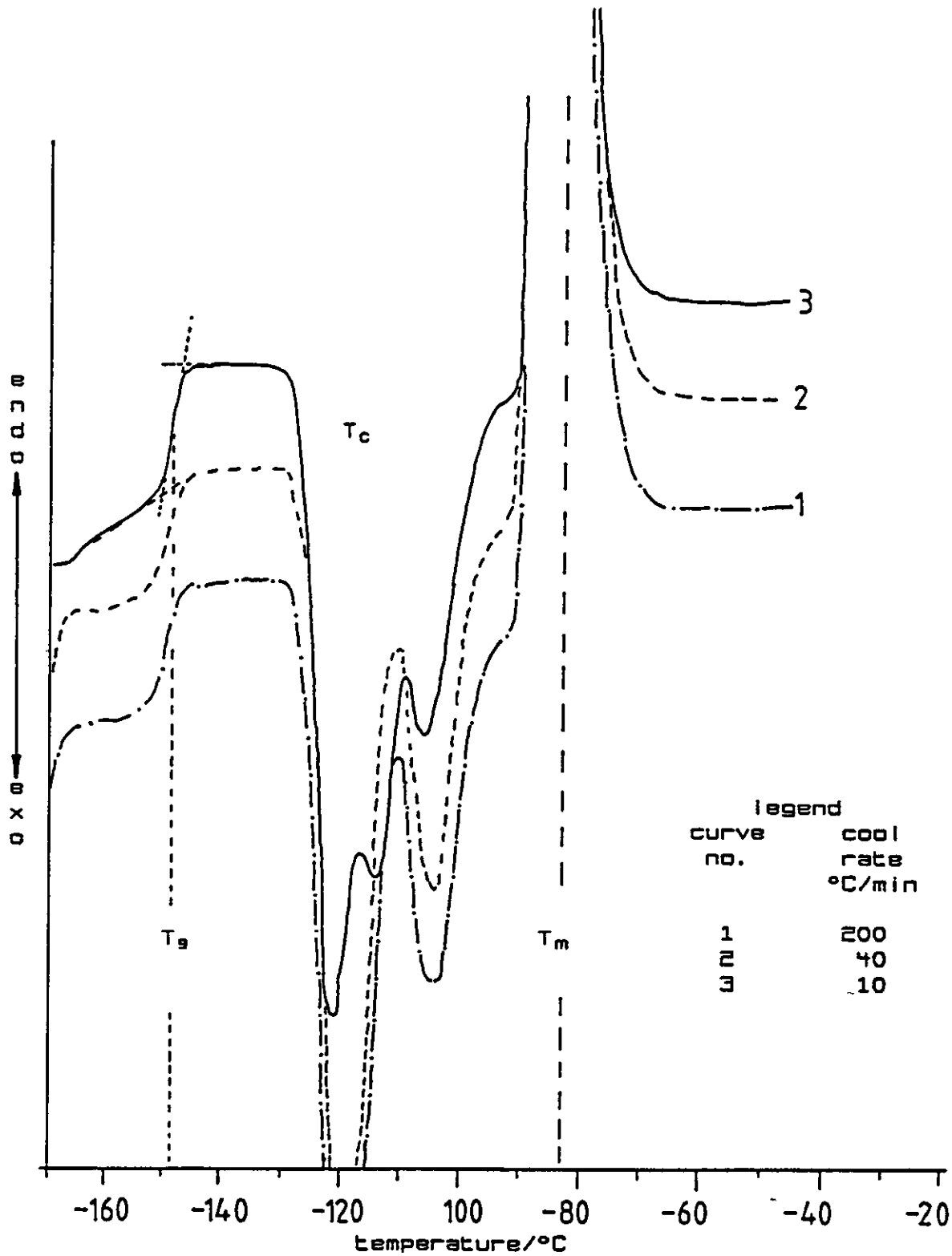

FIGURE 4.39

DSC thermogram on heating ethylbenzene, cooled and heated at 20°C/min

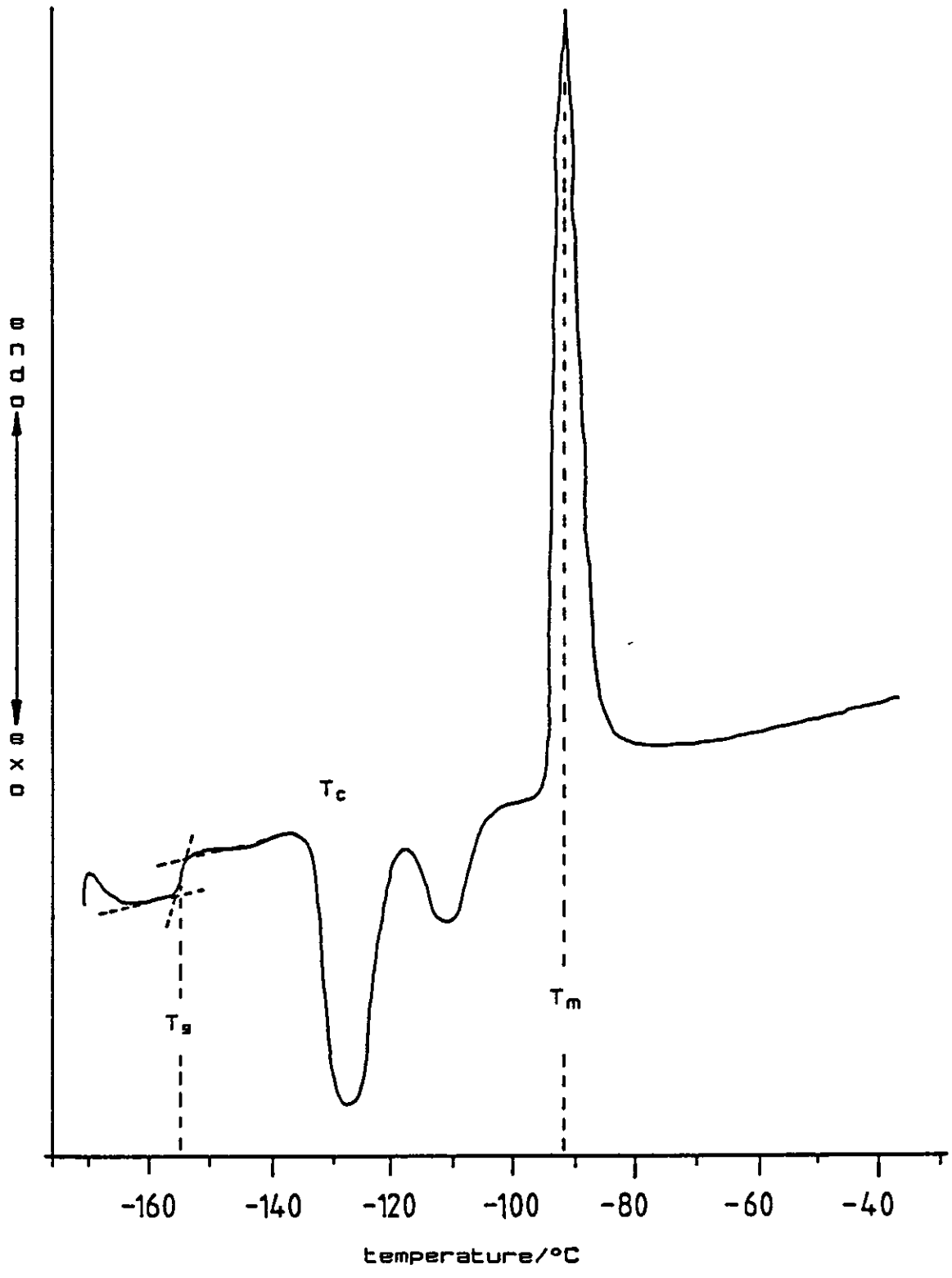

FIGURE 4.40

DSC thermogram produced on heating nitroethane, cooled and heated at 40°C/min (1), and for (2) and (3), quenched at 200°C/min prior to heating at 40°C/min

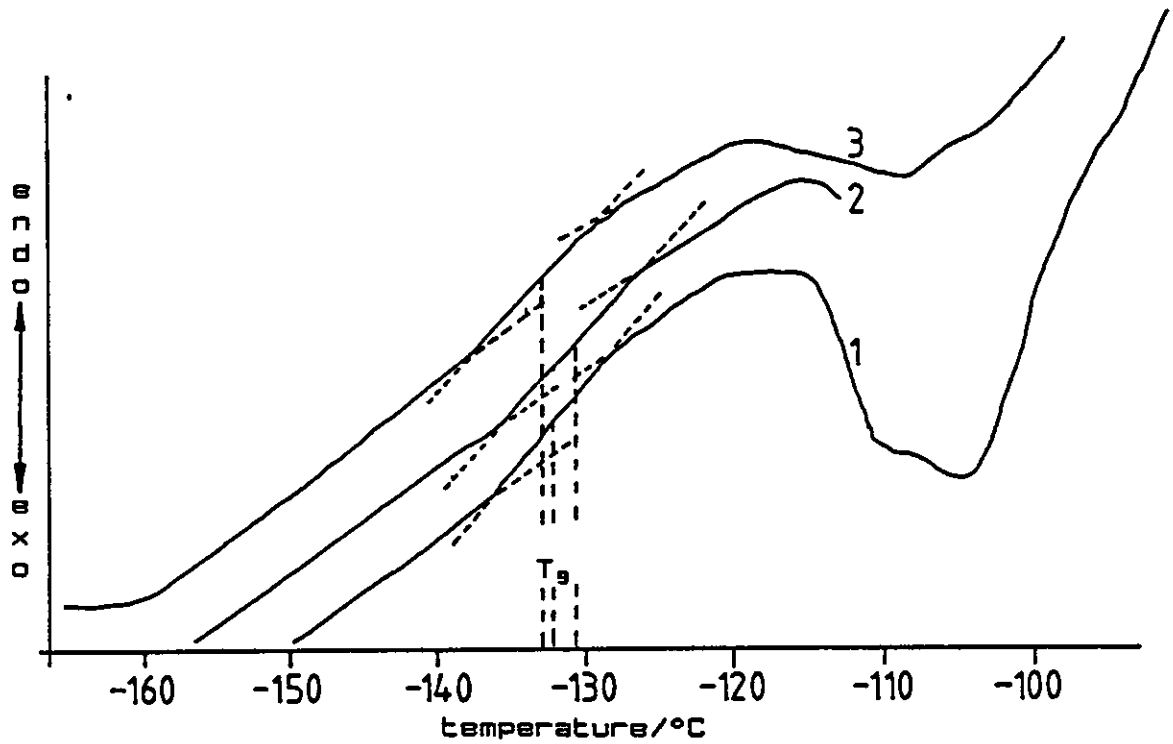

FIGURE 4.41

DSC thermogram produced on heating DOP plasticizer, cooled and heated at 20°C/min

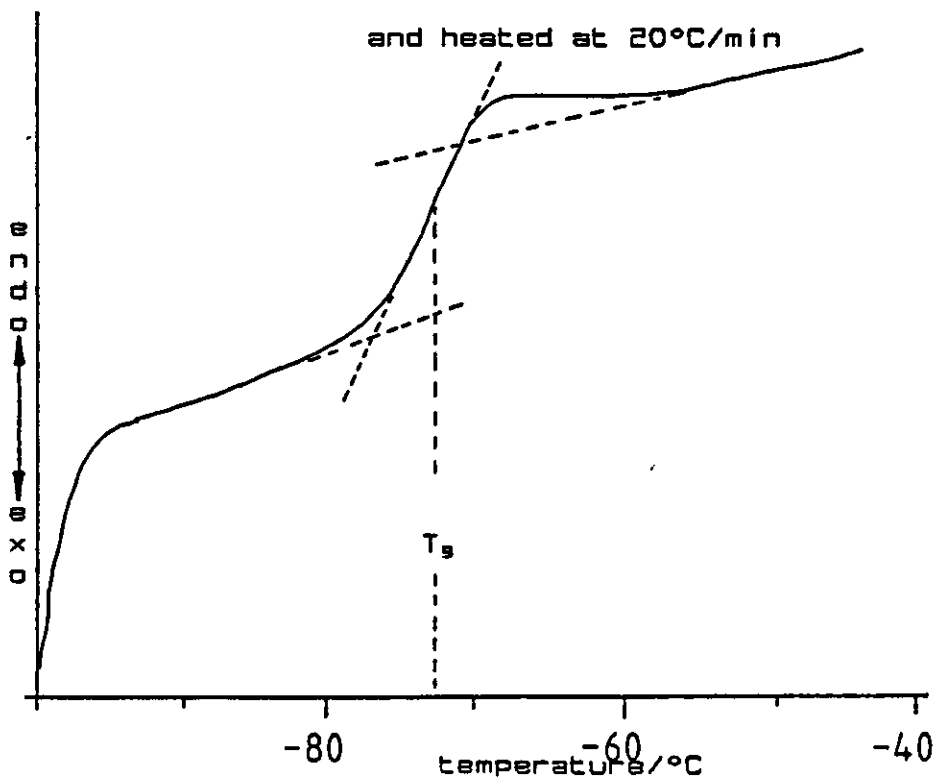

FIGURE 4.42

DSC thermograms produced on heating DMP (1), BBP (2) and Cereclor 552 (3); cooled and heated at 40°C/min

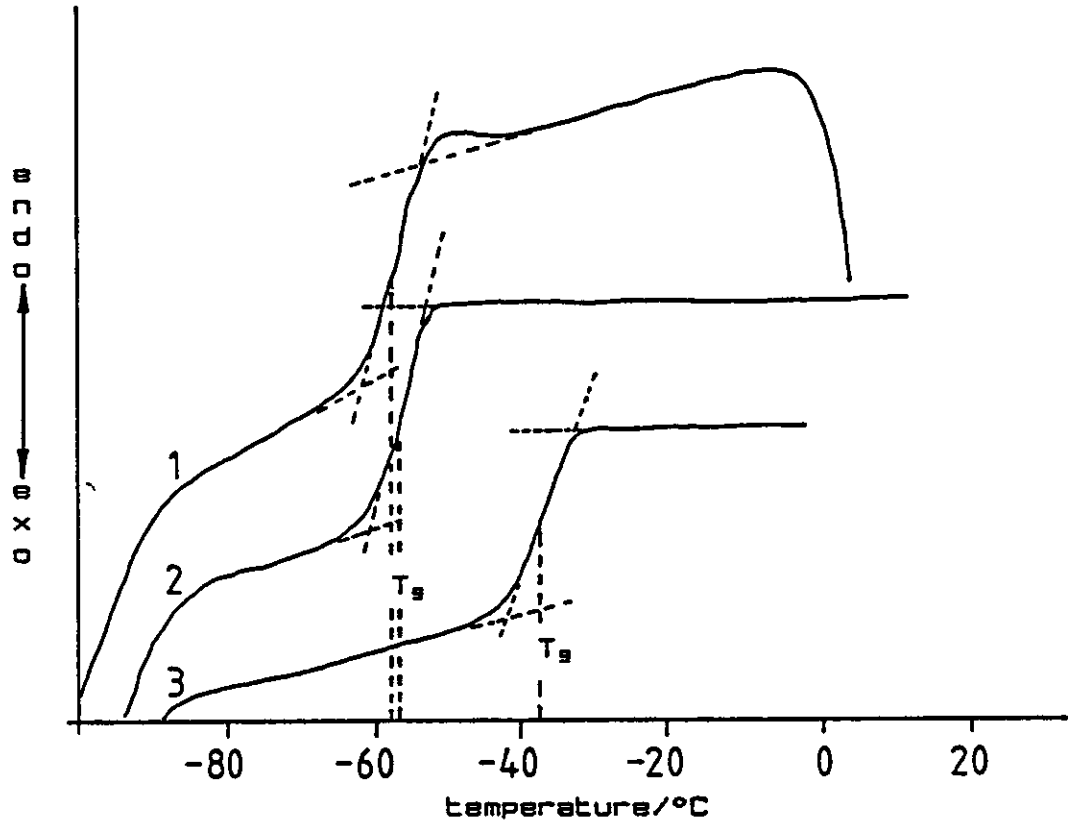

4.4 DYNAMIC MECHANICAL THERMAL ANALYSIS OF SWOLLEN POLY (VINYLCHLORIDE) PLAQUES

The results obtained from the PL-DMTA were in the form of thermograms depicting tan δ and log modulus with modulus units in Nm^{-2} plotted against temperature. A typical thermogram obtained for uPVC heated at 4°C/min at 1 Hz, with a constant strain of times one, is shown in figure 4.43. The normal Greek alphabetic labelling convention[156] is used running from high to low temperatures to describe the tan δ peaks and the convention used by McCrum et al.[157] is adhered to in labelling the modulus curve. E_u' is the unrelaxed storage modulus E' and E_r' the relaxed storage modulus.

4.4.1 The capabilities of the Polymer Laboratories Dynamic Mechanical Thermal Analyser

The mechanical spectrometer has a maximum force capability of 4N and a maximum sample displacement of 250 microns. The instrument can measure more than 4 and a half decades of sample modulus. A thick sample of high modulus material can present too high a stiffness for the instrument to achieve adequate displacement. On the other hand a very thin film of low modulus material will not provide enough restoring force for the system to calculate modulus variations with accuracy. In this minimum case data will be collected but of questionable accuracy.

The modulus of any sample, the restoring force per unit displacement, is provided by the product kE' in the

FIGURE 4.43

PL-DMTA dual-cantilever thermogram produced on heating S71/102 uPVC at 4°C/min with a frequency of 1 Hz and instrument strain of one

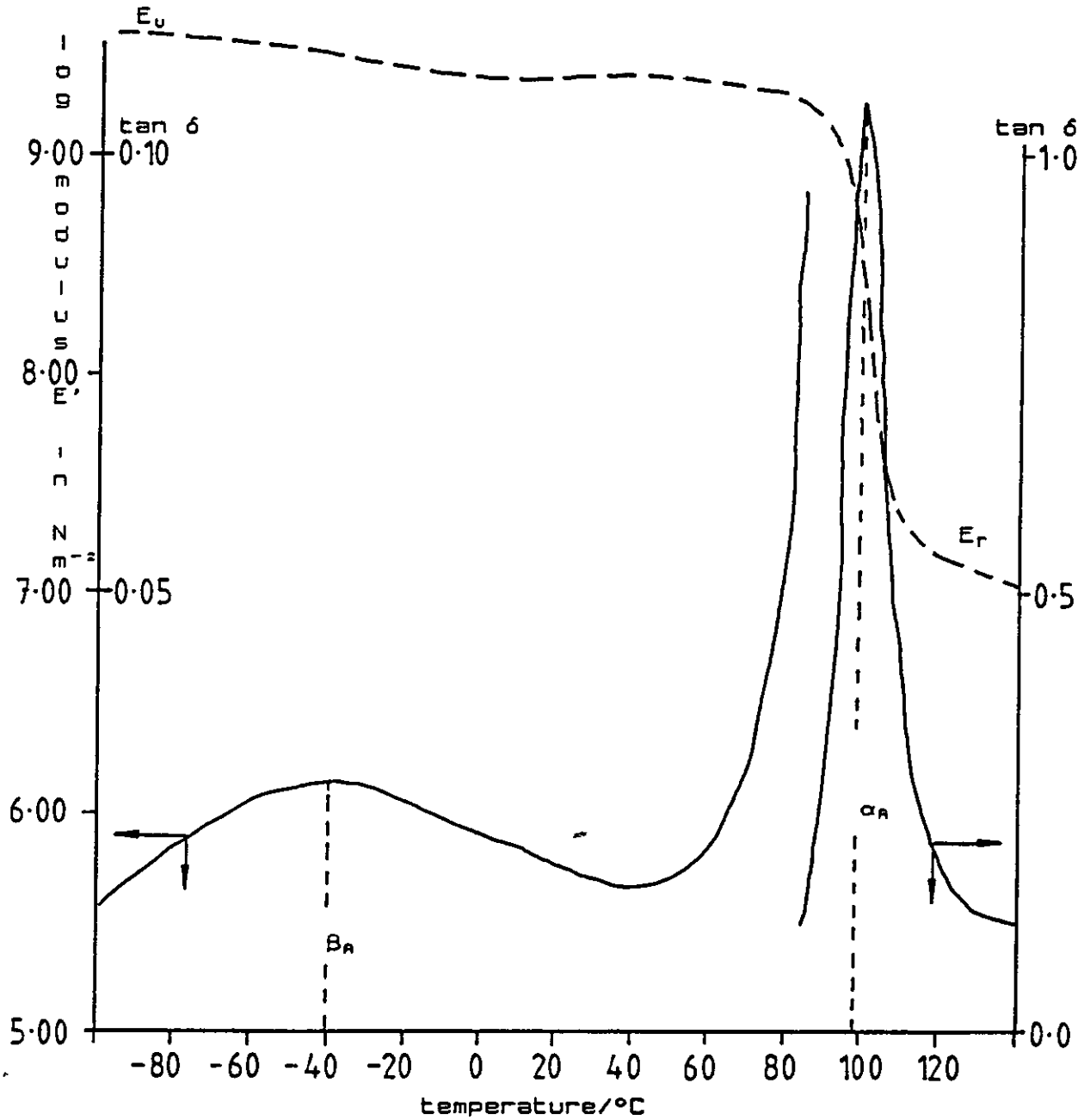

dual-cantilever mode and kG' in the shear mode, where k, the geometry constant, is calculated using equation 3.8. The maximum stiffness the machine can detect, shown as the product log (kE'), is 6.5 in the 'auto-strain' mode. All analyses have been carried out at constant displacement, strain times one, a displacement of 16 microns giving an upper working limit of log (kE') = 6.0. The minimum stiffness is log (kE') > 2.0.

The sample geometry is selected to ensure that the kE' product remains within the operational range of the instrument during analysis. In the dual cantilever mode the easiest parameter to control is the sample length. In the shear mode the sample length is the only parameter that can be changed and is kept less than twice the diameter to keep bending errors to a minimum.

The measurement through the T_g of PVC using the dual-cantilever mode produced a fall in modulus typically from log 9.4 in the "glassy" state to log 6.8 in the "rubbery" region. When the above considerations for accurate analysis during a complete thermal scan, i.e. from -130°C to 170°C, are taken into account, the respective k constants are 4.0 < log k > 3.0. In shear mode, however, using unswollen PVC samples having an original thickness of around 2 mm and swelling to a maximum thickness value of around 3.5 mm, it is impossible to keep within the machine's operating limits for the ideal complete temperature scan of -130°C to 170°C, reliable information only being obtained after the onset of softening. Thus, information on the β relaxation, occurring at -30°C in the shear mode is unobtainable. Also, due to the high modulus at low temperatures and considering

that the samples are only held in the frame by compression, a considerable amount of slippage occurs.

4.4.1.1 Experimental variation

The Log modulus and tan δ thermograms for the shear analysis of PVC plaques swollen with dimethylbenzene for 30 mins at 60°C are shown in figures 4.44 and 4.45 respectively. This experiment was designed to examine the accuracy of the experimental procedure. To test the consistency of the analysis within the sample a large plaque was swollen with dimethylbenzene for 30 mins at 60°C from which a number of samples were cut out and analysed. Any error produced would mainly be attributed to the clamping procedure and the micrometer measurement of the sample thickness. The log modulus readings at 60°C are shown in table 4.8 together with the tan δ peak positions. The tan δ peak position for the swollen region is denoted by $T_g\alpha'$ and the tan δ peak position for the dry unswollen portion is denoted by $T_g\alpha$.

4.4.2 Analysis of highly swollen poly (vinylchloride) plaques using dual-cantilever dynamic mechanical thermal analysis methods

4.4.2.1 Systems thought to be fully swollen

Room temperature liquid sorption of some of the swelling agents investigated produced a plaque,

FIGURE 4.44

Experimental variation of log modulus shown by PL-DMTA shear analysis of identical uPVC samples swollen with dimethylbenzene liquid at 60°C for 30 mins

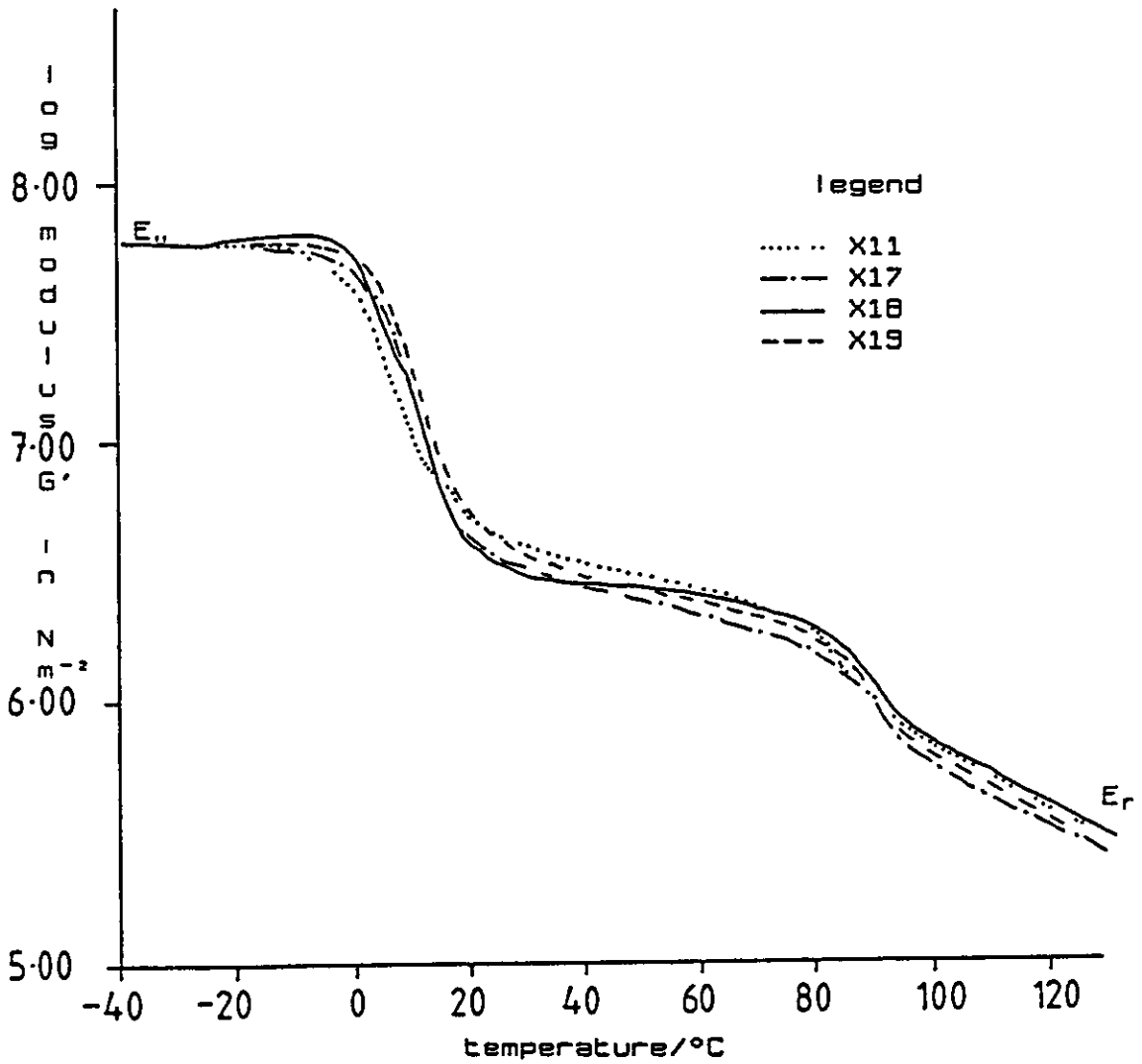

FIGURE 4.45

Experimental variation of tan δ shown by PL-DMTA shear analysis of identical uPVC samples swollen with dimethylbenzene liquid at 60°C for 30 mins

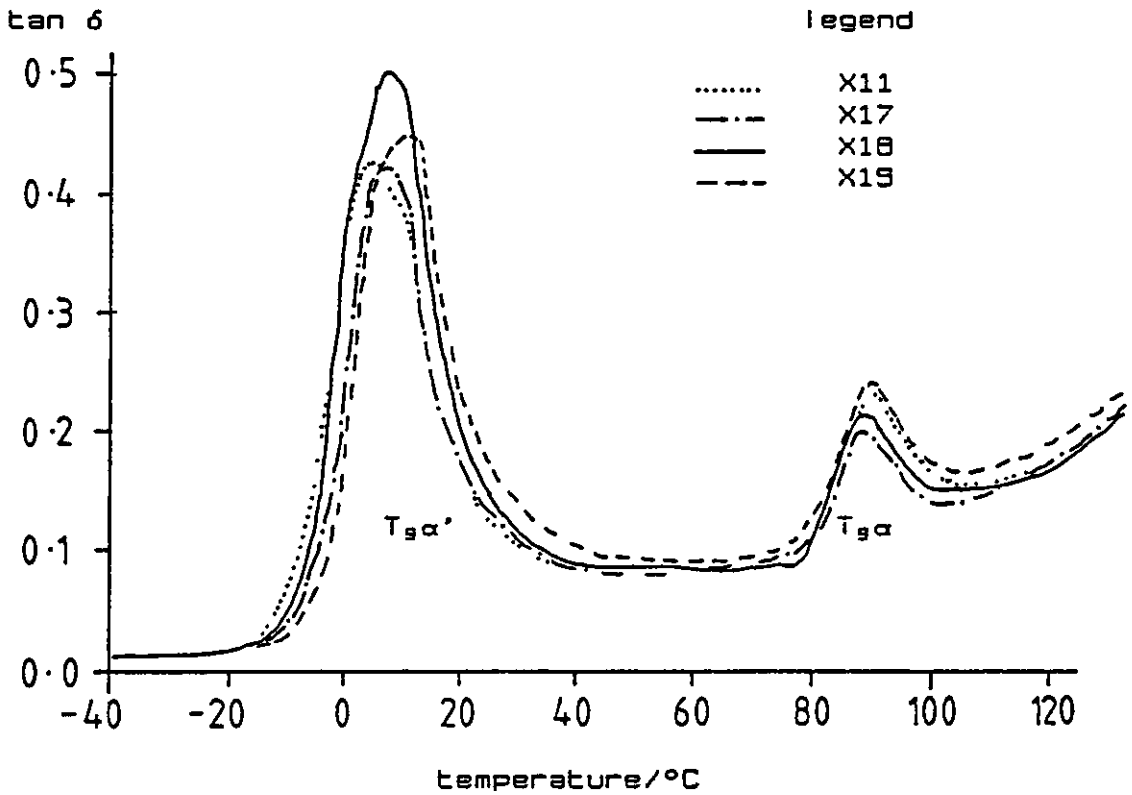

TABLE 4.8

Experimental variation between samples of PVC swollen, to the same extent, with dimethylbenzene liquid

sample number	percentage molar content	log modulus at 60°C (G' in Nm^{-2})	$T_g\alpha'$	$T_g\alpha$
X11	15	6.40	4	90
X17	14	6.46	7	89
X18	12	6.32	8	89
X19	14	6.44	10	90

which was opaque white in colour, very soft and rubbery in texture with no visual appearance of the dry inner core remaining. A typical thermogram is seen in figure 4.46. This depicts the tan δ plot exhibiting two peaks both at low temperatures, -37 and -124 °C. The larger broader peak, $T_g\alpha'$, occurring at -37°C is thought to be due to a transition associated with the swollen PVC region. In all of these highly swollen samples the PL-DMTA was operated until the sample disintegrated; in each case no tan δ peak associated with the T_g of uPVC was observed, thus, the PVC plaques employed were thought to be fully swollen. At the temperature where the sample began to break, shown by wide fluctuations in the modulus and tan δ readings, the experiment was terminated.

The small low temperature tan δ, $T_{g\ell}$, peak is thought to be a transition associated with the excess liquid present. Fully swollen plaques producing $T_{g\ell}$ peaks possibly associated with the pure liquid, are shown in figures 4.46 to 4.54. The results are tabulated in table 4.9. The temperatures of the transition due to excess ethylbenzene and nitroethane in fully swollen plaques shown in table 4.9 compare well with the PL-DMTA T_g values of the respective pure liquids in table 4.7.

4.4.2.2 Highly swollen diluent/Poly (vinylchloride) systems exhibiting an unplasticised poly (vinylchloride) glass transition

Extremely fast liquid sorption was observed with 1,2-dichloroethane and trichloromethane at 45°C into plaques

FIGURE 4.46

Low temperature tan δ peaks produced using dual-cantilever PL-DMTA on uPVC swollen with nitroethane liquid at room temperature

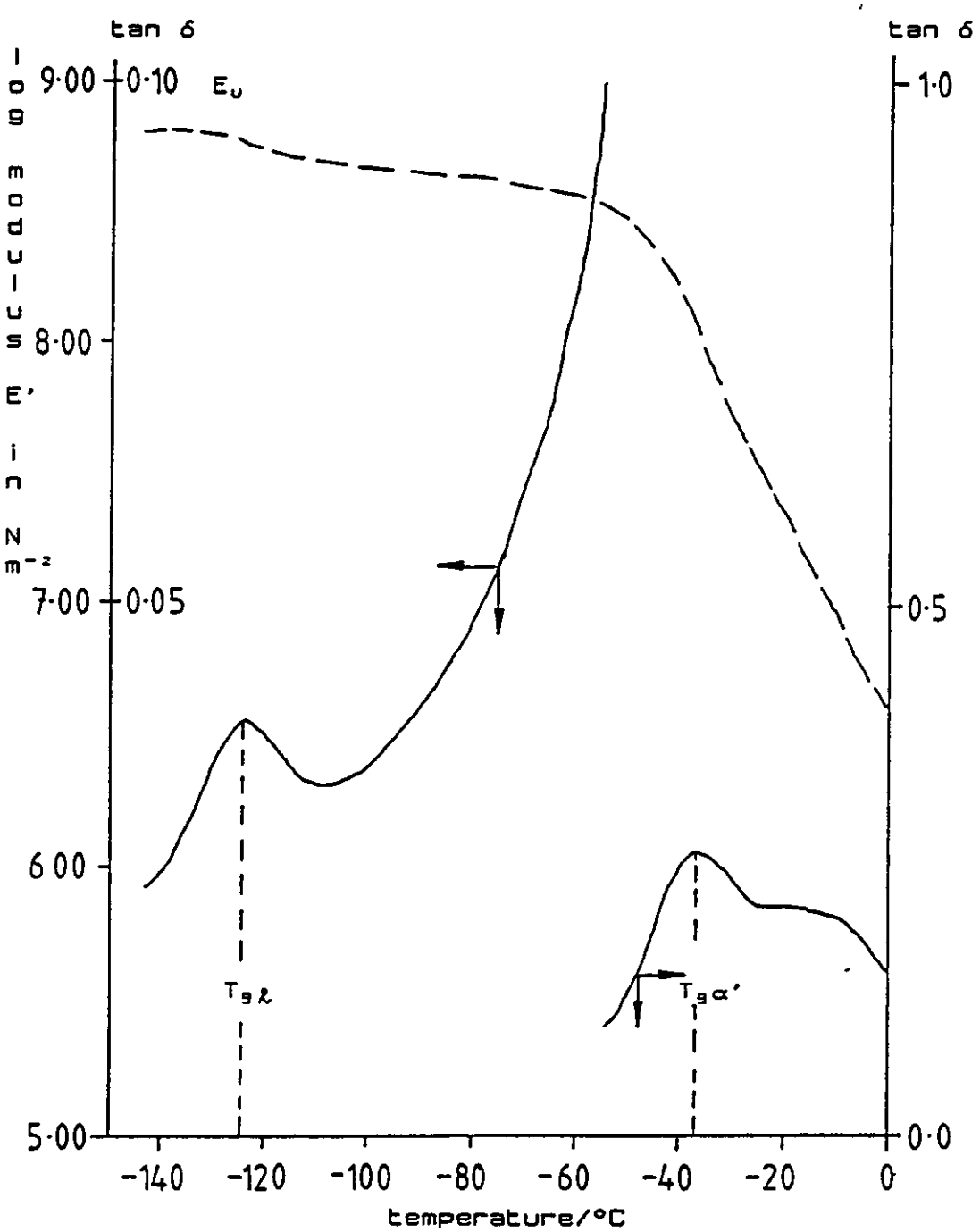

FIGURE 4.47

Low temperature tan δ peaks produced using dual-cantilever PL-DMTA on uPVC swollen with 1,2-dichloroethane liquid at room temperature

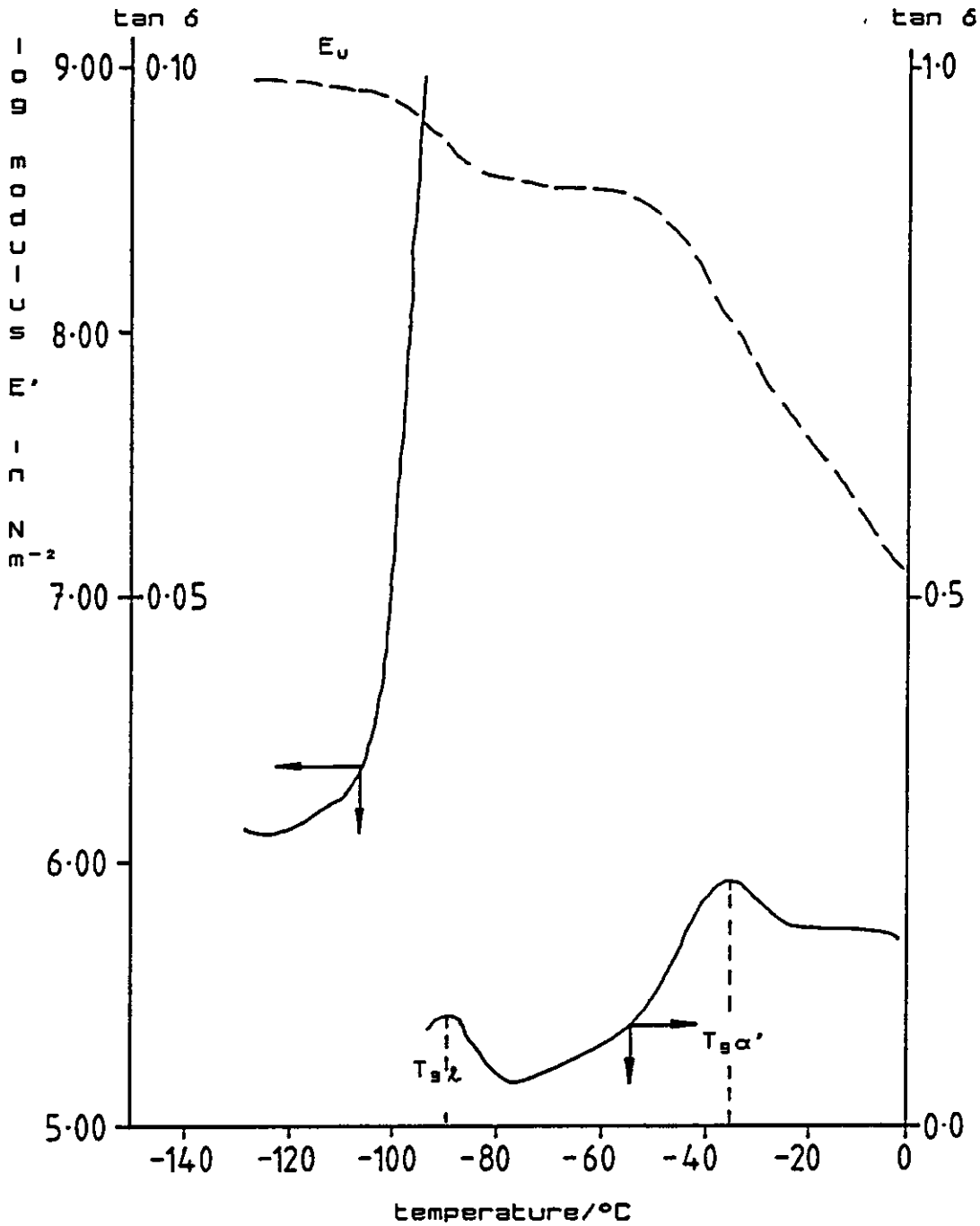

FIGURE 4.48

Low temperature tan δ peaks produced using dual-cantilever PL-DMTA on uPVC swollen with chlorobenzene liquid at room temperature

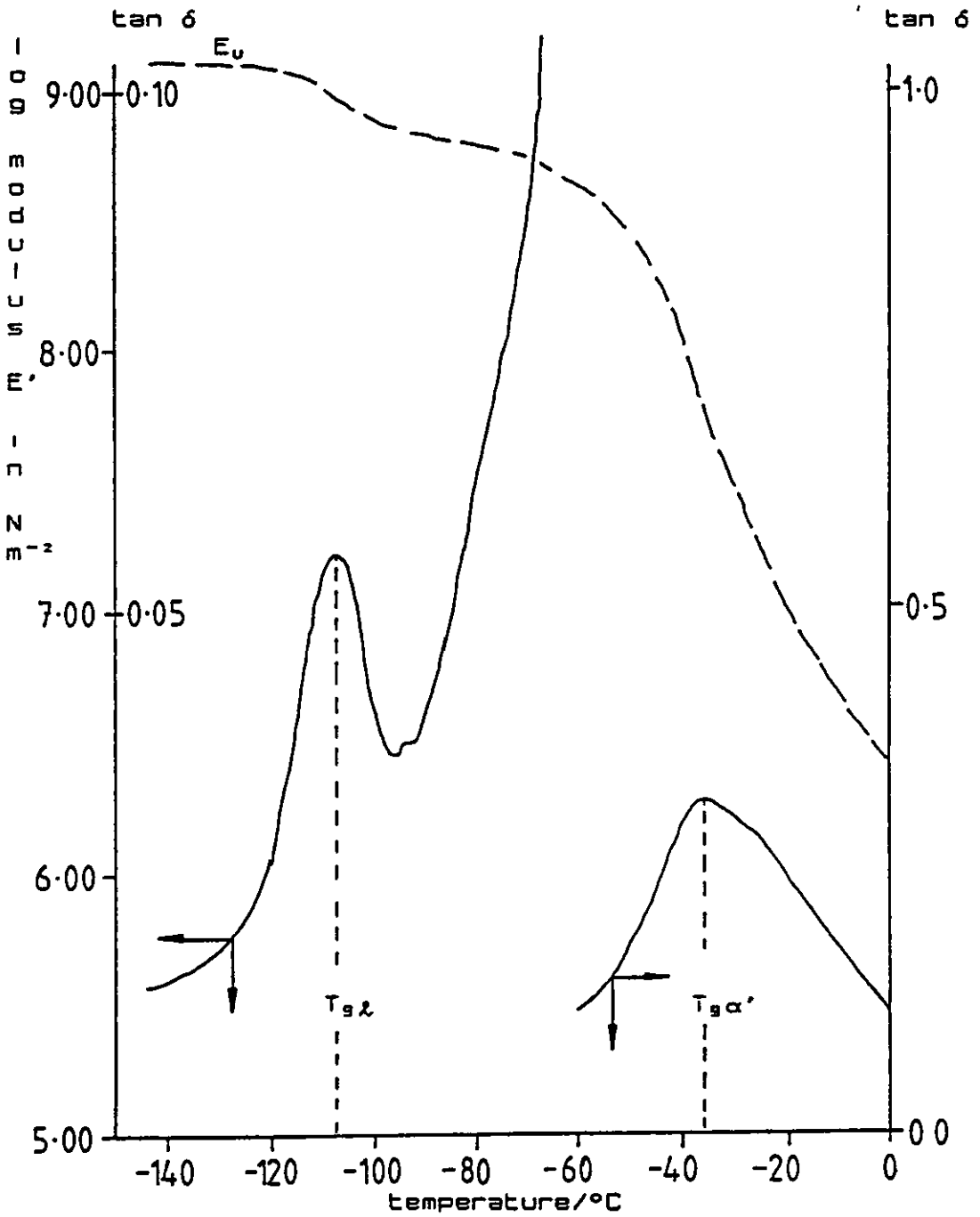

FIGURE 4.49

Low temperature tan δ peaks produced using dual-cantilever PL-DMTA on uPVC swollen with trichloroethane liquid at room temperature

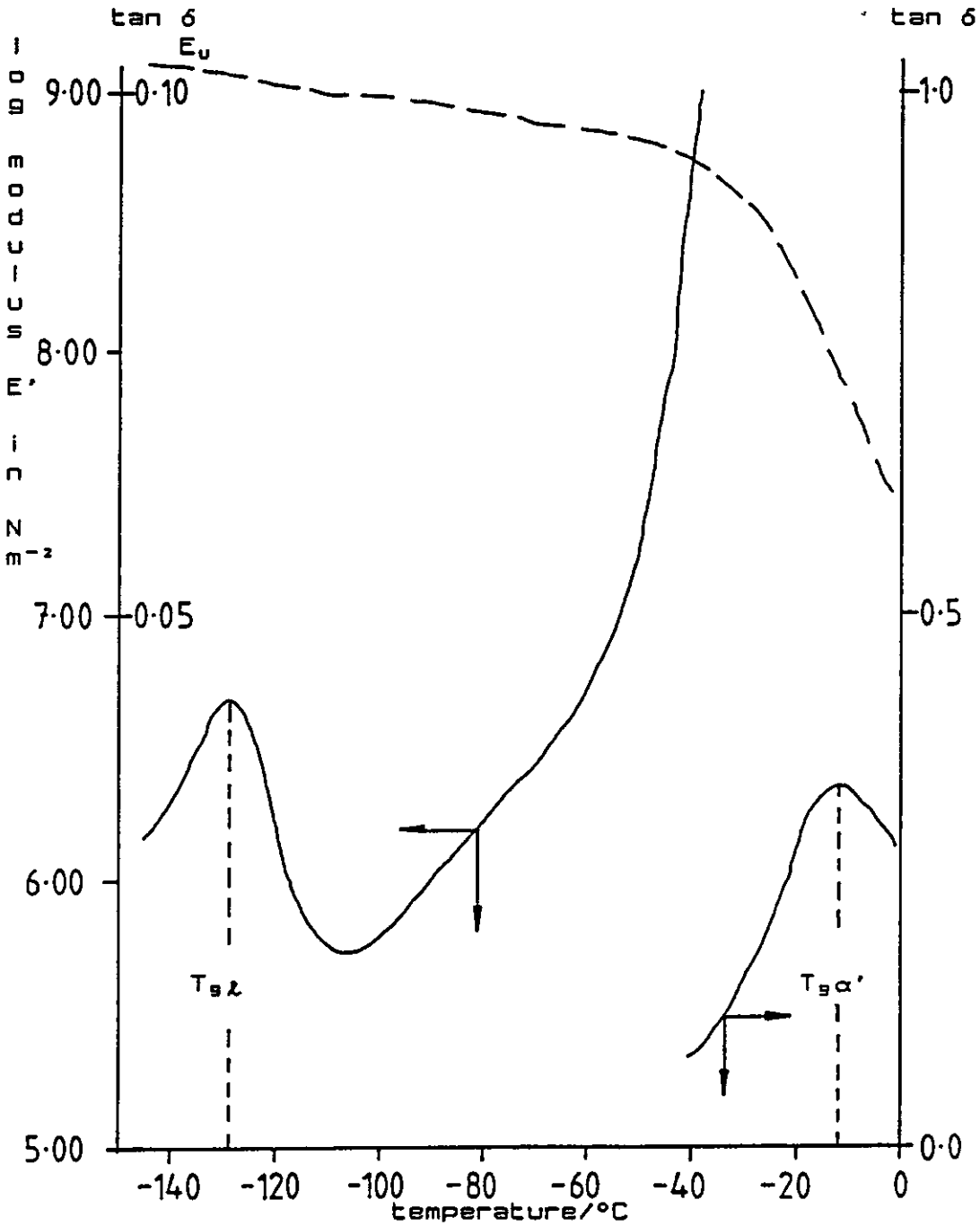

FIGURE 4.50

Low temperature tan δ peaks produced using dual-cantilever PL-DMTA on uPVC swollen with 2-nitropropane liquid at room temperature

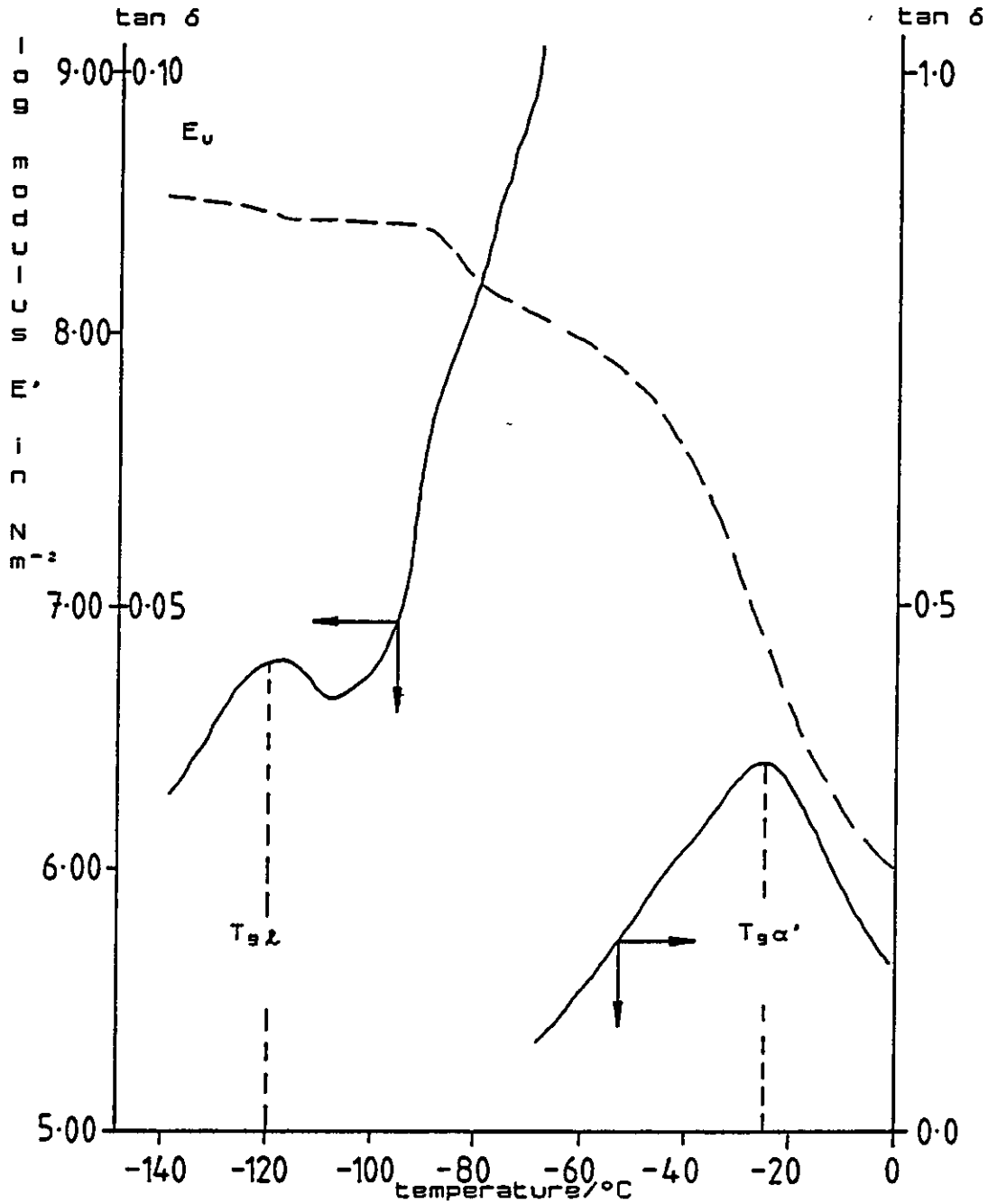

FIGURE 4.51

Low temperature tan δ peaks produced using dual-cantilever PL-DMTA on uPVC swollen with 1-nitrobutane liquid at room temperature

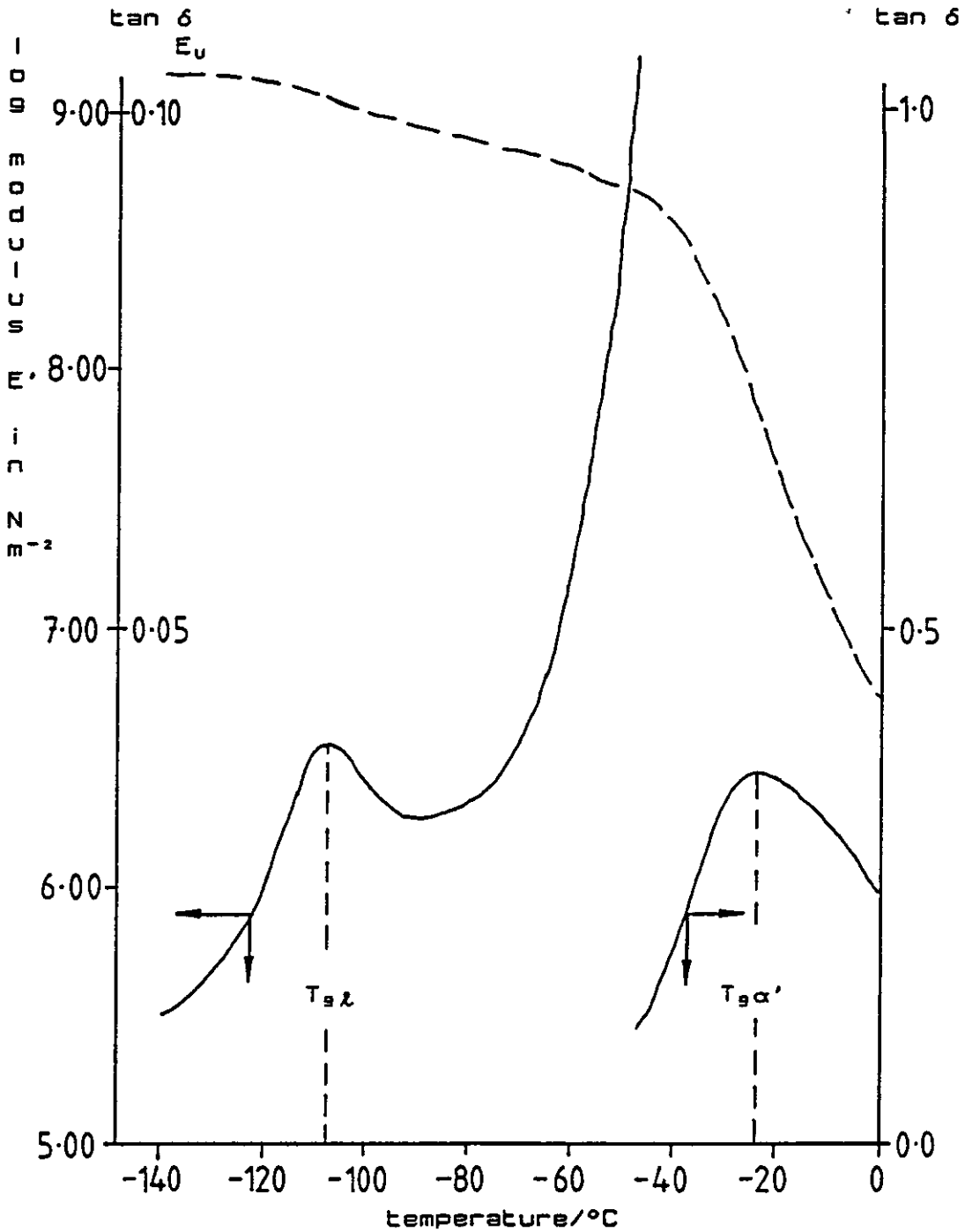

FIGURE 4.52

Low temperature tan δ peaks produced using dual-cantilever PL-DMTA on uPVC swollen with ethylbenzene liquid at room temperature

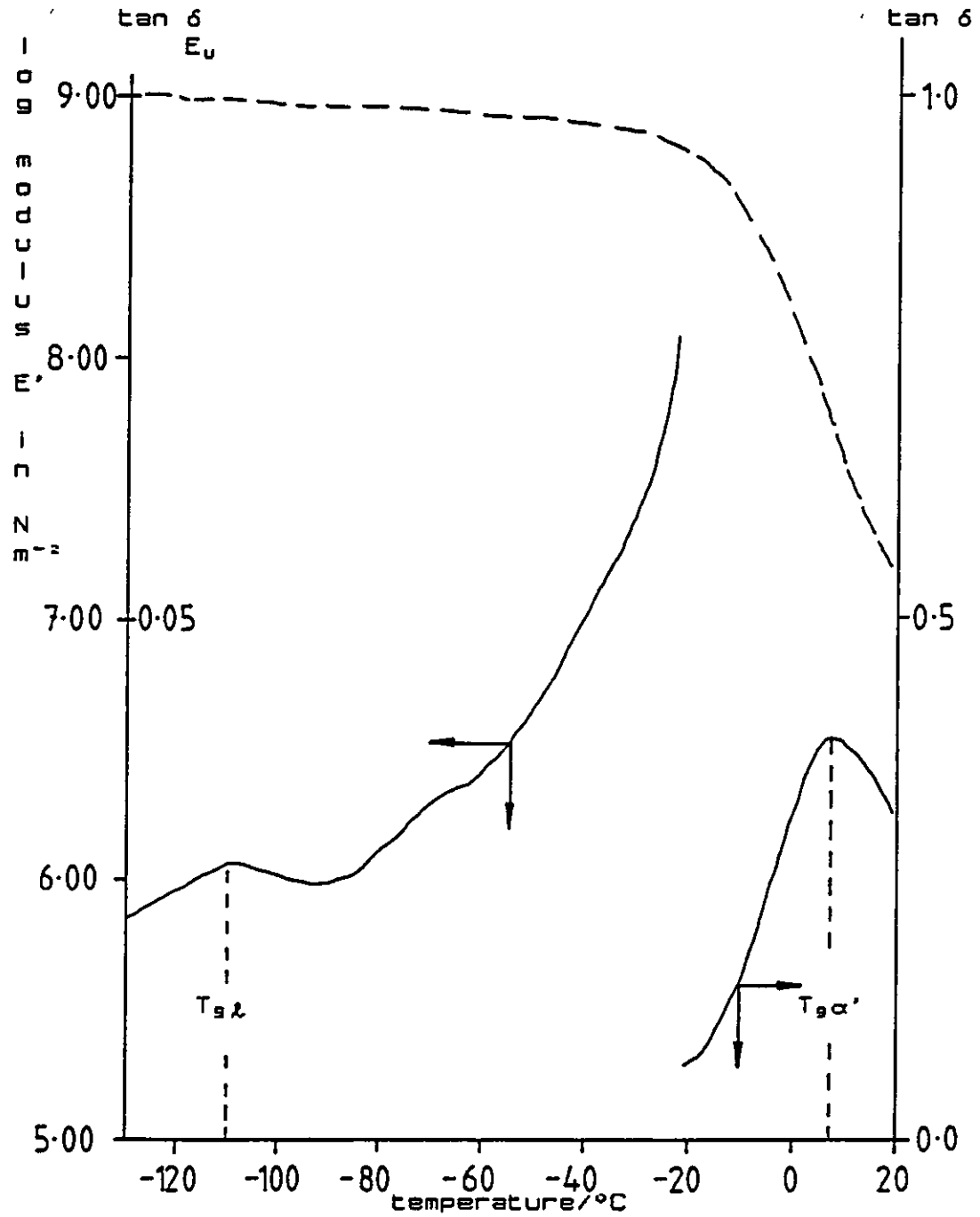

FIGURE 4.53

Low temperature tan δ peaks produced using dual-cantilever PL-DMTA on uPVC swollen with dichlorobenzene liquid at room temperature

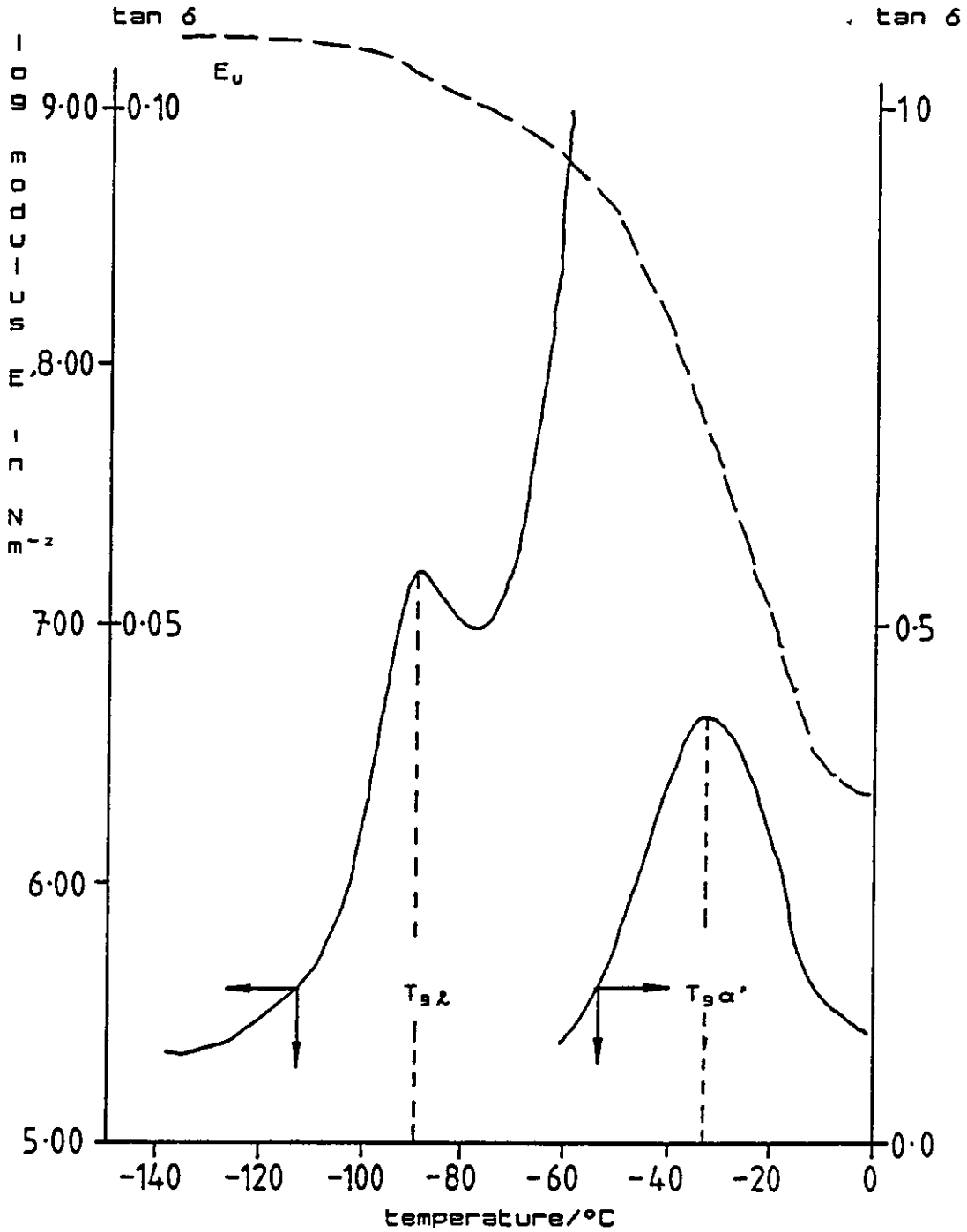

FIGURE 4.54

Low temperature tan δ peaks produced using dual-cantilever PL-DMTA on uPVC swollen with propanone liquid at room temperature

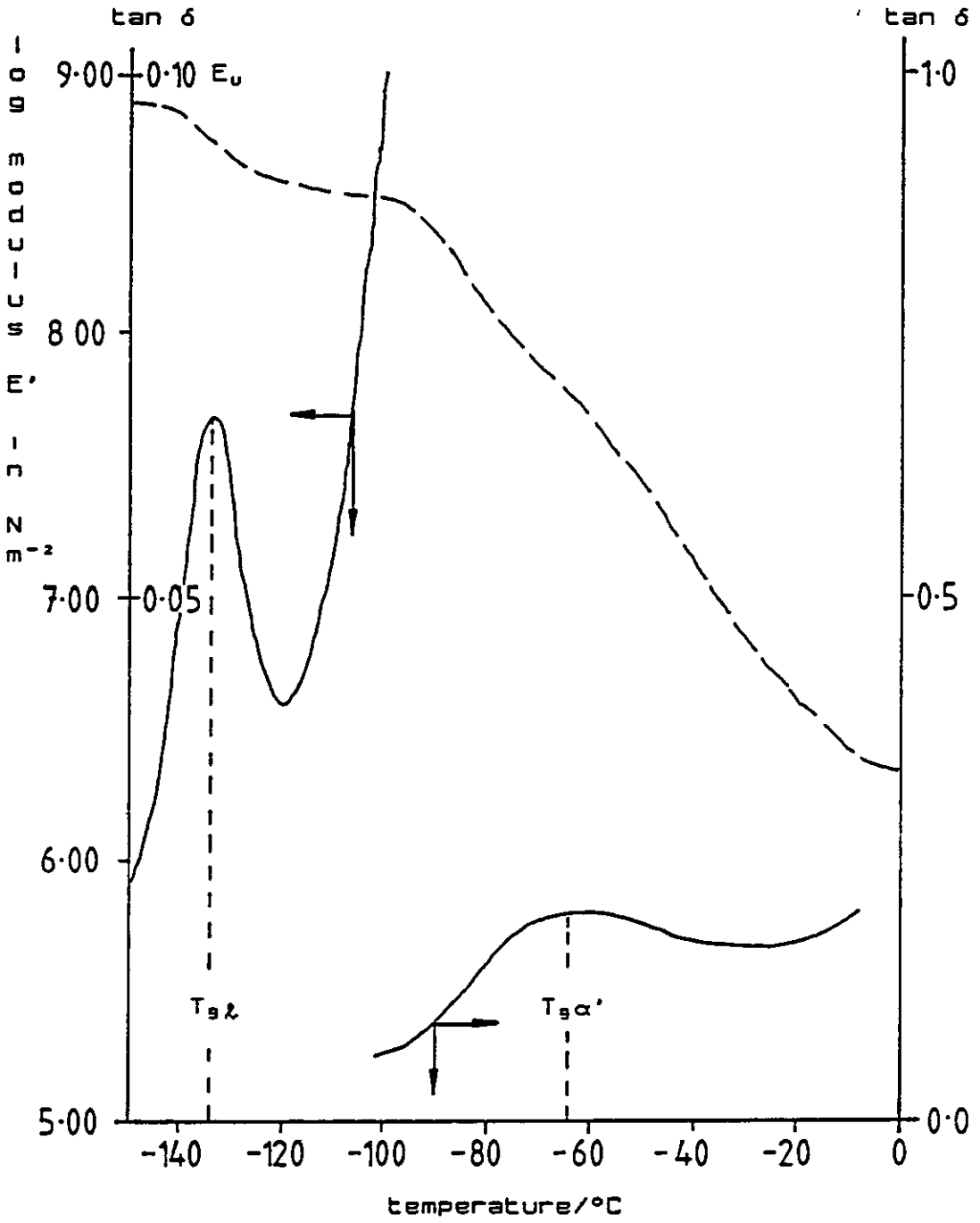

TABLE 4.9

Tan δ peak positions produced using fully swollen PVC plaques produced at room temperature; (PL-DMTA dual cantilever mode at 4°C/min and strain times one.)

swelling liquid	sorption time (days)	% molar content	transition due to excess liquid, $T_{g\ell}$ °C	$T_{g\alpha'}$ °C
ethylbenzene	85	19	-111	8
nitroethane	29	70	-124	-37
2-nitropropane	3	67	-120	-24
1-nitrobutane	24	56	-106	-22
chlorobenzene	15	61	-106	-35
dichlorobenzene	6	60	-79	-32
trichloroethane	16	32	-128	-12
1,2-dichloroethane	3	86	-88	-35
propanone	12	51	-132	---

FIGURE 4.55

Dual-cantilever PL-DMTA on uPVC rapidly swollen with trichloromethane liquid at 45°C

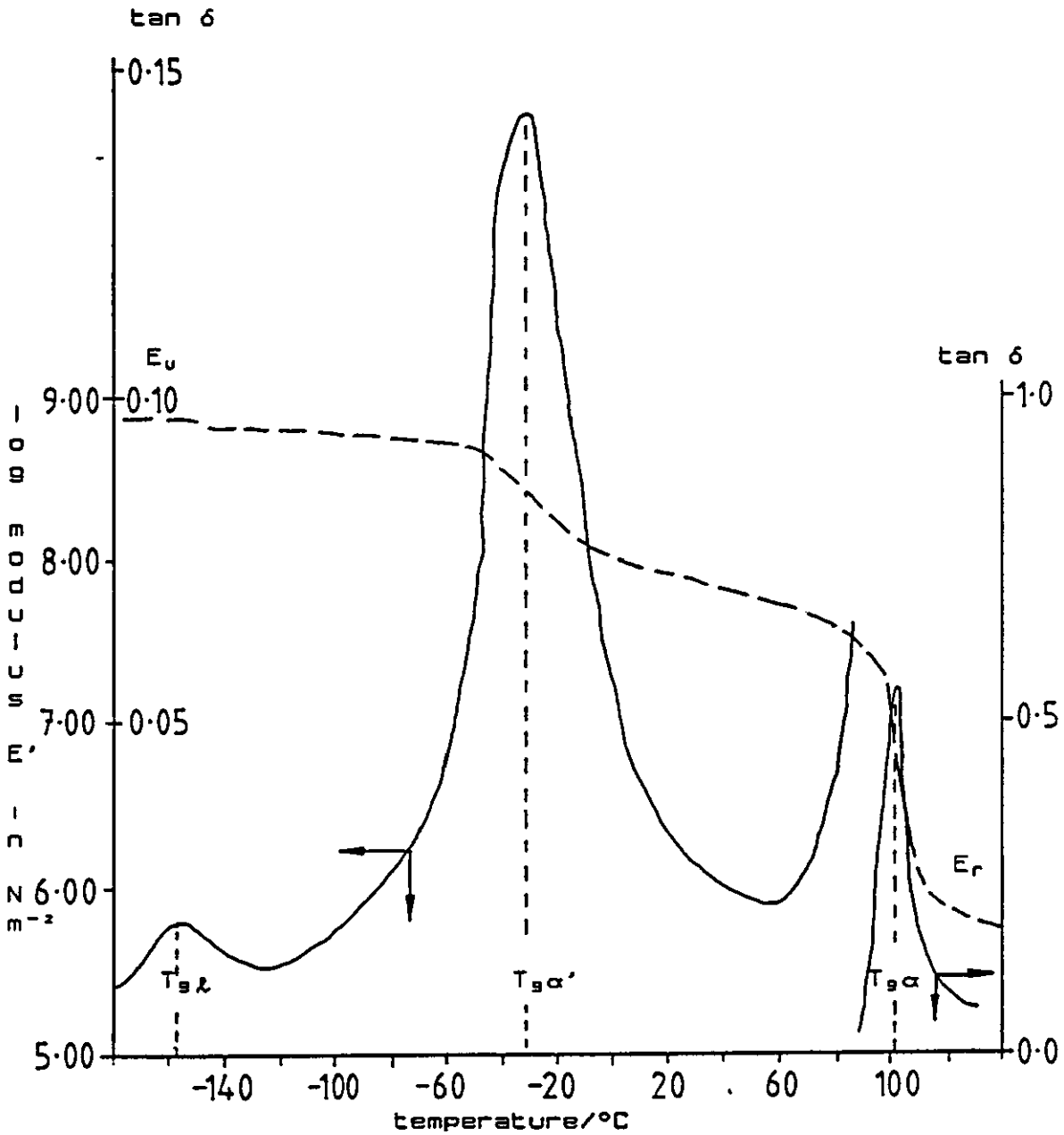

of PVC. When examined using PL-DMTA in the dual-cantilever mode, three tan δ transition peaks were observed, a small $T_{g\ell}$ peak thought to be associated with glassy regions of excess liquid present, a broad peak associated with the diluent swollen outer layer and a main $T_{g\alpha}$ peak, an example of which is shown in Figure 4.55. An approximate value for the T_g of trichloromethane is -149°C, shown in table 4.9, this compares to within 14°C of the $T_{g\ell}$ peak exhibited in figure 4.55. The $T_{g\ell}$ peak produced in the PL-DMTA of uPVC swollen with 1,2-dichloroethane occurs at -113°C a difference of 17°C with the $T_{g\ell}$ calculated value for 1,2-dichloroethane shown in table 4.9.

4.4.3 Examination of vapour swollen poly (vinylchloride) plaques using dual-cantilever, dynamic mechanical thermal analysis methods

Vapour swollen samples produced thermograms where the $T_{g\alpha'}$ peak occurred at higher temperatures than observed in section 4.4.2 for liquid swelling. This would indicate a low concentration of vapour in the polymer. In some cases, (see figure 4.56), the $T_{g\alpha'}$ peak is a shoulder on the low temperature side of the $T_{g\alpha}$ peak.

Using the conditions described in section 4.2 to produce table 4.6 it was found that the extent of sorption, with the exception of 1,2-dichloroethane, in each case was small and was not sufficient to produce a visible separate swollen layer. The sorption of 1,2-dichloroethane into PVC plaques was rapid when compared with the other vapours that were examined. The rate of sorption was some 50 times

FIGURE 4.56

Dual-cantilever PL-DMTA on a 0.4 g plaque of uPVC containing 1 mg of benzene introduced from the vapour state at 50°C

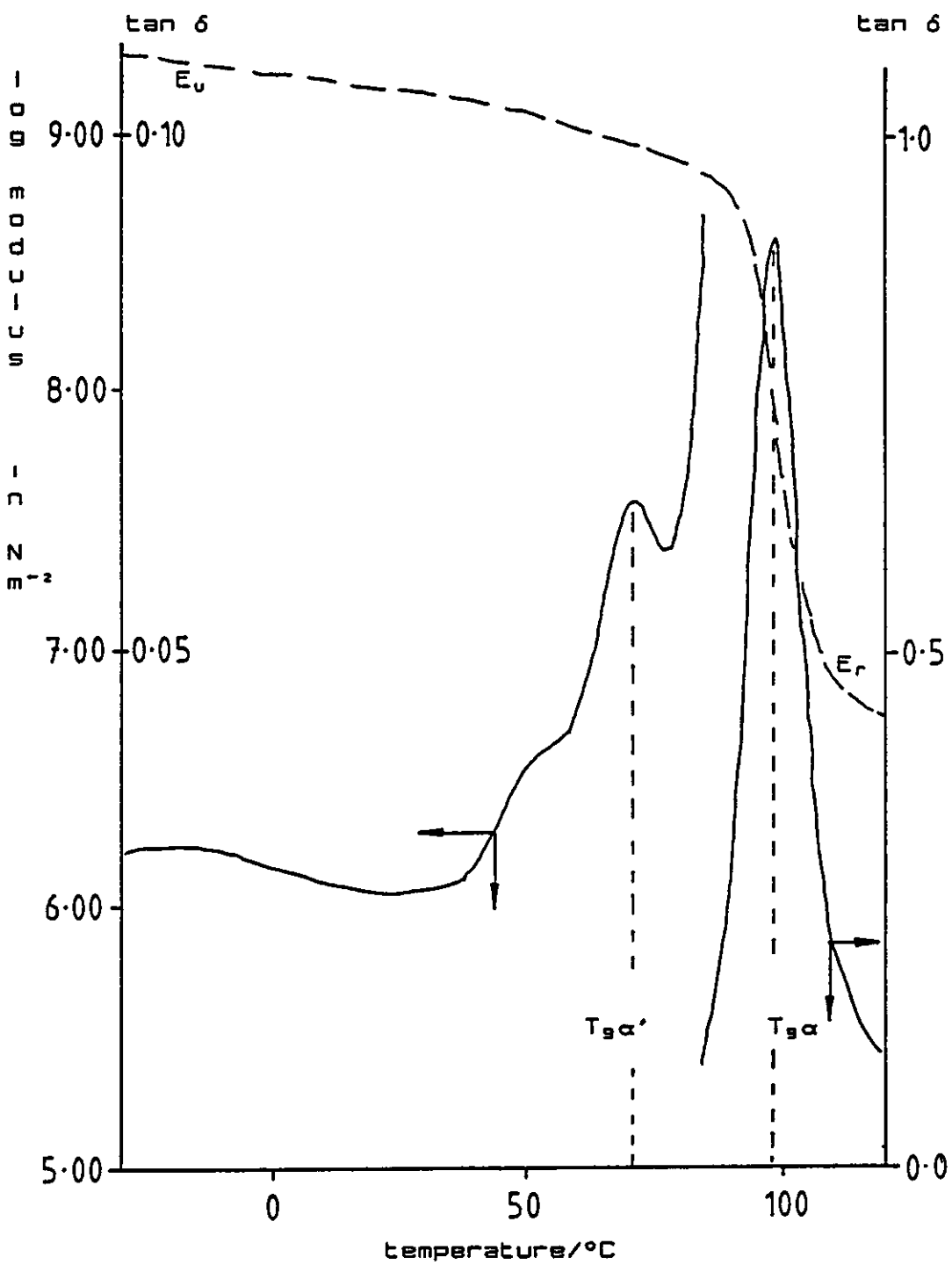

greater than that of benzene as shown in table 4.6, for experiments at the same vapour pressure and temperature. It was possible with 1,2-dichloroethane to sorb enough vapour in the plaque sufficiently to remove the $T_{g}\alpha$ transition as shown in table 4.10. There was, however, no indication of a solvent front moving through the polymer as compared with liquid swollen PVC plaques. PL-DMTA studies of uPVC swollen with 2-nitropropane produced a plaque where the $T_{g}\alpha'$ peak is more clearly resolved than uPVC swollen with benzene (see figure 4.56) or propanone vapour, as shown in figure 4.57.

Dual cantilever PL-DMTA was carried out on uPVC swollen with 1,2-dichloroethane and benzene vapour for a range of percentage mol vapour contents in the sample as shown in table 4.10. It is seen that the relatively rapid uptake of 1,2-dichloroethane precludes the examination of swollen plaques with vapour contents less than 6%. The $T_{g}\alpha$ peak is removed at vapour contents higher than 8.4%. The tan δ thermograms for uPVC swollen with 1,2-dichloroethane and benzene vapour for the percentage molar contents shown in table 4.10 are shown in figures 4.58 and 4.59. The numbers on the curves refer to the percentage molar content of vapour in the sample. The curves are numbered with increasing percent molar content of swelling agent present at the removal of the sample from the swelling environment. Although precautions were carried out to prevent vapour loss from the sample between weighings, before and after PL-DMTA loss of vapour is inevitable particularly during PL-DMTA. Since the ranges of percent molar contents of vapours shown in figures 4.58 and 4.59 are small the loss of vapour from the samples may account for the more highly swollen samples

TABLE 4.10

Tan δ peak positions shown by PVC, swollen with 1,2-dichloroethane and benzene vapours during PL-DMTA

vapour	%mol content in sample	$T_{g}\alpha'$ °C	$T_{g}\alpha$ °C
1,2-dichloroethane	6.1	28	95
	8.4	43	95
	9.7	47	--
	12.0	40	--
	13.4	36	--
	20.4	24	--
	22.1	36	--
benzene	0.2	72	99
	4.5	53	98
	4.8	49	99
	9.1	40	97
	13.6	43	--

FIGURE 4.57

Resolution of tan δ peaks of dual-cantilever PL-DMTA of uPVC plaques swollen with either 48 mg of 2-nitropropane or 33 mg of propanone introduced from the vapour state at 50°C

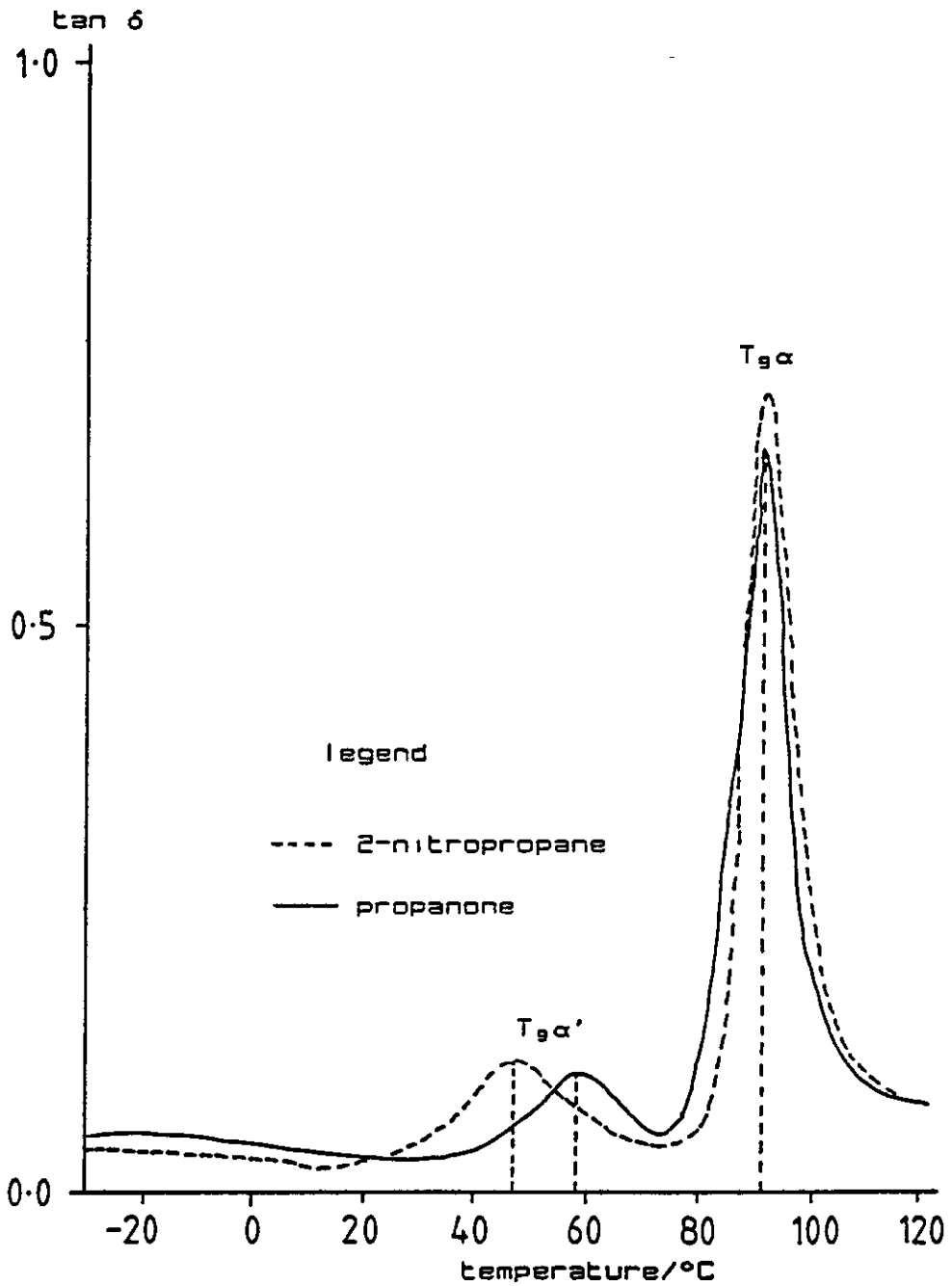

FIGURE 4.58

Tan δ thermograms produced on heating uPVC plaques swollen with 1,2-dichloroethane vapour at 50°C

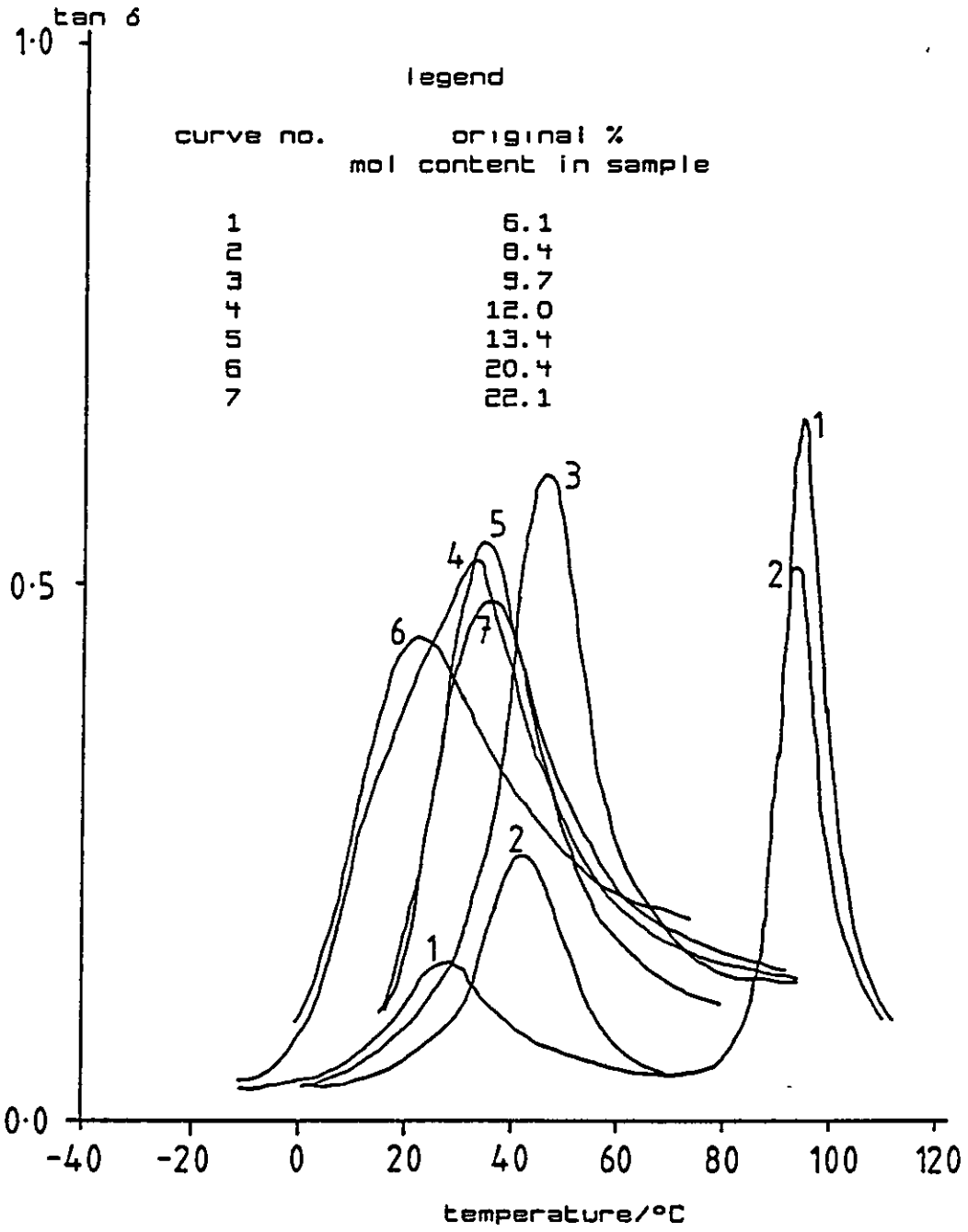

FIGURE 4.59

Tan δ thermograms produced on heating uPVC plaques swollen with benzene vapour at 50°C

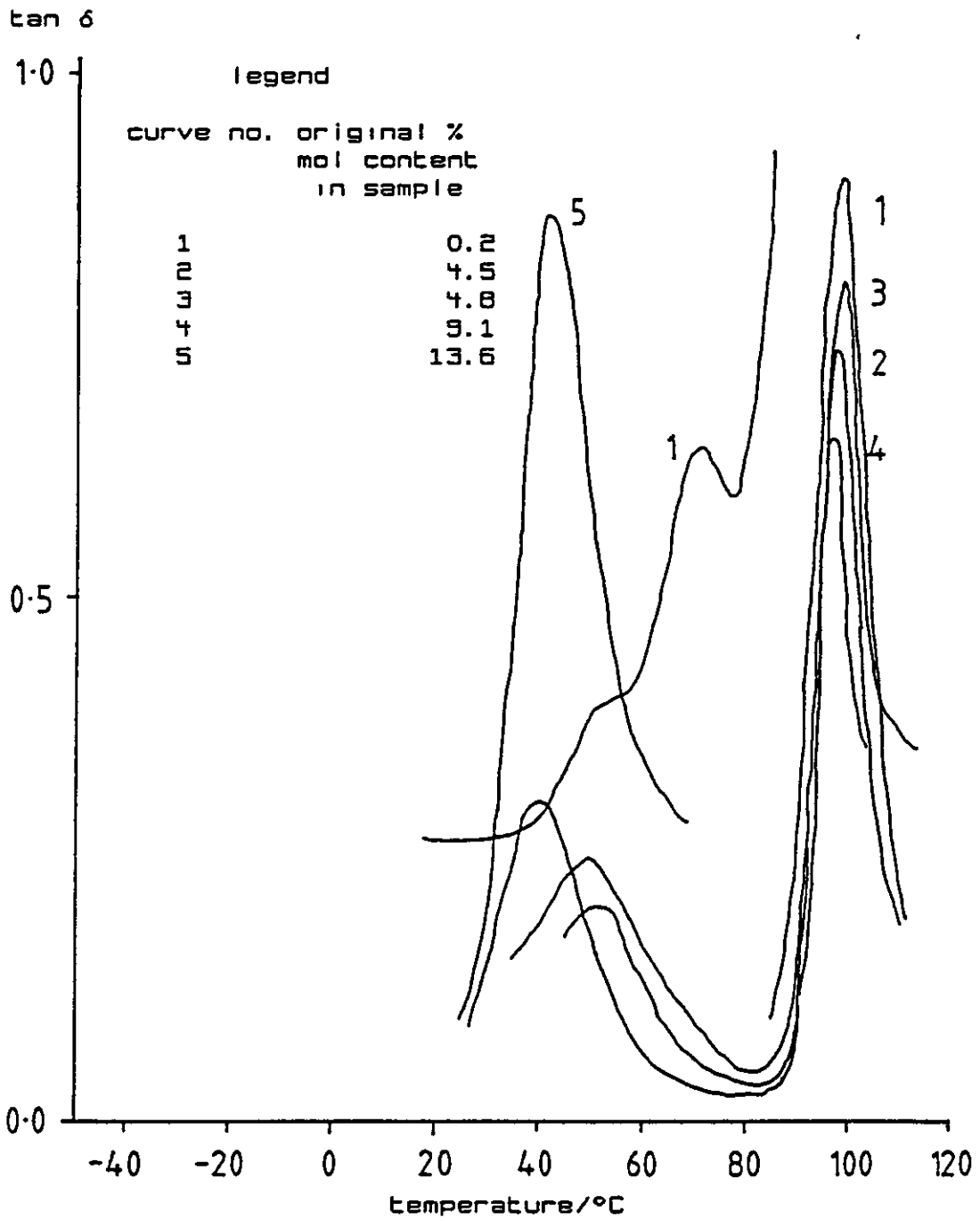

showing $T_g\alpha$''s higher than expected.

4.4.4 Analysis of highly swollen PVC plaques using shear PL-DMTA methods

4.4.4.1 Loss of vapour during analysis

The PL-DMTA temperature range employed, was approximately -130 to 120°C with a heating rate of 2°C/min for shear analysis, meant an approximate time for a single experiment would be around 125 min. Since some of the diluents had boiling points within this working range the sample may be losing diluent during the analysis, and in sample preparation and handling, therefore the concentration of liquid in the swollen region calculated at the start of the experiment will be greater than the concentration at 60°C. An indication of the loss of material from the sample by the time the temperature has reached 60°C in the analyser is required since the mechanical properties of the material discussed in chapter 5 will depend on the concentration of diluent present at that temperature. A series of experiments was thus designed to estimate the amount of liquid loss at any particular time during the PL-DMTA experiment, in particular the loss of liquid occurring up to 60°C.

Plaques of PVC were swollen at 60°C for various time intervals in order to produce samples with different liquid swollen layer thicknesses. Discs were cut from the swollen plaques as described in section 3.2. Knowledge of L_T and L_C allowed the computation of the respective volume fractions

of the swollen region, V_r, and the dry inner core, V_s, in the disc. The molar content of liquid present in the swollen region in the discs was calculated using methods described in Appendix 2. The discs were subsequently cooled and analysed in the PL-DMTA instrument. At least four samples were produced for each sorption time interval. The analyses were terminated at various times corresponding to produce a range of "removal temperatures" as stated in table 4.11. The loss of liquid was calculated using the methods outlined in Appendix 2 for each removal temperature. The results are tabulated in table 4.11 and the percentage loss of liquid in the sample was plotted with respect to the duration of the PL-DMTA experiment (shown as the sample removal temperature) in figures 4.60 to 4.64. The V_r fractions of the samples shown in these figures are approximations to the values given in table 4.11, in an attempt to model the loss of liquid from the sample to the extent of penetration of the liquid in the sample as shown by the V_r fraction. In the worst case, propanone, the loss of liquid at 60°C in the analyser is around 20% and around 10% for the other, higher boiling point liquids.

4.4.4.2 Shear log modulus thermograms of liquid swollen disc

Log modulus thermograms for swollen polymers for the various liquids employed using shear analysis techniques are shown in figures 4.65 to 4.69. Only a representative number of analyses are shown in each case for simplicity. The ascending numbers on the thermograms indicate the increasing

TABLE 4.11

Loss of solvent from samples during PL-DMTA

Sample no.*	sorption time mins	V_f fraction	removal temperature °C	liquid content in sample mg	loss of liquid from sample mg	% loss
A12	2	0.38	-30	11.8	2.6	22.03
A10	2	0.40	-20	7.3	0.9	12.33
A11	2	0.46	0	8.6	1.2	13.95
A21	2	0.43	30	8.0	1.2	15.00
A9	2	0.32	60	13.4	2.7	20.15
A19	2	0.41	60	7.8	1.7	21.79
A18	2	0.39	100	13.3	6.3	47.37
A13	2	0.40	110	16.2	6.8	41.98
A16	5	0.57	-20	30.2	10.5	34.77
A17	5	0.54	5	26.5	6.7	25.28
A15	5	0.50	50	25.8	6.6	25.58
A14	5	0.47	100	26.3	15.1	57.41
F23	5	0.30	-35	10.5	0.5	4.76
F22	5	0.29	0	10.0	0.1	1.00
F27	5	0.27	50	11.1	0.1	9.01
F28	5	0.31	70	6.8	1.1	16.18
F24	5	0.35	100	11.5	2.2	19.13
F25	15	0.45	0	19.2	1.5	7.81
F26	15	0.39	-40	15.8	0.5	3.16
F31	15	0.40	50	13.9	1.7	12.23
F29	15	0.34	106	13.6	3.6	26.47
F34	120	0.62	-20	42.1	0.9	2.14
F30	120	0.81	3	55.2	1.5	2.72
F40	120	0.89	20	76.5	6.0	7.84
F39	120	0.93	42	84.8	6.1	7.19
F36	120	0.73	55	43.6	6.2	14.22
F35	120	0.72	60	41.8	4.4	10.53
F38	120	0.89	70	83.7	10.2	12.19
F37	120	0.82	100	76.2	17.3	22.76
F33	120	0.84	102	58.5	14.3	24.44
N10	1	0.25	1	5.5	1.2	21.82
N8	1	0.24	50	8.2	3.0	36.59
N9	1	0.25	100	8.1	2.5	30.86
N12	5	0.20	-40	5.7	2.1	21.05
N14	5	0.25	0	10.3	1.6	15.53
N13	5	0.26	50	11.2	1.4	12.50
N11	5	0.28	126	11.7	5.7	48.72
N17	15	0.50	0	34.9	6.0	17.19
N16	15	0.51	60	33.4	9.4	28.14
N18	15	0.55	80	34.0	12.5	36.76
N15	15	0.55	110	37.3	16.0	42.90

*- Sample identification at foot of table

TABLE 4.11(cont)

Loss of solvent from samples during PL-DMTA

Sample no.*	sorption time mins	V_r fraction	removal temperature °C	liquid content in sample mg	loss of liquid from sample mg	% loss
X36	30	0.29	60	9.9	2.7	27.27
X38	30	0.36	63	13.1	2.2	16.79
X37	30	0.38	100	10.7	1.1	10.28
X39	30	0.32	110	12.4	3.3	26.61
X30	60	0.40	-20	12.4	0.05	0.40
X27	60	0.40	50	12.0	0.3	2.50
X29	60	0.39	60	12.0	0.9	7.50
X28	60	0.39	70	11.1	1.3	11.71
X26	60	0.41	127	11.9	2.6	21.85
X25	60	0.20	130	3.1	0.8	25.81
X42	240	0.84	0	45.9	1.3	2.83
X43	240	0.80	35	41.3	2.4	5.81
X41	240	0.84	66	45.0	4.1	9.11
X40	240	0.75	120	39.8	10.0	25.13
X33	300	0.42	0	28.6	1.0	3.50
X32	300	0.62	50	30.5	2.1	6.89
X34	300	0.65	70	30.3	4.4	14.52
X31	300	0.62	100	30.2	6.4	21.19
E17	30	0.34	15	8.3	0.0	0.00
E18	30	0.28	30	7.2	0.4	5.56
E16	30	0.31	60	7.2	0.8	11.11
E15	30	0.27	100	6.8	1.1	16.18
E21	90	0.33	0	9.6	0.3	3.13
E30	90	0.47	20	55.2	1.5	2.72
E29	90	0.44	42	15.5	1.5	9.68
E20	90	0.33	50	9.6	0.3	8.74
E22	90	0.37	70	9.6	1.0	10.42
E28	90	0.51	81	17.2	2.2	12.79
E19	90	0.37	100	9.5	2.0	21.05
E27	90	0.52	102	17.3	3.5	20.23
E25	900	0.81	0	38.4	0.4	1.04
E24	900	0.85	50	38.9	2.7	6.94
E26	900	0.84	75	36.9	3.8	10.30
E23	900	0.87	100	37.7	0.6	15.92
T9	150	0.73	100	47.7	9.2	19.00
T10	150	0.79	60	40.2	5.9	14.50
T11	150	0.64	30	45.2	4.0	8.50
T12	150	0.72	24	38.0	2.7	7.00

A -propanone
F -fluorobenzene
X -dimethylbenzene
E -ethylbenzene
N -nitroethane
T -methylbenzene

FIGURE 4.60

Loss of vapour from uPVC plaques swollen with dimethylbenzene liquid at 60°C, when analysed using shear techniques

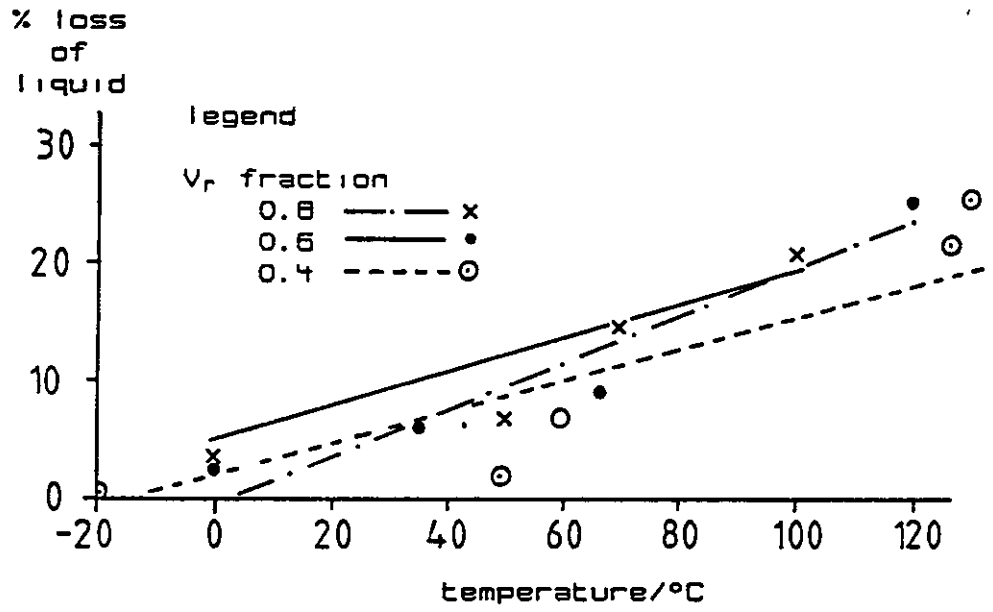

FIGURE 4.61

Loss of vapour from uPVC plaques swollen with ethylbenzene liquid at 60°C, when analysed using shear techniques

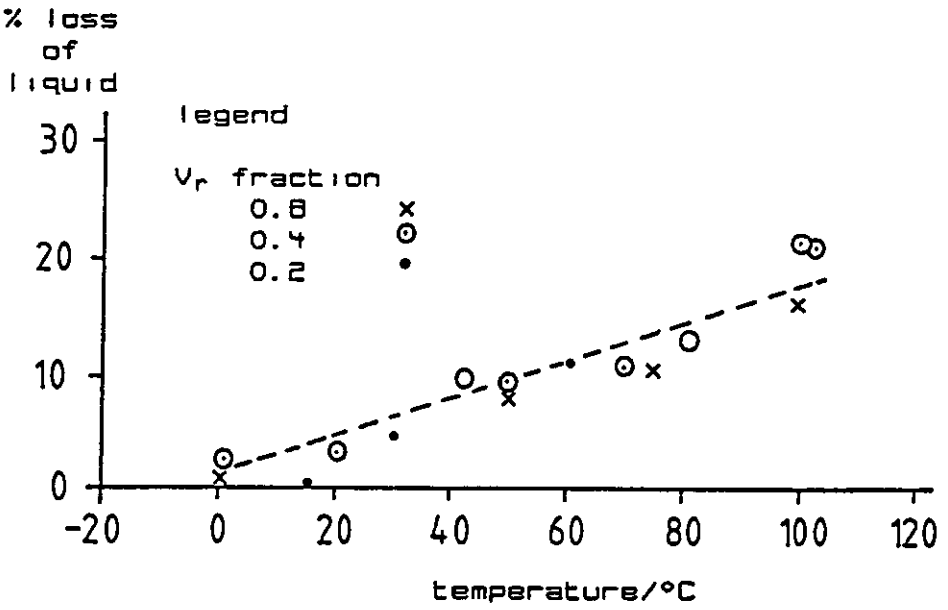

FIGURE 4.62

Loss of vapour from uPVC plaques swollen with methylbenzene liquid at 60°C, when analysed using shear techniques

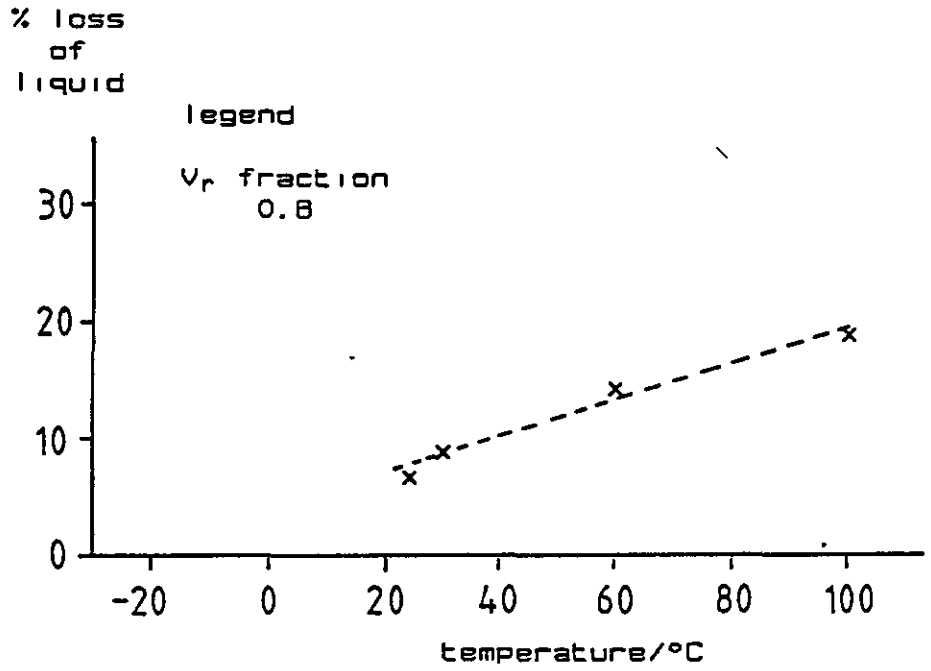

FIGURE 4.63

Loss of vapour from uPVC plaques swollen with nitroethane liquid at 60°C, when analysed using shear techniques

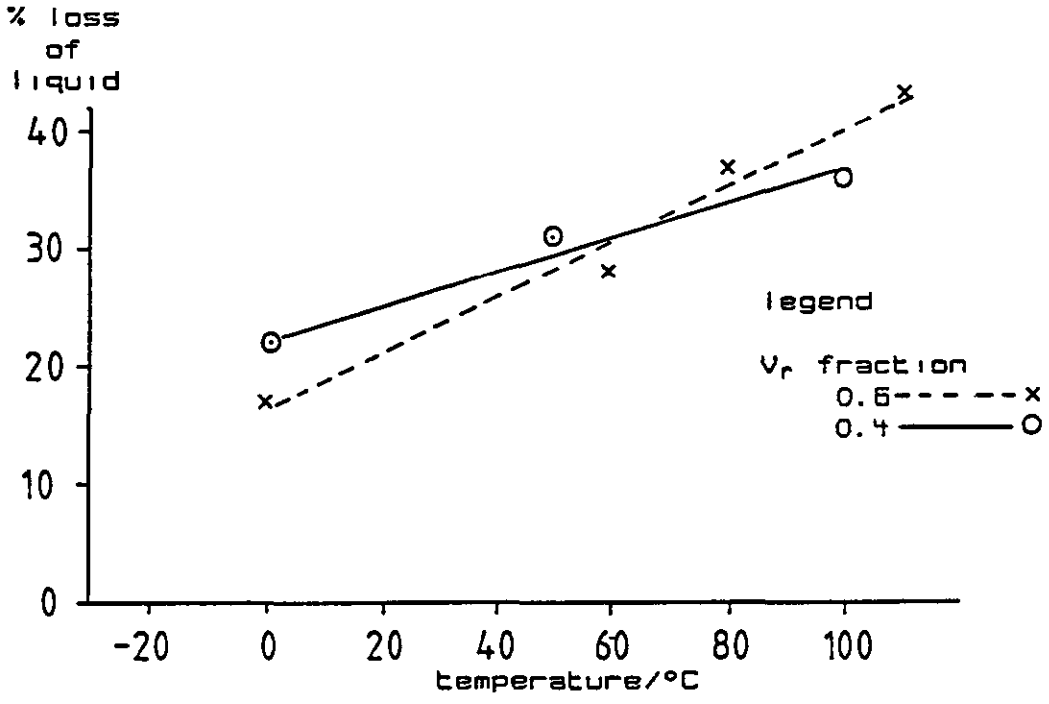

FIGURE 4.64

Loss of vapour from uPVC plaques swollen with fluorobenzene liquid at 60°C, when analysed using shear techniques

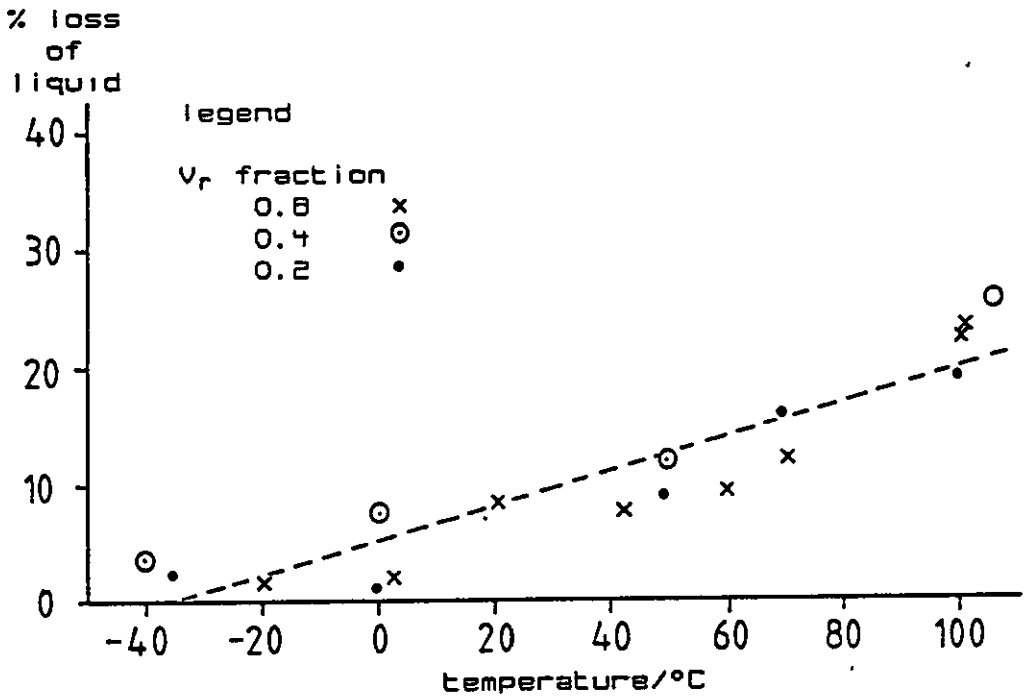

percentage liquid content in the swollen region. The calculated percent mol content of liquid in the swollen region at 60°C, in the analysis head, is given in the legend in each figure. The liquid content in the swollen region is that found after the discs had been cooled to the PL-DMTA starting temperature, around -100°C, and heated to 60°C in the analyser. The percentage liquid content values have been corrected for loss of liquid, calculated in section 4.4.4.1, for the temperature in the analyser of 60°C. The modulus curves generally show a decrease in value at any given temperature with increasing mol content of liquid in the swollen region, although some curves do not follow this trend. The deviations from this trend are probably due to errors in calculating the liquid content rather than instrument error. The main contributions towards this error would be the difficulty experienced in measuring the inner core thickness via the microscope and the losses of vapour from the sample during analysis.

4.4.4.3 Tan δ thermograms of swollen plaques

Tan δ thermograms for the various liquids used in the shear analysis of swollen PVC samples are shown in figures 4.70 to 4.74. The examples shown correspond to the log modulus plots in figures 4.65 to 4.69 discussed in section 4.4.4.2. The ascending numbers on the plots again correspond to the percentage liquid content of the swollen region in the discs given in the legends in the figures, after they had been cooled in the PL-DMTA to the starting temperature and heated with a rate of 2°C/min, corrected for

the loss of liquid from the swollen region at 60°C using the results shown in section 4.4.4.1. The $T_g\alpha$'s show a general trend, a decrease in temperature with increasing liquid contact, again anomalies occur from the trend producing higher than expected $T_g\alpha$' values.

FIGURE 4.65

Shear log modulus thermograms for uPVC swollen with ethylbenzene liquid at 60°C

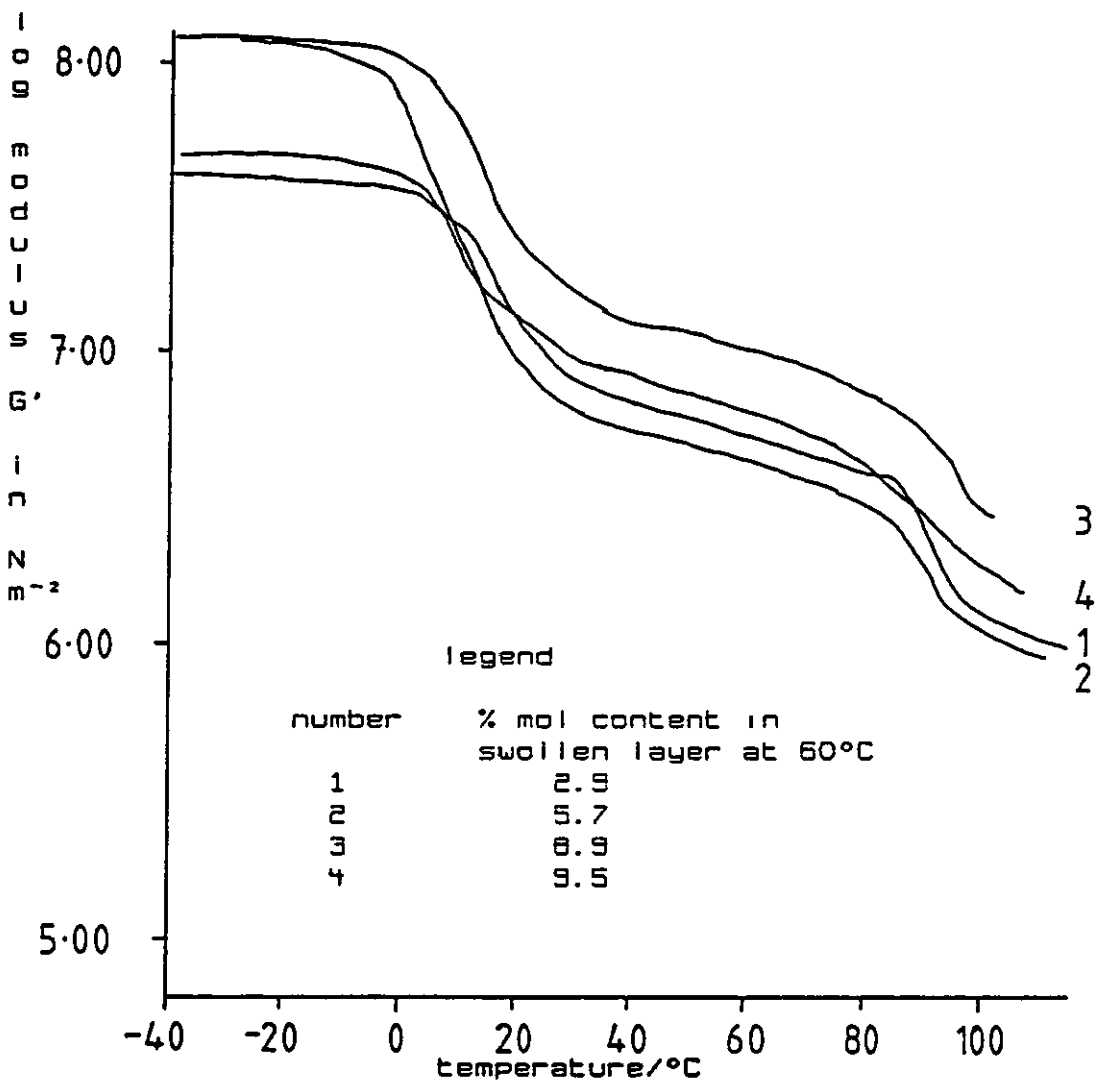

FIGURE 4.66

Shear log modulus thermograms for uPVC swollen with dimethylbenzene liquid at 60°C

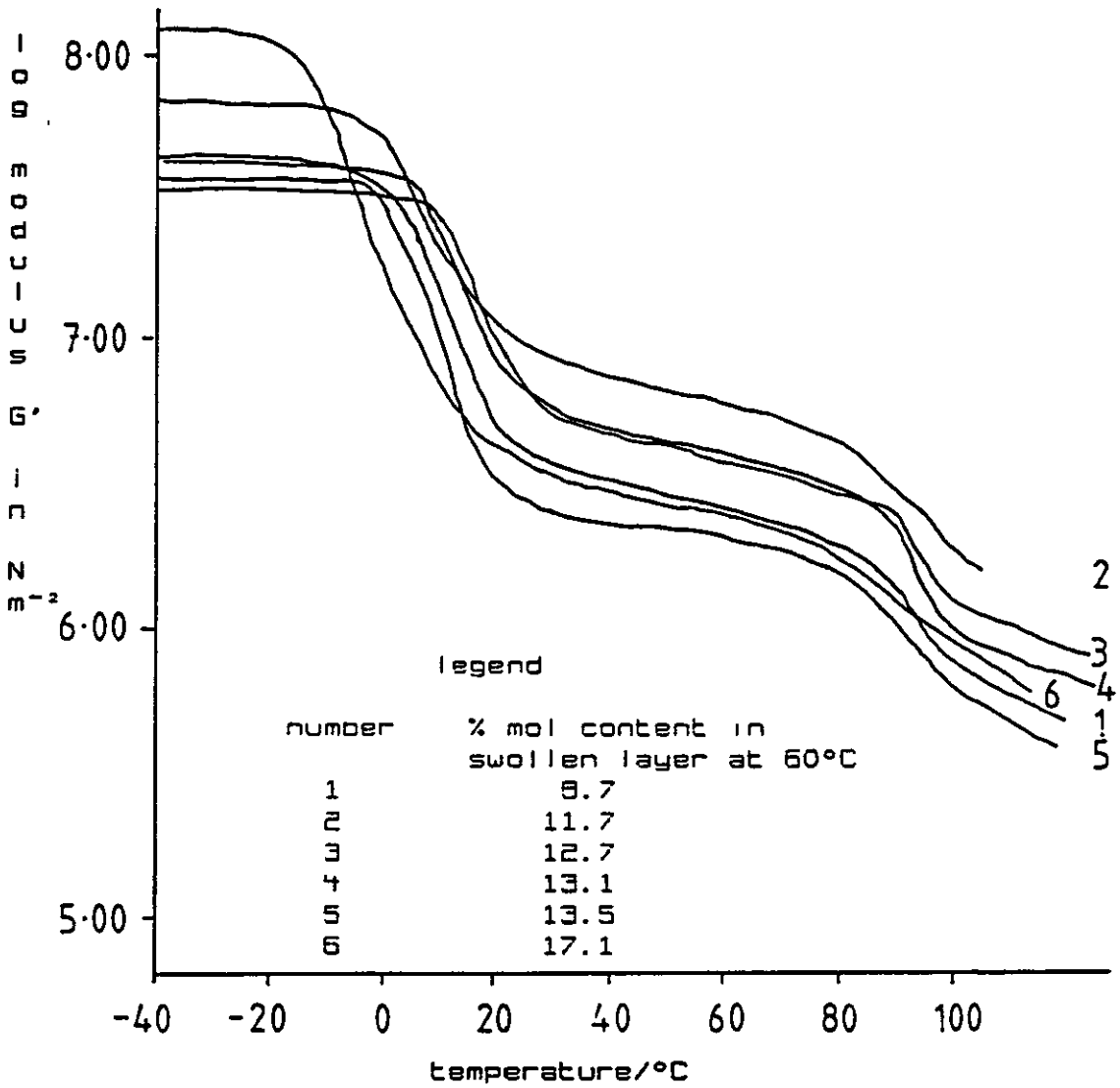

FIGURE 4.67

Shear log modulus thermograms for uPVC swollen with nitroethane liquid at 60°C

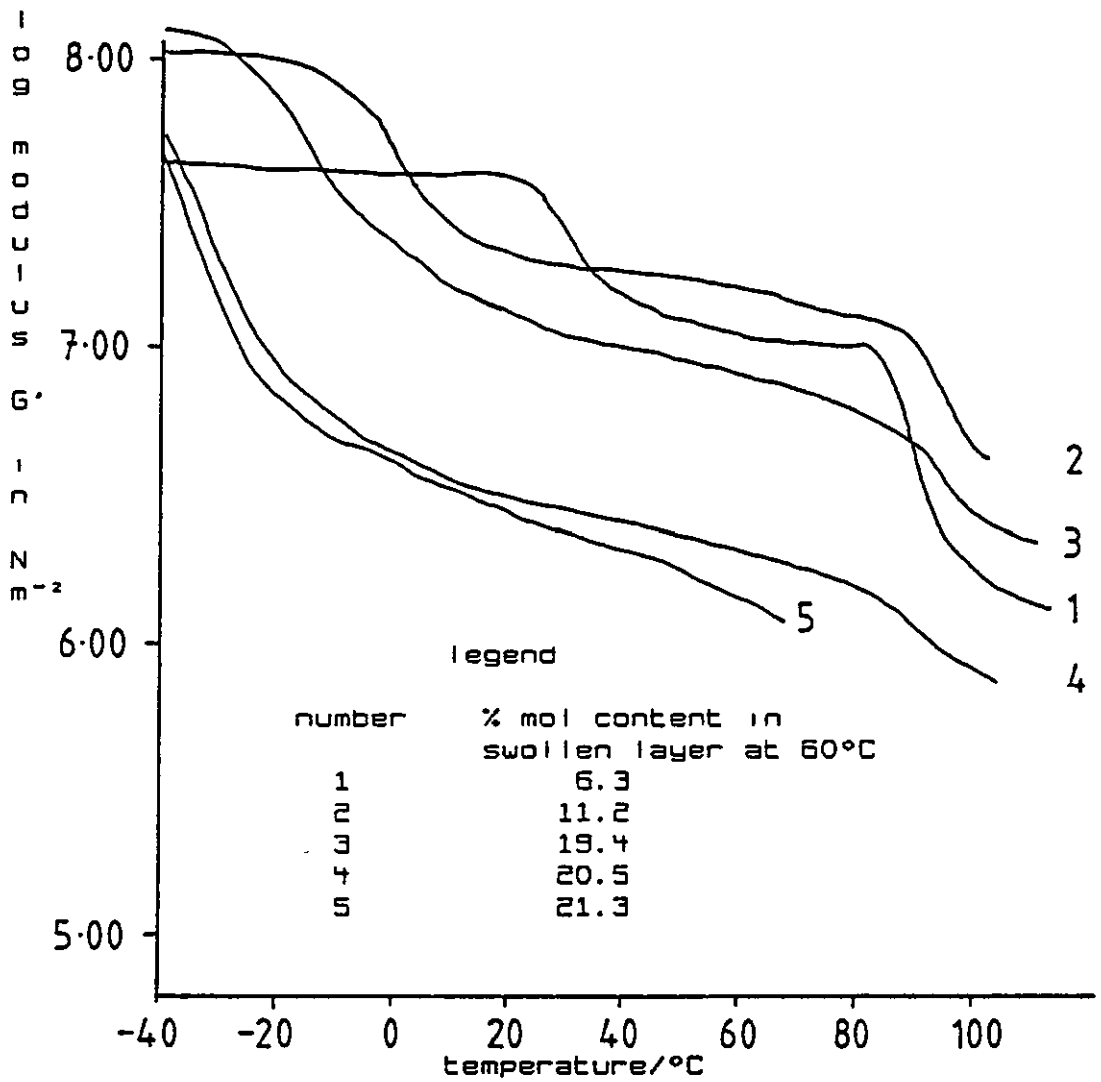

FIGURE 4.68

Shear log modulus thermograms for uPVC swollen with propanone liquid at 56°C

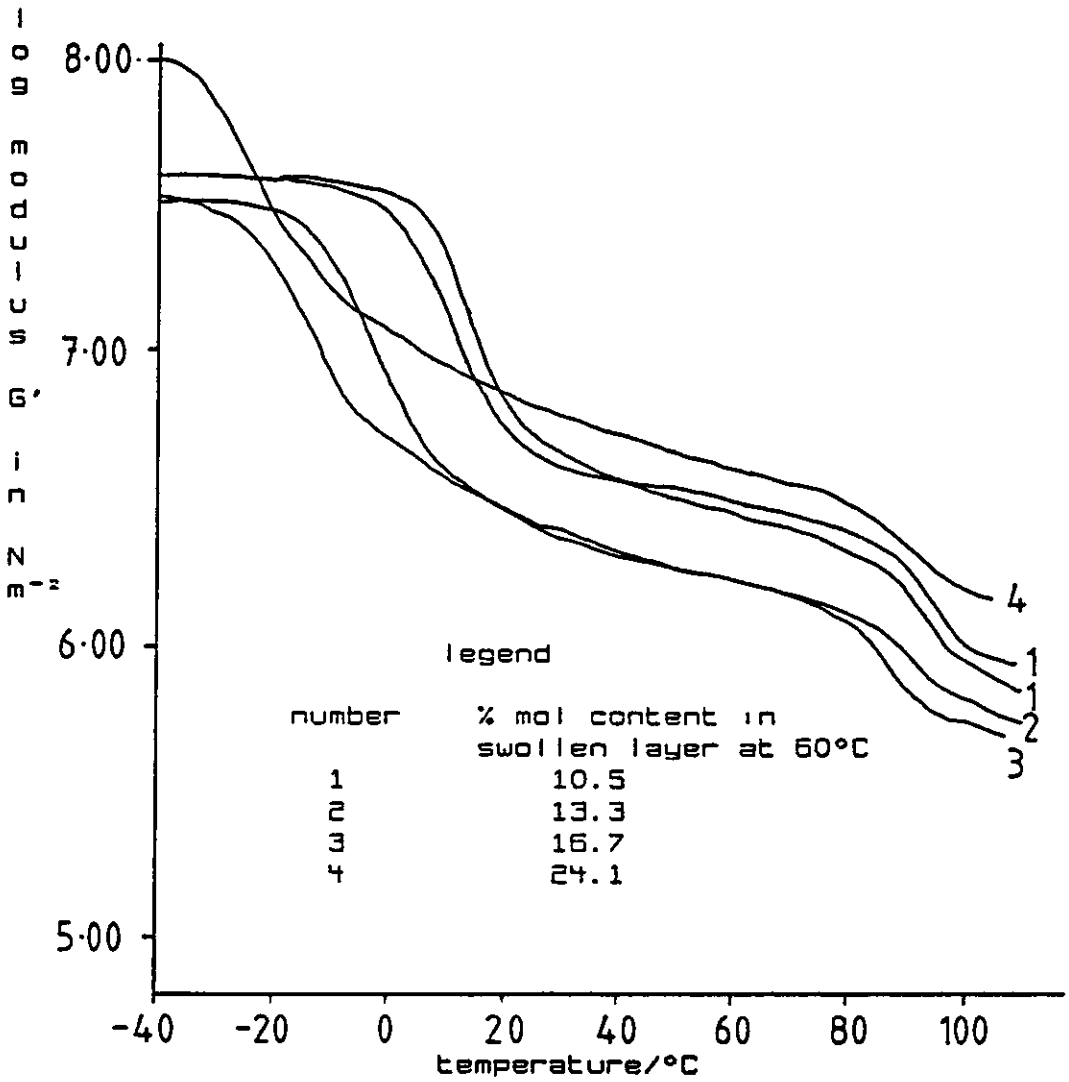

FIGURE 4.69

Shear log modulus thermograms for uPVC swollen with fluorobenzene liquid at 60°C

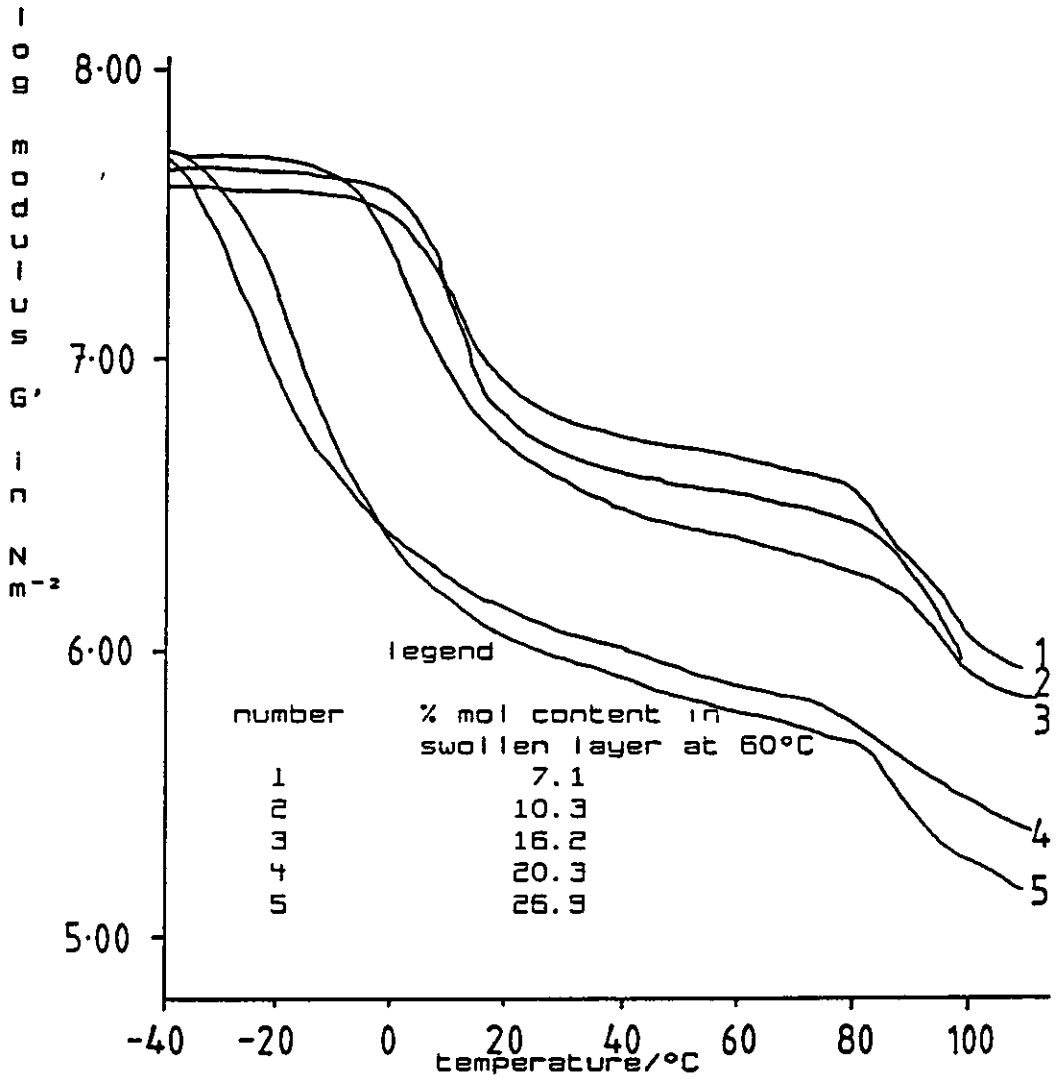

FIGURE 4.70

$T_{g\alpha'}$ and $T_{g\alpha}$ peak produced with shear PL-DMTA for uPVC swollen with nitroethane liquid at 60°C

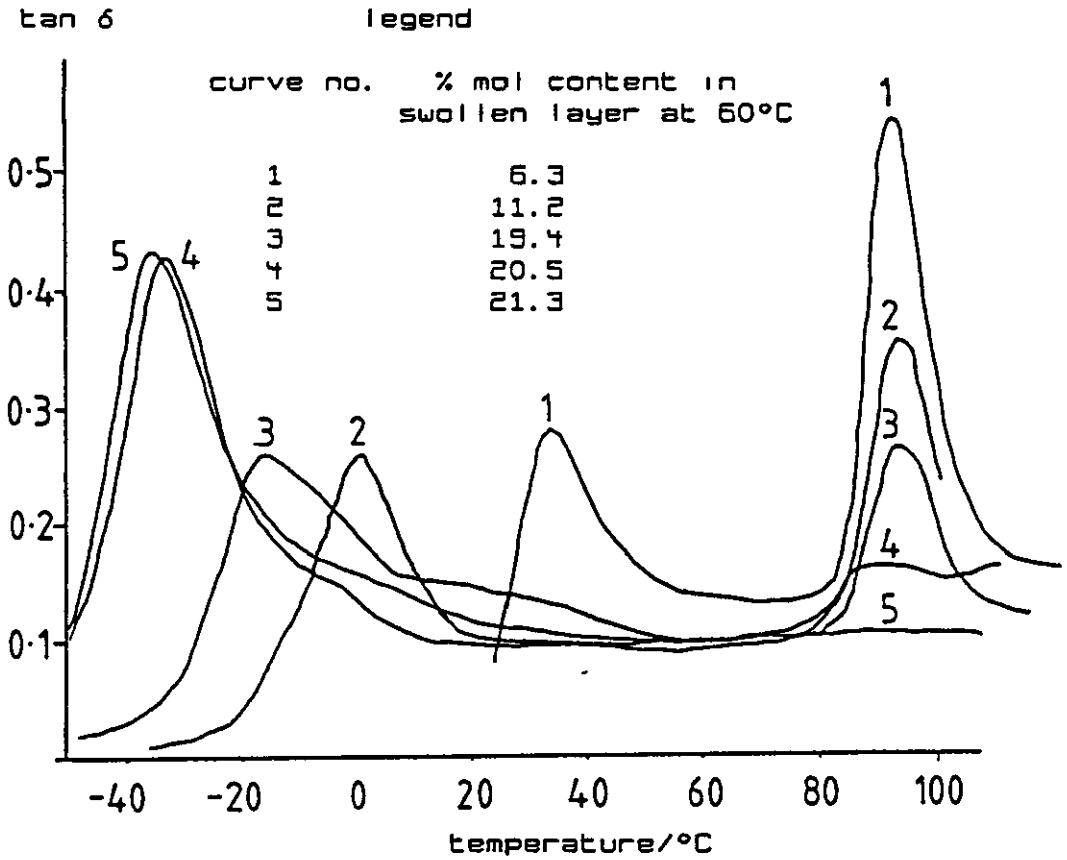

FIGURE 4.71

$T_g\alpha'$ and $T_g\alpha$ peak produced with shear PL-DMTA for uPVC swollen with dimethylbenzene liquid at 60°C

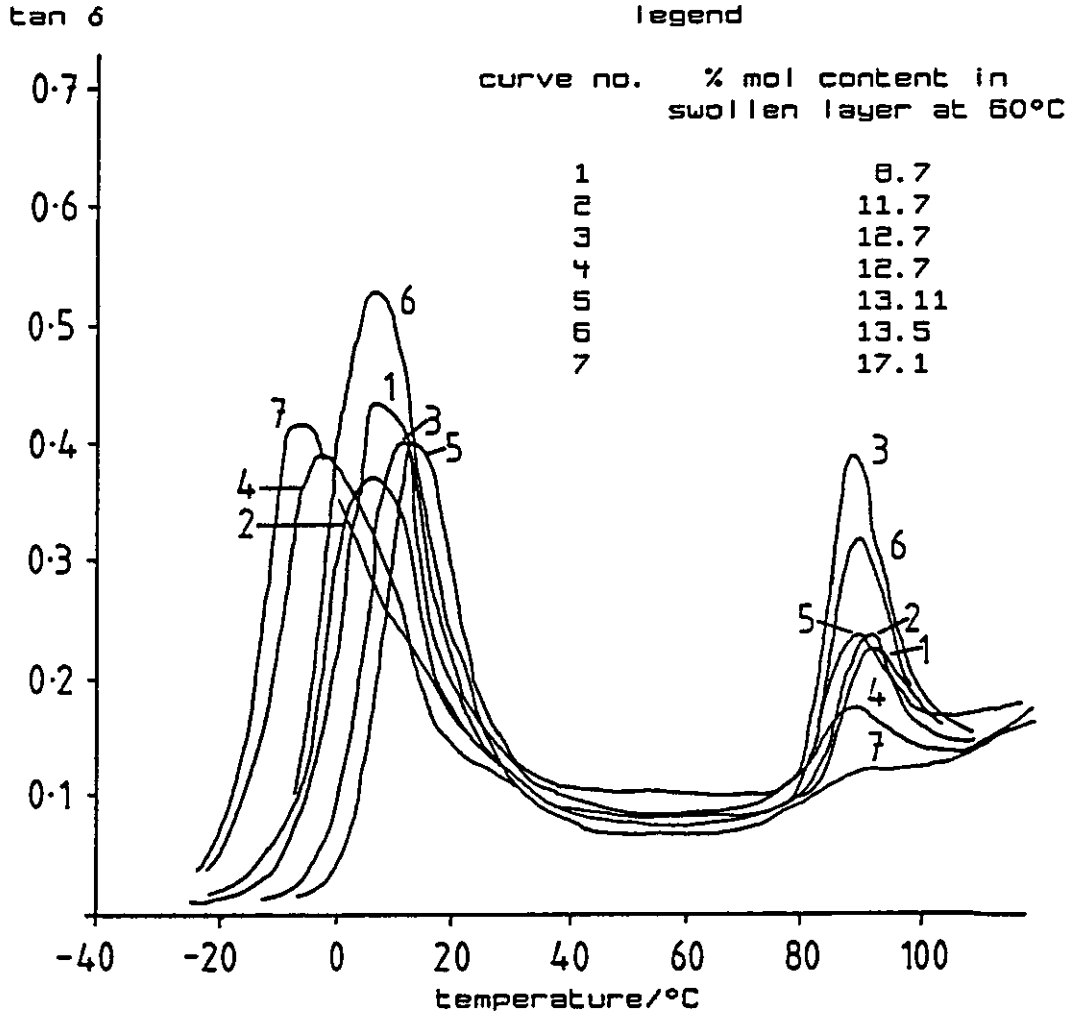

FIGURE 4.72

$T_g\alpha'$ and $T_g\alpha$ peak produced with shear PL-DMTA for uPVC swollen with fluorobenzene liquid at 60°C

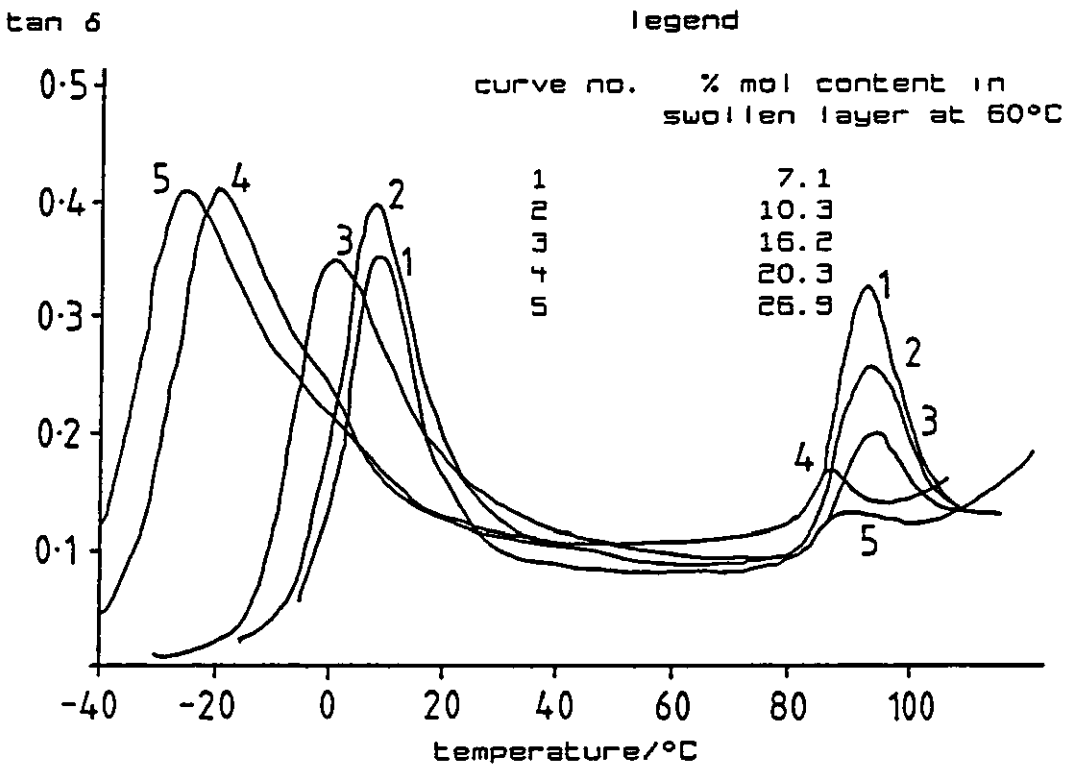

FIGURE 4.73

$T_g\alpha'$ and $T_g\alpha$ peak produced with shear PL-DMTA for uPVC swollen with propanone liquid at 56°C

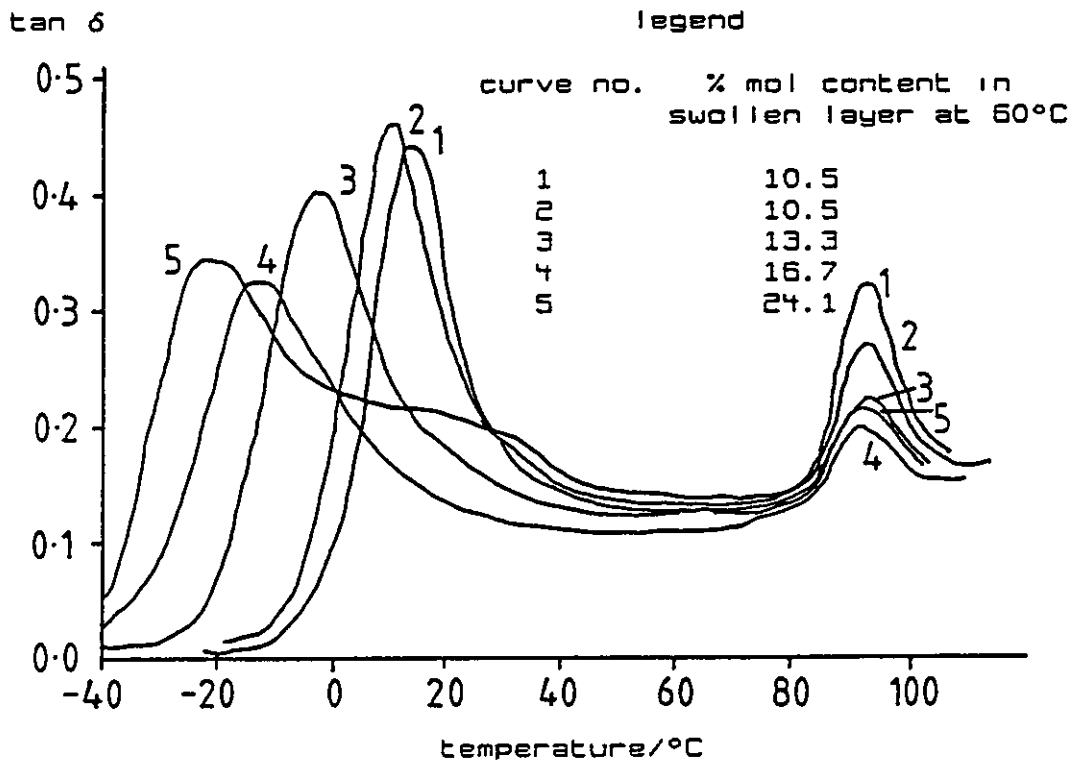

FIGURE 4.74

$T_g\alpha'$ and $T_g\alpha$ peak produced with shear PL-DMTA for uPVC swollen with ethylbenzene liquid at 56°C

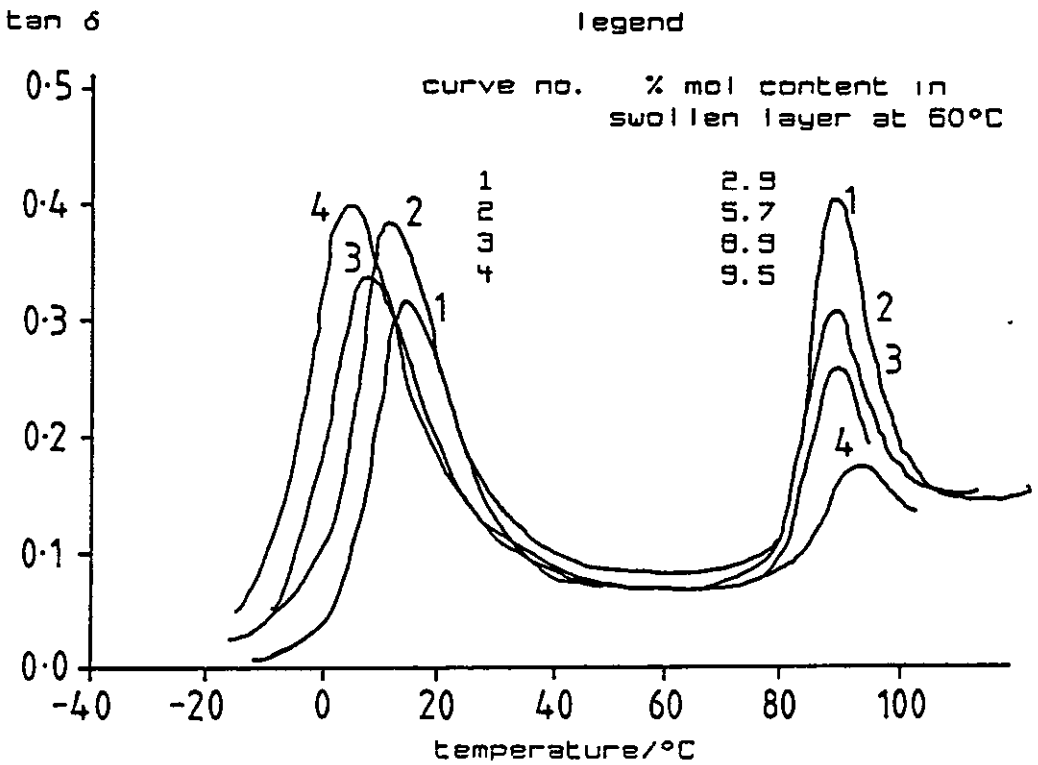

4.5 EXAMINATION OF SEPARATED CORE AND SWOLLEN LAYER

In one instance, DOP, it was found to be possible to separate the swollen layer from the inner uPVC core and run a PL-DMTA on the shaved layer. The resulting thermograms are shown in figure 4.75. Tan δ is shown to be lowered by 13°C and the size of the $T_{g\alpha}$ peak, for the analysis of the swollen region only, is much diminished. The modulus of the swollen layer is shown as the dotted line.

With DSC methods it has been possible to separate the swollen and inner core layers and run analyses on both layers independently for a large number of swollen systems, the results of which are shown in figures 4.76 to 4.80. The samples were prepared by cutting the swollen layer away from the inner core using a scalpel. The respective portions, swollen and dry, were separately chopped into small enough pieces to fit into the DSC pan. Difficulty was experienced in achieving optimum baselines for the inner core samples and also for the propanone swollen layer, (see figure 4.78). The dry inner core was glassy and difficult to cut into small pieces and it was thought that the poor baselines may be due to lack of physical contact between the glassy inner core pieces and the sample pan. A summary of the results is given in table 4.12. Instrument calibration was carried out using the method described in section 4.3.2

FIGURE 4.75

Shear PL-DMTA of uPVC swollen with DOP liquid at 60°C. The dotted curve is the shear analysis of the separated swollen region

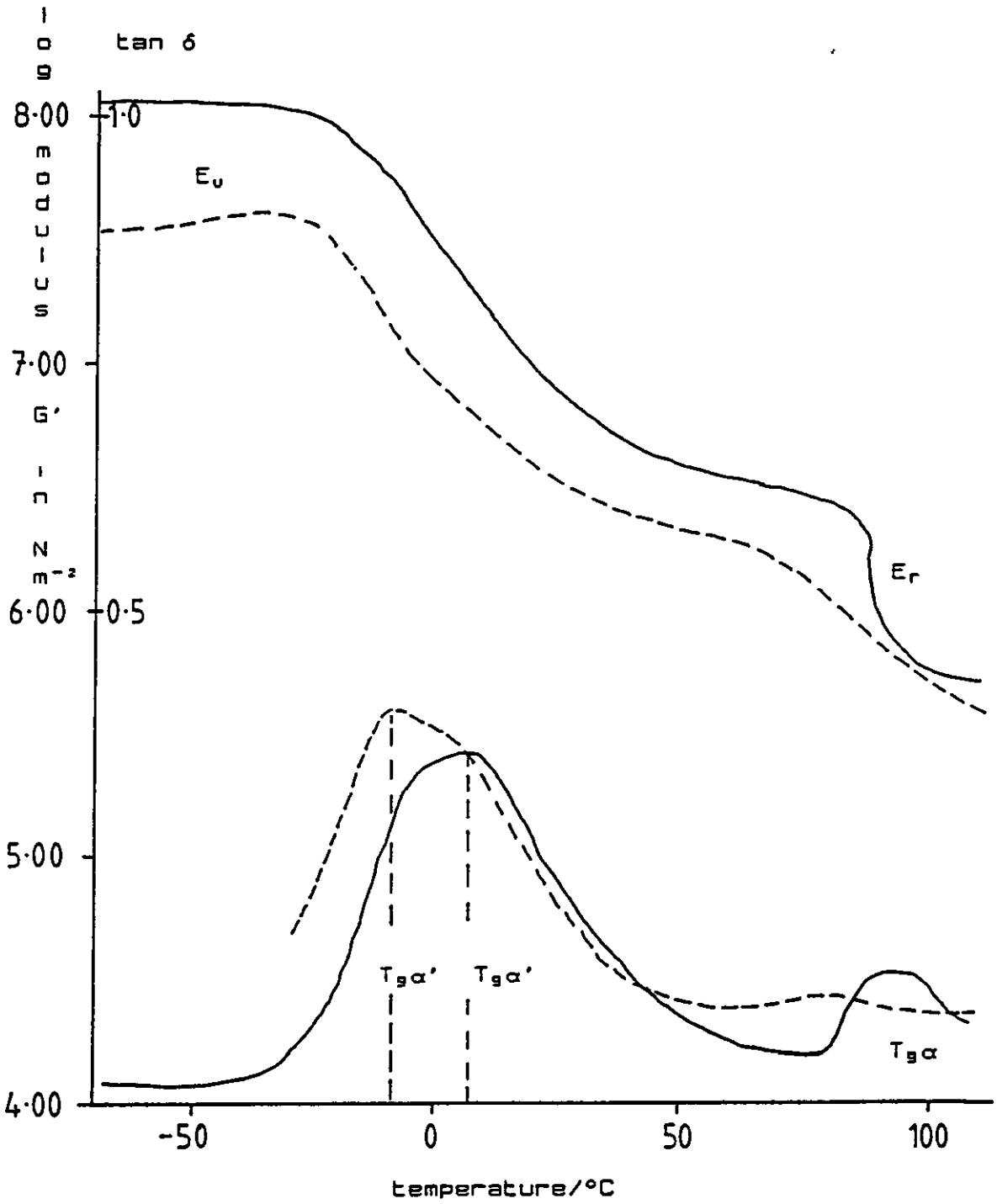

FIGURE 4.76

DSC thermograms for separated ethylbenzene swollen and core regions, samples were cooled and subsequently heated at 40°C/min

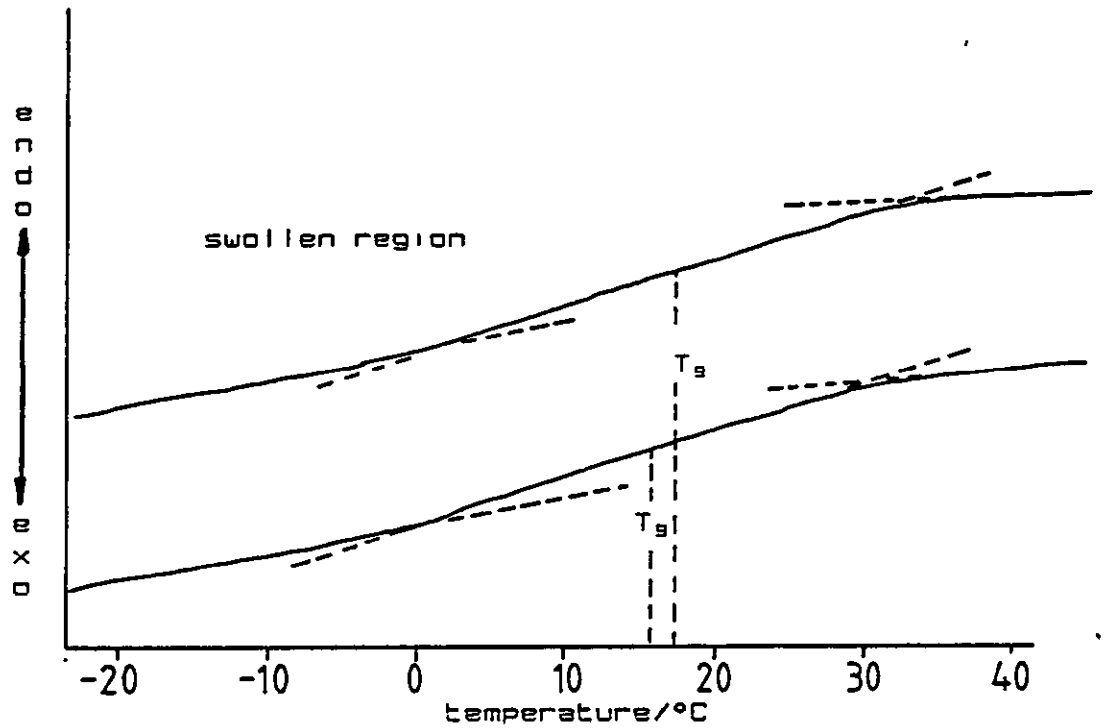

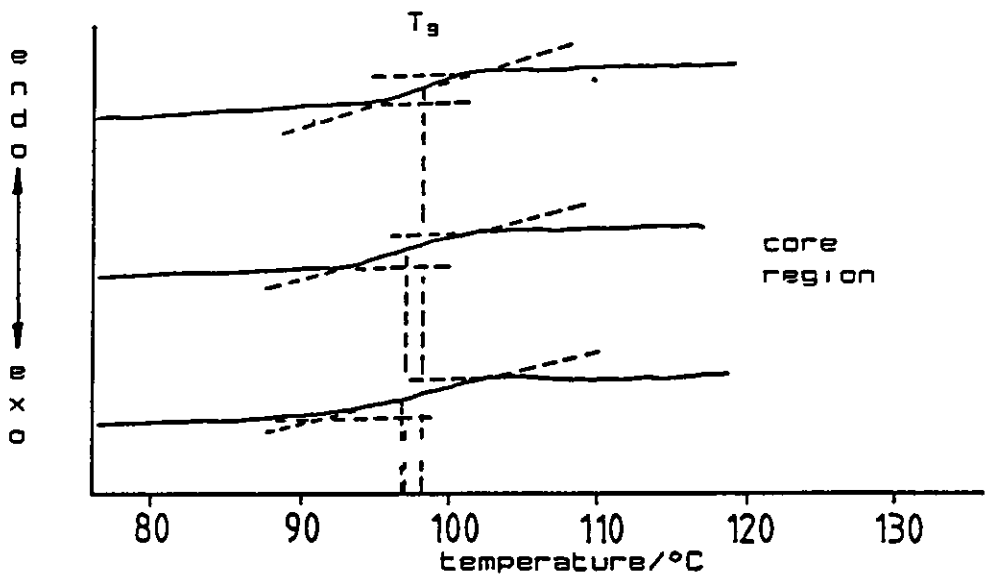

FIGURE 4.77

DSC thermograms for separated nitroethane swollen and core regions, samples were cooled and subsequently heated at 40°C/min

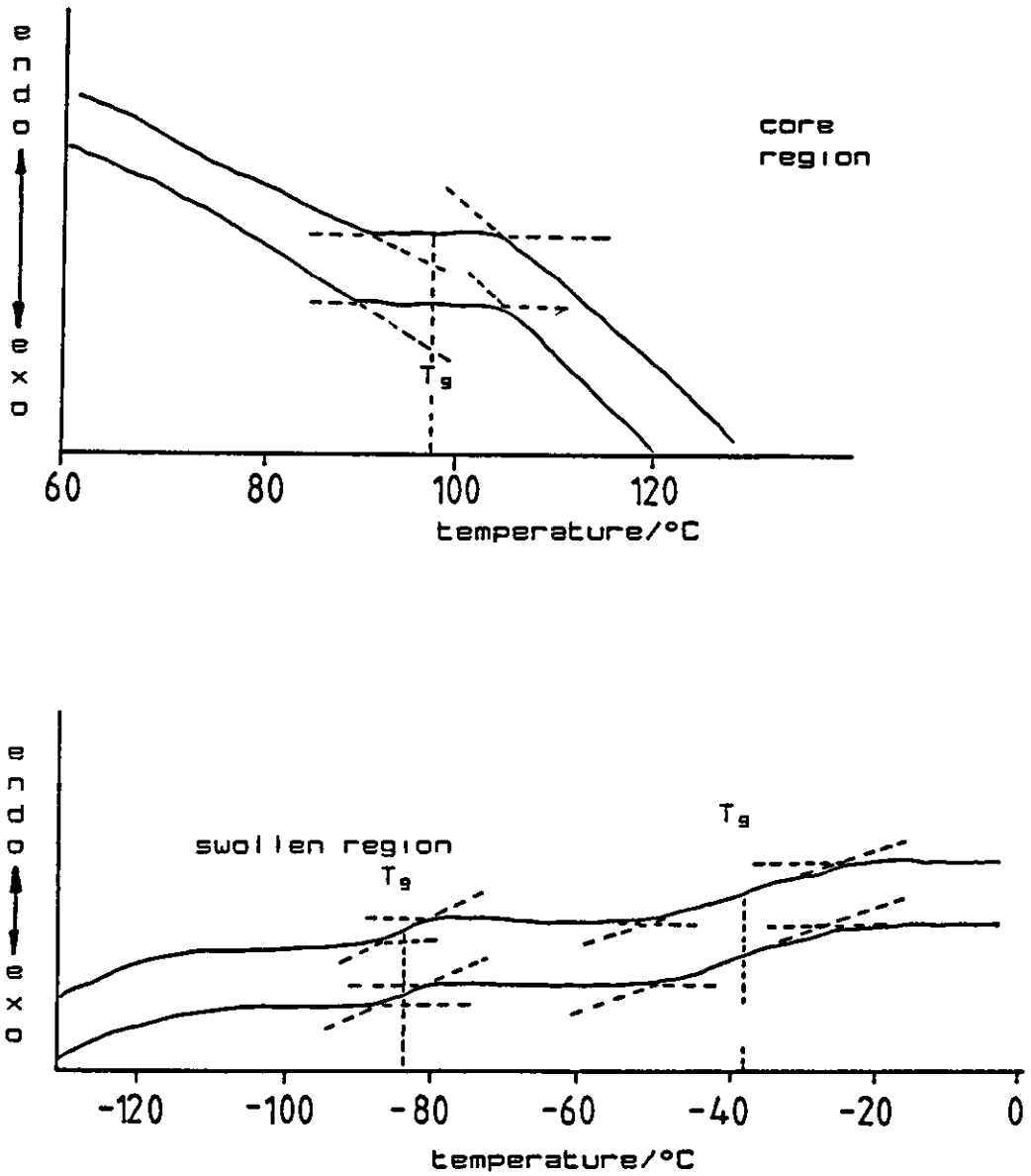

FIGURE 4.78

DSC thermograms for separated propanone swollen and core regions, samples were cooled and subsequently heated at 40°C/min

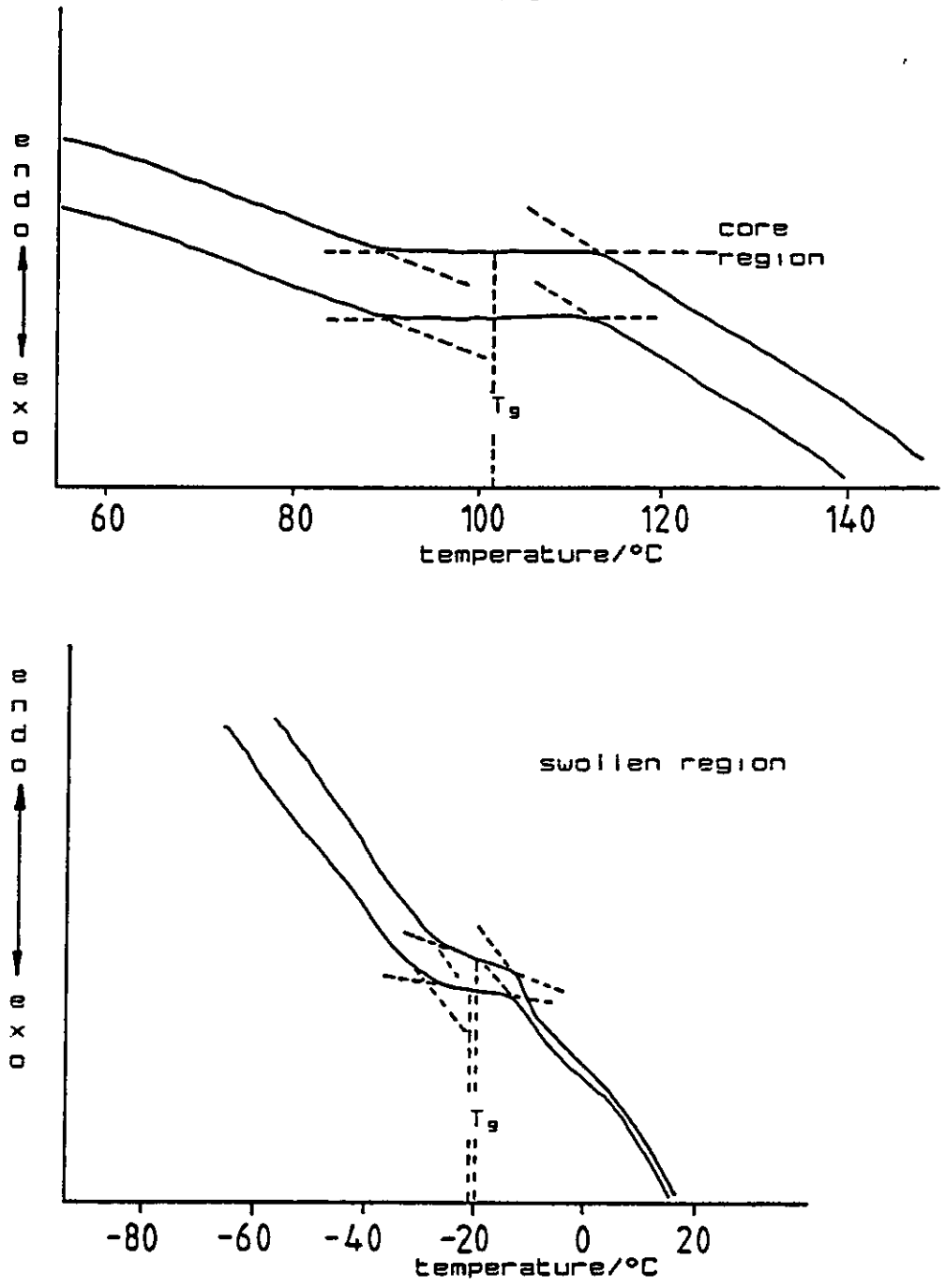

FIGURE 4.79

DSC thermograms for separated DOP swollen and core regions, samples were cooled and subsequently heated at 40°C/min

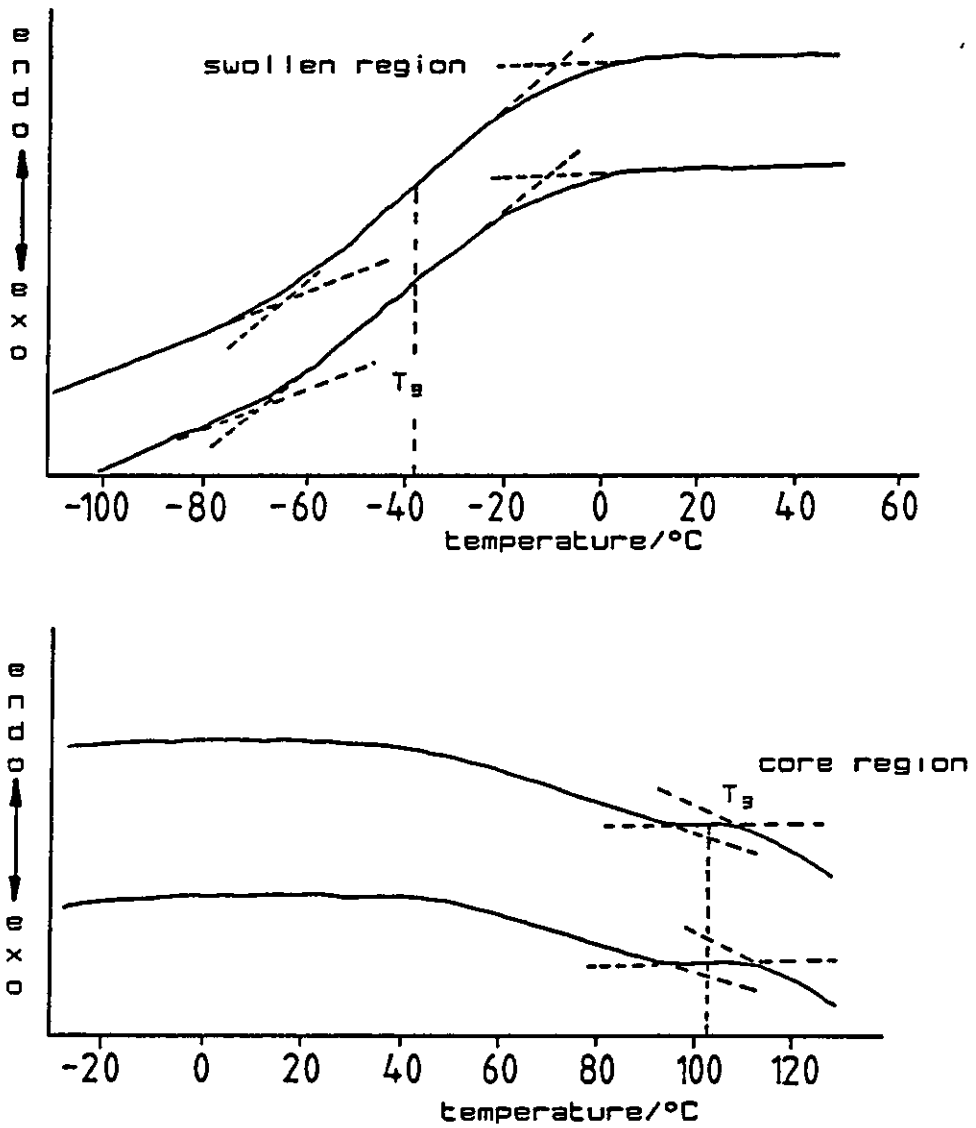

FIGURE 4.80

DSC thermograms for separated DMP swollen and core regions, samples were cooled and subsequently heated at 40°C/min

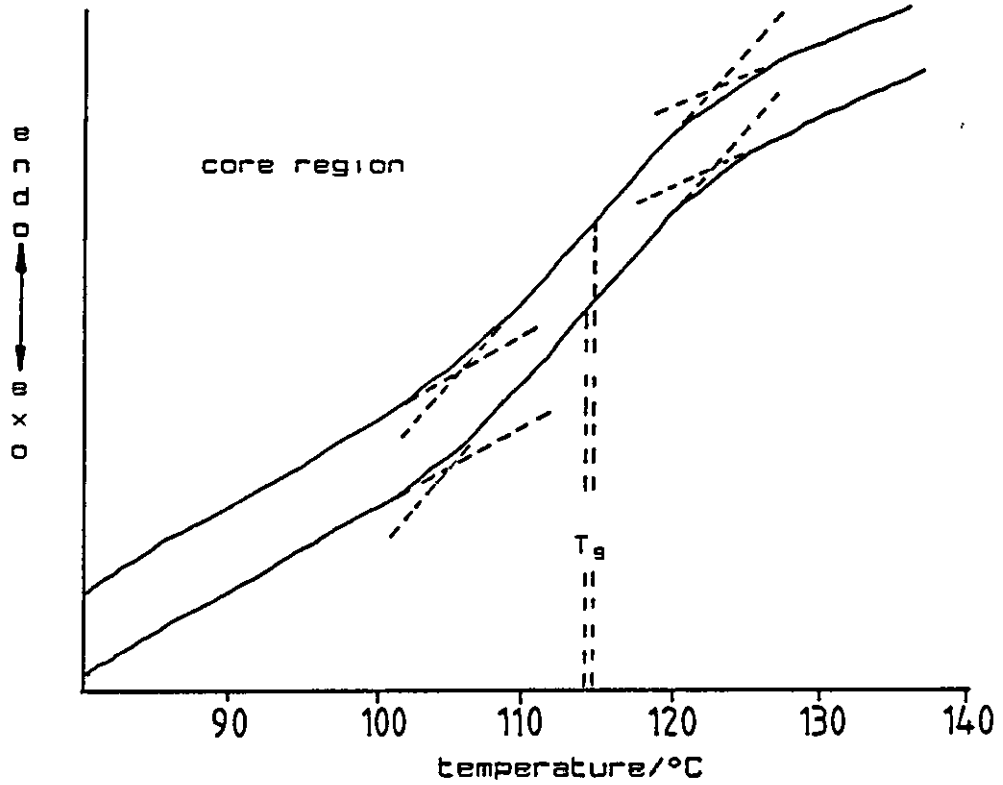

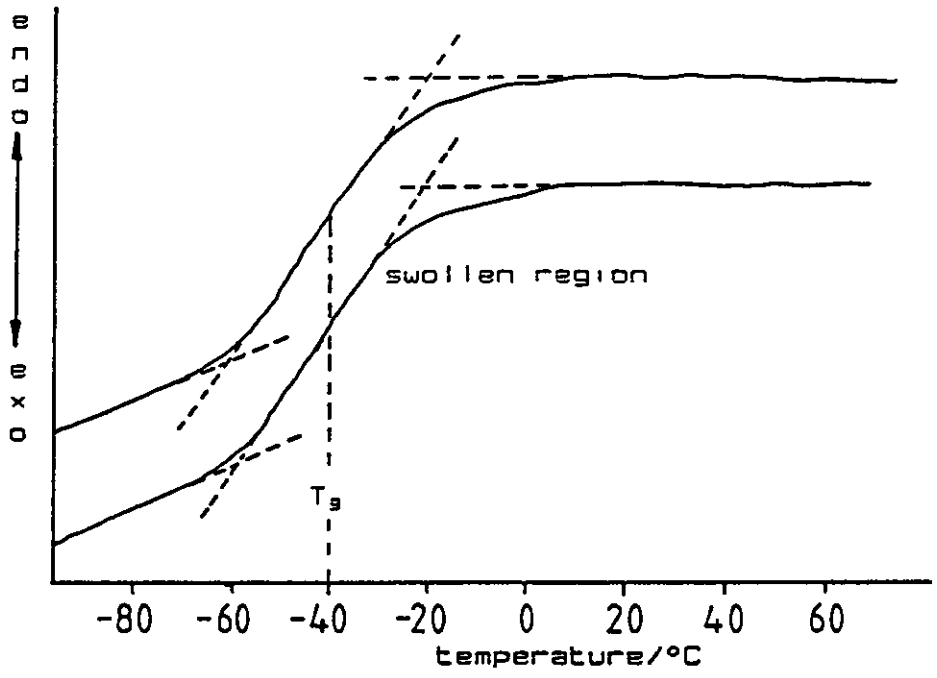

TABLE 4.12

DSC transition values for separated swollen and core regions; (cooled and heated at 40°C) and corrected for a heat rate of 4°C/min

liquid	swollen* region	core* region	% molar content in swollen layer	V_r
ethylbenzene	14.3	93.0	13.0	0.63
nitroethane	(-88.7)-42.5	93.9	31.2	0.44
propanone	-25.1	97.9	31.1	0.54
DOP	-42.6	98.9	5.4	0.48
DMP	-15.6	102.9	81.0	0.93

* - average value on removal from the swelling environment

CHAPTER 5 — DISCUSSION

5.1 DIFFUSION OF LIQUIDS INTO uPVC

The diffusion of a limited number of liquids into uPVC plaques has been reported[21,25]. Kwei et al.[25] investigated the mass uptake and distance of liquid penetration as a function of time and analysed their experimental data by a generalized diffusion equation which took into account both Fickian and case II mechanisms, obtaining excellent agreement between this equation and experimental results. Lapcik et al.[21] have investigated the penetration of a number of liquids into uPVC as a function of time and temperature. To produce diffusion coefficient data, Fick's second law was solved assuming a discontinuous change of D with concentration. Both methods took into account the swelling of the plaque by employing Danckwert's[148] methods of representing moving frames to measure the liquid front in the swelling system. These two groups of workers found excellent agreement between theoretical predictions and experimental data, but application of a classical Fickian, treatment was not discussed.

5.1.1 Validity of classical diffusion theories with changing sample thickness

The effect of the solvent front movement in equation 2.111 is to alter the sample thickness term, L_T, thus directly altering the diffusion coefficient. This effect is shown in figure 5.1 and table 5.1 where the thickness of the unswollen core is taken into account, with respect to time in calculating the diffusion coefficient for fluorobenzene at 60°C. The core thickness values were obtained from an averaged core thickness of a number of samples at a particular time. It is seen that the diffusion coefficient changes by a factor of a 100.

The line, drawn in figure 5.1, is a polynomial fit to the experiment data. Although the line is close, on visual inspection to a straight line, as would be given by Fickian diffusion on such a plot as figure 5.1, the slope with respect to time is changing slightly, see table 5.1. This alone, according to equation 2.111, will change the value of D.

In taking into account the sample thickness it is assumed that the concentration throughout the swollen layer is that of the concentration at the polymer-liquid interface and the polymer-diluent layer offers no resistance to further movement of liquid. The changing core thickness seems to be the dominating factor in changing the value of D rendering the use of purely Fickian treatments inappropriate.

FIGURE 5.1

Diffusion of liquid fluorobenzene at 60°C into uPVC.

$M_T/M(max)$ versus square root time

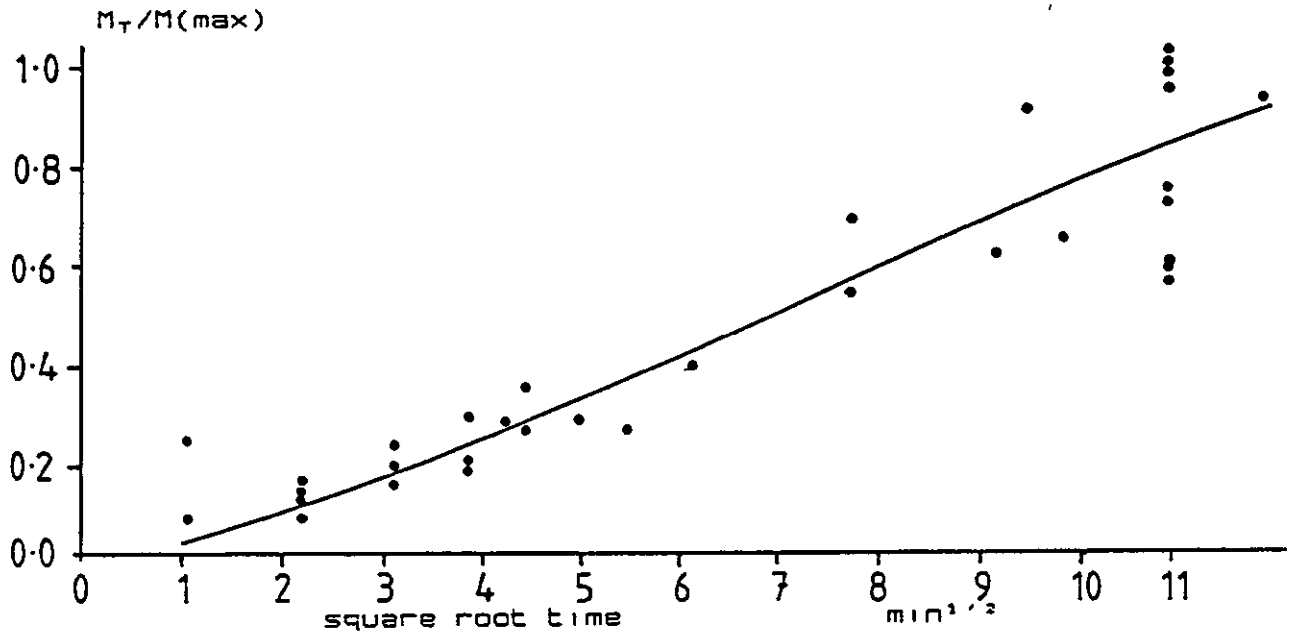

TABLE 5.1

The classically derived diffusion coefficient for the diffusion of fluorobenzene into uPVC plaques at 60°C taking into account the changing sample thickness

sorption time min	average core cm	slope$\times 10^{8}$ cms^{-1}	$D \times 10^{7}$ $cm^{2}s^{-1}$
2.25	0.14	8.8	3.11
3.16	0.13	9.2	2.98
4.50	0.12	10.1	2.79
7.75	0.08	11.6	1.69
10.95	0.05	8.3	0.34

5.1.2 The Case II contribution to diffusion into a system which swells

5.1.2.1 Validity of Case II theories with liquid diffusion into uPVC samples

At large experimental times according to equation 2.124 the mass uptake is linear, the slope being is $C_o v$ and the intercept given by $C_o D/v$. Accordingly, values may be computed for D and v from the data produced in table 4.4. Using the values for C_o, D and v it is possible to calculate the total amount of penetrant per unit area for any time as described in equation 2.123, and as shown in figures 5.2 to 5.9. The algorithm for equations 2.121 and 2.123 is given in Appendix 3. The dotted line in the figures shows the calculated total mass uptake per surface area with respect to time. Table 5.2 shows D and v values for the sorption of the liquids and plasticizers employed at the two temperatures. A sorption experiment was conducted at room temperature, with propanone as the penetrant, for comparison purposes with the literature quoted values produced by Kwei *et al.*, at room temperature,[25] upon which this model is based. The room temperature propanone data are shown at the foot of table 5.2. The values given by Kwei *et al.* pertain to a compression moulded uPVC sheet, with a thickness of 0.33 cm, subjected to the liquid sorption of propanone at room temperature. The equilibrium concentration of propanone in the swollen sheet was taken as the surface concentration and was found to be 0.50 g cm^{-3}. The reported diffusion coefficient and the velocity of liquid penetration

FIGURE 5.2

Diffusion of propanone into uPVC at 56°C

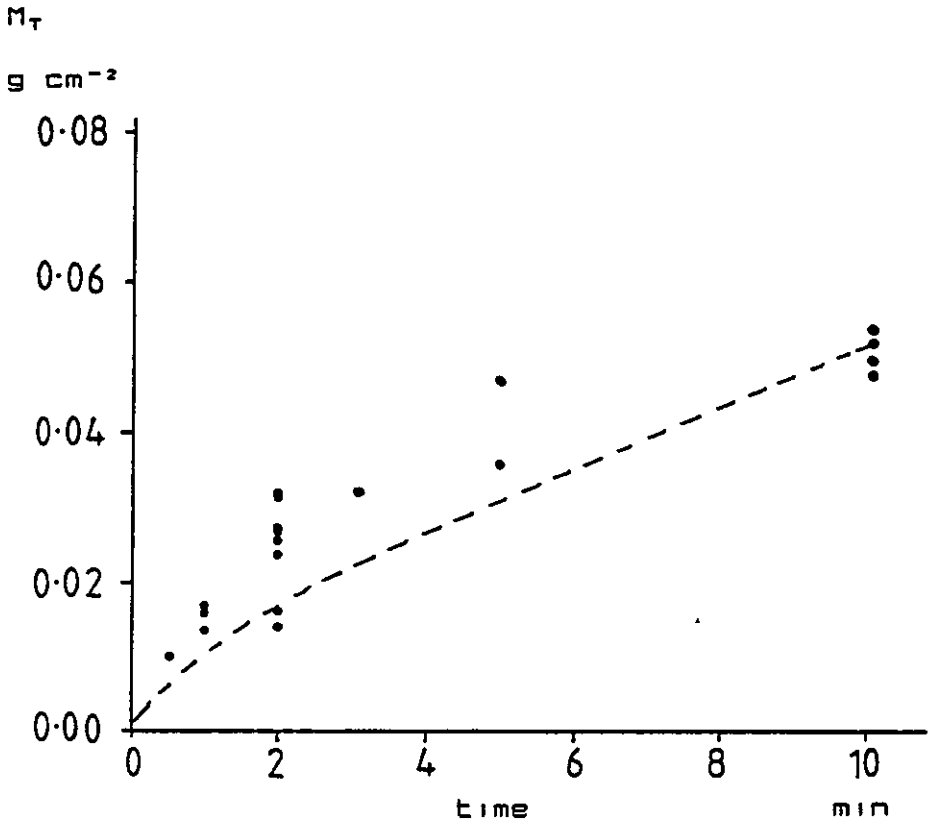

FIGURE 5.3

Diffusion of ethylbenzene into uPVC at 60°C

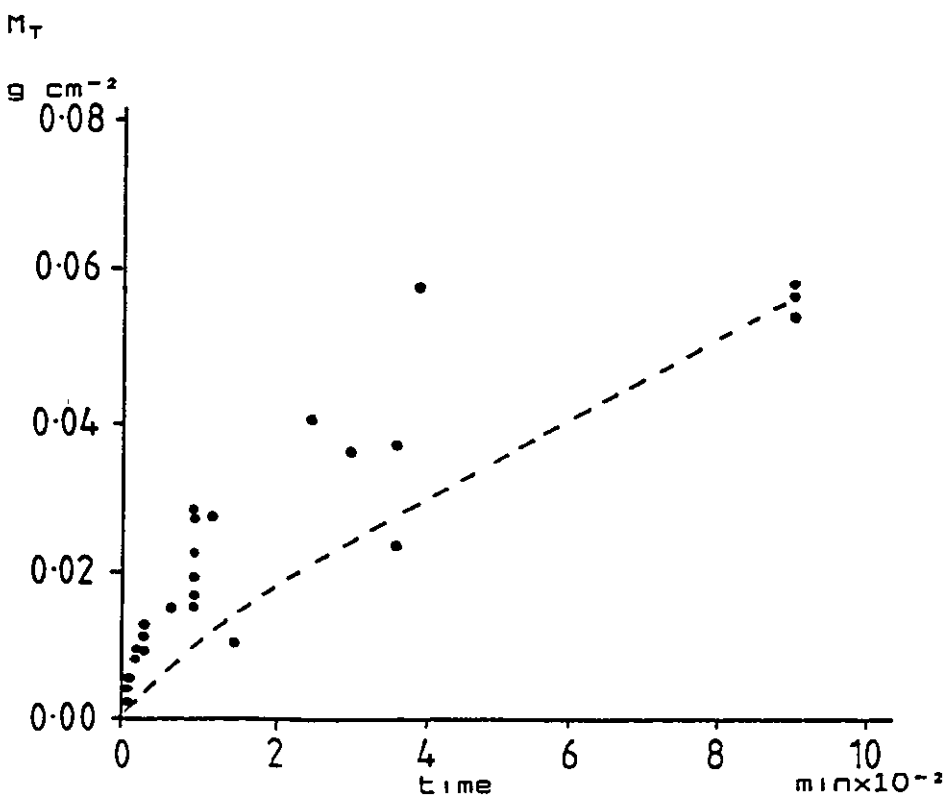

FIGURE 5.4

Diffusion of dimethylbenzene into uPVC at 60°C

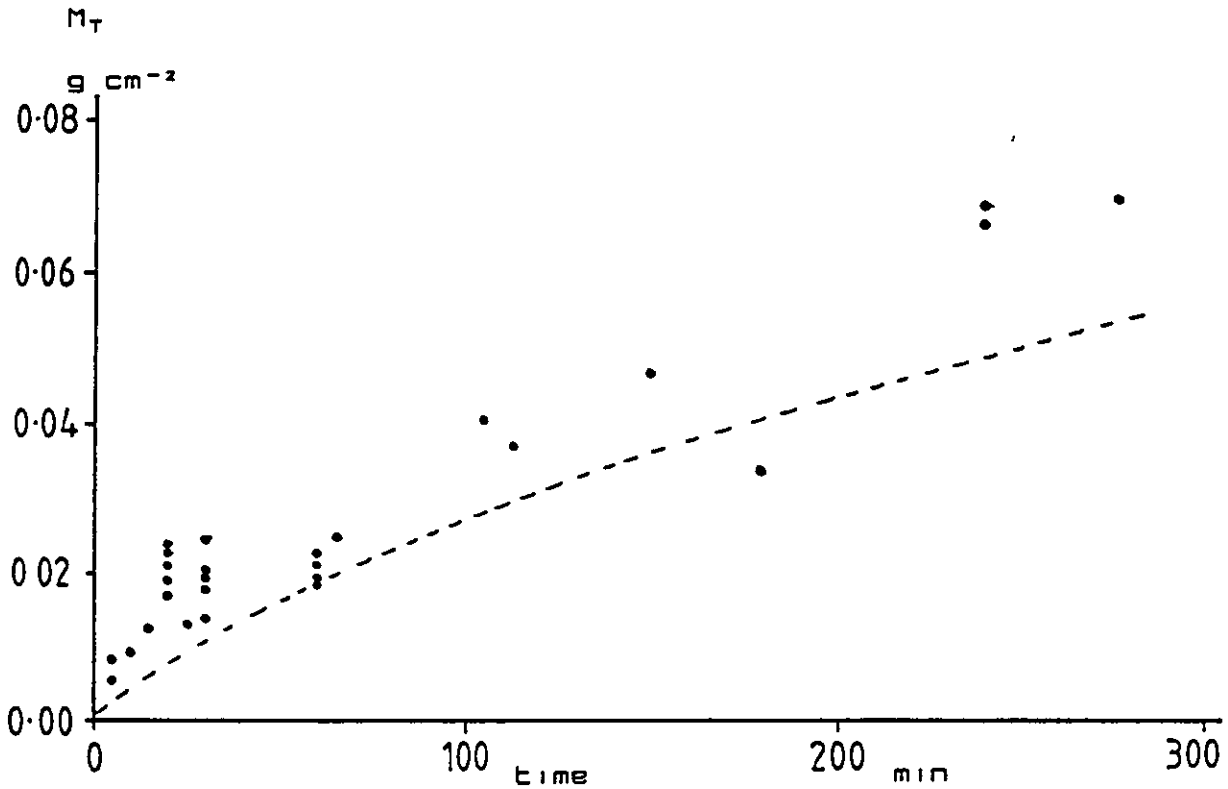

FIGURE 5.5

Diffusion of nitroethane into uPVC at 60°C

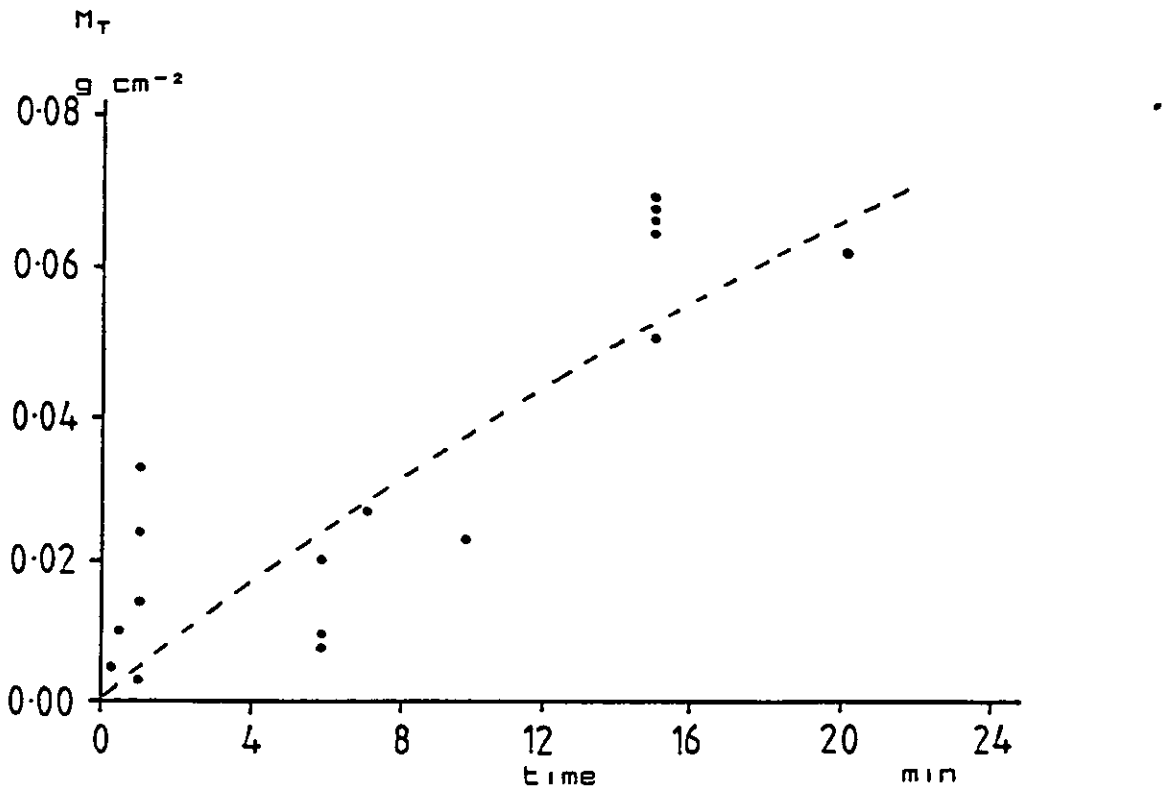

FIGURE 5.6

Diffusion of fluorobenzene into uPVC at 60°C

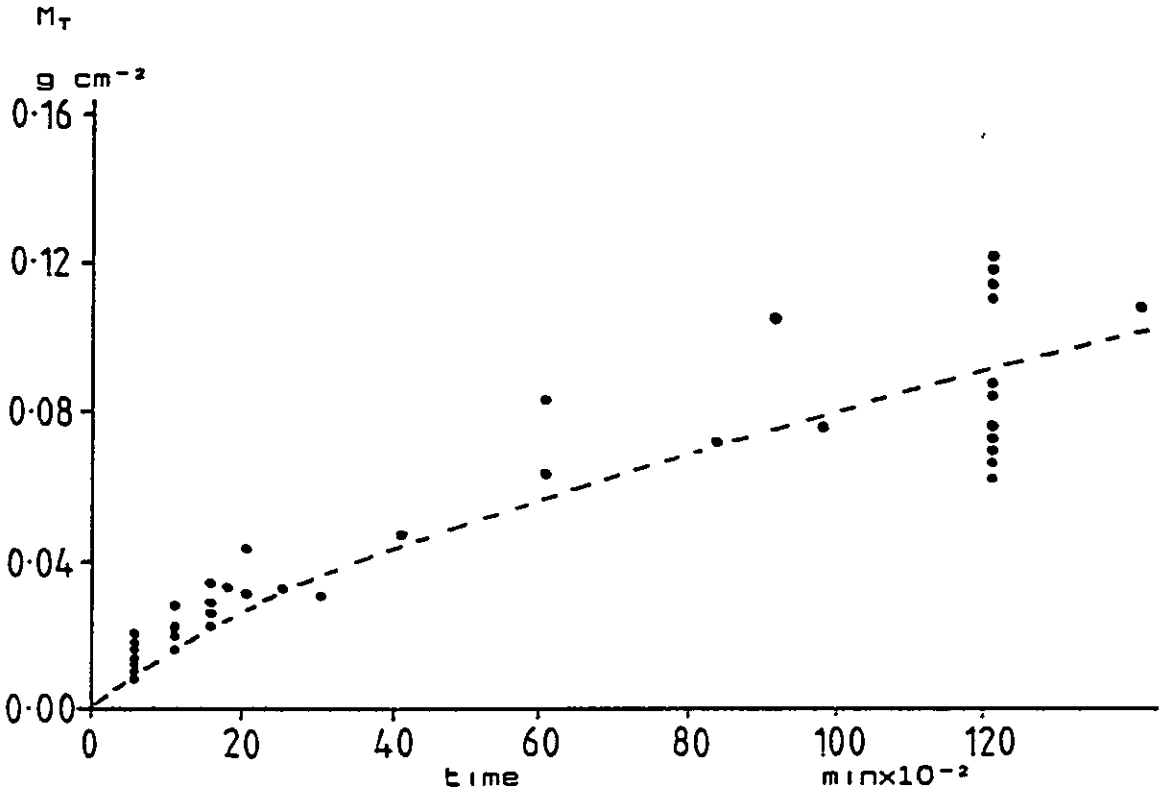

FIGURE 5.7

Diffusion of BBP, (•), and DMP, (x), plasticizers into uPVC at 60°C

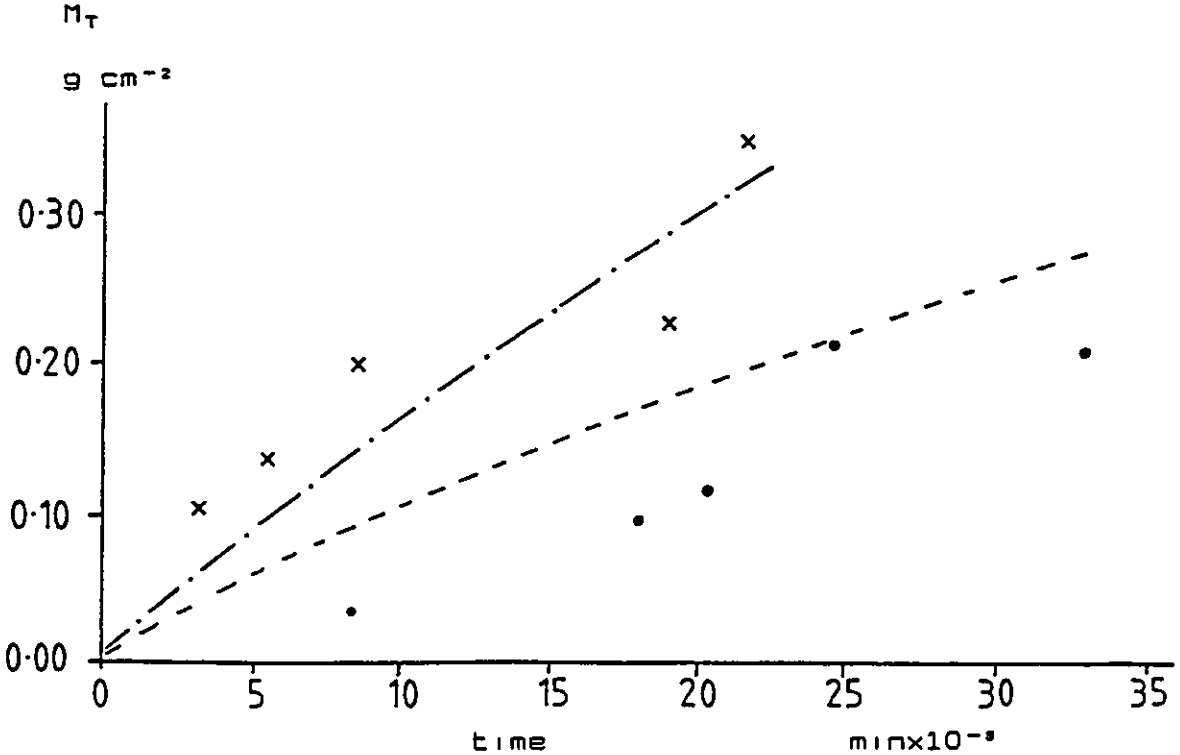

FIGURE 5.8

Diffusion of DOP plasticizer into uPVC at 60°C

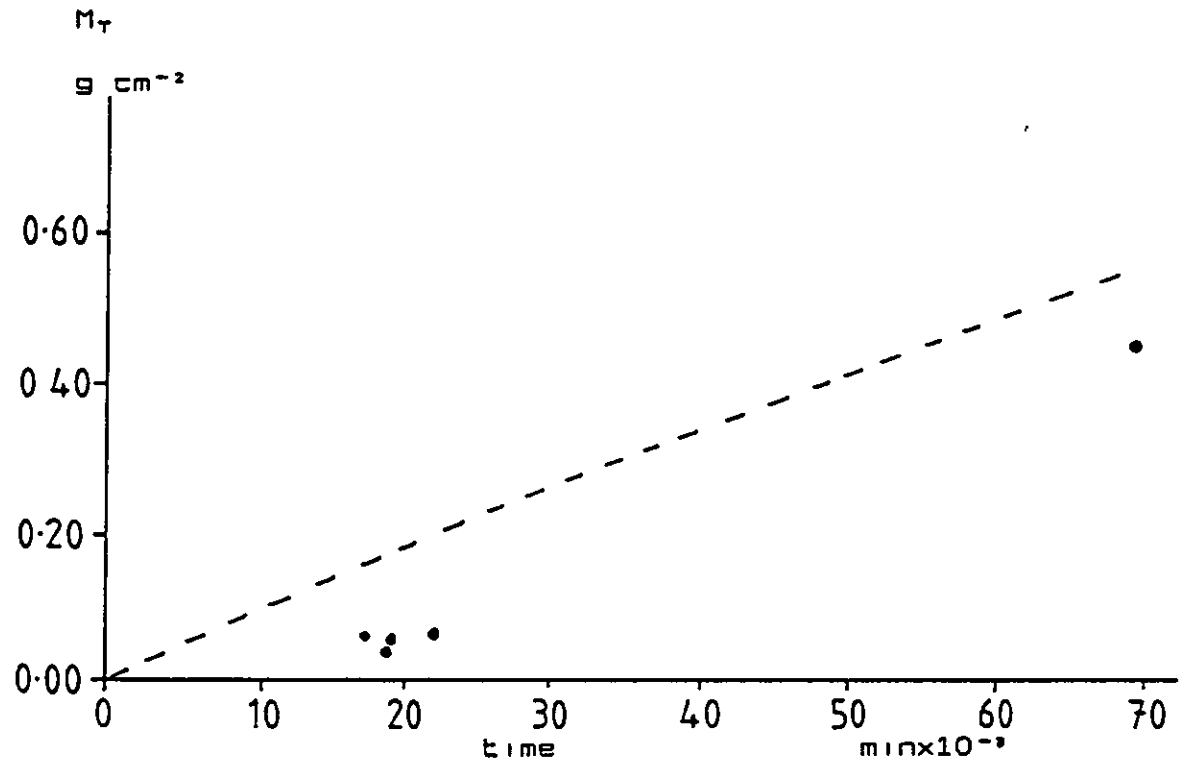

FIGURE 5.9

Diffusion of Cereclor 552 plasticizer into uPVC at 60°C

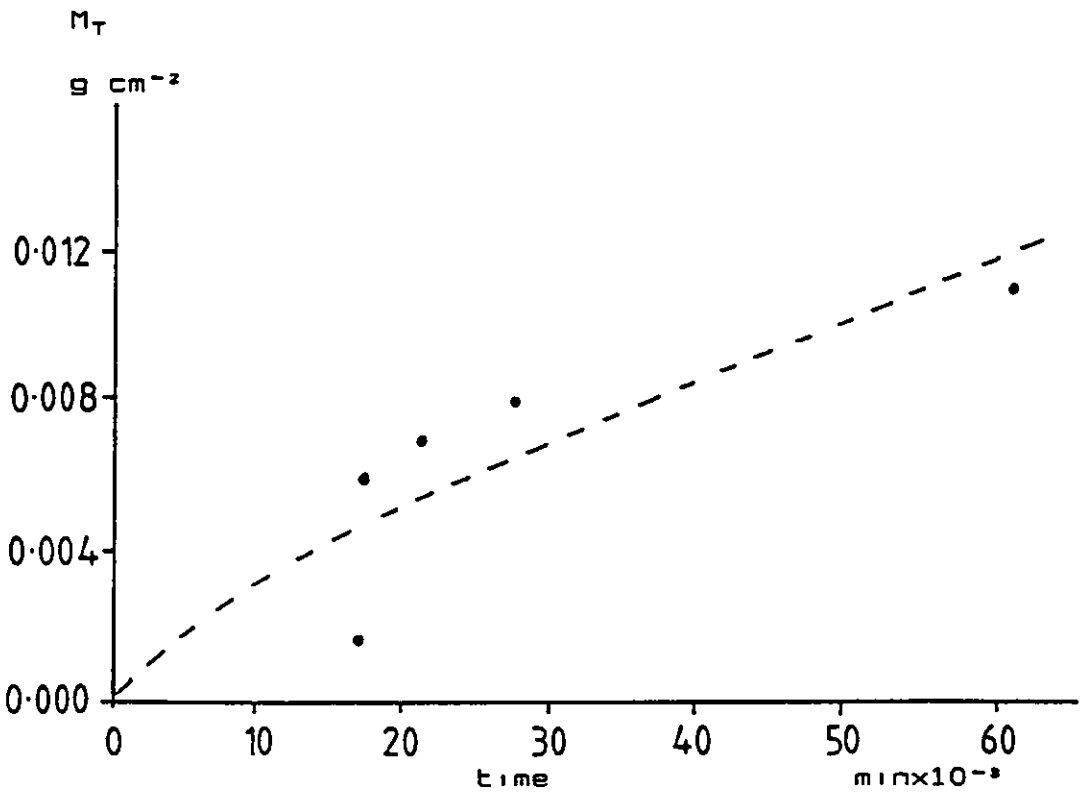

TABLE 5.2

Diffusion coefficients and liquid front velocities calculated using least-square calculations from mass per surface area versus time data

liquid	at 30°C		at 60°C	
	$D \times 10^6$ cm^2s^{-1}	$v \times 10^6$ cms^{-1}	$D \times 10^6$ cm^2s^{-1}	$v \times 10^6$ cms^{-1}
propanone	40.10	13.50	1230.00	233.00
fluorobenzene	1.81	2.09	181.00	36.30
dimethylbenzene	1.06	0.82	73.90	11.00
ethylbenzene	1.58	1.09	16.00	3.20
nitroethane	----	----	81.90	108.00
BBP	----	----	1.75	0.28
DMP	----	----	4.93	0.63
DOP	----	----	8.88	0.41
Cereclor S52	----	----	0.25	0.06
1,2-dichlorobenzene	0.36	0.71	----	----
chlorobenzene	175.00	44.20	----	----
benzene	1.83	1.66	----	----
methylbenzene	0.82	1.19	----	----
2-nitropropane	1.64	1.48	----	----
1-nitrobutane	0.02	0.02	----	----
	at room temperature			
propanone	6.38	24.1		

reported by Kwei *et al.* were,

$$v = 1.82 \times 10^{-5} \text{ cm s}^{-1}$$

$$D = 7.05 \times 10^{-8} \text{ cm}^2 \text{ s}^{-1}$$

These compare well with the room temperature propanone sorption experiment reported in table 5.2

5.1.2.2 Prediction of the thickness of the liquid swollen layer

The increasing thickness of the swollen layer with respect to time was reported in section 4.1.2.3. The diffusion coefficient and liquid velocity front values, obtained in section 5.1.2.1, were used in equation 2.121 to fit a calculated curve to the experimental swollen layer thickness, L, curves in figures 4.20 to 4.27. The results are shown in figures 5.10 to 5.17. A series of curves was calculated for different values of C_x, and compared with the experimental L curve. C_x is identified as being the critical concentration at which point the "apparent" discontinuity in D is seen, shown as the liquid front. This treatment was restricted to the sorption experiments conducted at 60°C and the C_x values are tabulated in table 5.3. Kwei *et al.* produced a calculated liquid front curve for $C_x = 0.034$ g cm^{-3} which fitted experimental data. The experiment, in this present work, using liquid sorption of propanone at room temperature produced an equilibrium concentration, $C_o = 0.97$ g cm^{-3} and when used together with D and v values, a curve which fits the swollen layer-time

FIGURE 5.10

Diffusion of propanone into uPVC at 56°C,

movement of liquid front into plaque

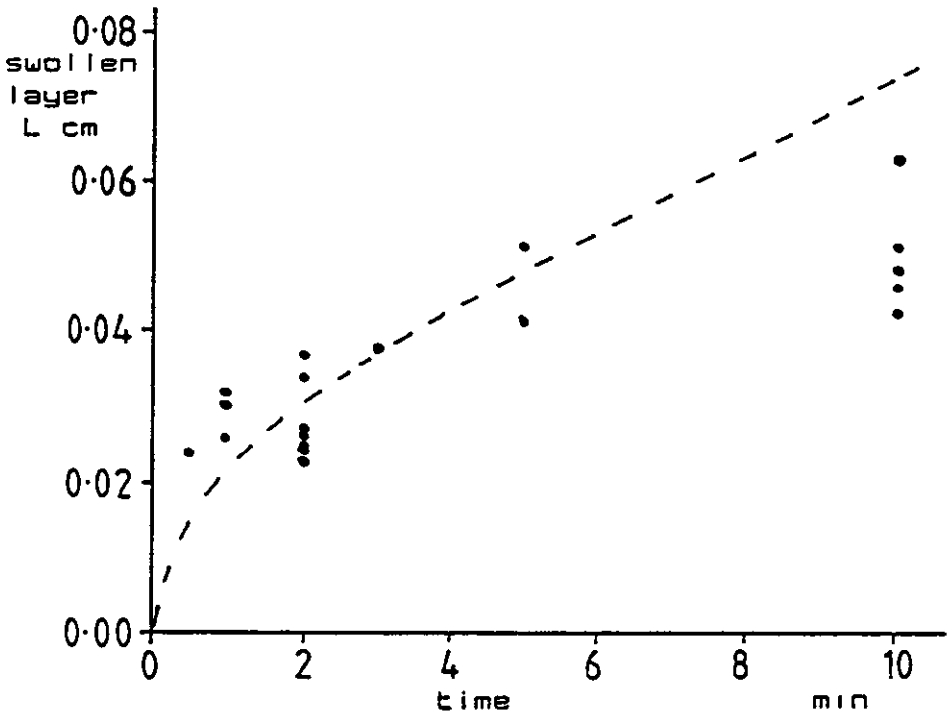

FIGURE 5.11

Diffusion of ethylbenzene into uPVC at 60°C,

movement of liquid front into plaque

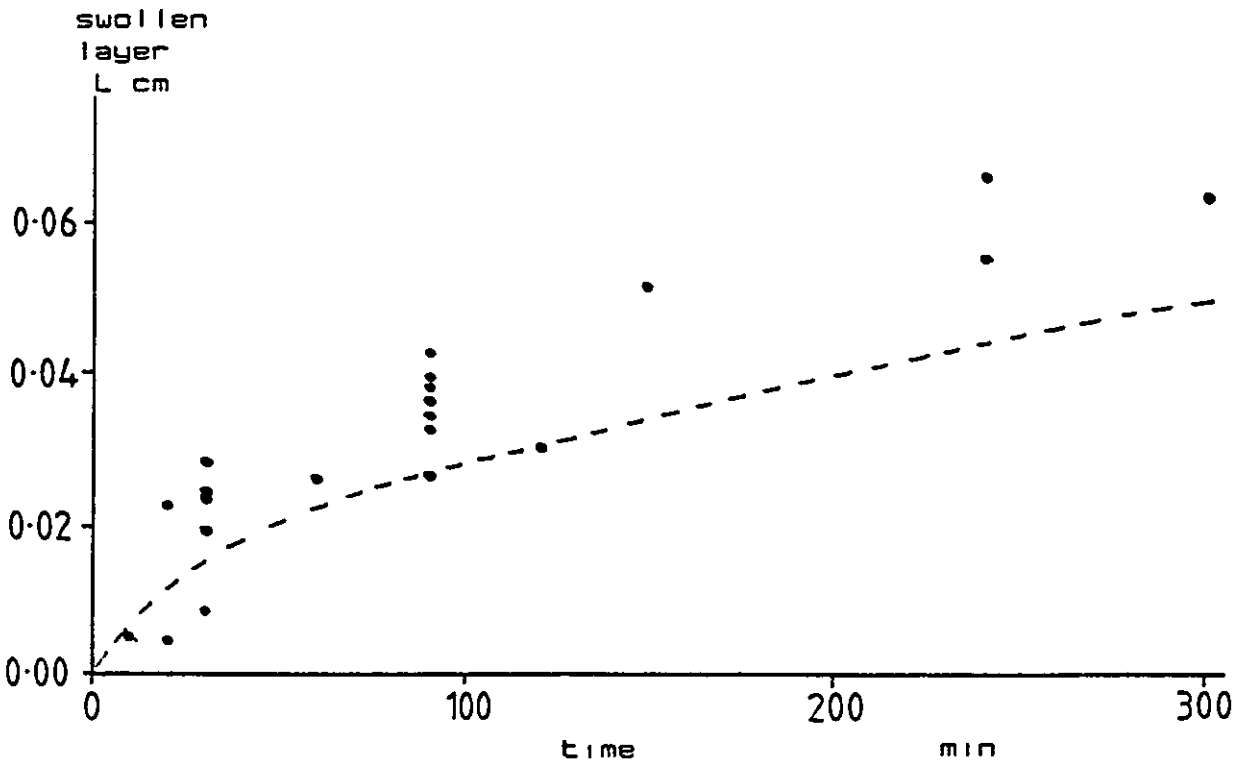

FIGURE 5.12

Diffusion of dimethylbenzene into uPVC at 60°C,

movement of liquid front into plaque

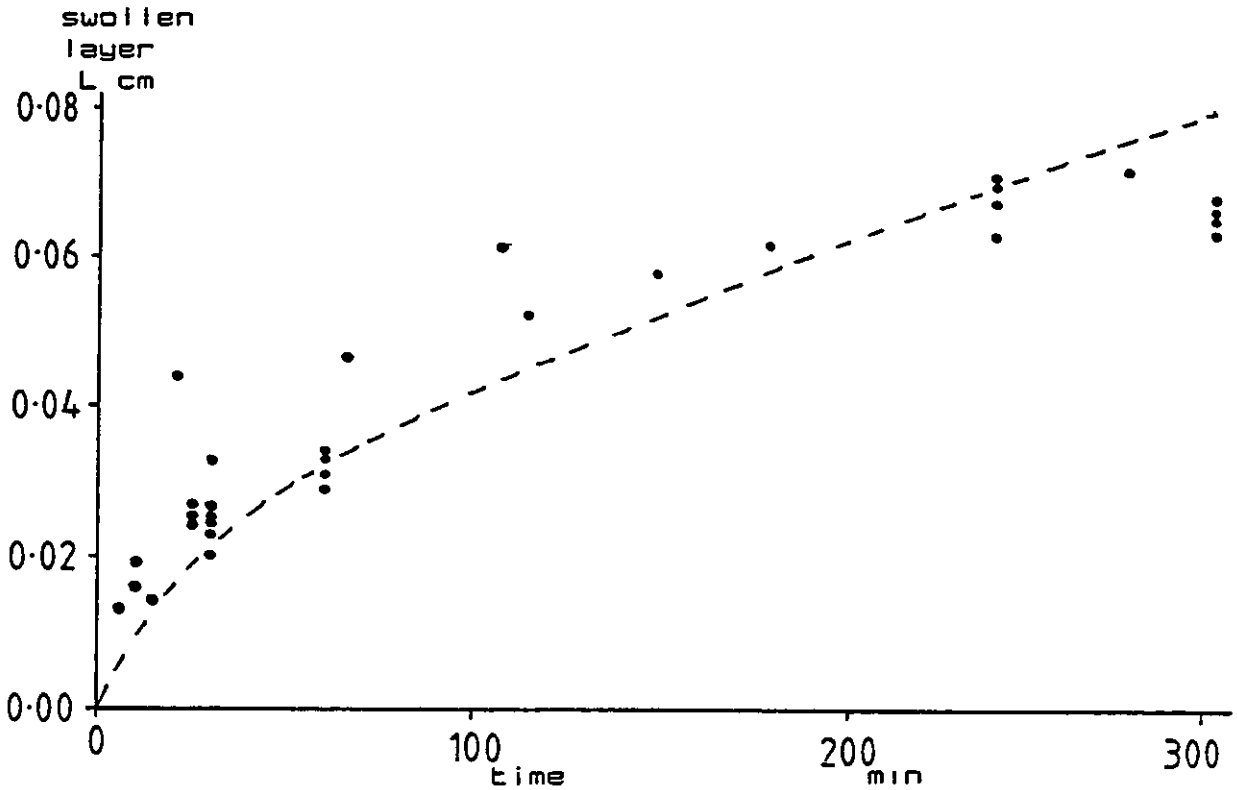

FIGURE 5.13

Diffusion of fluorobenzene into uPVC at 60°C,

movement of liquid front into plaque

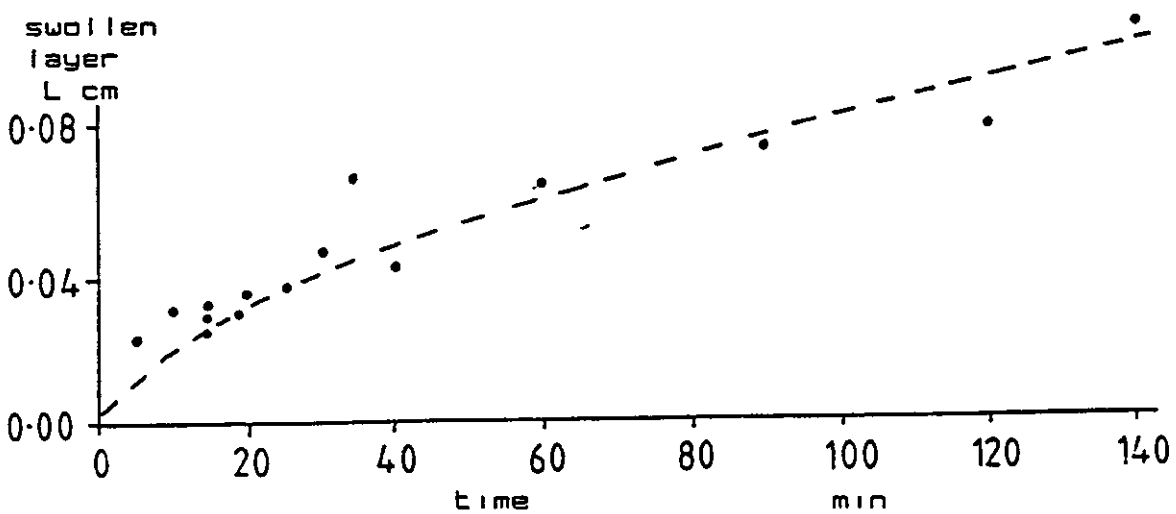

FIGURE 5.14

Diffusion of nitroethane into uPVC at 60°C.

movement of liquid front into plaque

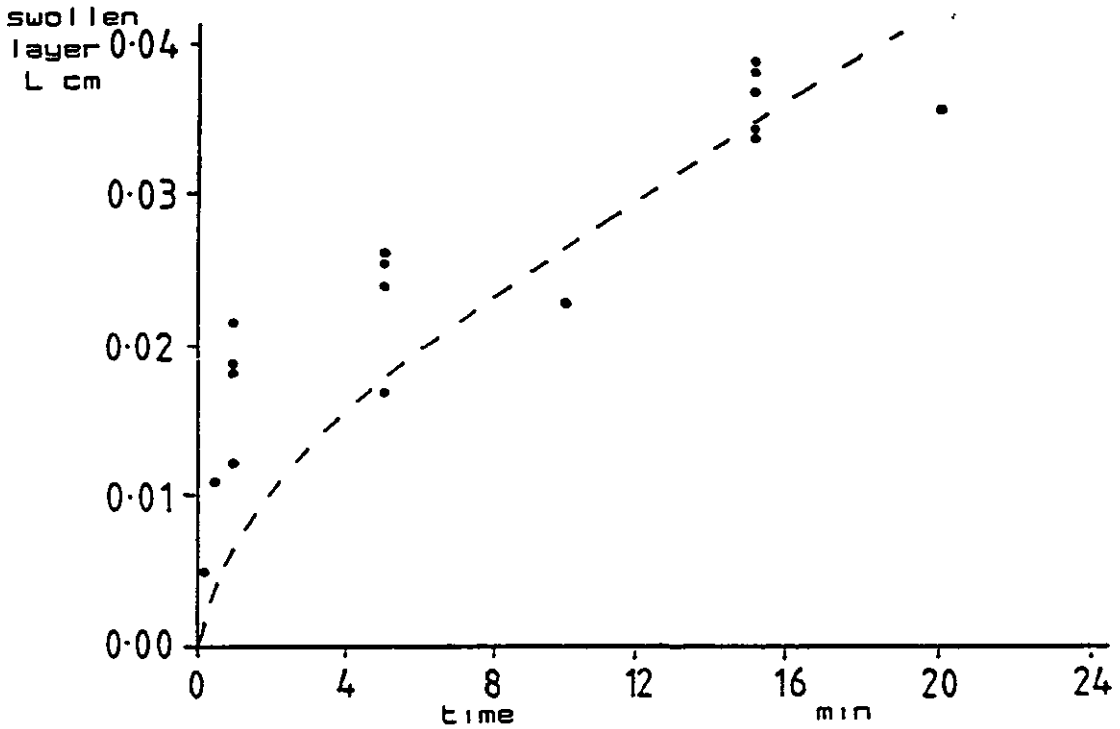

FIGURE 5.15

Diffusion of BBP (•) and DMP (x) plasticizers into uPVC at 60°C, movement of liquid front into plaque

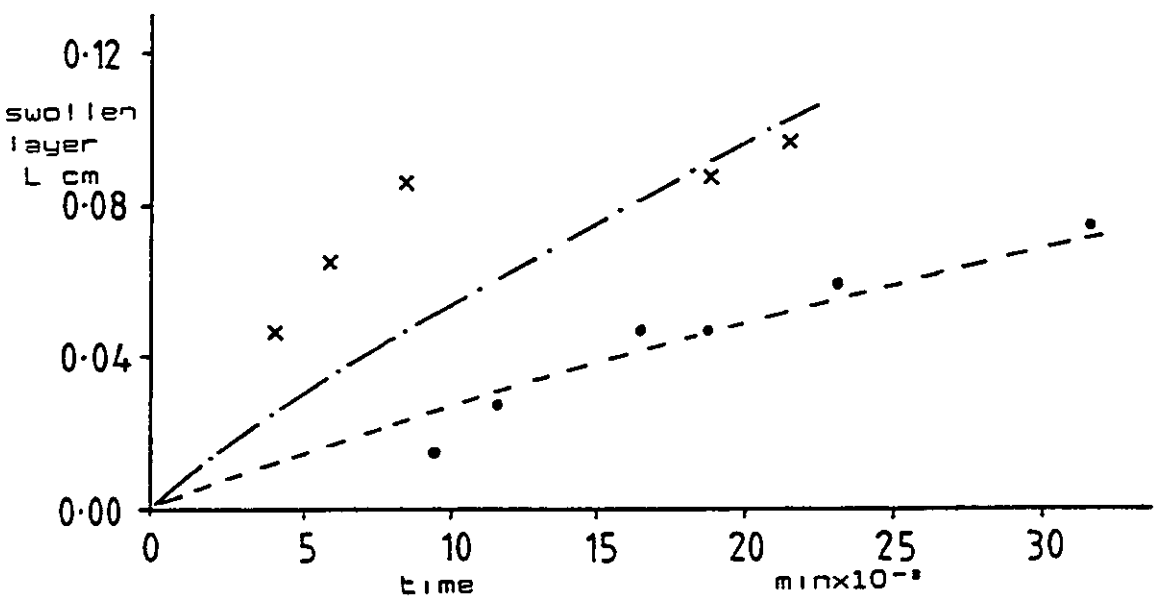

FIGURE 5.16

Diffusion of Cereclor 552 plasticizer into uPVC at 60°C,

movement of liquid front into plaque

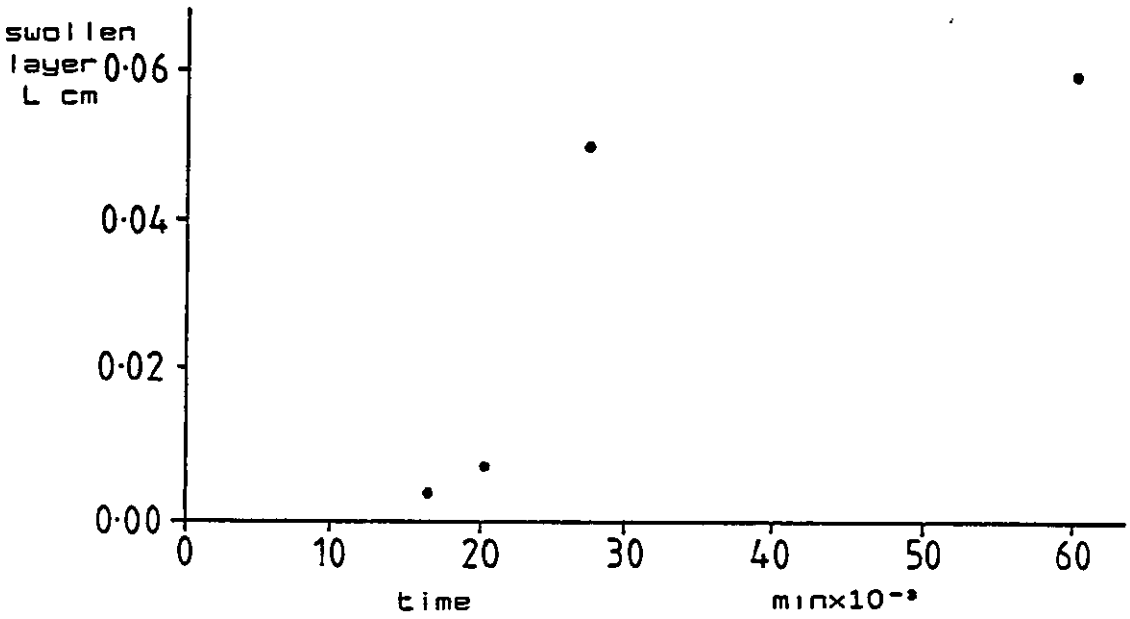

FIGURE 5.17

Diffusion of DOP plasticizer into uPVC at 60°C,

movement of liquid front into plaque

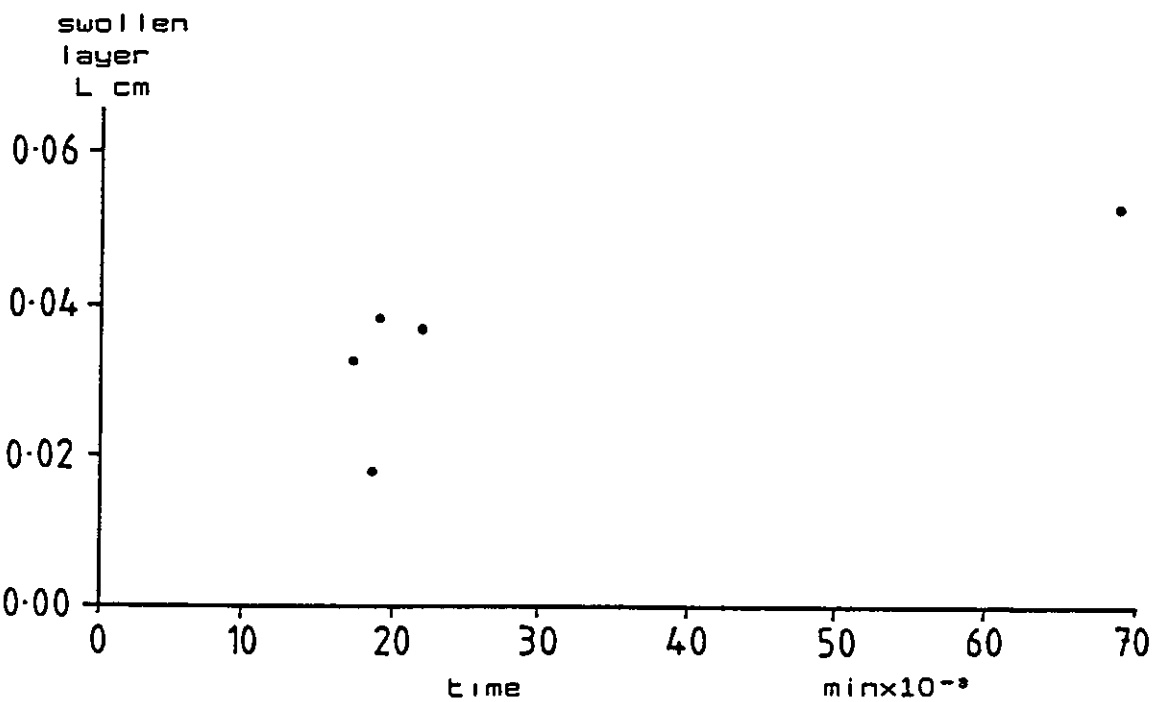

TABLE 5.3

Critical liquid concentrations giving rise to the "apparent" discontinuity in D and the sharp advancing front

liquid	critical liquid concentration C_x g cm^{-3}
fluorobenzene	2.0×10^{-5}
ethylbenzene	8.0×10^{-10}
propanone	1.3×10^{-7}
dimethylbenzene	3.3×10^{-5}
nitroethane	1.0×10^{-10}
BBP	0.135
DMP	0.105
DOP	0.27
Cereclor 552	1.0×10^{-4}
propanone (room temperature)	0.033

dependency produces a C_x of 0.033 g cm^{-3}; a value which compares well with the Kwei figure. The increase of the swollen layer thickness with respect to time for the sorption of propanone at room temperature is shown in figure 5.18.

5.1.3 The effect of diffusant size, hydrogen bonding number and solubility parameter on the diffusion coefficient

A comparison of the diffusion coefficient with respect to diffusant size, hydrogen bonding number and solubility parameter is given in figures 5.19 to 5.21. The dotted lines in each figure represent the best fit to the experimentally derived diffusion coefficients. Both the solubility and hydrogen bonding number figures, at both temperatures, show small increases in D with increasing values of solubility parameter and hydrogen bonding number. D, when examined with respect to increasing molar volume, shows a decrease in value, at both temperatures.

FIGURE 5.18

Diffusion of propanone into uPVC at room temperature,

movement of liquid front into plaque

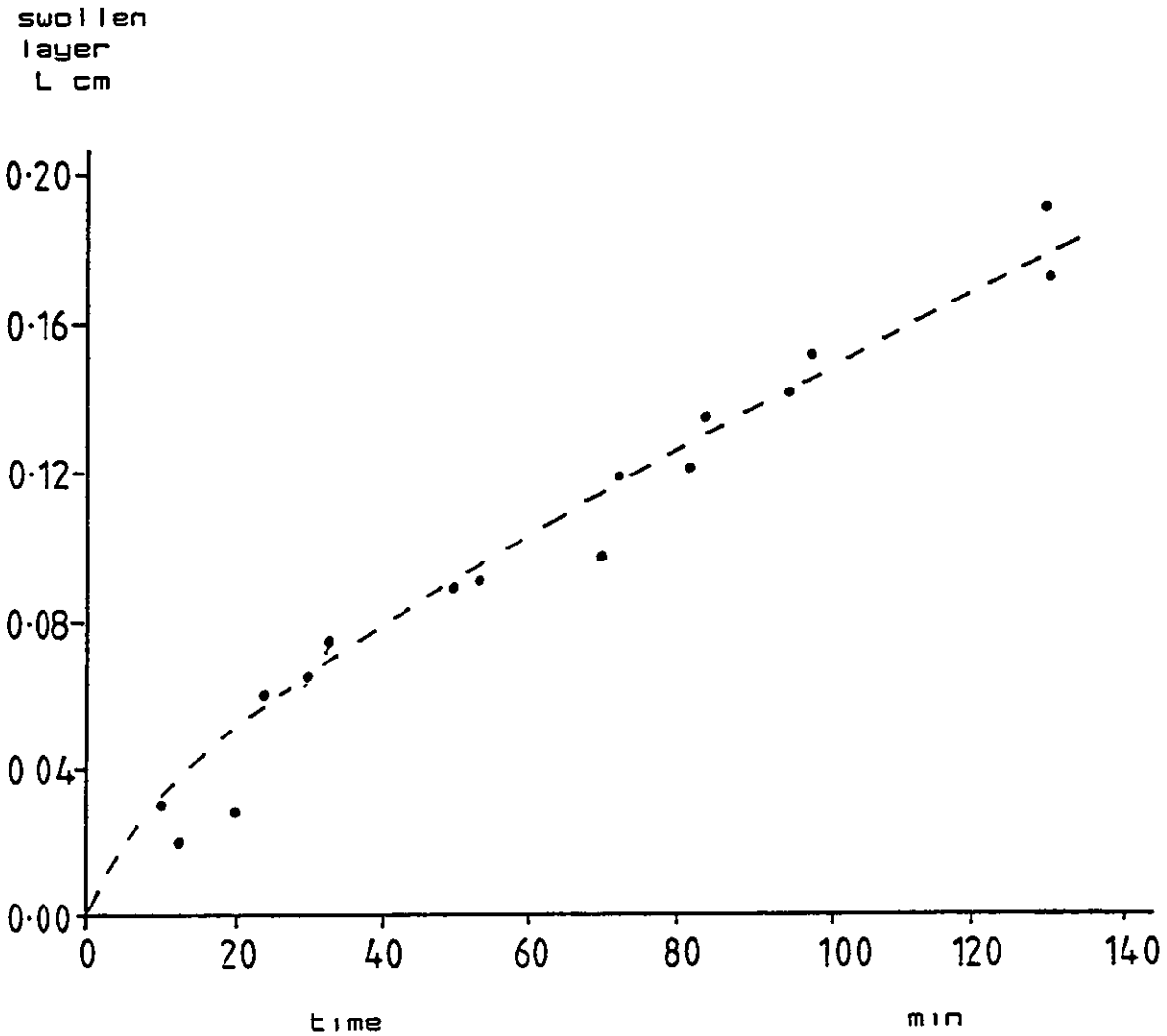

FIGURE 5.19

The diffusion coefficient of liquid in uPVC as a function of the liquid solubility parameter, at 30 and 60°C

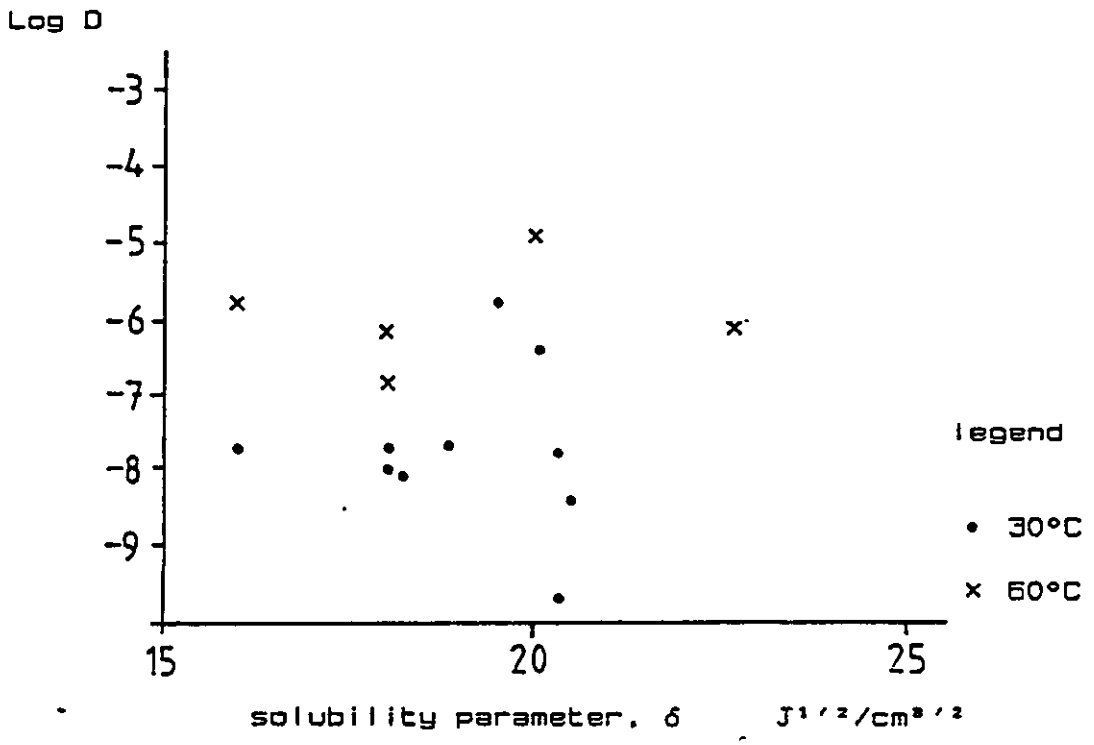

FIGURE 5.20

The diffusion coefficient of liquid in uPVC as a function of the liquid molar volume, at 30 and 60°C

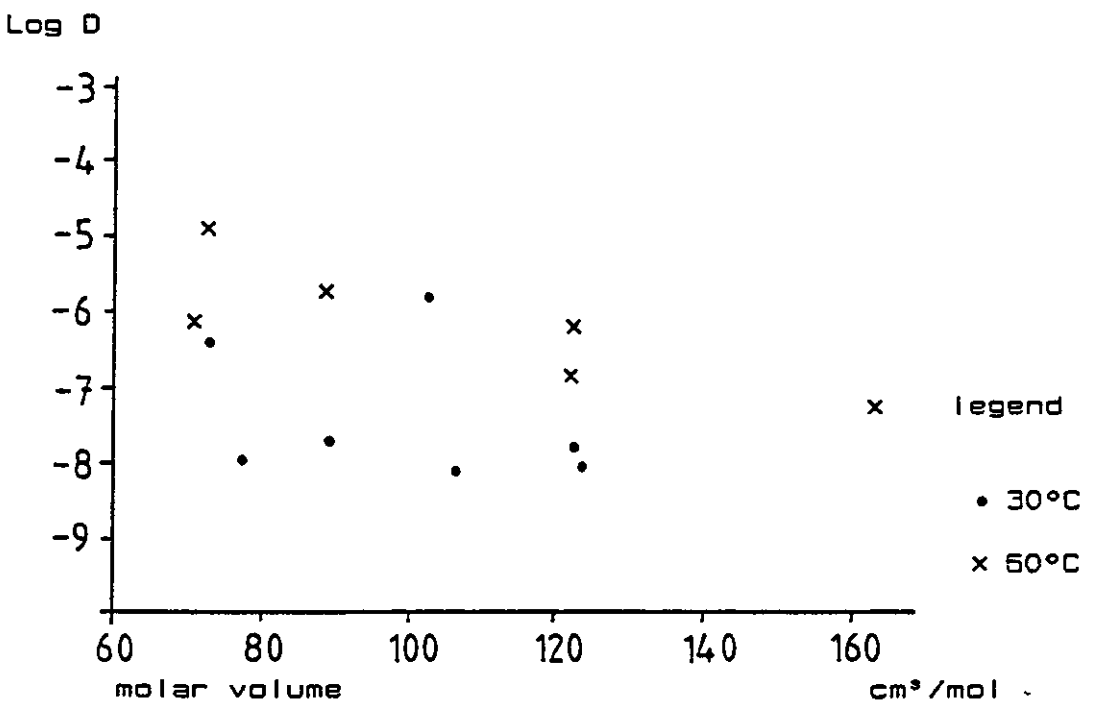

FIGURE 5.21

The diffusion coefficient of liquid in uPVC as a function of the liquid hydrogen bonding number, at 30 and 60°C

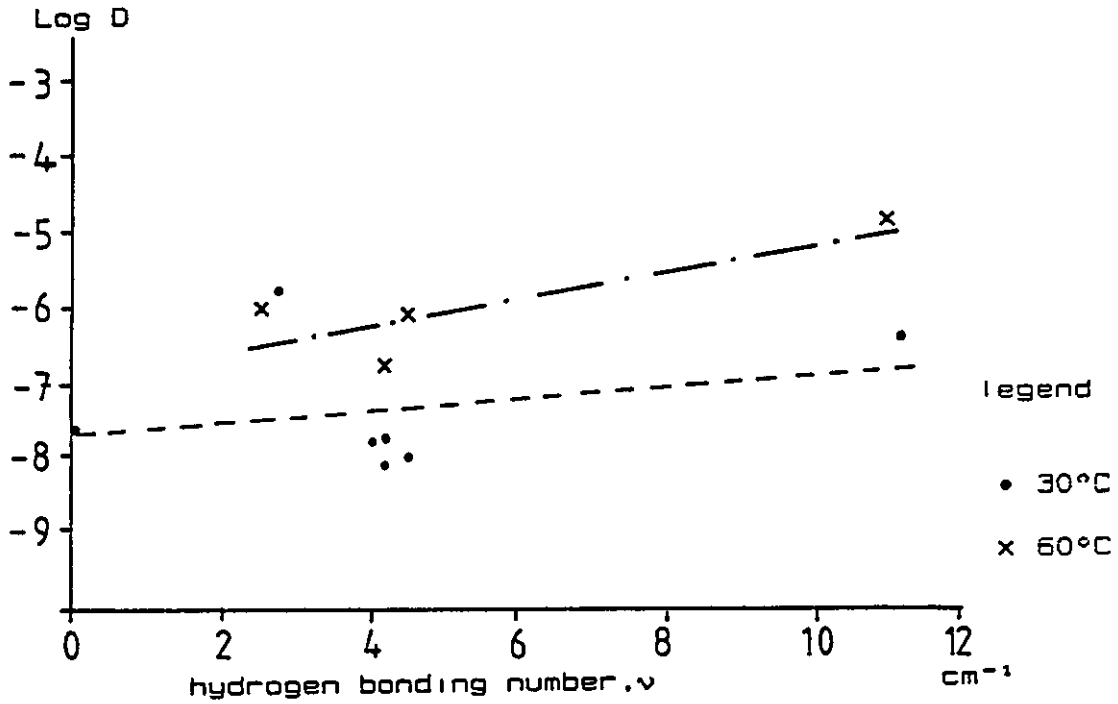

5.2 DYNAMIC MECHANICAL THERMAL ANALYSIS AND DSC ANALYSIS OF LIQUIDS AND PLASTICIZERS

The number of liquids in which it was possible to observe a T_g was small using both, PL-DMTA and DSC techniques. The major difficulty, as already mentioned in section 4.3.1, for PL-DMTA was that on quenching the liquid held in the filter paper support, in liquid nitrogen, the solid became extremely brittle and shattered when clamped into the sample clamp. The filter paper support technique was more successful for the plasticizers than the liquids. The plasticizer molecules are obviously larger than the liquids and the BBP thermogram shown in figure 4.34 is of particular interest, exhibiting two tan δ peaks. It may be proposed that the smaller, lower temperature, (-75°C), tan δ peak may be attributed to a β relaxation for the molecule. From the BBP molecule shown in figure 5.22, it can be postulated that the β relaxation can be attributed to either the benzyl or butyl group. The β relaxation in quenched, therefore amorphous, poly(ethylene teraphthalate) is thought to be due to the ester linkage and has a transition temperature of -65°C[156]. The chemical structure is;

$$-\{-COC_6H_4COO(CH_2)_2O-\}_n$$

If only the butyl group was considered, i.e. polyethylene, from the BBP molecule, it has been shown that a co-operative movement, causing a relaxation at around -120°C is observed[37]. A β relaxation in the BBP molecule between -65 and -120°C is therefore more likely to be due to the ester and butyl components. for the larger benzyl group, because of its size, then the β relaxation if observed would be

higher than -65°C. β relaxations have also been demonstrated for di-2-ethylhexyl phthalate in the literature[158] where the β relaxation occurring at -170°C was ascribed to the ethylhexyl groups.

The use of a substrate to support the liquid during PL-DMTA analysis will affect the magnitude of the tan δ peak, making the transitions appear smaller than if the support was absent. The tan δ peak position, however, is unaffected by the support[152].

FIGURE 5.22

A schematic diagram of the butylbenzyl phthalate molecule

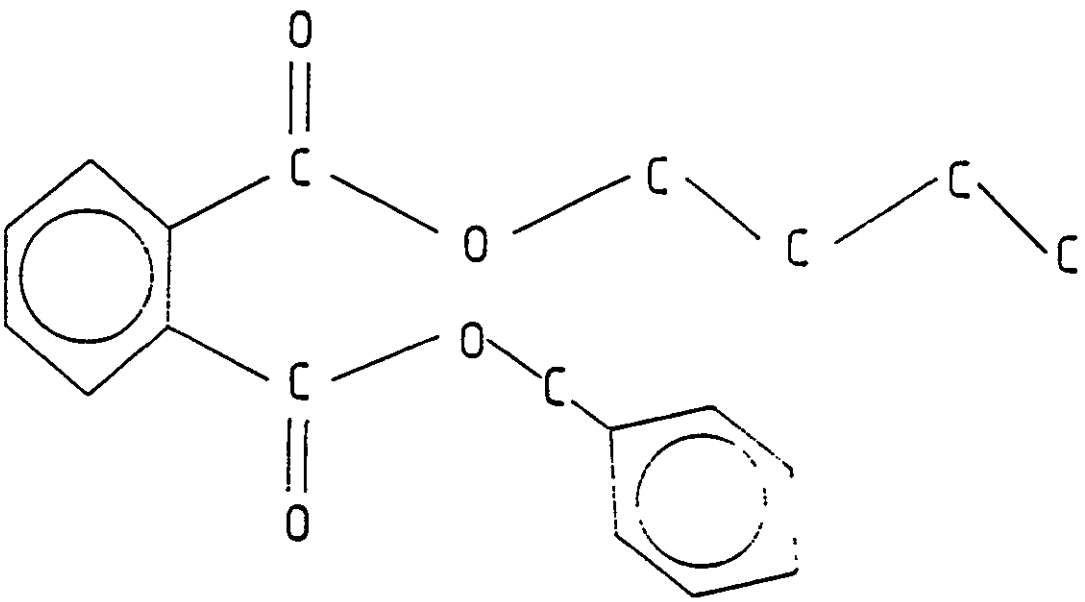

5.3 THE DYNAMIC MECHANICAL THERMAL ANALYSIS OF SWOLLEN UPVC COMPRESSION MOULDED PLAQUES

Work carried out by Harrison[159] in this laboratory showed that the behaviour of uPVC swollen with liquid VCM at room temperature is similar to that shown by many of the liquids employed in this work. Figure 5.23 shows a PL-DMTA thermogram, using the dual-cantilever mode, for uPVC swollen with liquid VCM at room temperature over a number of hours[160] giving a PVC/VCM gel with a T_g of -3°C. The sample used was produced from S71/102 resin processed in the same manner as the plaques used in this present work, except that the resin was preheated in the press for 5 mins and pressed at 9600 KNm^{-2} for 10 mins at 181°C, conditions only slightly more severe. The tan δ trace in figure 5.23 became visibly noisy at around 20°C, possibly due to the VCM (bp of -13°C) boiling off and disrupting the sample structure. There is no sign of any unswollen material present as shown by a uPVC tan δ occurring at 88°C, the sample fracturing between 50 and 90°C.

5.3.1 The stability of the glass transition peak position of the swollen material

5.3.1.1 Movement of $T_g\alpha'$ peak on the rerunning of highly swollen samples using dual-cantilever PL-DMTA

Trichloromethane and 1,2-dichloroethane swollen samples, prepared by swelling the samples in the respective liquid at 50°C, were run for a second time using PL-DMTA.

FIGURE 5.23

PL-DMTA dual-cantilever thermogram produced on heating uPVC swollen with liquid VCM at room temperature

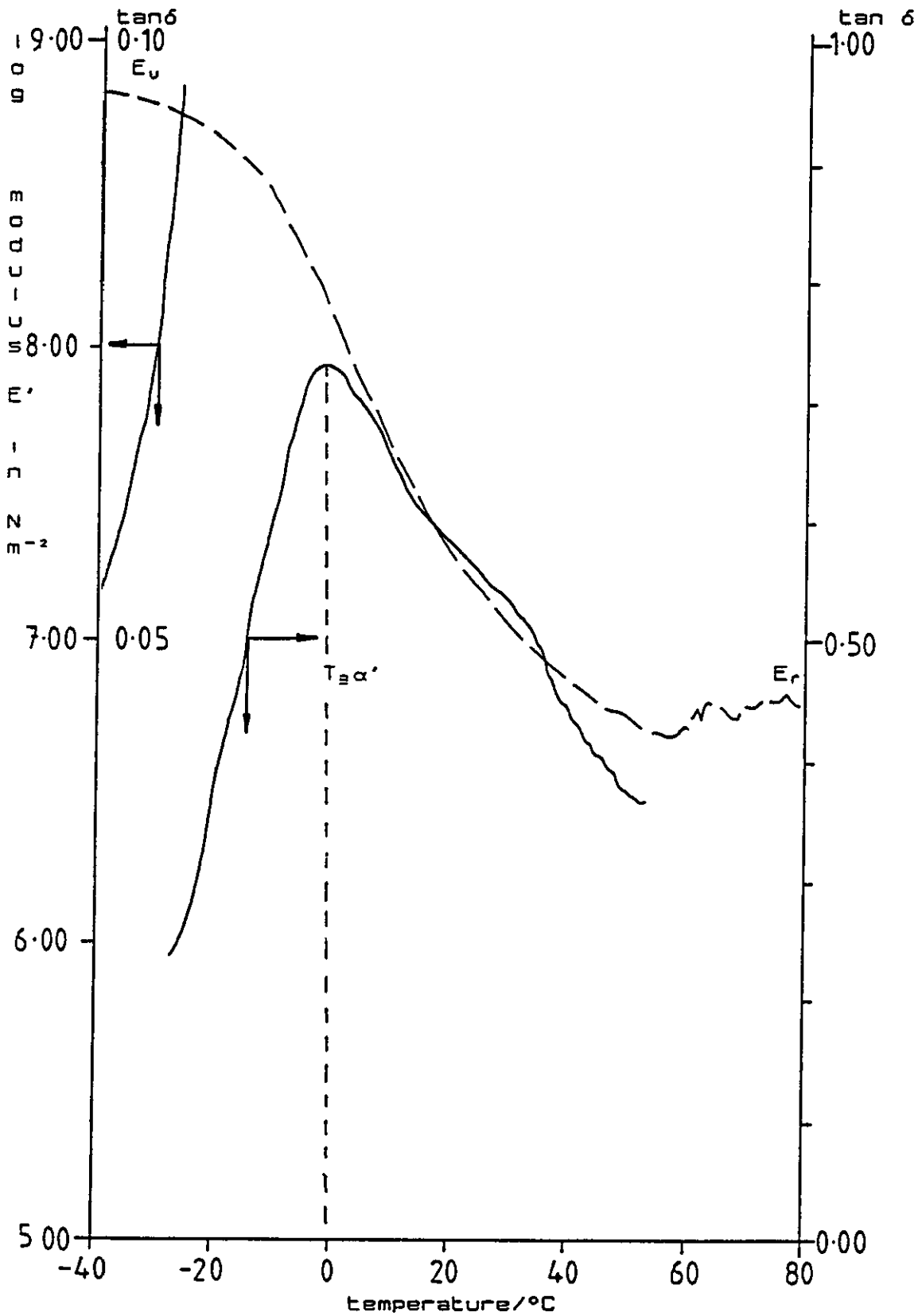

At the end of the first experiment the samples were cooled *in situ* and the same analysis conditions used for the repeat experiment. The clamping of the samples was checked once the temperature of the analysis head was well below the temperature of the $T_g\alpha'$ peak in the first experiment. The outer layer of these samples proved to be very fragile making intermediate weighings impracticable. In all cases the lower temperature tan δ peak associated with the T_g of the imbibed liquid disappeared in the second experiment together with an upward shift in the position of the tan δ peak due to $T_g\alpha'$. It has been suggested[161] that the formation of the $T_{g\ell}$ peak is caused by the swelling agent in the swollen region of the plaque, coming out of solution with the PVC, as the plaque is cooled from room temperature to -100°C forming micro-environments of pure liquid within the polymer. These micro-environments are removed on heating during PL-DMTA and due to loss of liquid from the sample during analysis do not recur in the second experiment. The boiling points for trichloromethane and 1,2-dichloroethane are 61 and 83°C respectively. The results of the tan δ peak positions in the two runs and their shifts are shown in table 5.4. The substantial changes in the $T_g\alpha'$ peak position on rerunning the experiment was thought to be due to the evaporation of the imbibed liquid from the plaque. However, it was impracticable to weigh the samples after PL-DMTA due to the fragile swollen layer breaking and sticking to the clamping frame.

TABLE 5.4

Tan δ peak positions and their shifts shown by uPVC, swollen with 1,2-dichloroethane and trichloromethane, during dual-cantilever PL-DMTA

liquid	original %mol content	solvent peak °C 1st. run	2nd. run	$T_g\alpha'$ °C 1st. run	°C 2nd. run	$\Delta T_g\alpha'$ °C	$T_g\alpha$ °C
1,2-dichloroethane	46	-115	---	-50	14	64	82
	23	-112	---	-44	29	73	84
trichloromethane	30	-135	---	-20	31	51	82
	13	-140	---	-28	32	60	82

5.3.1.2 Movement of $T_g\alpha'$ peak on the rerunning of vapour swollen samples using dual-cantilever PL-DMTA

Liquid swollen uPVC plaques show considerable changes in the $T_g\alpha'$ peak position, perhaps, due to the speed by which the plaques were first swollen producing a non-equilibrated system. Vapour sorption is carried out over long time intervals, typically 100 hours to produce a 30 mg uptake of propanone in a 1.3 g plaque of uPVC at 50°C. The plaque is more likely to be in equilibrium in atmospheric conditions unlike rapidly liquid swollen plaques. The shift in the tan δ peak position for $T_g\alpha'$ in vapour swollen samples would thus be expected to be smaller. To examine this proposal similar experiments were carried out as those described in section 5.3.1.1 using 1,2-dichloroethane and benzene. In this case however, due to the nature of the swelling agent and/or the experiment conditions, the nature of the swollen layer allowed the weighing of the sample between the first and second PL-DMTA experiments. The results are given in table 5.5 showing the movement of the $T_g\alpha'$ peak and change in percent molar content between the first and second runs. The percent molar content stated as measured is that at the beginning of the experiment and would be changing with respect to time and temperature and is, therefore, only an approximation to the content present at the transition region.

Since these experiments were carried out using dual-cantilever analysis it was possible to examine the β relaxation which occurs at -30°C in unswollen uPVC as shown in figure 4.43. It is interesting to note that, for the two

TABLE 5.5

Tan δ peak positions and their shifts shown by uPVC, swollen with 1,2-dichloroethane and benzene during dual-cantilever PL-DMTA

vapour	%mol content 1st. run	%mol content 2nd. run	$T_g\alpha'$ °C 1st. run	$T_g\alpha'$ °C 2nd. run	$\Delta T_g\alpha'$ °C	$T_g\alpha$ °C
1,2-dichloroethane	6.1	5.1	28	35	7	95
	8.4	7.5	43	48	5	95
	9.7	9.5	47	47	0	--
	12.0	11.0	40	44	4	--
	13.4	13.0	36	38	2	--
	20.4	19.2	24	25	1	--
	22.1	19.4	36	39	3	--
benzene	0.2	0.2	72	--	-	99
	4.5	4.0	53	60	7	99
	4.8	4.8	49	53	4	99
	9.1	8.5	40	47	7	99
	13.6	8.5	43	45	2	--

liquids examined in this manner, the position of the β relaxation peak is unaffected by the swelling agent content in the sample and the type of swelling agent involved. The swollen samples were cooled *in situ* from room temperature to the starting temperature, of around -150°C; at a rate of 8°C/min, the fast cooling rate will not affect the position of the β relaxation peak[162]. The position of the β relaxation peak is shown in figure 5.24 for the samples swollen with 1,2-dichloroethane or benzene vapour at 50°C. The β relaxation peak value remains almost constant with a slight overall decrease in value with increasing content of swelling agent.

5.3.1.3 Movement of $T_g\alpha'$ peak on the desorption of liquid swollen samples using shear PL-DMTA mode

Rapidly swollen samples such as those produced using the swelling agent in liquid form show significant shifts in the $T_g\alpha'$ position if desorption was allowed to occur prior to PL-DMTA. For example, a uPVC plaque swollen with dimethylbenzene at 60°C for 30 mins produces a sample with a swollen layer of approximately 0.4 fraction of the sample thickness. When this sample was allowed to equilibrate at atmospheric pressure and at room temperature for a number of hours, followed by shear mode PL-DMTA, a shift in $T_g\alpha'$ of 25 degrees was produced when compared with an identical sample that was analysed directly after removal from the swelling environment. A similar set of experiments is shown in figure 5.25 where two sets of samples were identically produced, by swelling plaques of uPVC in propanone at 56°C, one being desorbed prior to PL-DMTA. Desorption was carried

FIGURE 5.24

β relaxation peaks for uPVC swollen with (a) benzene and (b) 1,2-dichloroethane vapour at 50°C. numbers refer to legends in figures 4.58 and 4.59

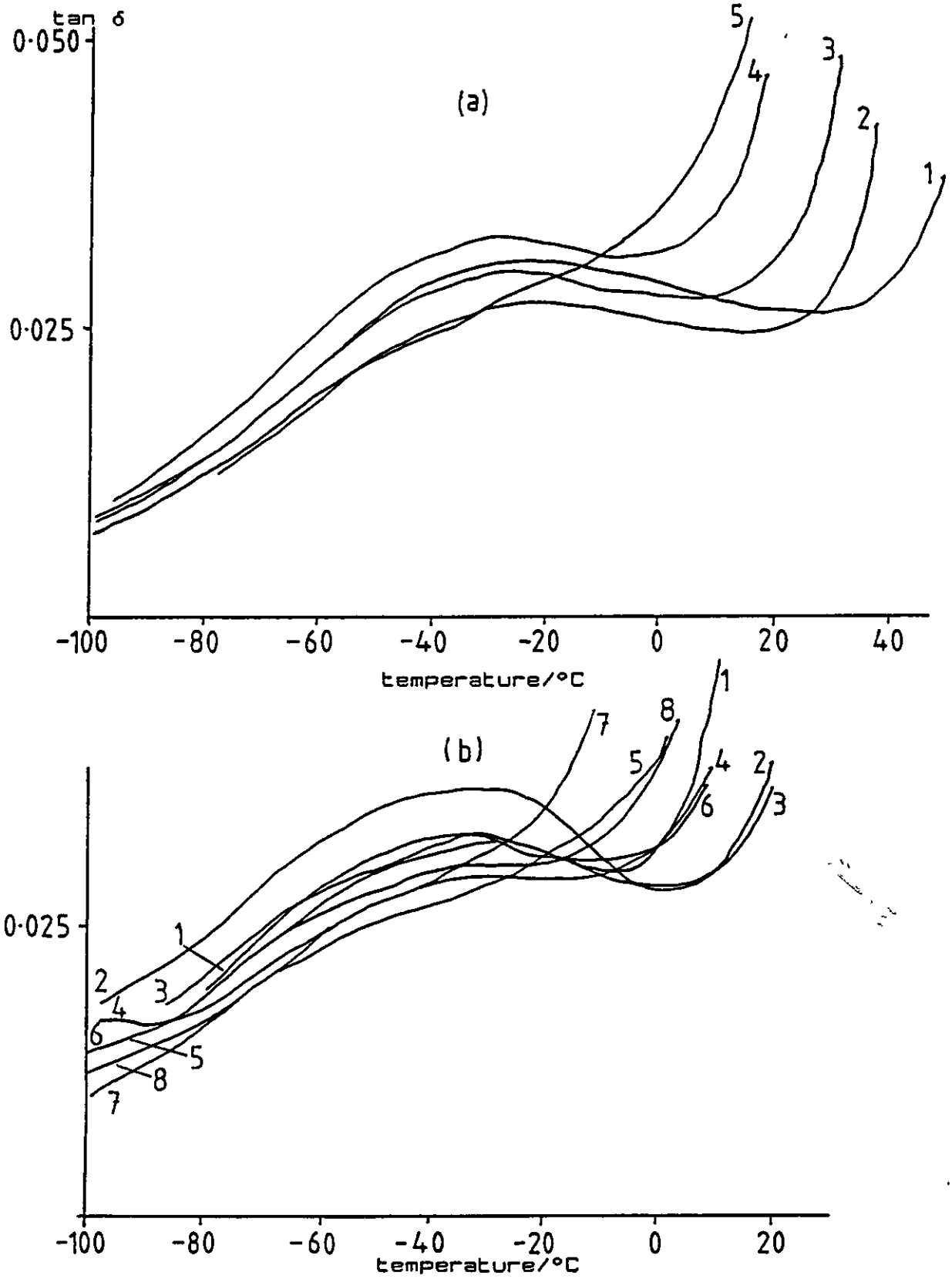

FIGURE 5.25

PL-DMTA shear mode thermogram produced on heating uPVC swollen with propanone at 56°C, dotted line - sample used as swollen, solid line - sample desorbed prior to analysis

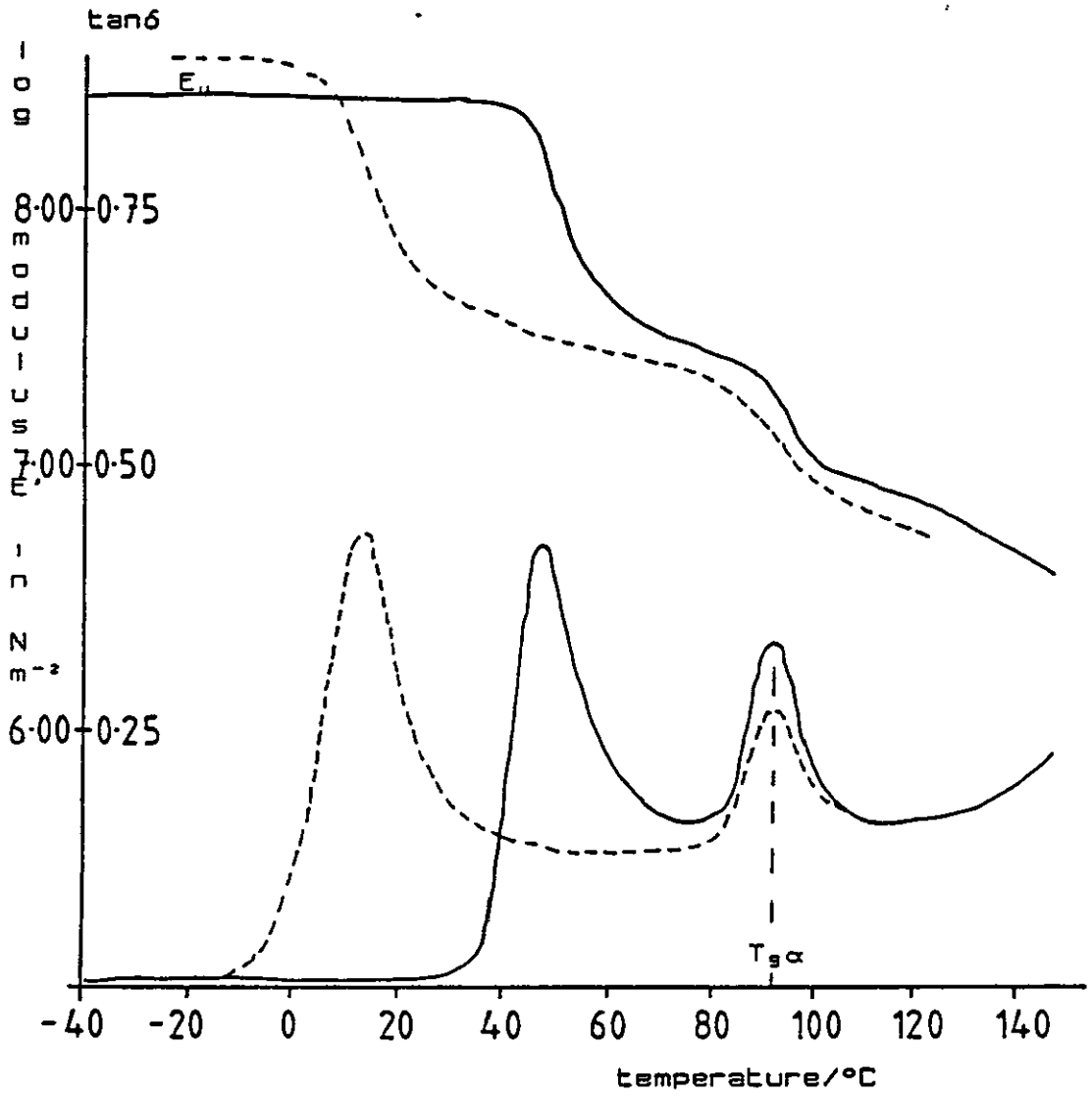

out at room temperature and pressure and was followed using the microbalance, the resulting desorption plot can be seen in figure 5.26 where it is seen that over a period of 50 hours approximately 45% of the original propanone content is lost. The $T_g\alpha'$ of the propanone-uPVC system which was allowed to desorb prior to PL-DMTA, shown by the solid line in figure 5.25, is shown to be 36°C higher than the swollen sample analysed directly after removal from the swelling environment. It is clear therefore that the time between removal of the swollen sample from a thermostat bath after the diffusion experiment and cooling to the starting temperature in the PL-DMTA experiment should be minimised. In order to illustrate the problem of desorption, even at low temperatures, three identical experiments were performed with the exception that the samples were treated differently after sorption. The samples were extracted from the same plaque, and swollen with dimethylbenzene at 60°C for 30 mins producing a sample with a swollen layer of approximately 0.4 fraction of the total sample thickness. One sample, (a), was not allowed to equilibrate after liquid sorption and was analysed immediately on removal from the swelling environment; this was the normal procedure for analysing swollen samples in shear mode PL-DMTA and is detailed in the experimental section. A second sample, (b), after the sorption experiment was stored in liquid nitrogen for 24 hours and a third sample, (c), after removal from the swelling environment was stored at 0°C for 72 hours prior to PL-DMTA. The results of this experiment are shown in figure 5.27 where sample c shows a $T_g\alpha'$, 25°C higher than samples a and b. This experiment suggests that swollen samples,

FIGURE 5.26

The desorption of propanone

followed using the microbalance

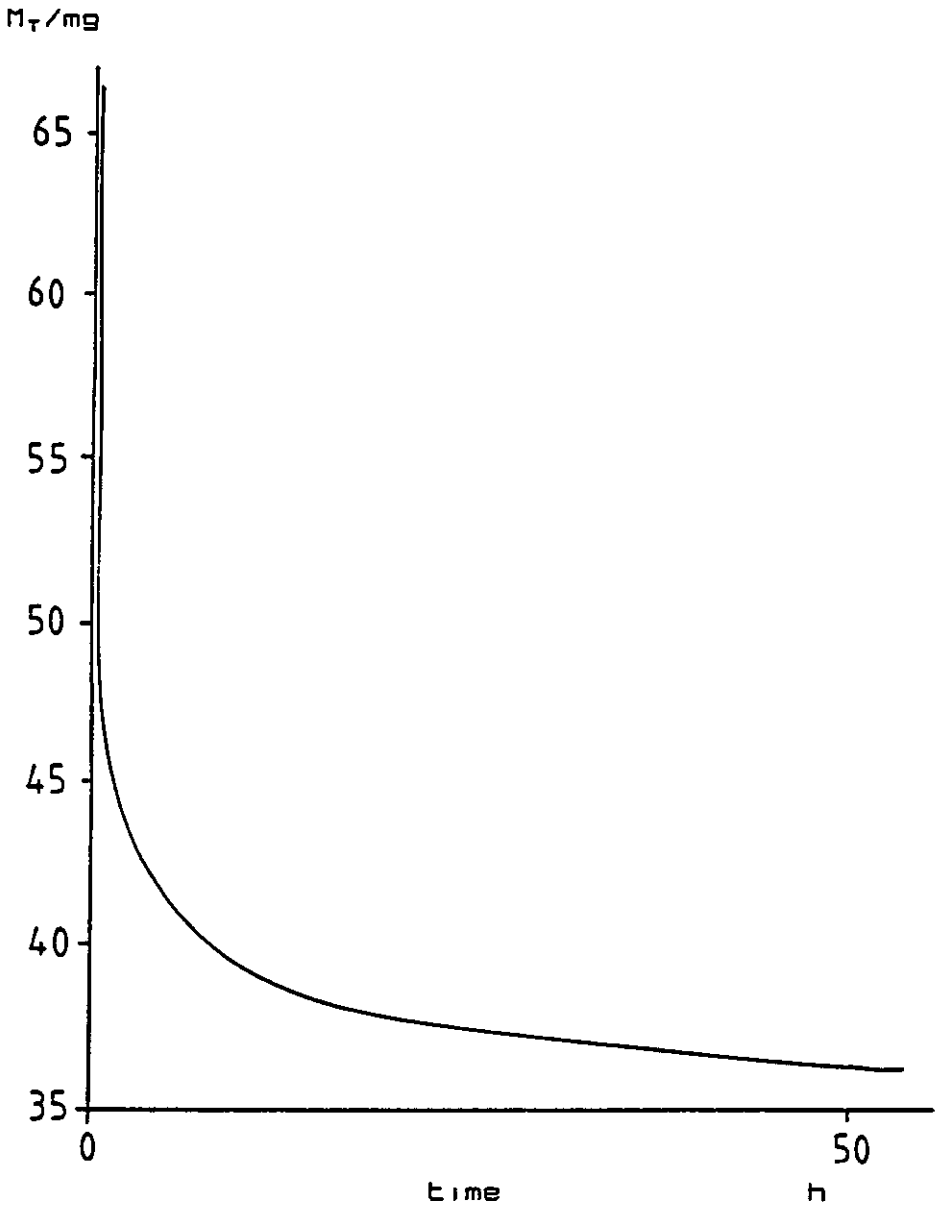

FIGURE 5.27

PL-DMTA shear mode thermogram produced on heating uPVC swollen with dimethylbenzene at 60°C for 30 mins, with a heating rate of 2°C/min, a frequency of 1 Hz and a instrument strain of one

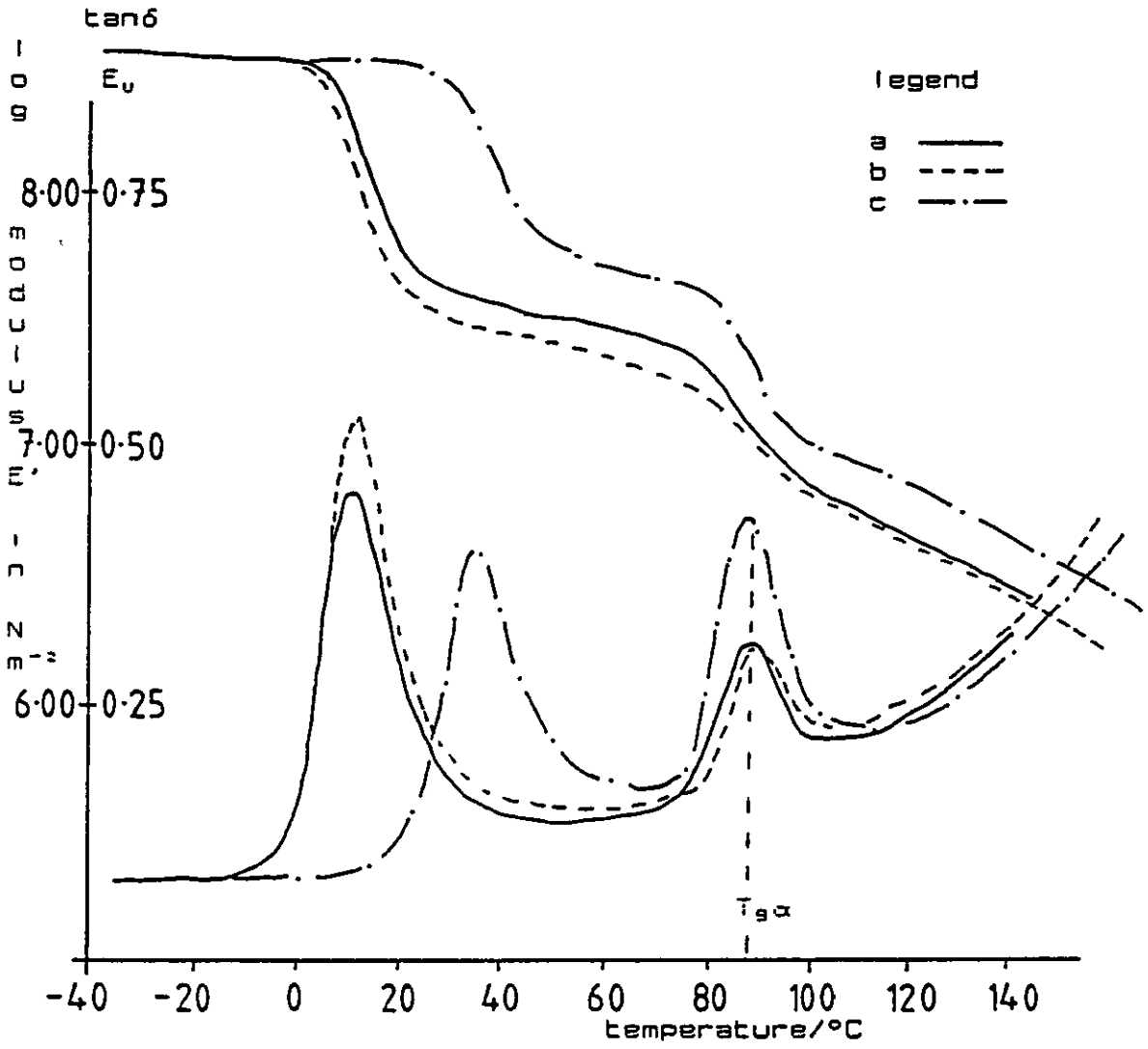

unless stored at liquid nitrogen temperatures, should be analysed immediately after the diffusion experiment.

5.3.2 Dynamic mechanical thermal analysis of shear mode results

As a direct consequence of the work described in section 4.4.1 above, the information obtainable from PL-DMTA, using the shear mode, below the $T_g\alpha'$ is limited. The following analysis, therefore, does not attempt to examine any relaxations or modulus readings below that of the $T_g\alpha'$ peak. All tan δ and modulus readings were confined to temperatures greater than the $T_g\alpha'$ position where the modulus value drops sufficiently to be within the machine's capabilities. The treatment below requires the use of a standard modulus value at a temperature below the T_g of uPVC. Since this is unobtainable using shear PL-DMTA, values of E' obtained using dual-cantilever PL-DMTA were employed. In converting these modulus values, E', to G' a Poisson's ratio of 0.42[65] was assumed in Equation 2.4.

The modulus value obtained from the PL-DMTA was a combination of the modulus for the glassy core and the rubbery region. Experiments carried out in shear mode, (see figure 3.9), together with Takayanagi's model for parallel connection allowed computation of the modulus of the rubbery region, G_r'. Log G_r' was calculated using the following method. First, log G' was converted into the compliance J'

$$J' = (1/G')/(1+\tan^2\delta) \qquad (5.1)$$

This measured J' from the PL-DMTA was denoted by J'(meas), and consisted of two portions produced from the rubbery fraction V_r and the fraction of solid material V_s.

$$J'(meas) = V_r J'_r + V_s J'_s \qquad (5.2)$$

The only unknown is J'_r which is calculated and converted back to G' as G'_r using

$$G' = (1/J')/(1+\tan^2\delta) \qquad (5.3)$$

The procedure described in Appendix 4 to calculate the log G_r' at 60°C and the algorithm in Appendix 1 to find the percent molar content of diluent or plasticizer in the swollen region at 60°C during PL-DMTA allowed figures 5.28 to 5.33 to be compiled. In section 4.4.4.4 the variation of the modulus value at 60°C due to the experimental procedure was investigated. The standard deviation in the log modulus value at 60°C was shown to be 0.06. This deviation is shown in figures 5.28 to 5.33 as a vertical error bar on the log modulus.

5.3.2.1 Calculation of molecular weight between cross-links from PL-DMTA modulus results

Viscoelastic theory suggested that chain entanglements were the cause of the rubber-elastic properties in a polymer. On a thermogram the rubber-elastic region is the "plateau" after the polymer has undergone a glass transition and before the rubber begins to flow.

FIGURE 5.28

Log G_r' calculated from the shear analysis, at 60°C, of uPVC swollen with nitroethane

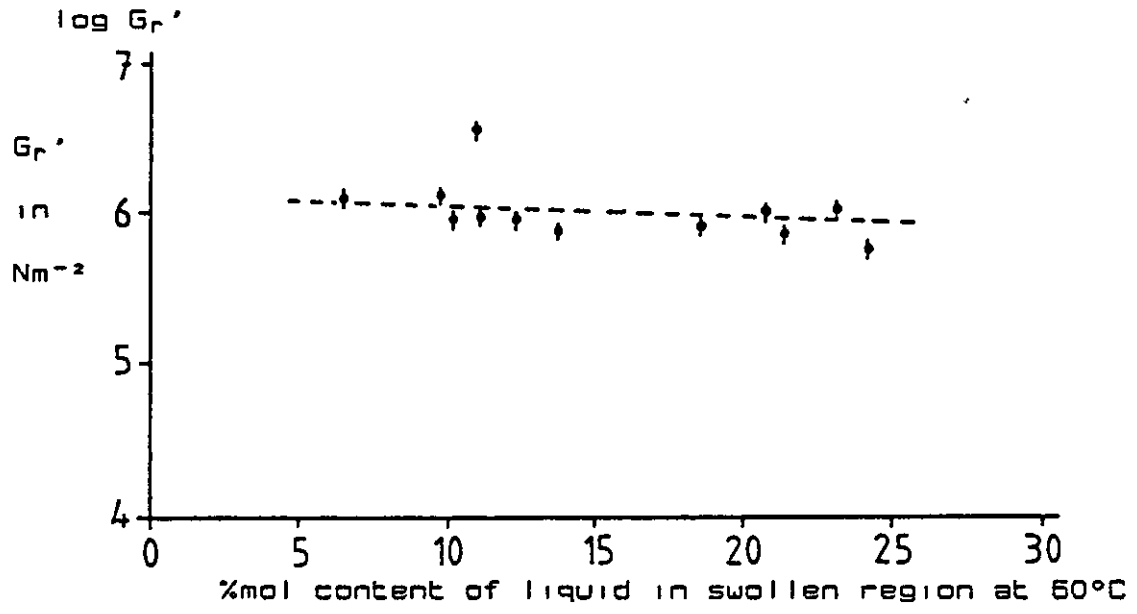

FIGURE 5.29

Log G_r' calculated from the shear analysis, at 60°C, of uPVC swollen with fluorobenzene

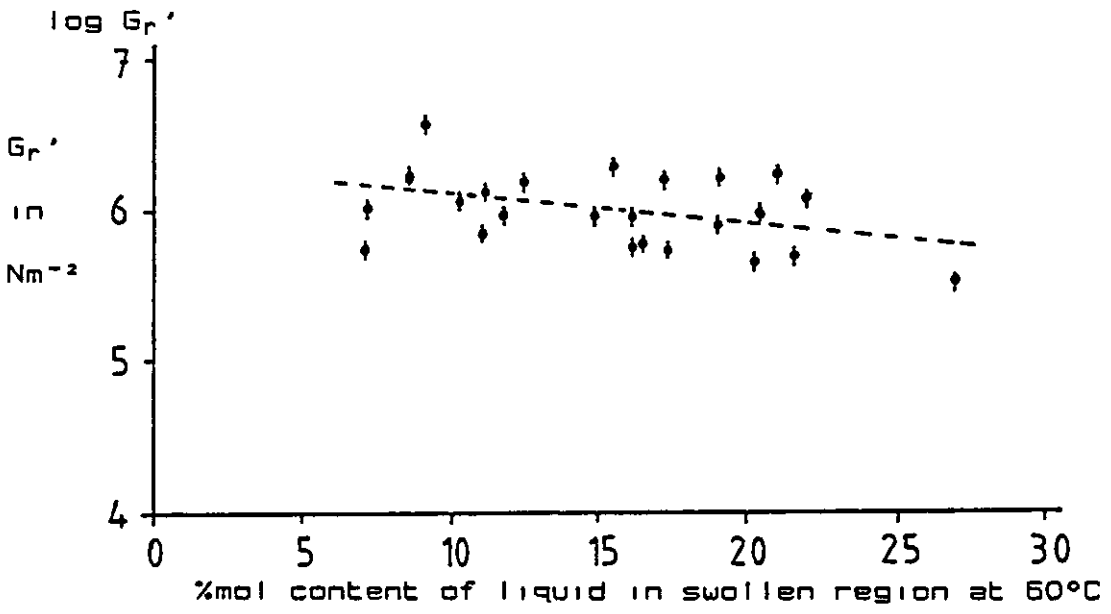

FIGURE 5.30

Log G_r' calculated from the shear analysis, at 60°C, of uPVC swollen with ethylbenzene

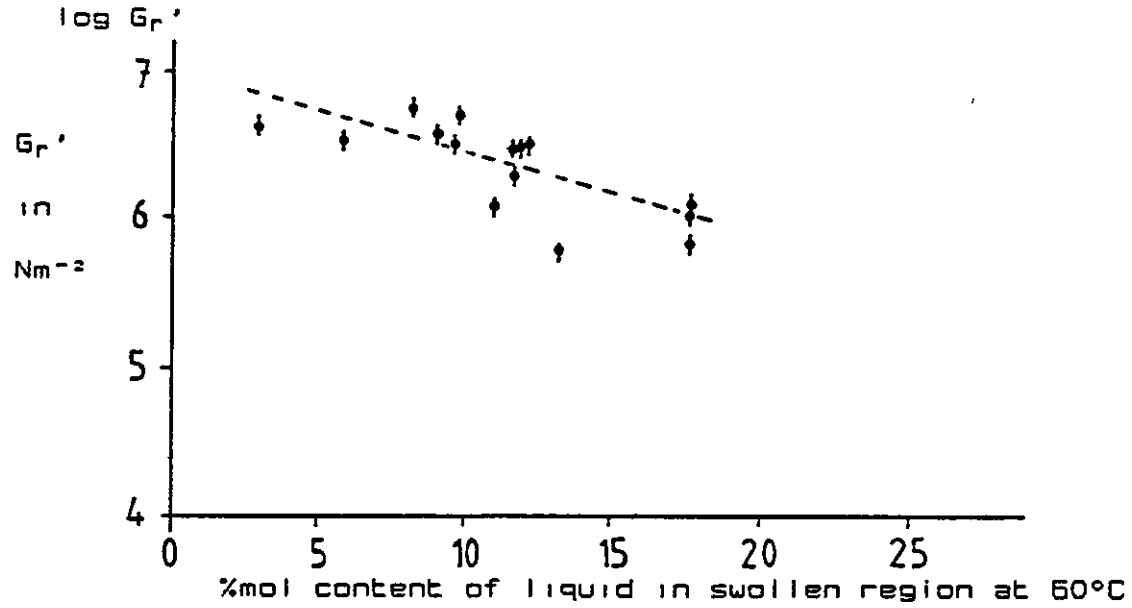

FIGURE 5.31

Log G_r' calculated from the shear analysis, at 60°C, of uPVC swollen with dimethylbenzene

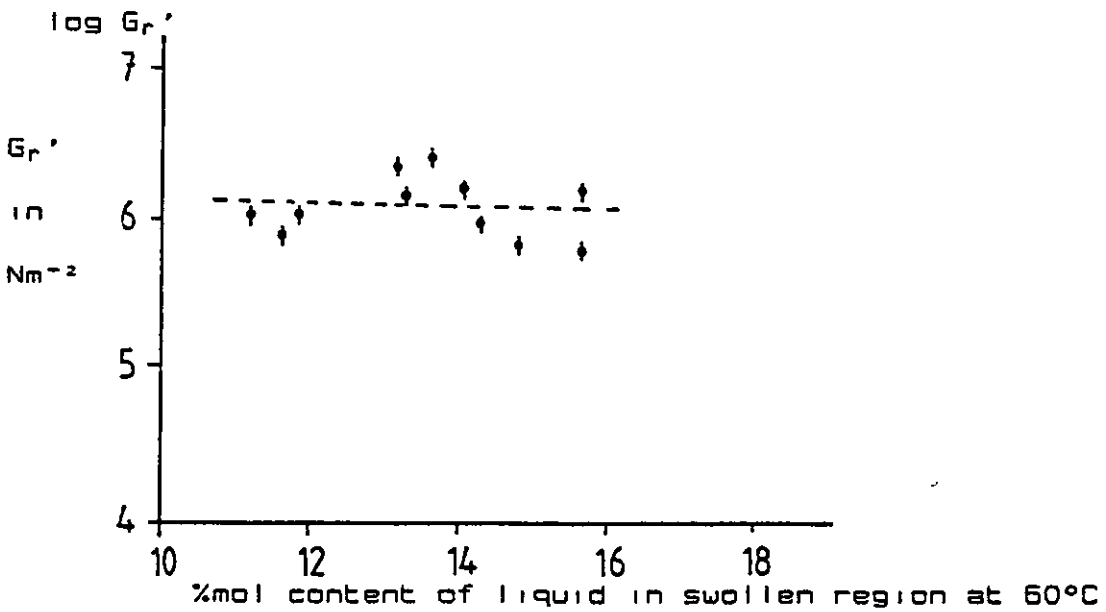

FIGURE 5.32

Log G_r' calculated from the shear analysis, at 60°C, of uPVC swollen with propanone

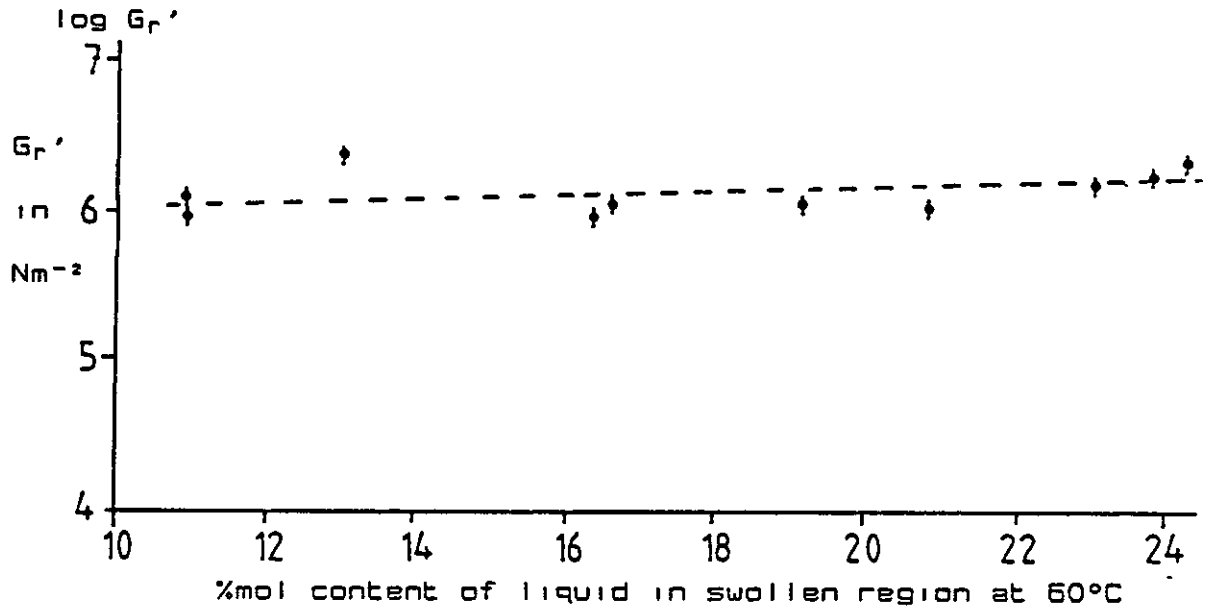

FIGURE 5.33

Log G_r' calculated from the shear analysis, at 60°C, of uPVC swollen with plasticizers

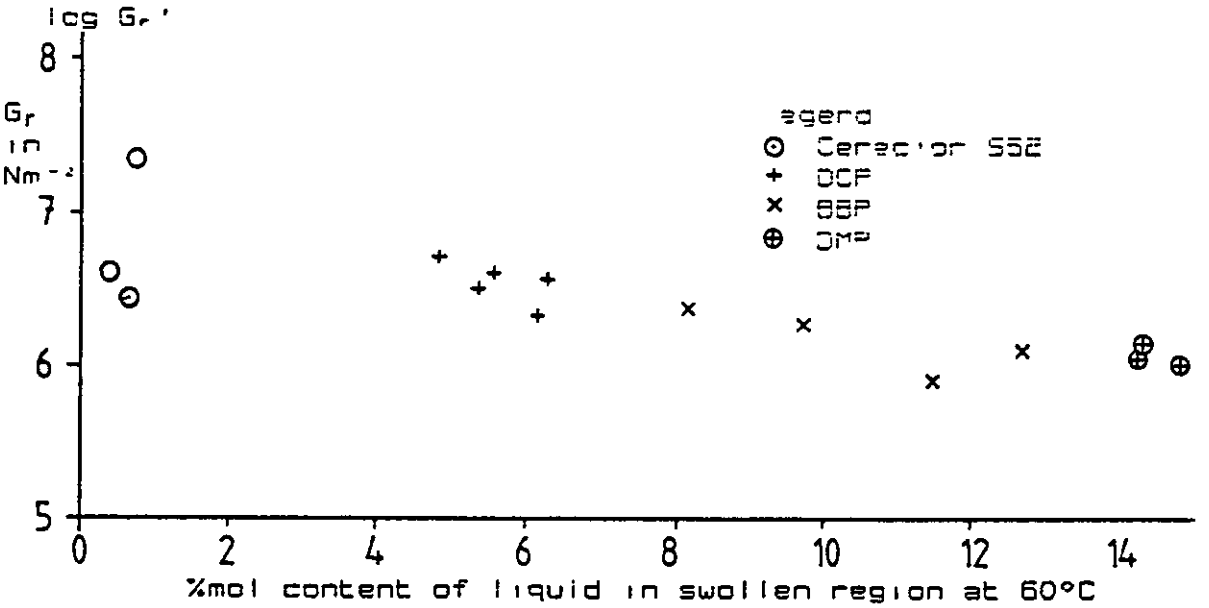

The height of the rubbery plateau can be correlated to M_c, the molecular mass between cross-links and/or entanglements; and by substituting G_r' for G in equation 2.63, M_c in the swollen region may be found.

$$G_r' = gpRT/M_c(1 - 2M_c/M_n) \qquad (5.4)$$

where G_r' is the shear modulus of swollen uPVC, ρ is the density of sample; ρ is calculated from the sum of the products of the relevant mass fractions and their densities and has units of Kg/m^3. R is the gas constant, 8.314 J $mol^{-1}K^{-1}$ and g is a numerical constant as defined in equation 2.63 and has the value of 3.3. The value obtained for M_c using PL-DMTA on uPVC was 1452 g/mol, calculated from the modulus value at 130°C given in figure 4.43. In a swollen uPVC sample exhibiting two tan δ peaks such as those in figures 4.70 to 4.74 the corresponding modulus curves shows two plateaus as seen in figures 4.65 to 4.69. The above treatment calculating M_c for the swollen region of the sample requires an average value of G_r' between the two tan δ peaks and the temperature at which the lower tan δ peak occurs. Appendix 4 describes the algorithm used to calculate G_r' values at temperatures of 10 degree intervals between 20 and 150°C. The log E' modulus data used in Appendix 4 was obtained using the PL-DMTA thermogram for polystyrene, an amorphous polymer. The validity of it s usage will now be discussed. The modulus data obtained from an amorphous polymer was preferred to the modulus data from uPVC since the experimental modulus curve obtained for a swollen sample, such as shown in figure 5.34, would have

FIGURE 5.34

Fitting of experimental G'meas to a calculated G'meas

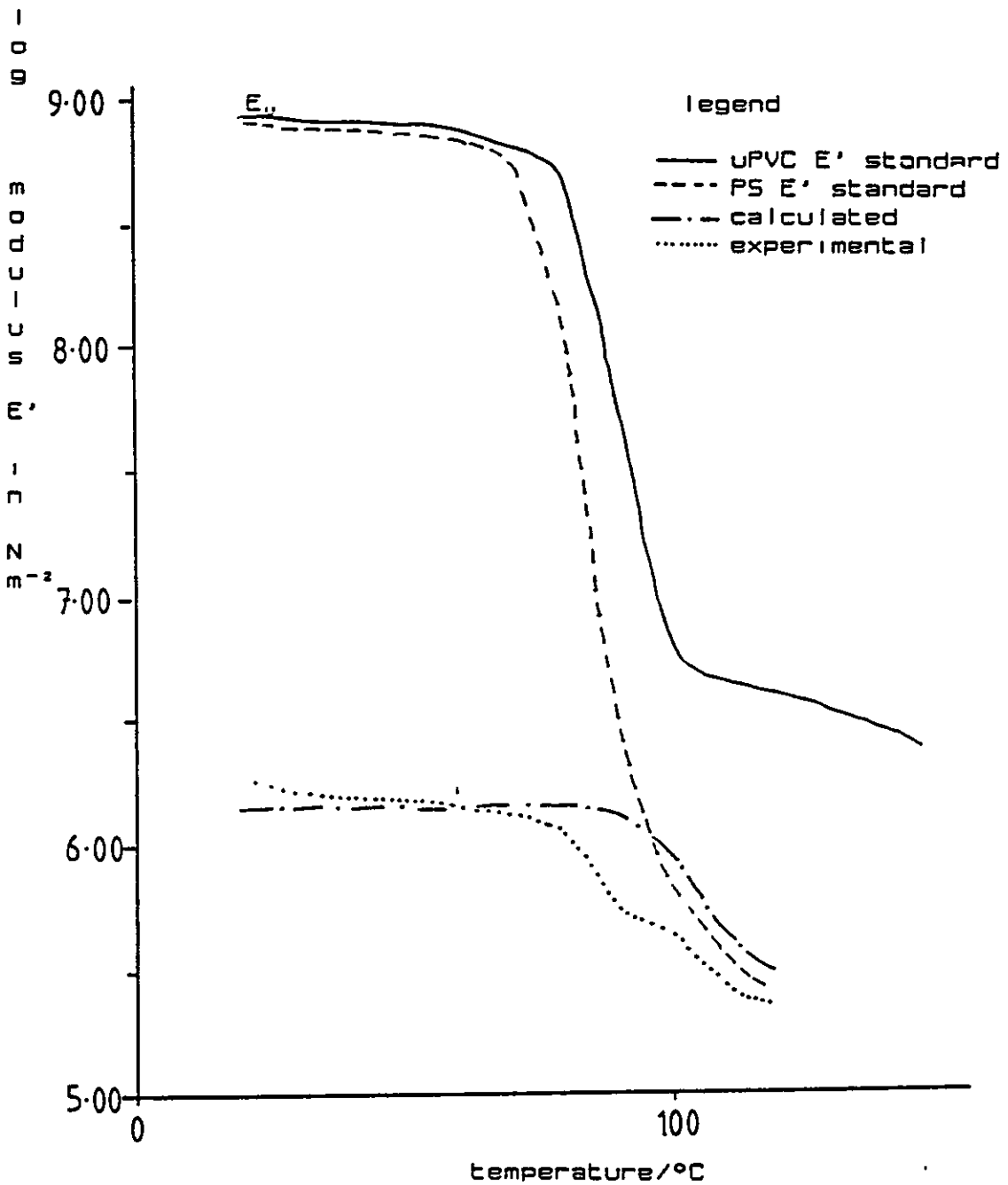

none or little crystallinity present, the swelling liquid having "softened" or "dissolved" any crystallites. Figure 5.34 shows, superimposed, the thermogram for uPVC, polystyrene by dual-cantilever PL-DMTA, a typical trace shown by a sample swollen with propanone at 56°C for 20 mins producing at sample exhibiting a large swollen layer, and the calculated trace for the modulus of the whole sample by shear PL-DMTA. Discrete polystyrene E' modulus values were first converted into shear modulus values. Equation 5.2 was then used to calculate J'(meas), using the J'_r value obtained at 60°C and assuming this value to be constant over the temperature range employed. The resulting calculated curve obviously coincides at 60°C with the experimental curve, the maximum deviation from the experimental curve occurring around 95°C. The modulus of the rubbery region, G_r, is assumed to be constant over the temperature range involved in this calculation and no correction was made for the effect of the loss of swelling agent on the modulus. At higher temperatures good agreement is found between the calculated and experimental curves. By using the modulus obtained with polystyrene rather than uPVC, closer agreement is obtained over the temperature range.

The plateaus shown in the modulus curves, for swollen samples, shown in figures 4.65 to 4.69, between the $T_{g\alpha'}$ and $T_{g\alpha}$ allows the computation of the molecular mass between cross-links and entanglements, M_c, using equation 2.63. Since the plateaux shown in the modulus curves in figures 4.65 to 4.69 are not exactly constant an average modulus value was employed[65]. Average values obtained for M_c for the various uPVC swollen systems are shown in table

TABLE 5.6

Average M_c values for uPVC swollen with various liquids

liquid	M_c via Equ. 2.63 g/mol	M_c via Equ. 2.70 g/mol
nitroethane	9049	9240
ethylbenzene	9877	8220
dimethylbenzene	9118	9009
fluorobenzene	14797	12936
propanone	----	8867
cereclor 552	2511	1947
BBP	6455	7636
DOP	2818	2739
DMP	7141	7725

5.6. The use of equation 2.70 at 60°C allows an alternative method for calculating the length of the chain between cross-links[81], the results being shown in table 5.6. The relative M_c values will give an indication of the liquids ability to dissolve the crystallinity in the polymer, the greater the M_c value the more efficient the liquid is in dissolving the crystallites. The values of M_c show little variance between diluent-uPVC systems. In the following section it will be shown that the variance in M_c between systems is equivalent to that found between identically swollen samples.

With the use of equation 2.81 and M_c it is possible to calculate the Flory-Huggins interaction parameter, λ. The results of which are shown in table 5.7. Theory[74,75] and experimental work[73] shows that liquids having λ values greater than 0.55 would be non-solvents for the polymer in question. The data in table 5.7 falls into two distinct sections, λ values obtained for liquids and values obtained for plasticizers. Of the liquids employed in this work only propanone is found in the literature[73] where λ was found to be 0.60 at 53°C, A better correlation with literature values[73] is found for DOP (λ = 0.01) and DMP (λ = 0.56), Both values were calculated at 53°C.

5.3.2.2 Estimation of the variation between identical shear experiments

The data obtained in section 4.4.1.1 was employed in the method discussed above to obtain an idea of the variance of M_c. The log modulus and tan δ thermograms for the shear analysis of uPVC plaques swollen with dimethylbenzene for 30

TABLE 5.7

Flory-Huggins interaction parameters for various liquids

liquid	λ using M_c via Equ. 2.63	λ using M_c via Equ. 2.70
nitroethane	1.016	1.017
ethylbenzene	1.280	1.277
dimethylbenzene	1.006	1.005
fluorobenzene	1.019	1.018
propanone	-----	1.015
cereclor S52	3.976	3.918
BBP	0.447	0.456
DOP	0.292	0.285
DMP	0.471	0.474

mins at 60°C are shown in figures 4.44 and 4.45 respectively. This extension to the experiment was designed to examine the precision obtained with the optical microscope.

To test the consistency of the analysis within the same plaque, a large plaque of uPVC was swollen with dimethylbenzene for 30 mins at 60°C from which a number of samples were extracted. A value for M_c for each experiment was calculated. By using the same large plaque and calculating an average value for the unswollen core thickness the error produced in this measurement by the microscope was reduced. The results for both these experiments are shown in table 5.8.

5.3.3 Glass transitions of swollen layers

Using the results obtained in section 4.3 it is possible to predict the T_g value of a swollen system if the concentration of the polymer is known, using equation 2.37. After accounting for the percentage loss of imbibed liquid as shown in Appendix 2, the volume composition of the swollen uPVC may be found using points 4 and 7, in Appendix 2, together with the respective densities of uPVC (1.369 g cm^{-3}) and diluent. The results for various swollen compositions all produced at 60°C are shown in figures 5.35 to 5.39. The dashed line indicates the theoretical value obtained using the Kelly-Bueche[55,65] plasticizer equation 2.37 and the dashed-dotted line is a polynomial regression fit through the data. Correlation between experimental and theoretical was only found for the nitroethane and

TABLE 5.8

The variation of the shear modulus, $T_g\alpha'$ and the resulting M_c values for dimethylbenzene swollen uPVC from: (a) the same plaque and (b) identical experiments.

expt.	average Log G_r' modulus	$T_g\alpha'$ °C	M_c via Equ 2.63 g/mol	Log G_r' modulus at 60°C	$T_g\alpha'$ °C	M_c via Equ 2.70 g/mol
a	5.96	10	10834	5.96	10	11993
	6.01	10	9615	6.02	10	10500
	6.03	9	9184	6.03	9	10268
	6.02	10	9491	6.01	10	10737
	5.97	10	10748	5.98	10	11474
b	5.93	4	11504	5.95	4	----
	6.24	7	5778	6.22	7	6575
	5.90	8	12210	5.88	8	13601
	6.03	9	9233	6.00	9	10457

FIGURE 5.35

Glass transition temperature of uPVC-propanone swollen layer found by shear mode PL-DMTA as a function of propanone volume fraction

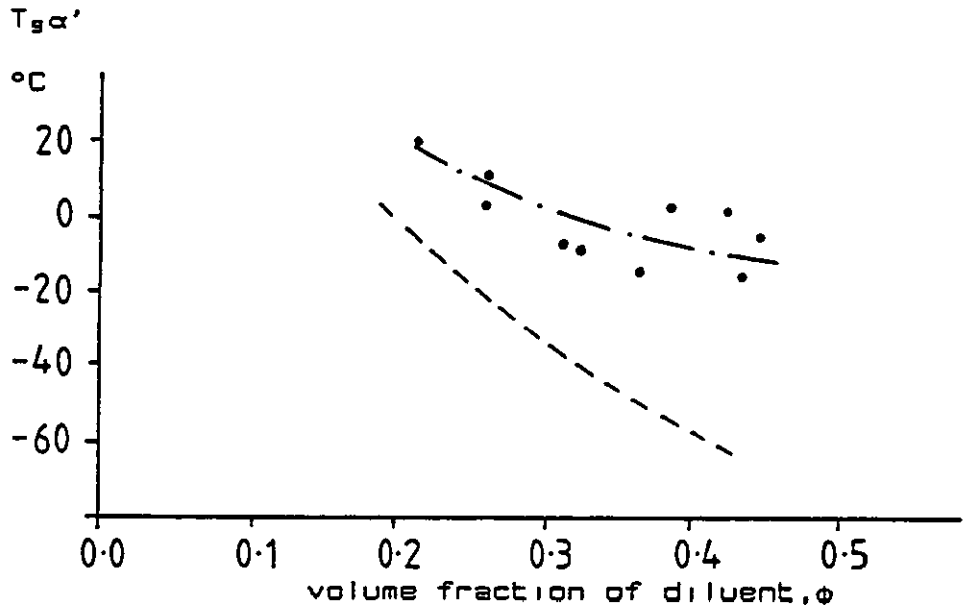

FIGURE 5.36

Glass transition temperature of uPVC-fluorobenzene swollen layer found by shear mode PL-DMTA as a function of fluorobenzene volume fraction

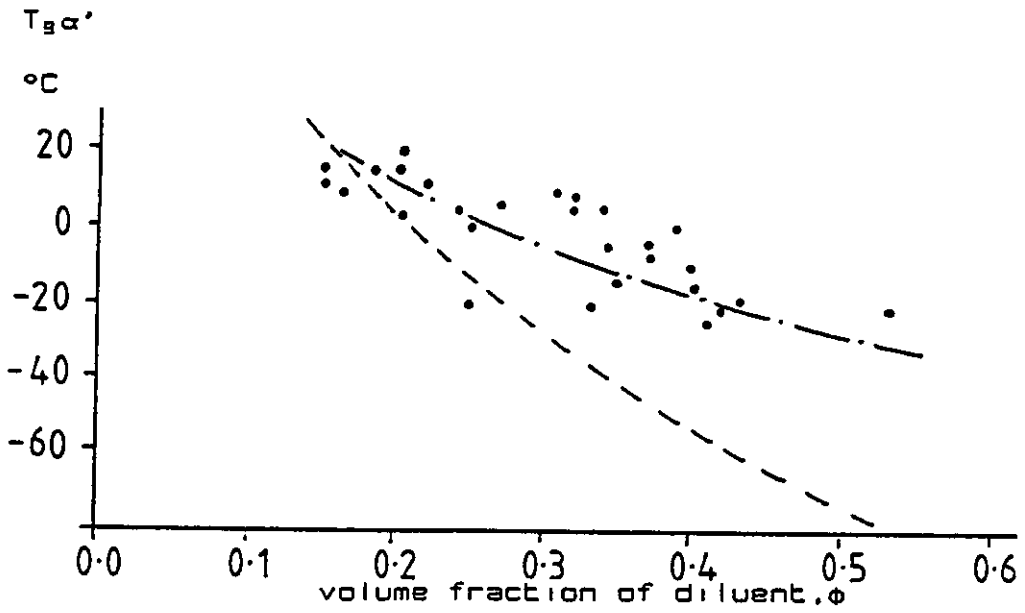

FIGURE 5.37

Glass transition temperature of uPVC-dimethylbenzene swollen layer found by shear mode PL-DMTA as a function of dimethylbenzene volume fraction

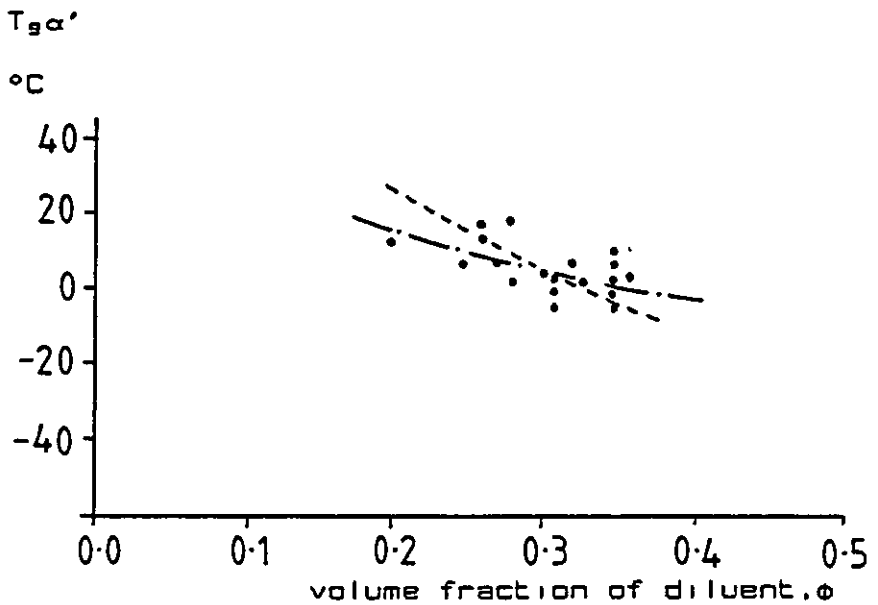

FIGURE 5.38

Glass transition temperature of uPVC-ethylbenzene swollen layer found by shear mode PL-DMTA as a function of ethylbenzene volume fraction

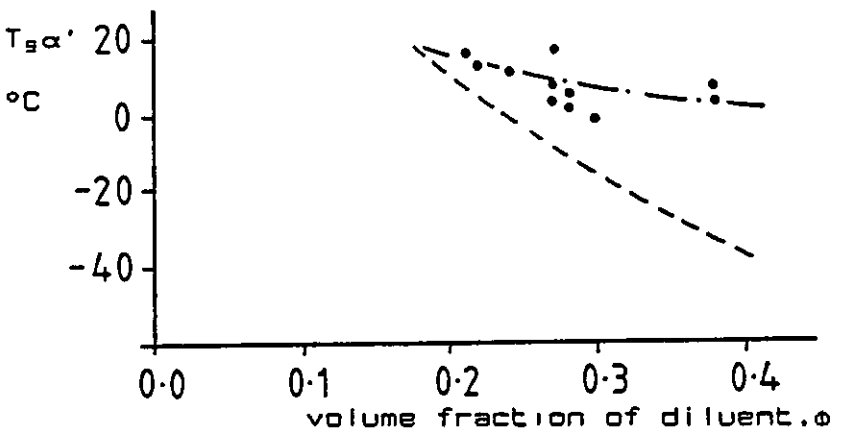

FIGURE 5.39

Glass transition temperature of uPVC-nitroethane swollen layer found by shear mode PL-DMTA as a function of nitroethane volume fraction

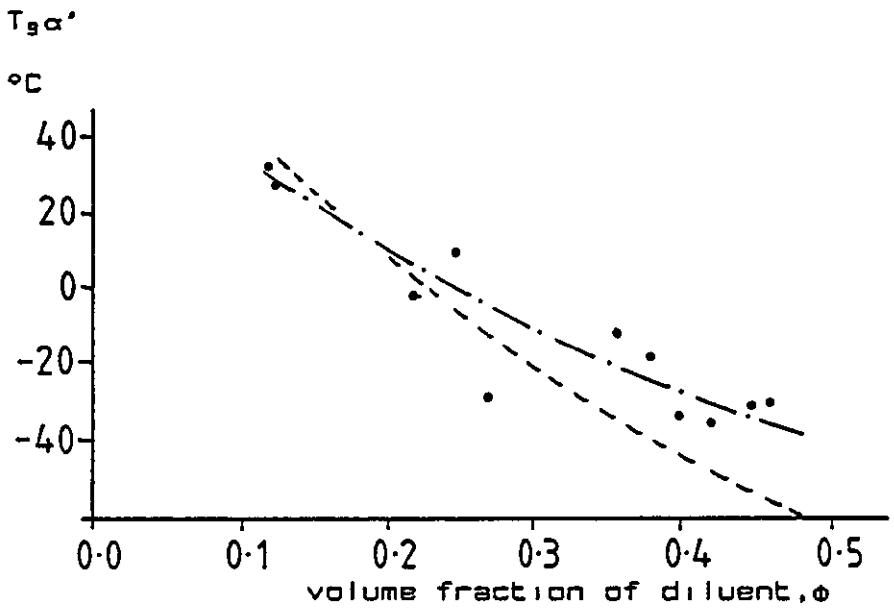

dimethylbenzene uPVC swollen systems. Deviations from the theoretical $T_g\alpha'$ increased with increasing volume fraction, ϕ, of swelling agent or diluent. This effect is in contradiction to recent work by Scandola et al.[163] where the T_g-concentration dependence for plasticized PVC showed two monotonically decreasing sections, having different curvatures and forming a cusp at a diluent-polymer concentration of 0.4.

5.3.3.1 Comparison of the glass transition temperature produced in highly swollen liquid sorbed uPVC plaques with the solubility parameter of swelling agent

In measuring the indentation modulus of PVC gels, produced from 10% (w/w) solutions of PVC in various solvents, Guerrero and Keller[31] were able to explain how the solubility parameter affected the nature of the gel network. It is possible to carry out a similar exercise using the systems where the polymer is fully swollen by the swelling agent, plotting $T_g\alpha'$ versus the solubility parameter of the swelling agent shown in figure 5.40. The $T_g\alpha'$ data was drawn from table 4.9 and the solubility data from table 3.1. The dotted line drawn through the data shows a minimum close to the solubility parameter value for propanone which nears the solubility parameter value for uPVC, (19.6 $J^{1/2}/cm^{3/2}$). The low $T_g\alpha'$ value for propanone is consistent with the idea that gels produced with similar solubility parameter values give weak polymer networks and there is good polymer-liquid interaction. The higher $T_g\alpha'$

FIGURE 5.40

The glass transition temperature of the swollen polymer modelled against the solubility parameter for the respective swelling agent for a number of liquids

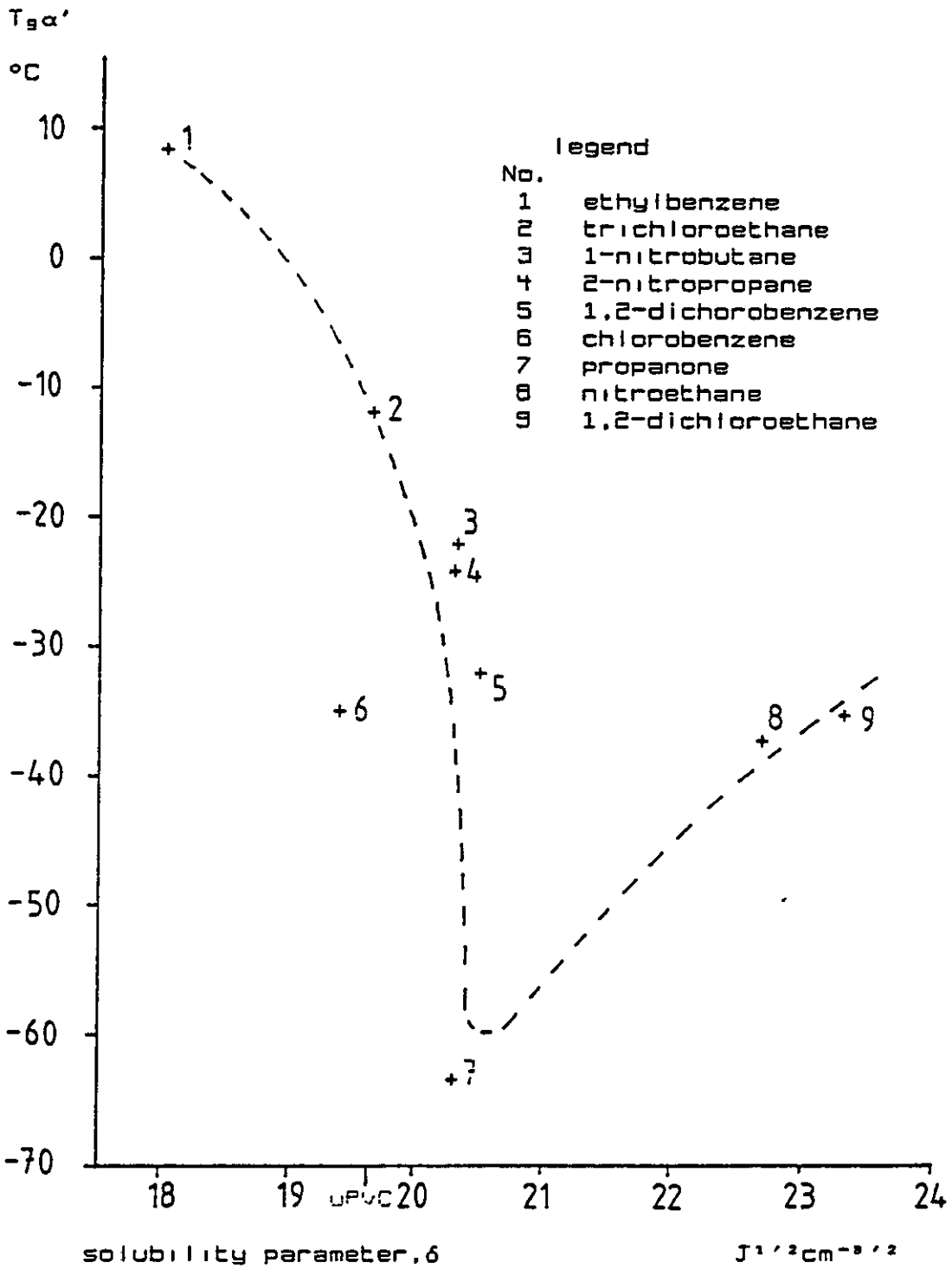

values would indicate that gels are produced using poor swelling agents that do not fully "dissolve" or "soften" the crystallite regions. Using this method it is not possible to show the formation of weak gels with swelling agents which show large differences in solubility parameter values from that for uPVC due to the insolubility of such liquids in uPVC plaques.

5.3.3.2 The glass transition investigated using differential scanning calorimetry methods

The use of DSC methods to investigate transitions in the swelling agents employed in this work has been particularly successful in determining the melting points of the liquids used. The analysis of the separated layers from the swollen sample has shown that the inner core $T_{g}\alpha$ is unaffected by the swelling agent but due to the poor physical contact between the polymer and sample pan, and hence poor DSC baseline, it has not been possible to investigate, with any precision, the presence of swollen material in the inner core nor the presence of dry unswollen material in the swollen layer.

5.3.4 Variation of $T_{g}\alpha$ peak height with volume fraction of unswollen core

The samples used in shear PL-DMTA are of the same diameter the only difference from sample to sample being the thickness, in particularly the core thickness. The height of the tan δ peak of $T_{g}\alpha$ gives an indication of the amount

of energy being dissipated during the transition and hence the peak height should show a relationship with the core thickness, the amount of uPVC present. This is shown in Figure 5.41.

FIGURE 5.41

Change in the tan δ peak height of the glass transition produced by the unswollen core

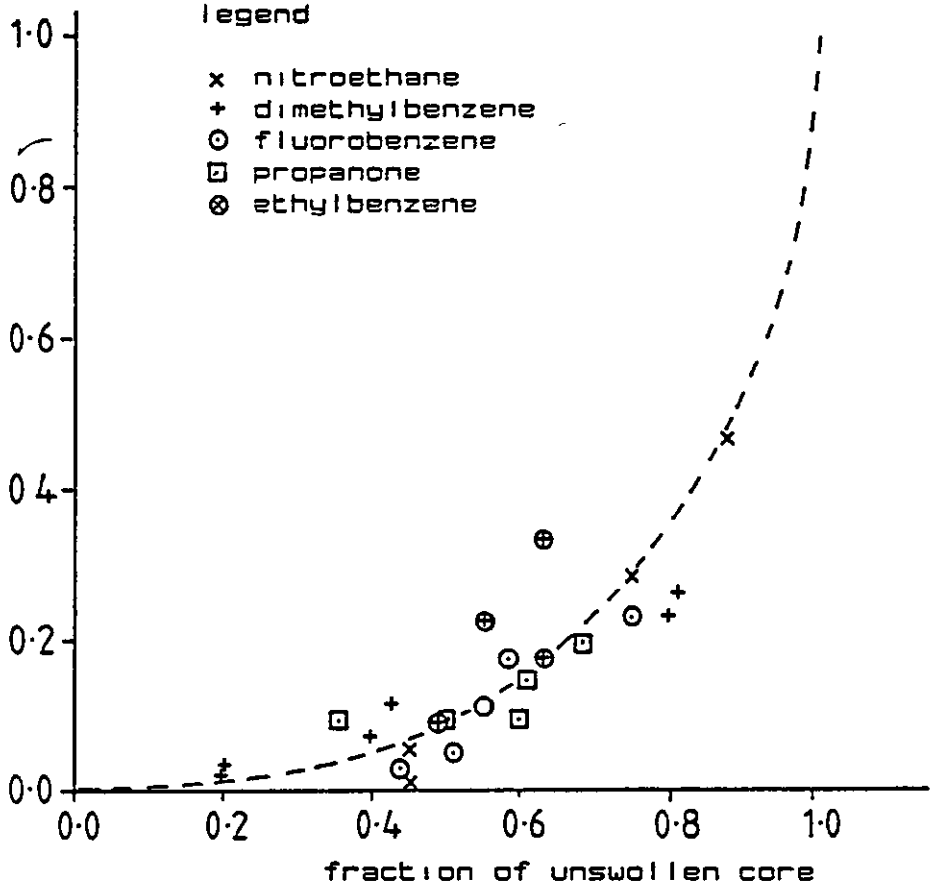

5.4 GENERAL DISCUSSION

The modulus curves shown in figures 4.65 to 4.69 in each case show thermograms for swollen plaques all of which exhibit window frames before analysis. At the start of heating the sample in the PL-DMTA, both inner core and swollen region, are glassy giving log moduli values of around 8. As the sample warms the $T_g\alpha'$ is passed, the outer swollen layer softens and the modulus falls by between 1 and 1.5 decades. The regime between $T_g\alpha'$ and $T_g\alpha$ arises from a sample having an outer elastic layer and a glassy inner core. The modulus in this temperature regime is a composite of these two regions. In section 5.3.2 a method was employed to separate the respective moduli of the two regions at 60°C. This temperature was chosen so that the inner core is still glassy and the outer swollen layer is in a rubbery state i.e. the sample is in a inhomogeneous state. The component value contributed by the glassy inner core, if unaffected by the swelling agent will be virtually a constant value, and variation in the measured modulus will be that due to the effect of the swelling agent on the swollen region. The modulus of the swollen region will depend on how the swelling agents affect the "cross-linked" network.

The structure of uPVC in the solid state has recently been reviewed by Blundell[164] and Walsh[165]. The "cross-linked" network structure of uPVC is thought to arise from one of two origins. Chemical cross-links might arise from bimolecular termination of branched propagating centres during polymerization or physical cross-links are present

due to low levels of crystallinity. The crystallinity of uPVC has recently been reported to be about 15%[166]. A swelling agent would first interact with the amorphous regions and depending on the swelling ability of the liquid could then interact with the crystallites, swelling and removing the crystallinity so that the network is disrupted.

It has been shown in the diffusion work in section 4.1.2.1 that the concentration of swelling agent reaches, in most cases, an equilibrium value in the swollen layer. A good swelling agent, one that dissolves, or swells the crystallites quickly, would produce a swollen layer in which the modulus is almost constant for the range of percent mol content of swelling agent measured in the swollen layer, since the modulus would then be due to entanglements in the network, the crystallites having been removed. It was not possible to measure very low values of liquid concentration in the swollen region because of the difficulty in measuring such small swollen layer thicknesses. This situation is shown in curve 1 in figure 5.42 and may be shown by the propanone-uPVC system. Swollen systems which show a decrease in the modulus value, curve two in figure 5.42, of the swollen region with increasing percent mole content of swelling agent in the swollen region would suggest that the liquid employed is a poor swelling agent and the crystalline region is still present and is only softening, or melting, slowly as the liquid content in the swollen region is increased. This situation would be shown by a ethylbenzene-uPVC system. A system showing a constant high modulus value, curve 3, in figure 5.42, for the swollen region would be exhibited in a system where the swelling

FIGURE 5.42

A schematic diagram showing the effect of diluent concentration in the swollen polymer with the modulus

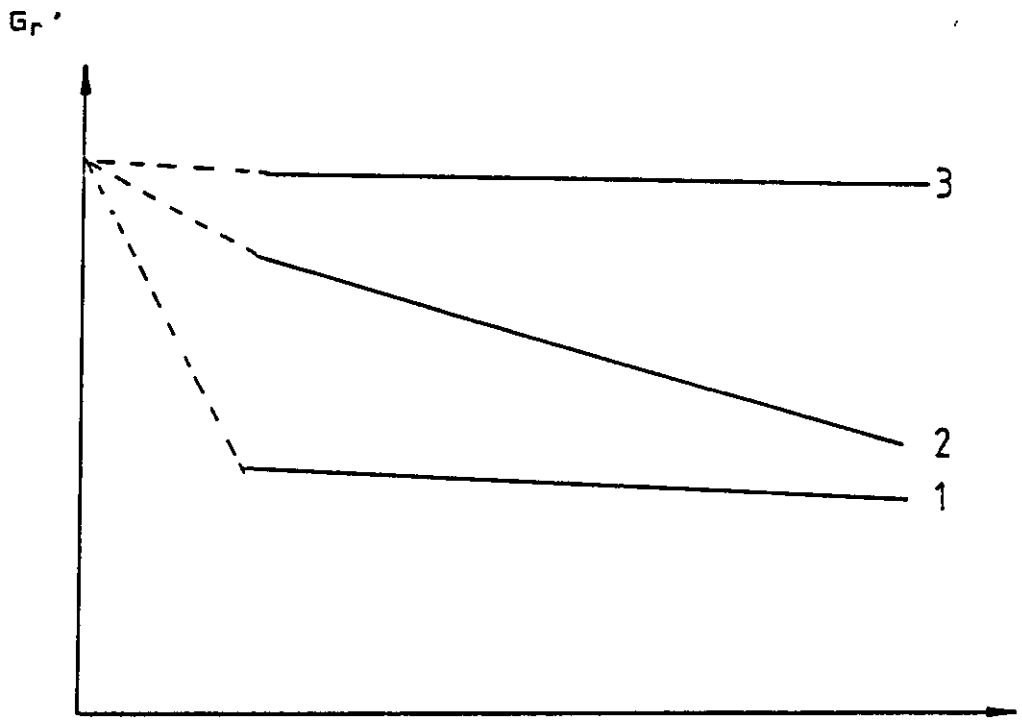

agent does not affect the crystalline regions. The dashed line in figure 5.42 shows the predicted change in G_r' at very low concentrations of swelling agent.

The arguments used above, in predicting the modulus of swollen uPVC with respect to the percent mole content of swelling agent in the swollen region, to some extent have been shown to be consistent with the experimental work. Of the five liquids used at 60°C, according to figure 4.3 ethylbenzene is the least efficient swelling agent and propanone the most able liquid to swell the polymer Examination of the linear least-squares fit of the best straight line through the data, shown as the dashed line in

figures 5.28 to 5.32, shows that G_r exhibits the greatest change with respect to mol content of liquid for the ethylbenzene-uPVC system. Propanone swollen systems give an almost constant G_r value at any liquid content, showing that any crystallinity present is swollen and removed for the swollen layer liquid concentrations examined.

Examination of the rate of change of G_r with respect to increasing percent mol content in the swollen region, i.e. the slopes of the best fit lines through the data show a parallel comparison with the ranking order given in table 5.2 with respect to the diffusion coefficient, D, and liquid front velocity, v. Ethylbenzene with the largest negative slope has the smallest, D and v, values and propanone, the largest D and v values of the five liquids employed at 60°C swelling conditions.

The ability of liquids to swell uPVC can be examined by the effect of the solubility parameter, δ, on the value of D. Examination of figure 5.19 shows, particularly at 30°C, a maximum D value at the δ of 19.5 $J^{1/2}/cm^{3/2}$ (for chlorobenzene at 30°C). The δ value for uPVC is 19.6 $J^{1/2}/cm^{3/2}$. Chlorobenzene at 60°C was found to be a solvent for uPVC. The maximum D value measured at 60°C was that for propanone (δ = 20.3 $J^{1/2}/cm^{3/2}$). Ethylbenzene (δ = 18.0 $J^{1/2}/cm^{3/2}$) has a greater difference in δ from uPVC and would thus be a poorer swelling agent according to theory. Ethylbenzene indeed exhibits a lower D value and as mentioned before is less efficient in "softening" or "melting" the crystallinity present. Both, the swelling agent molar volume and hydrogen bonding number, effect the value of D. An increase of 100% in the swelling agent molar

volume can cause a decrease in D of up to 1.5 decades, as shown in figure 5.20, but an increase in the hydrogen bonding number from 2 to 11 only shows an increase in D of 1 decade. The effect of molar volume seems to have a greater influence on the value of D than the hydrogen bonding number. The solubility parameter, though not completely able to describe the swelling ability of a liquid in uPVC alone, does show a greater change in D than a change in molar volume or hydrogen bonding number does. The above arguments used in correlating the ranking order of D with the solubility parameter can be extended to include the thermal properties of the swollen polymer. Figure 5.40 shows a distinct minimum in $T_g\alpha'$ at a solubility parameter value of δ = 20.5 $J^{1/2}/cm^{3/2}$, very close to that for propanone (δ = 20.3 $J^{1/2}/cm^{3/2}$). The low D for ethylbenzene particularly at 60°C when compared with D for propanone correlates well with figure 5.40 in that a high $T_g\alpha'$ (8°C) is observed together with a low δ value (18.0 $J^{1/2}/cm^{3/2}$). It is interesting to note that some liquids at 30°C, whilst exhibiting low D and v values when compared with D and v values for propanone, are solvents for uPVC at 60°C and others remain swelling agents, e.g. ethyl*benzene* is a swelling agent at both temperatures, 2-nitropropane and 1,2-dichlorobenzene both disrupt the polymer structure at 60°C. It can be concluded that the ability of a liquid to swell a polymer depends on a number of factors, δ, hydrogen bonding ability, molar volume and the temperature of the system, no one single factor can alone predict the swelling ability of a liquid with a polymer.

Very long diffusion times were required for the

swelling of uPVC plaques with the plasticizers and hence insufficient data were obtained to make any real qualitative statement about the modulus of the swollen region. It would appear that the crystalline regions are more intact, as shown by the higher G_r values obtained, when compared with the liquid swollen systems. Values of M_c in table 5.6 are calculated to be around 10,000 g/mol, which is still relatively small, as compared with the M_n value for this polymer (200,000 g/mol). This would suggest that changes in the network either due to an entangled chemical cross-linked structure, any crystallinity being removed by the swelling liquid, or due to the swelling liquid being unable to remove all the crystallinity do not significantly influence M_c. These M_c values are somewhat higher than the value (6200 g/mol) of a soft entangled uPVC[65]. The lack of a modulus plateau in the samples that were fully swollen produced using dual-cantilever mode PL-DMTA, see figures 4.46 to 4.54, would suggest that the liquids employed were all able to remove any crystallinity and that no chemical cross-links were present, and so it is not possible to evaluate an M_c value. The values obtained for the Flory-Huggins interaction parameter for the liquids swelling systems at 60°C were consistently high, at around 1. This suggests that these liquids are not solvents for uPVC. Whilst this appears to be correct for ethylbenzene, fluorobenzene, dimethylbenzene, propanone and nitroethane may well dissolve uPVC completely if sufficient time is allowed for a swelling experiment. Therefore, it is probable that the values for liquids in table 5.7 are over estimated. Since a liquid which is a solvent for a polymer will have a value of λ less

than 0.6[73-75].

Examination of the glass transition of the swollen region with respect to the volume fraction of diluent in the swollen polymer, as displayed in figures 5.35 to 5.39, shows the $T_g\alpha'$ to be higher than would be predicted from free-volume theories in three of the five liquid systems. Propanone, fluorobenzene, and ethylbenzene swollen systems all show higher than expected $T_g\alpha'$ values. Close agreement to free-volume theories is found for the systems swollen with dimethylbenzene and nitroethane. The higher than expected $T_g\alpha'$ value may arise from one or more of four origins; firstly, the swelling agent may be ineffective in removing the crystallinity. Crystallite content in a polymer will act as physical cross-links and could therefore produce higher T_g's than if the polymer was amorphous. This could indeed be the case for systems swollen with fluorobenzene or ethylbenzene since there is a distinct rate of change in G_r' with respect of mol content of diluent as shown in figures 4.36 and 4.38 indicating slow "melting" of "softening" of the crystalline regions as discussed earlier. However, this argument does not explain the propanone-uPVC system in figure 4.35. Secondly, if the polymer contains cross-links that arise from both, chemical and physical origins, and the imbibed liquid is only able to remove, by "melting" or "softening" crystalline regions, leaving the chemical originated cross-links intact, a constant higher than expected $T_g\alpha'$ would be exhibited. This could possibly explain the $T_g\alpha'$ behaviour with respect to volume fraction of diluent for systems swollen with propanone. Thirdly, the higher than expected $T_g\alpha'$ values may be due to the mode of

the experiment itself. The value of $T_g\alpha'$ may be affected by the unswollen inner core. This idea was explored in section 4.5, where in one instance it was possible to separate the outer swollen layer from the dry inner core and analyse this swollen layer using PL-DMTA techniques. A downward shift in $T_g\alpha'$ of 13°C was recorded for the separated outer swollen layer. Obviously, at the interface between swollen and core layers there is chain bridging. This may account for the high $T_g\alpha'$ values in figure 4.35, for the propanone-uPVC system, where the volume fraction of the unswollen core, V_s, was substantial, around 0.6. However, nitroethane-uPVC systems were analysed with a V_s fraction of approximately 0.5 and close agreement between predicted T_g value and $T_g\alpha'$ was found. Fourthly, although, attempts were made to minimise the effect of vapour loss during PL-DMTA, in figures 5.35 to 5.39, it is interesting to note that the most volatile system, that produced with propanone, shows the largest deviation from the predicted free-volume T_g value and a system which gave close agreement, uPVC swollen with dimethylbenzene, was the least volatile liquid employed. No single one of the above arguments can fully describe the discrepancies between $T_g\alpha'$ and the value expected to be found using free volume theories. A combination of the above ideas would seem more plausible.

At temperatures above the $T_g\alpha$ the inner glassy region is softened, as shown by the second fall in modulus in figures 4.65 to 4.69. The modulus value again reaches a plateau, at temperatures above $T_g\alpha$ which could be due to the crystalline region of the inner core. This is most easily seen in figure 5.34, where the plateau modulus for uPVC is

shown together with the beginning of the plateau exhibited by a sample swollen with dimethylbenzene. The plateau modulus value, above $T_g\alpha$, for uPVC is greater than the value for the swollen sample by a factor of 5, this is after converting the E' value obtained using dual-cantilever analysis, for uPVC, to G' consistent with the shear mode analysis. This region, however, was not fully explored due to the volatility of the liquids employed in producing the swollen layer. In most cases, at temperatures above 100°C the swelling agents would be beginning to boil or at least evaporate out of the sample. This very often caused cavitation in the sample making data acquisition impossible due to signal noise. Because of the volatility of the swelling agents the stability of the $T_g\alpha'$ was investigated for both the liquid evaporating from the discs prior to analysis and the effect of PL-DMTA itself by running a repeat analysis on the same sample.

CHAPTER 6 — SUMMARY AND RECOMMENDATIONS

It has been shown that the analysis of very soft, swollen polymers, which may lose part of the volatile component upon heating is possible by using a Polymer Laboratories Dynamic Mechanical Thermal Analyser in the shear mode. The use of PL-DMTA in the shear mode for laminated materials, one component being very soft, is a relatively new and untried technique. The modulus of the swollen region, G_r', has been modelled with the concentration of swelling agent present and has successfully been explained by data for diffusion coefficients and liquid velocities. The change in diffusion coefficient from one swelling agent-uPVC system to another was explained using data for solubility parameter, molar volume and the hydrogen bonding ability. It has been shown that the decrease in G_r' with respect to increasing swelling agent content, for swelling agents showing relatively small diffusion coefficient values, may be due to the presence of residual crystallinity, which is removed only with high contents of swelling agent. Liquids which show a relatively high diffusion coefficient value are efficient swelling agents and appear to remove the crystallinity even at low concentrations in the polymer, and so the change in G_r' with concentration of swelling agent is not observed. This has

been shown to be the case by examining the thermal properties of the swollen material, in particular the glass transition of the swollen polymer. The validity of the $T_g\alpha$''s of the swollen materials were examined by predicting the $T_g\alpha$' of the swollen polymer, using free volume methods.

By following the uptake of liquid per unit volume of uPVC with respect to time, it was possible to show that the diffusion process could be discussed in terms of a combination of Fickian and case II mechanisms. The generalized diffusion equation was applied successfully to the analysis of experimental data. The method employed required the swollen region to be in equilibrium with the concentration of liquid at the surface of the polymer. With the swelling experiments being carried out at 60°C, the equilibrium concentration of liquid in the swollen region with any particular liquid would be the same.

The diffusion of liquid VCM into uPVC compression moulded plaques at room temperature followed a similar behaviour seen in many of the liquids employed in this work[159], in that a moving liquid front is observed during sorption. No work was possible on VCM swollen samples showing an unswollen core since extraction of the disc would have meant allowing the sample to warm to room temperatures. This would have caused massive vapour loss, due to the low boiling point for VCM, (-13°C), and perhaps disruption of the sample structure during evaporation. The fully swollen sample discussed in this work, (figure 5.23), on removal from the liquid VCM was kept in liquid nitrogen, evaporation of VCM was therefore not a problem, until the sample had warmed during PL-DMTA.

CHAPTER 6 - SUMMARY AND RECOMMENDATIONS

6.1 APPLICATIONS FOR THE TECHNIQUE

Perhaps, the major application for this particular PL-DMTA method is the analysis of laminated polymers. The simple geometry of the sample, in the shear mode analysis, allows the use of the Takayanagi model for parallel composites, particularly when one component of the composite is very soft making sample clamping difficult.

The thermal stability of cross-links in uPVC may be investigated. This could be accomplished by conducting sorption experiments on uPVC compression moulded samples at increasing temperatures. The sorption temperature range used would show Fickian and case II behaviour and hence the observance of a liquid front moving towards the centre of the sample. The liquid concentration in the swollen region should show temperature dependent behaviour. The $T_g\alpha'$ for each swelling temperature can be plotted against volume fraction of liquid in the liquid/PVC system for a greater range than demonstrated in this work. Close examination of the modulus value at a temperature between $T_g\alpha'$ and $T_g\alpha$ and subsequent calculation of M_c at different swelling temperatures may lead to information regarding the stability of the crystalline regions to the imbibed liquid and the temperature of the polymer.

If a sample of polymer, e.g. epoxy resin, was cross-linked to a known degree and then partially swollen, the M_c value expected may be evaluated using a number of methods; standard dual-cantilever PL-DMTA, analysing the swollen layer using shear analysis methods and finally calculating M_c via more traditional methods including (a)

stress-strain data and (b) swelling ratios with solvents of known thermodynamic interaction parameters. If reasonable correlation is found between the methods, greater confidence can be given to the value of M_c.

6.2 POSSIBLE IMPROVEMENTS IN INSTRUMENTATION

The head of the PL-DMTA instrument, figure 3.7, although it can be run in an inert atmosphere, such as nitrogen being introduced into the head via an inlet port at the rear of the bulk head, cannot be run at a pressure much greater than atmospheric pressure, since the bulk head seal with the environmental chamber and the hole through which the ceramic drive shaft passes are not designed to be vapour tight seals.

By running the head in the same type of vapour as that used in producing the swollen discs, the amount of vapour lost during the analysis would be minimised. An instrument, in development in this laboratory[167], in conjunction with ICI, Plastics and Petrochemicals Division, The Heath, Runcorn, UK. runs on such a principle[168]. The stainless steel environmental chamber can withstand several atmospheres pressure. A Viton sealing ring between the chamber and the bulkhead provides the necessary seal and a stainless steel bellows arrangement on the ceramic drive shaft provides a seal between chamber and bulkhead. To enable the bellows to function correctly an equalizing pressure (nitrogen gas) in the chamber carrying the motor on the other side of the bellows is required. This machine is still under development, the major technical difficulties

being the balancing of the gas pressures either side of the bellows as the sample under test is being heated from subambient to elevated temperatures.

6.3 IMPROVEMENTS IN EXPERIMENTAL TECHNIQUE

From the moment a swollen plaque is removed from the environment employed for swelling, the swollen plaque will begin to desorb. This desorption has been kept to a minimum by quick transference of the plaque to a liquid nitrogen bath, for temporary storage. Once the discs have been removed from the plaque a slice is cut from the remaining portion for examination under the optical microscope, cutting the slice from the plaque without damaging the outer swollen layer was difficult. The use of a technique which circumvents the cutting of a slice for microscopy, and allows direct measurement of the dry inner core and total swollen thickness would be beneficial to the accuracy of the experiment. The measurement of the inner core using a depth gauge (or needle point micrometer) that is able to penetrate the swollen soft layer should be explored.

REFERENCES

1. R H Burgess in "Manufacturing and Processing of PVC", (Ed. R H Burgess), Applied Science Publishers Ltd., London, (1982)
2. M W Allsopp in "Manufacturing and Processing of PVC", (Ed. R H Burgess), Applied Science Publishers Ltd., London, (1982)
3. M Clark in "Particulate Nature of PVC", (Ed. G Butters), Applied Science Publishers Ltd., London.(1982)
4. H S Mickley, A S Michaels & A C Moore, J. Polym. Sci. 60, 121, (1962)
5. H Behrens, G Gribel, L Meinel, H Reichenbach, G Schulze, W Schenk & K Watter, Plaste und Kautschuk, 22, 414, (1975)
6. W D Cooper, R M Speirs, J C Wilson & E L Zichy, Polymer, 20, 265, (1979)
7. J E Glass & J W Fields, J. Appl. Polym. Sci. 16, 2269, (1972)
8. J A Brydson, "Plastics Materials", 3rd. ed., Newnes-Butterworths, London, (1975)
9. K H Illers, Makromol. Chem. 127, 1, (1969)
10. K U Pohl & D O Hummell, Makromol. Chem. 113, 203, (1968)
11. H Germar, Kolloid Z. 193, 25, (1963)

12. N Nakajima, A Hamada & S Hayashi, Makromol. Chem. 95, 40, (1972)

13. G A R Matthews in "Advances in PVC Compounding and Processing", (Ed. M Kaufman), Maclaren, London, (1962)

14. G C Portingell in "Particulate Nature of PVC", (Ed. G Butters), Applied Science Publishers Ltd., London, (1982)

15. M Gilbert & J Vyvoda, Polymer, 22, 1134, (1981)

16. E G Harrison, J V Dawkins, & R E Wetton, Polym. Comm. 26, 194, (1985)

17. J J Aklonis, "Introduction to polymer viscoelasticity", 2nd. ed., Wiley-interscience, New York, (1983)

18. J Corbiere, P Terra & R Paris, J. Polym. Sci. 8, 101, (1952)

19. K H Illers, Makromol. Chem., 127, 1, (1969)

20. L Lapcik & L Valko, J. Polym. Sci. part A2, 9, 633, (1971)

21. L Lapcik, J Panak, V Kello & J Polavka, J. Polym. Sci. 13, 981, (1975)

22. T K Kwei, T T Wang & H M Zupko, Macromol., 5, 645, (1972)

23. H L Frisch, J. Polym. Sci. part 2A 10, 1849, (1972)

24. H L Frisch, T T Wang & T K Kwei, J. Polym. Sci. part 2A 7, 879, (1969)

25. T T Wang & T K Kwei, H L Frisch, J. Polym. Sci. part 2A 7, 2019, (1969)

26. T T Wang, T K Kwei, Macromol., 6, 919, (1973)

27. A R Berens, Polymer, 18, 697, (1977)

28. A R Berens, Polym. Eng. Sci. 20, 95, (1980)

29. A S Michaels, W R Vieth & J A Barrie, J. Appl. Phys. 34, 1, (1963)

30. J W Summers, J. Macromol. Sci. Phys. B20, 219, (1981)

31. S J Guerrero & A Keller, J Macromol. Sci. Phys. B20, 167, (1981)

32. J M G Cowie, "Polymers: chemistry & physics of modern materials", Intertext books, London, (1973)

33. J D Ferry, "Viscoelastic properties of polymers", Wiley, N. Y. (1961)

34. R N Haward, "The physics of glassy polymers", Appl. Sci., London (1973)

35. A Ledwith & A North, "Molecular behaviour and the development of polymer materials", Chapman and Hall, London (1975)

36. G Rehage & W Borchard in "Physical properties of polymers", (Ed. A M Bueche), Wiley, N. Y. (1962)

37. R. T. Bailey, A. M. North & R. A. Pethrick, "Molecular motion in high polymers", Clarendon Press, Oxford, (1981)

38. R. Buchdahl & L. E. Nielson, J. Polym. Sci. 15, 1, (1955)

39. W. Reddish, Pure Appl. Chem. 5, 723, (1962)

40. R Simha & R F Boyer, J. Chem. Phys. 37, 1003, (1962)

41. A K Doolittle, J. Appl. Phys. 22, 1471, (1951)

42. A K Doolittle, J. Appl. Phys. 23, 236, (1952)

43. M L Williams, R F Landel & J D Ferry, J. Am. Chem. Soc. 77, 3701, (1955)

44. W Kauzmann, Chem. Rev. 43, 219, (1948)

45. J H Gibbs, J. Chem Phys. 25, 185, (1956)

46. J H Gibbs & E A DiMarzio, J. Chem. Phys. 28, 373, (1958)

47. J H Gibbs & E A DiMarzio, J. Polym. Sci. 1A, 1417, (1963)

48. J H Gibbs & E A DiMarzio, J. Res. Nat. Bur. Std. 68A, 611, (1964)

49. P J Flory, J. Chem. Phys. 10, 51, (1942)

50. M L Huggins, Ann. N. Y. Acad. Sci. 43, 1, (1942)

51. M L Huggins, J. Chem. Phys. 46, 151, (1942)

52. M L Huggins, J. Am. Chem. Soc. 64, 1712, (1942)

53. A J Kovacs, J. Polym. Sci. 30, 131, (1958)

54. G Adam & J H Gibbs, J. Chem. Phys. 43, 139, (1965)

55. A M Bueche, "Physical properties of polymers", Wiley, N. Y. (1962)

56. J H Gibbs & E A DiMarzio, J. Polym. Sci. 40, 121, (1959)

57. L A Wood, J. Polym. Sci. 28, 319, (1958)

58. M Gordon & T S Taylor, J. Appl. Chem. 2, 493, (1952)

59. L E Nielson, "Mechanical properties of polymers and composites", Marcel Deker, N. Y. (1974)

60. L E Nielson, "Mechanical properties of polymers", Van Nostrand Reinhold, N. Y. (1962)

61. L E Nielson, J. Macromol Sci. Revs. Macromol. Chem. C3, 69, (1969)

62. T G Fox & S Loshaek, J. Polym. Sci. 15, 371, (1955)

63. T G Fox & P J Flory, J. Appl. Phys. 21, 581, (1950)

64. K Ueberreiter & Rhode-Liebenau, Makromol. Chem. 49, 164, (1961)

65. D.W.van Krevelen, "Properties of polymers", Elsevier, Amsterdam, (1980)

REFERENCES

66. J H Hildebrand, J. Am. Chem. Soc. 38, 1452, (1916)

67. P J Flory, J. Chem Phys. 10, 51, (1942)

68. M L Huggins, Ann. N.Y. Acad. Sci. 43, 1, (1942)

69. A R Miller, Proc. Camb. Phil. Soc. 39, 54, (1943)

70. E A Guggenheim, Trans. Faraday Soc. 44, 1007, (1948)

71. S H Maron, J. Polym. Sci. 38, 329, (1949)

72. R F Blanks & J M Prausnitz, Ind. Eng. Chem. Funda. 3, 1, (1964)

73. P Doty & H S Zable, J. Polym. Sci. 1, 90, (1946)

74. P J Flory, J. Chem Phys. 9, 660, (1941)

75. P J Flory, J. Chem Phys. 10, 51, (1942)

76. M L Huggins, Ann. N. Y. Acad. Sci. 44, 431, (1943)

77. W Kuhn, Kolloid Z. 76, 258, (1936)

78. L R G Treloar, Trans. Faraday Soc. 39, 36, (1943)

79. L R G Treloar, Trans. Faraday Soc. 39, 241, (1943)

80. James H M & Guth E, J. Chem. Phys. 11, 455, (1943)

81. L R G Treloar, "The physics of rubber elasticity", 3rd. ed. Oxford University Press, London, (1975)

82. L R G Treloar, Trans. Faraday Soc. 40, 59, (1944)

83. A V Tobolsky, D W Carson & N Indictor, J. Polym. Sci. 54, 175, (1961)

84. W R Krigbaum & R-J Roe, Rubber Chem. & Tech. (Rubber Reviews), 38, 1039, (1965)

85. P J Flory, Chem. Rev. 35, 51, (1944)

86. P J Flory & J Rehner, J. Chem Phys. 11, 512, (1943)

87. P J Flory, J. Chem. Phys. 18, 108, (1950)

88. F T Wall & P J Flory, J. Chem. Phys. 19, 1435, (1951)

89. P J Flory, Ind. Engng. Chem. 38, 417, (1946)

90. G Gee, Trans. Faraday Soc. 42B, 33, (1946)

91. J C Maxwell, Phil. Trans. Roy. Soc. 157, 49, (1867)

92. W Voigt, Ann. Physik. 47, 671, (1892)

93. Lord Kelvin, Quart. J. Math. (1855)

94. L Boltzmann, Prog. Ann. Phys. Lpz. 7, 624, (1876)

95. P Meares, "Polymers: Structure & bulk properties", Van Nostrand, London, (1976)

96. E Weichart, Ann. de Phys. 50, 335, (1893)

97. A V Tobolsky, "Properties and structure of polymers", Wiley, N.Y. (1960)

98. P E Rouse, J. Chem. Phys. 21, 1272, (1953)

99. F Bueche, J. Chem. Phys. 22, 603, (1954)

100. D J Ferry, R F Landel & M L Williams, 26, 359, (1955)

101. M L Williams, J. Polym. Sci. 62, 57, (1962)

102. J B Jackson P J Flory, R Chaing & M J Richardson, Polymer, 4, 237, (1963)

103. L E Nielson & F D Stockton, J. Polym. Sci. A1, 1995, (1962)

104. W R Krigbaum, R-J Roe & K J Smith, Polymer, 5, 533, (1964)

105. M Takayanagi, Mem. Fac. Eng. (Kyushu Uni.) 23, 41, (1963)

106. M Takayanagi, H Harima & Y Iwata, Mem. Fac. Eng. (Kyushu Uni.) 23, 1, (1963)

107. M Takayanagi, K Imada & T Kajiyama, J. Polym. Sci. C15, 263, (1966)

108. A Fick, Ann. Phys., 170, 59, (1855)

109. J Crank "The mathematics of diffusion", 2nd. ed., Oxford Univ. Press, London, (1975)

110. P Meares, J. Polym. Sci., 27, 391, (1958)

111. H Fujita, A Kishimoto & K Matsumoto, Trans Faraday Soc, 56, 424, (1960)

112. A Kishimoto & Y Enda, J. Polym. Sci., A1, 1799, (1963)

113. A Kishimoto & K Matsumoto, J. Phys. Chem., 63, 1529, (1953)

114. S Prager & F A Long, J. Am. Chem. Soc., 73, 4072, (1951)

115. R J Kokes & F A Long, J. Am. Chem. Soc., 75, 6142, (1953)

116. G S Park, Trans. Faraday, 46, 684, (1950)

117. H Fujita, J. Phys. Soc. Japan, 8, 271, (1953)

118. W W Brandt, J. Phys. Chem., J. Phys. Chem., 63, 1080, (1959)

119. R M Barrer, J. Phys. Chem., 61, 178, (1957)

120. H Fujita, Adv. Polym. Sci., 3, 1, (1961)

121. H Fujita, A Kishimoto, J. Polym. Sci., 28, 547, (1958)

122. M H Cohen & D Turnbull, J. Chem. Phys., 31, 1164, (1959)

123. M J Hayes & G S Park, Trans. Faraday Soc., 52, 949, (1956)

124. R M Barrer & R R Ferguson, Trans. Faraday Soc., 54, 989, (1958)

125. H B Hopfenberg & H L Frisch, Polym. Letters, 7, 405, (1969)

126. T Alfrey, E F Gurnee & W G Lloyd, J. Polym. Sci., C12, 248, (1966)

127. J Crank & G Park "Diffusion in polymers", Academic Press, London, (1968)

128. H L Frisch, Polym. Eng. & Sci., 20, 2, (1980)

129. C H M Jaques, M B Hopfenberg & V T Stannett in "Permeability of plastic films & coatings", (Ed. H B Hopfenberg), Plenum Press, New York, (1974)

130. C E Rogers in "Physics & chemistry of the organic solid state", (Ed. D Fox, M M Labes, & A Weissberger), vol 2 chap. 6. Interscience, New York. (1965)

131. E Bagley & F A Long, J. Am. Chem. Soc., 77, 2172, (1955)

132. J Crank, J. Polym. Sci., 11, 151, (1953)

133. W Jost, "Diffusion in solids liquids and gases", Academic Press, N. Y. (1960)

134. "Handbook of tables for probability and statistics", 2nd. ed. Chemical Rubber Company, Ohio. (1968)

135. P G Faulkner, J. Macromol Sci. Phys. B11(2), 251, (1975)

136. A Gonze, Plastica, 24, 49, (1971)

137. D A Tester, in "Manufacturing and Processing of PVC" (Ed. by R H Burgess), Applied Science Publishers Ltd., (1982)

138. P A Small, J. Appl. Chem, 3, 71, (1953)

139. H Burrell, Official Digest 27, 726, (1955)

140. P I Vincent & S Raha, Polymer, 13, 283, (1972)

141. W Gordy & S C Stanford J. Chem. Phys, 7, 93, (1939)

142. W Gordy & S C Stanford J. Chem. Phys, 8, 170, (1940)

143. W Gordy & S C Stanford J. Chem. Phys, 9, 204, (1941)

144. N Kornbleum, H O Larson, R K Blackwood, D D Mooberry, E P Oliveto & G E Graham, J. Am. Chem. Soc. 78, 1497, (1956)

145. "Handbook of solubility parameters and other cohesion parameters" ed. A F M Barton, Chemical Rubber company, Florida, (1983)

REFERENCES

146. PL-DMTA users manual, Polymers Laboratories Ltd., The Technology Centre, Epinal Way, Loughborough, Leicestershire, LE11 0QE, UK.

147. M M Morton, PL-DMTA Users Newsletter, P.L. Laboratories No. 2, (1986)

148. P V Danckwerts, Trans. Faraday Soc. 46, 701, (1950)

149. P Higginbotham, "Microtab, BBC software", Edward Arnold Publishers Ltd., London, (1985)

150. J V Koleske & J A Faucher, J. Chem Ed., 43, 254, (1966)

151. R T Morrison & R N Boyd, "Organic Chemistry", 3rd. ed., Allyn and Bacon, Inc., Boston, (1976)

152. J A Faucher & J V Koleske, Phys. Chem. Glasses, 7, 202, (1966)

153. M Scandola & G Ceccorulli, Polymer, 26, 1958, (1985)

154. M Scandola & G Ceccorulli, M Pizzoli & G Pezzin, Polym. Bulletin, 6, 653, (1982)

155. J G Aston, G J Szasz & H L Fink, J. Am. Chem. Soc., 65, 1135, (1943)

156. R E Wetton in "Developments in Polymer Characterisation - 5", (Ed. J V Dawkins), Elsevier Applied Science Pubishers, London, (1986)

157. N G McCrum, B E Read & G Williams, "Anelastic and Dielectric Effects in Polymeric Solids", Wiley, New York, (1967)

158. J V Koleske in "Polymer Monograph - 3, PVC", (Ed. H Morawetz), Macdonald Technical and Scientific, London, (1969)

159. E G Harrison, Chemistry Department, Loughborough University,Leicestershire, UK, to be published

160. E G Harrison, Chemistry Department, Loughborough University,Leicestershire, UK, unpublished data

161. R E Wetton, Polymer Laboratories Ltd., The Technology Centre, Epinal Way, Loughborough, Leicestershire, UK., private communication.

162. L C E Struik, Polymer, 28, 57, (1987)

163. D J Blundell, Polymer, 20, 934, (1979)

164. D J Walsh, J S Higgins, C P Druke & J S McKeown, Polymer, 22, 168, (1981)

165. D G H Ballard, A N Burgess, L M Dekoninck and E A Roberts, Polymer, 28, 3, (1987)

166. E G Harrison, R E Wetton, I Hovell, J V Dawkins, Chemistry Department, Loughborough University, Leicestershire, UK, unpublished work

167. A Faraday, P V Smallwood & R Stevenson, ICI Petrochemicals and Plastics Division, The Heath, Runcorn, Cheshire, UK., unpublished work

168. A Faraday, ICI Petrochemicals and Plastics Division, The Heath, Runcorn, Cheshire, UK., private communication.

169. Users manual, C.I. Electronics Salisbury Wiltshire U.K.

APPENDIX 1

Calculation of liquid concentration in the swollen layer

The surface concentration, C_o, was taken to be the concentration that the system attained at equilibrium. The swelling experiments carried out at 60°C were not taken to full swelling equilibrium of the sample in the diluent. However the percentage molar content in the swollen layer was known. The following algorithm allowed the computation of M_f in the swollen layer.

$$\text{Mol fraction content in swollen layer} = \frac{\text{dm/diluent MM}}{\text{dm/diluent MM} + 0.0155} \div \text{vol fraction of swollen layer}$$

where 0.0155 is the number of moles of 1 g of uPVC. The liquid sorption experiments carried out at 30°C were taken to equilibrium sorption and the mass uptake per cm^3 of PVC was calculated from knowledge of the PVC density. The insertion of M_f, at equilibrium, in to equation 4.1 allows computation of the mass of diluent per gram of uPVC i.e. C_o.

APPENDIX 2

Sample molar content, percentage loss of liquid from sample, and volume composition of swollen layer

The calculation of the molar content of swelling agent in the sample, the percentage loss of swelling agent from a single disc and the volume composition of diluent and polymer required the following measurements from the sample of PVC during preparation;

a. Average original thickness of sample, L_o, measured in millimetres
b. Original mass of sample, om, measured in grams
c. Average swollen sample thickness, L_T, measured in millimetres
d. Swollen mass of sample, sm, in grams
e. Thickness of unswollen core, L_c, measured in millimetres
f. Mass of discs before PL-DMTA, mb, in grams
g. Mass of discs after PL-DMTA, ma, in grams
h. Volume fraction of core of the original sample, L_c/L_o.

1 $$\text{\%mol content in sample} = \frac{(sm - om) \times 64.52}{\text{diluent MM} \times om}$$

2 mass of swollen disc = mb/2

3 mass of original unswollen disc
$= \rho_{PVC} \times$ disc volume = md

APPENDIX 2

4 mass of liquid originally present in one disc prior to PL-DMTA = mb/2 - md = W

5 percentage loss in one disc = ((mb-ma)/2)/W x 100

The liquid is only present in the swollen layer and the fraction of sample that is swollen is given by;

6 $1-L_c/L_o$ = fraction of sample that is swollen

The mass of polymer that is in the swollen region is therefore given by;

7 $md(1-L_c/L_o)$

Using points 4 and 7 above, and density values for diluent and polymer, it is possible to evaluate the volume fractional composition of polymer and diluent in the swollen layer.

APPENDIX 3

The algorithm required to calculate the generalised diffusion equation of a penetrant into a semi-infinite surface[168]

```
 10 REM ***************************************
 20 REM *      SOLUTION OF GENERAL            *
 30 REM *    DIFFUSION EQUATION FOR           *
 40 REM *  FICKIAN AND CASE II DIFFUSION      *
 50 REM *           BY A FARADAY              *
 60 REM *         ADAPTED FOR BBC             *
 70 REM ***************************************
100 @%=&0002050A
101 A1=.0705230784
102 A2=.0422820123
103 A3=.0092705272
104 A4=.0001520143
105 A5=.0002765672
106 A6=.0000430638
110 INPUT "DIFFUSION COEFFT",D
120 INPUT "VELOCITY",V
130 INPUT "THICKNESS",H0
132 H9=10
134 IF H0*V/D<40 THEN 140
136 PRINT "THICKNESS TOO LARGE "
138 GOTO 130
140 INPUT "TIME",TS:TS=TS*60
142 IF H0>V*TS THEN 150
144 PRINT " TIME TOO LARGE"
```

```
146 GOTO 140
150 C0=.22
160 IF TS=0THEN STOP
170 T=TS
180 CM=0
190 REMVDU2
195 PRINT"THICKNESS";H0;"TIME";TS
200 FOR H=H0/H9 TO H0 STEP H0/H9
210     X=(H+V*T)/2/(D*T)^.5
220     GOSUB 1000
230     ERFC1=1-ERF
240     X=(H-V*T)/2/(D*T)^.5
250     GOSUB 1000
260     ERFC2=1-ERF
262     C=C0/2*(EXP(H*V/D)*ERFC1+ERFC2)
264     PRINT H TAB(20),C/C0
266     CM=CM+C
268 NEXT H
270 X=V/2*(T/D)^.5
280 GOSUB 1000
290 ERF1=ERF
300 X=-V/2*(T/D)^.5
310 GOSUB 1000
320 ERFC3=1-ERF
360 MT=C0*(D/V*ERF1+V*T/2*ERFC3
                    + (D*T/PI)^.5*EXP(-V*V*T/4/D))
420 PRINT
430 PRINT
435 PRINT"MASS ABSORBED","   MEAN CONCN"
440 PRINTMT TAB(13),CM/H9
```

```
 450 PRINT
 455 VDU3
 500 GOTO 140
1000 REM ERF CALC
1010 IF X<3 THEN 1050
1020 MERF=.527*EXP(-(X^2))/X
1030 ERF=1-MERF
1040 GOTO 1070
1050 NERF=1-1/(1+A1*X+A2*X^2+A3*X^3+A4*X^4+A5*X^5+
                                          A6*X^6)^16
1060 ERF=NERF
1070 RETURN
```

APPENDIX 4

The calculation of G_r' modulus value

```
1   REM **********************
2   REM *                    *
3   REM * Gr' calculation *
4   REM * using BBC BASIC *
5   REM *   © I. Hovell    *
6   REM *                    *
7   REM **********************
10 MODE1:CLS
20 @%=131594
30 REM"DATA TAKEN FROM S71/179"
40 REM"PRESSED AT 50 TON FOR 6 MIN"
50 REM"16/10/85.RUN DATE 13/8/86"
60 CLS
80 INPUT"VOL. FRACTION OF RUBBERY REGION":N
90 FOR TEMP=20 TO 150 STEP 10
100    READ GS,D
110    INPUT"LOG SHEAR MODULUS MEASURED":GM
120    GM=10^GM:GS=10^GS
130    INPUT"TAN DELTA AT SAME
       TEMPERATURE":DE
140    GS=GS/2.84:REM POISSON RATIO
150    GS=(1/GS)/(1+D^2)
160    GM=(1/GM)/(1+DE^2)
170    JR=(GM-((1-N)*GS))/N
180    JR=(1/JR)/(1+DE^2)
190    JR=LOG JR
```

APPENDIX 4

```
200    REMVDU2
210    PRINTTEMP,JR
220    VDU3
230 NEXT TEMP
240 DATA9.38,.0175,9.36,.0155,9.35,.0155
250 DATA9.34,.018,9.31,.0275,9.26,.0515
260 DATA9.16,.265,8.18,1,7.15,.315
270 DATA7.12,.15,7.05,.115,6.97,.11
280 DATA 6.9,.115,6.85,.125
```

APPENDIX 5

Microbalance data acquisition[169]

The following routine uses an IEEE interface between the Commodore computer and the Robal control unit. The main control loop, K, allows the acquisition of 4000 readings being printed on the computer screen. The loop, J, is simply a delay routine. The mass reading is read into B$ in the subroutine starting at line 4000. The routine is terminated when the value of A$ is 13. The mass reading is then printed at 2045 and the routine is repeated via the main loop.

```
2000 REM TEST ROUTINE
2005 FOR K=1 TO 4000
2010     FOR J=1 TO 5000
2020     NEXT J
2030   GOSUB 4000
2035   IF VAL(B$)=0 THEN
       PRINT"RE-TRY":GOTO 2030
2045   PRINT K,B$
2050 NEXT K
2070 STOP
2999 REM*********
4000 OPEN 4,5
4010 B$=""
4020 GET#4,A$
4030 IF ASC(A$)=13 THEN 4060
4040 B$=B$+A$
```

APPENDIX 5

```
4050 GOTO 4020

4060 CLOSE 4

4080 RETURN
```